Bedload transport and channel change in gravel-bed rivers

Submitted for the degree of

Doctor of Philosophy

Philip John Ashworth B.Sc. (Hons)

May 1987

Environmental Science Department

University of Stirling

ABSTRACT

Spatial and temporal variations in channel morphology, near-bed velocity, shear stress, bedload transport rate, pebble tracer movement, and bedload and bed material size distribution were measured in seven different channel patterns in two gravel-bed rivers in the Scottish Highlands (the Dubhaig and Feshie) and a proglacial stream in Norway (the Lyngsdalselva). The results showed that there were discernible links between the channel processes and changes which were consistent for all river types.

169 shear stress estimates from velocity profiles with changing discharge showed that Keller's (1971) velocity-reversal hypothesis holds true in different channel patterns of gravel-bed rivers and can be extended to include subunits of the pool/riffle cycle. At discharges near bankfull there is a decrease in the flow strength and amount of bedload movement from the poolhead down to the pooltail (and then riffle). On a broader scale 72 Helley-Smith bedload samples and the movement of over 3700 pebble tracers showed that the entrainment of different size fractions from heterogeneous bed material is inefficient and is overpredicted by the traditional bedload transport equations. Empirical analyses showed that when the armour is mobile/broken large and small particles have almost equal mobility as first proposed by Parker et al. (1982) and Andrews (1983). However for the majority of flow conditions the armour is static and entrainment is selective to a greater or lesser degree depending on the availability of appropriate-sized sediment at the surface and from bank erosion.

The magnitude and direction of flow strength and bedload transport helps

to explain the location and mode of channel development as revealed by repeated levelling and mapping. The accelerating convergent/decelerating divergent cells of flow alter the channel morphology in predictable ways. The positions of these cells can change with increasing discharge as the channel becomes generally, rather than locally, competent to move coarse sediment. The rates of bank erosion and volumetric scour and fill decreased from the active multi-braided system through to the stable straight channel type.

CONTENTS

LIST OF FIGURES

LIST OF TABLES

ACKNOWLEDGMENTS

I would like to express my thanks to Dr. Rob Ferguson for arranging this project and for his excellent supervision throughout my time in Stirling. The research reported here has been stimulated by many hours of enthusiastic discussion with Rob and is a tribute to his patience and willingness to help me.

Within the department I would like to thank Professor Mike Thomas for allowing access to all the departmental facilities and continued support during my research, Mary Smith and Ken Dockery for cartographic advice and producing some of the drawings presented here, and all the technical staff (particularly Ina Mack) for making my stay in Stirling so enjoyable.

In the field I would like to thank Mr R. Kennedy of Dalnaspidal Farm and the Nature Conservancy Council for permission to work at Drumochter, Lord Dulverton for access and permission to undertake research in Glen Feshie, and the executive director of the British Schools Exploring Society Peter Steer, the 1984's expedition scientific leader Brian Whalley, and over 80 young expeditioners for providing the opportunity and help with my research on the Lyngsdalselva in Norway.

None of the research reported here would have been possible if I had not had the help of many enthusiastic field assistants. I am particulary in debt to John Phizacklea (technician) who was my reliable, keen, and conscientious field assistant at Drumochter. Other volunteers (?!) included Rob, Alan Werritty, Alan Jenkins, Tim Stott, and Philippa Rowling.

Finally I would like to thank the Natural Environment Research Council for providing me with a studentship and extra funds for my research in Norway, John Lewin at Aberystwyth for first directing me towards wet, cold rivers and frequently offering advice and constructive criticism, Philippa Rowling for her constant support, friendship and culinary delights, and my mother and father for their interest and continual support (both moral and financial!) throughout my time in Stirling.

1 INTRODUCTION AND BACKGROUND TO THE STUDY

1.1 Introduction

Rivers with beds consisting predominantly of material with median sizes greater than 2 mm can be termed gravel-bed rivers (Charlton et al. 1978, Bathurst 1982). Such rivers dominate upland and proglacial areas where either thick gravel deposits exist beneath the river bed or where the bedrock is covered by a thin veneer of gravelly till. These rivers are becoming increasingly important to help fulfil man's needs for power generation, resources and leisure. To control the river's natural system effectively, large sums of money need to be invested often leading to huge construction schemes and the alteration of the river channel. In order for the engineer to efficiently change and modify the natural river system he must be able to predict and assess the response of the river to any man-induced interference. This information and understanding can only arise from detailed investigations of the interrelationships between the channel processes and changes for the full range of channel types.

To date there is still a lack of knowledge of these interrelationships in gravel-bed rivers. Up to the 1970s research concentrated predominantly on rivers with fine alluvial beds. The popular laboratory-based studies often used the simplified case of straight uniform channels with steady flow over bed material that was uniform in size and small relative to water depth. Only recently has attention been focused on flow in gravel-bed rivers with their characteristic coarse heterogeneous bed material. This research is still in its infancy and is limited to a few channel types, discharge regimes, and bed grain sizes. Much more work is

still required to investigate and compare the morphology, flow characteristics and sediment movement within the broad continuum of gravel-bed river channel types. Basic information is still needed to help assess the geomorphological and sedimentological importance of gravel-bed rivers in the present and past environment. The study here provides results from integrated field measurements in seven different channel patterns of three rivers. Whilst the results are used to look at individual relationships between the channel processes and changes the study also provides a general overview of the functioning and development of the whole gravel-bed river system.

1.2 Reasons for studying bedload transport and channel change in gravel-bed rivers

With continued urban and industrial growth the natural physical character of many gravel-bed rivers has been significantly affected by river and catchment development projects. The utilisation of river systems for water resources, navigation, flood control and power generation has led to channels being dredged and straightened, flows regulated, and banks protected and raised (Hey 1982). Similarly, catchment developments related to such activities as forestry, gravel mining, road and pipeline construction and urban growth have considerably altered the quantity and quality of the sediment and water carried into rivers (Hey et al. 1982). The impact of these major constructions and engineering works on the natural river system can lead to channel instability and vast financial penalties on society - even resulting in the loss of life. It is therefore essential that the engineer is provided with an extensive and accurate data set so that he can improve existing designs and modelling techniques and minimise the adverse consequences of any proposed

engineering works.

Neill and Hey (1982) summarise their review on engineering problems related to gravel-bed rivers by stating that there are still "many deficiencies in current engineering design and management practice for gravel-bed rivers." They note that of particular importance to the engineer is information on velocity distribution, the stability of pebbles and the forces required to transport them, and the rate and location of maximum channel scour and adjustment. However despite such data being fundamental to engineering schemes the understanding in these areas is still incomplete.

Information on the movement of different size fractions from heterogeneous gravel-bed material is particularly important to the fisheries industry. Two main European Salmonid species, the Atlantic salmon (*Salmo salar* L.) and the trout (*Salmo trutta* L.) in both the freshwater and anadromous forms use the gravel beds of upland rivers for egg deposition. As Carling (1984) notes, the successful development of the fish eggs is directly affected by the physical nature of the stream bed and the flow hydraulics. The interaction between discharge, bed grain size, and sediment movement can have an important influence upon "spawning site choice, survival of intragravel stages, emergence of swim-up fry and the growth and survival of older stages" (Milner et al. 1981).

Factors which are known to have a detrimental effect on egg development are gravel movement and the proportion of fine particles in the surface and subsurface layers of the bed. Gravel movement causes washout of eggs which are consequently damaged by crushing, are preyed upon by other fish, or are subsequently deposited in environments unsuitable for egg

development (Carling 1984). McNeil (1966) working on Pacific salmon spawning beds on North American west coast rivers reported that such losses can be up to 90% for pink and chum salmon. Similar work by Harris (1970) observed that up to 58% of brown trout and sea trout eggs were washed away in tributaries of the Afon Dyfi, in Wales, and concluded that erosion was a major cause of egg loss.

Gravel composition and structure influence the oxygen supply to the eggs and the removal of toxic metabolic wastes by controlling the water movement through the gravel. Many workers have shown that the proportion of fine particles in the spawning gravel will reduce void space and the water percolation through the gravel and thus have a major effect on egg survival (e.g. McNeil and Ahnell 1964, Hall and Lantz 1969, Turpenny and Williams 1980). An understanding of the sediment movement and deposition in gravel-bed rivers can therefore be of great value to the fisheries industry as well as having implications for the aquatic ecosystem in many upland rivers.

Finally, studies of ancient sediments of previously tropical and glacial areas have shown that an understanding of contemporary gravel-bed river processes and associated depositional forms can be rewarded by vast financial gains. As Miall (1978) concludes "in terms of resource extraction, fluvial deposits act as hosts for a variety of non-renewable resources, including coal, hydrocarbons, and many placer deposits." Work by Smith and Putnam (1980) and Smith (1983) on Canadian anastomosing river systems of sand and gravel bed channels showed that the preservation potential for resources such as coal, oil and gas reserves should be excellent in many rapidly aggrading fluvial environments. Indeed, Smith and Putnam (1980) state that an understanding of rapidly aggrading systems

is "paramount to the geologist exploring for oil, gas and coal."

An investigation into the mechanics of gravel-bed river behaviour of various channel patterns and forms can therefore be a useful aid to scientists and entrepreneurs of many disciplines. The recent influx of financial support for such studies by governments, mining, oil, and engineering companies and the fisheries industry underlines the magnitude of the financial gains that can be achieved from this understanding. This funding has been reflected in several major international conferences in the past four years. Recent Symposium volumes include Gravel-bed Rivers (Hey et al. 1982), Special Publication of International Association of Sedimentologists (6) - Modern and Ancient Fluvial Systems (Collinson and Lewin 1983), River Meandering (Elliot 1984), and Sediment Transport in Gravel-Bed Rivers (Thorne et al. in press).

1.3 The gravel-bed river system and associated research

The cause-effect relationships operating in gravel-bed rivers are closely interlinked with substantial feedback, both positive and negative. This system can be presented as a flow diagram as shown in Fig. 1.1 from Ashworth and Ferguson (1986). The system is best entered at the top left and followed round in a clockwise direction. Unsteady discharge through a system of highly nonuniform channels with rough beds produces a complicated spatial and temporal pattern of water velocity. The vertical velocity gradient at any point determines the shear stress on the bed and this together with sediment availability governs the size and amount of bed material that can be moved as bedload. In turn, bedload transport either maintains the existing size, shape and pattern of channels or alters the morphology by scour, fill and maybe lateral migration. It may also alter the existing texture and structure of bed sediments by selective entrainment and deposition.

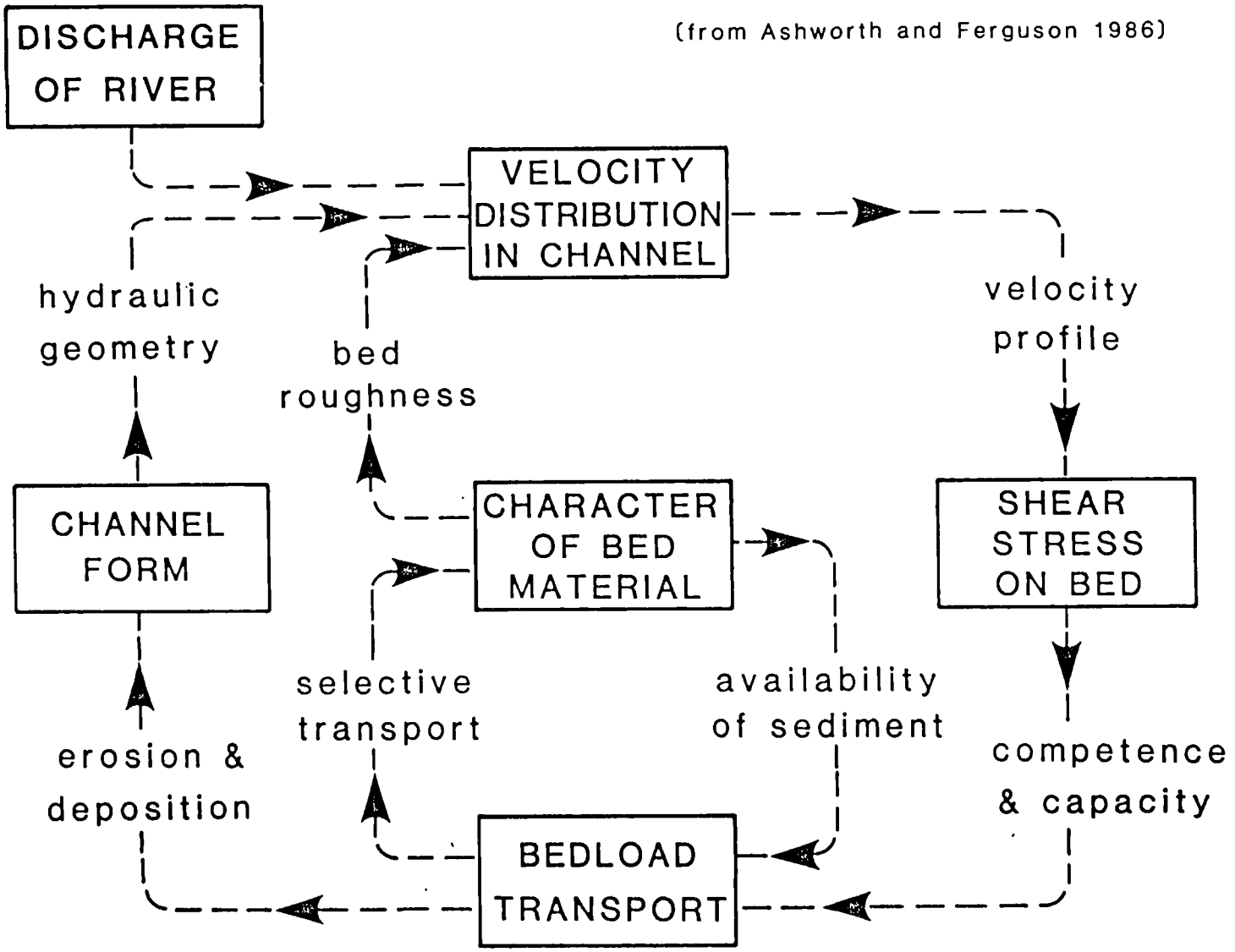

Fig. 1.1 Interrelationships amongst form, flow, and sediments in active gravel-bed rivers

In conditions of fluctuating discharge the system is obviously dynamic not static. Even at a constant discharge the streamwise variations in channel form and hydraulics that are inevitable where channels divide and recombine must cause differences in sediment transport and consequent erosional and depositional modification of channel form and sedimentology.

Up to the 1970s little research had been undertaken to describe the role and importance of each component of this system in gravel-bed rivers. Previous work had been dominated by either flume and laboratory studies, research in rivers with fine alluvial bed material, or theoretical two dimensional modelling on straight and trapezoidal channel forms. In recent years gravel-bed river research has accelerated dramatically and often the conclusions of earlier work have been found to be partly or wholly inapplicable to describe the processes and functioning of the gravel-bed river system. The development of this research is outlined below and is discussed in relation to the forementioned system's diagram (Fig. 1.1). Only a very brief synopsis of previous work is described for each major link in the system's framework since it is more useful and relevant to include a detailed discussion within each of the result Chapters 3-5.

Recent research has shown that the fundamental morphologic and functional component of gravel-bed rivers is the pool/riffle unit (Parker and Peterson 1980, Church and Jones 1982, Ferguson and Werritty 1983, Thompson 1986). This usually consists of a deep pool leading onto an oblique/tranverse topographic high (riffle/bar front) characterised by rough turbulent flow through interspersed coarse bed material. In gravel-bed rivers at low flow this pool/riffle sequence is easy to recognise, though more stringent methods of objectively identifing the division between pools and riffles exist (Richards 1976a, O'Neill and

Abrahams 1984). The spacing of the pools has been found to vary systematically between 3 and 10 channel widths, but more commonly for 4 to 7 channel widths (Leopold et al. 1964, Harvey 1975, Keller and Melhorn 1978, Milne 1980).

The pool/riffle unit has a major effect on flow geometry (and therefore bedload competence and capacity) which often changes from low to high stage. As early as 1914 Gilbert observed that there may be a reversal (or cross-over) in velocity between pools and riffles as the discharge increased. This has since been used by Keller (1971) in his 'velocity reversal' hypothesis to explain the areal sorting of channel material (whereby riffles have coarser bed material than pools). Keller's (1971) hypothesis was based on the proposal (supported by limited field measurements, see 3.1) that with increasing discharge the average bottom velocity of a pool increases faster than that of a riffle until at relatively high flow the average bottom velocity of the pool exceeds that of a riffle (i.e. the 'reversal velocity'). At high flows the riffles would aggrade with coarse transported pool sediment whilst at low flow the pools would be infilled with fine sediment winnowed out of the riffles.

As the discussion in 3.1 will show since Keller's (1971) paper few field measurements have been undertaken to test the validity of his proposal (though there are many documented theoretical or hypothetical arguments for and against the velocity-reversal hypothesis). The only two sets of direct field measurements which can be found in the literature (Andrews 1979, Lisle 1979) both support Keller's (1971) hypothesis but are limited to the same river, the East Fork, which is not a true gravel-bed river but has a distinct bimodal (sand and gravel) bed size distribution (Klingeman and Emmett 1982). Furthermore previous studies have <u>assumed</u> that Keller's (1971) velocity-reversal hypothesis can be universally applied to explain bed sorting and channel changes in all river types with different flow

characteristics (for example Hirsch and Abrahams (1981), Campbell and Sidle (1985)), but Keller's (1971) hypothesis still has to be tested in channels of different patterns (including divided channels), and different magnitudes of discharge, hydraulics, bedload transport rates, and bed grain size.

The pool/riffle nonuniform geometry also influences the structure and direction of flow. Recent work in gravel-bed rivers has shown that at low flow there is a streamwise alternation of convergent accelerating flow into the pool and divergent decelerating flow onto the riffles (Church and Gilbert 1975, Ferguson and Werritty 1983, Thompson 1986). At high flows areas of flow divergence can be responsible for substantial bar aggradation as the water's depth, slope, and shear stress decreases (Hein 1974, Ferguson and Werritty 1983, Southard et al. 1984, Rundle 1985, Davoren and Mosley 1986). In contrast the convergent zones tend to be associated with deep, fast flow which can lead to extensive bed scour and bank collapse (Ferguson and Werritty 1983, Ashworth and Ferguson 1986, Davoren and Mosley 1986). The role of these convergent/divergent cycles in channel development is only just beginning to come clear. However much more data is needed relating the flow strength and direction and bedload transport to the resulting channel changes before any firm conclusions can be expected to emerge. In particular more information is required on the spatial and temporal (especially with changing discharge) variations in the convergent/divergent cycle and to establish whether there is any common behaviour for all channel types.

As Fig. 1.1 shows the vertical velocity distribution at a point determines the shear stress acting on the bed. The amount and size of sediment moving over the bed is expected to depend on this flow strength. The transport of sediment particles can be in the form of bedload and/or suspended load, depending on the size and arrangement of the bed material

particles and flow conditions. In natural conditions there is no sharp division between the two forms of transport, but usually three modes of particle motion are distinguished : (1) rolling and sliding; (2) saltation, and (3) suspended particle motion. If all other factors are assumed to be equal, when the value of the shear velocity just exceeds the critical for the particle size the particles will begin rolling and sliding or both in continuous contact with the bed. With increasing values of shear velocity the particles will move along the bed by more or less regular jumps which are called saltations. These two types of particle motion are conveniently termed bedload transport in which the successive contacts of the particles with the bed are strictly limited by the effect of gravity (Bagnold 1973).

Research on bedload movement has been ongoing since the pioneering work of Gilbert (1914) in the U.S. Most of the work has been directed towards trying to understand the threshold of sediment movement and then using this to help predict transport rates of individual size fractions and total bedload. The classic work of Shields (1936) showed that the size of a particle just competent to move was proportional to the shear stress acting on the particle. Therefore as the shear stress increased, larger and larger sizes could be transported. However, more recent work has shown that the transport of a particle is not dependent solely on its size (and weight) but the character of the bed material and its structural arrangement. Gravel-bed rivers have typically heterogeneous bed material which has tight interlocking structures and a mixture of protruding and sheltered pebbles. Thus the entrainment of any particular size fraction is dependent on a complex interaction between the flow strength and the availability of appropriate-sized sediment. The considerable research in this area is not reported on here since it closely overlaps with the results from this study reported in Chapter 4. A more comprehensive background to the development of modern sediment transport theory can be

found in 4.1.

The amount, size and frequency of bedload movement determines whether a channel alters its geometry and in turn its hydraulic properties and stability. The evolution and development of channel patterns has been studied in great detail both in the laboratory and field. Early research concentrated on describing channel development in meandering rivers with generally fine/sand alluvial bed material (e.g. Leopold and Wolman 1960, Langbein and Leopold 1966, Bluck 1971, Hooke 1975). The dominant work in this field was the classic 'sine-generated curve' of Langbein and Leopold (1966). Although their model did not tackle the problem of the development of meandering channels it did provide the first theoretical basis for understanding the meandering form. More recently work has concentrated on developing mathematical models to help simulate meander development (for example Ikeda et al. 1981, Parker et al. 1982a, Dietrich and Smith 1984, Ferguson 1984). These models together with extensive field surveys have shown that some modes of meander development are more common than others (for example Hooke (1977) reported that of 444 eroding banks on rivers in Devon 55% were either translated downstream, extended laterally, or both). Although erosion rates at a particular meander bend may fluctuate substantially (and unpredictably) from one period of years to the next it seems that most types of meander development involve some form of bank erosion complemented by point bar deposition on the inside of the bend. Often this means that the hydraulic geometry of the channel remains unchanged since the migration of the scour pool is compensated for by the growth of the point bar.

In contrast to the meandering pattern, the evolution of straight channels has received little attention in recent years. Although many flume studies begin with a straight channel the objective is often to find the critical slope or hydraulic conditions at which channel migration occurs

and few notes are taken of earlier developments (though see for example Schumm and Khan 1972 and Ashmore 1982). Field observations of straight channels are also uncommon. The best documented example is Knighton's (1974, 1977) study of straight sections on a meandering reach of the River Dean in Cheshire. He showed that since the banks were steep, any rise in discharge was accommodated almost entirely, by increased depth and velocity without leading to erosion since no point of the flow was concentrated on one bank more than the other. This observation does not seem unreasonable since the straight channel is often the form that engineers try to emulate to minimise channel scour and bank erosion.

The most active and unstable channel patterns are the low sinuosity, high gradient, and usually poorly vegetated multichannel systems of upland and proglacial areas. In Britain, extensive braiding or channel division is limited to these upland areas although the situation would have been very much different at the close of the last glaciation. Divided rivers in Britain tend to have cobble or gravel beds with wide valley floors that are not densely wooded, so that banks are weak and readily eroded. Their steep valley gradients increase the specific stream power and bed material is frequently moved creating and modifying the channel's bar system. These divided channels are often found in an overall gently sinuous pattern (Lewin and Weir 1977, Werritty and Ferguson 1980), but also confined to small shifting areas of complicated channel division (Thompson in press).

In contrast, the proglacial environment offers an abundant sediment supply which is usually reworked on a broad unconfined outwash plain. Work on these streams has shown that channel changes are frequent and bar development is complex (for example Krigström 1962, Fahnestock 1963, Smith 1974, Church and Gilbert 1975, Hein and Walker 1977). No single mode of bar development is common to any divided channel which leads to problems

of classification and description (Smith 1978, Ashmore 1982).

For many years the work of Leopold and Wolman (1957) was accepted as being the explanation for most forms of bar development in high gradient environments with non-cohesive material. From both flume and field observations they showed that during high flows a short, submerged central bar would be deposited because of differences in local competence (why this should be in the centre of the channel was not discussed by Leopold and Wolman (1957)). Gradual enlargement of this deposit by the entrapment of other particles would ultimately result in diversion of the flow, incision by the divided flow, and the exposure of a mid-channel bar. The bar itself is thus viewed as a *static* feature which may be modified by erosion or accretion as the surrounding channels migrate. More recently Hein (1974) and Hein and Walker (1977) have suggested an origin by winnowing out of fine sediments from a 'diffuse gravel sheet' of material transported along the bed and deposited in a lobate form at an avalanche face. This has been supported by further observations by Rust (1975, 1978), Cant and Walker (1978) and a similar sequence of events described by Southard et al. (1981). Ashmore (1982) using both field and flume observations disagreed with both of these explanations and put forward a model of bar development based on the accretion of a series of active lobate bars. These increased in surface area to a point where the flow over part of the bar surface became incapable of moving sediment and the flow then became concentrated on both sides of this area. Bar growth was by deposition at the avalanche face and bars in his model showed a distinct downstream fining.

The mechanisms of bar formation in divided channels are therefore complex and difficult to explain. Direct field observations to support these changes in bed morphology are not easy to obtain since they occur at high discharges, when the water is turbid, and measurement almost impossible

(Smith 1974, Hein 1974, Rust 1978). The situation is complicated further in floods due to the decrease in the degree of braiding with rising stage as channel bars are drowned, although this can be compensated for by the reactivation of previously dry abandoned channels. The behaviour of divided channels is therefore often irrational and difficult to predict and their evolution and development is not as simple to describe as the meandering, straight, and intermediate channel forms.

The interrelationships of the different components in the gravel-bed river system depicted in Fig. 1.1 vary in form and magnitude for different channel patterns. Until the past decade the convenient but rigid classification of channel patterns into straight, meandering or braided types put forward by Leopold and Wolman (1957) was still popular with fluvial geomorphologists. Each channel pattern was assumed to have its own characteristic system and a clear division for each channel type. However, more recently it has been recognised that not only do different channel patterns exist - for example the anastomosing rivers of Smith and Putnam (1980) and the wandering river type described by Church et al. (1981), but also that no strict classification exists, only a continuum controlled by hydraulic variables (Ferguson 1981, Lewin 1983).

The flow diagram in Fig. 1.1 is a useful framework to help describe the interrelationships operating in the gravel-bed system. If these interrelationships can be quantified it may be possible to model the response of the gravel-bed river to a change in any of the parameters (or links). However before a general model can be considered the system has to be tested using integrated sets of field measurements to see if the interrelationships can be distinguished in the true field situation. In addition data sets from different channel patterns must be compiled and compared to see if the gravel-bed system is a model that represents the full range of channel types.

1.4 Objectives

The previous discussion of the relationships between form, flow, and sediments in the gravel-bed system has given a brief introduction to some of the uncertainties and problems facing the engineer and environmental scientist. These are discussed in more detail in the literature reviews later in Chapters 3-5 (particularly 3.1 and 4.1). The aim of this study is to help clarify and solve some of these problems by providing information on..

(1) The influence of changing discharge on channel flow and sediment transport in the pool/riffle unit. Pool/riffle units of different channel types will be divided into four subunits; the poolhead, midpool, pooltail, and riffle and measurements taken in each subunit to see if Keller's (1971) velocity-reversal hypothesis holds true.

(2) The affect of flow conditions and bed material availability on bedload transport. Of particular interest is to determine whether the entrainment of different size fractions of the bed can be related to the measured fluid forces acting on them. The analysis will include a review and testing of the most commonly used bedload transport formulae to see which equations and reasoning are the closest to predicting the movement of gravel from heterogeneous bed material.

(3) Whether channels of different patterns change at (a) in different ways (b) at different rates. An understanding of the flow pattern and bedload movement over a range of discharges will highlight the ability of the convergent/divergent flow unit to modify the channel form.

(4) The cause-effect relationships operating in gravel-bed rivers and

indicating to what extent channel changes and bar development can be predicted/modelled from information on the flow strength and direction, bed grain size, and the rate, frequency, and sizes of bedload transport.

All the objectives will be tested in a broad range of channel patterns to see if any common relationships emerge. The results are presented with accompanying discussions in Chapters 3, 4, and 5 with a brief general discussion in 6.1.

2 METHODS

2.1 Site description

2.1.1 Rationale for river selection

The criteria for river selection was threefold. Firstly since no single channel type is representative of gravel-bed river morphology or behaviour a broad range of gravel-bed river channel patterns with different levels of activity to compare with each other were required. These different channel patterns must be located in the same area as far as is possible to reduce the number of field visits needed. Secondly the rivers selected must be in areas where there would be little risk of human disturbance either to the river or instrumentation. Finally the field sites should have easy access, especially near the study reaches to aid the carrying of heavy equipment and samples. Three rivers were selected that satisfied these conditions; the Allt Dubhaig, River Feshie and Lyngsdalselva. These rivers provided both the conventional straight, meandering, and braided channel patterns, but also the transitional forms between them to give a continuum according to sinuosity and the degree of braiding (see 1.3).

The Allt Dubhaig in the Scottish Highlands has a sharp drop in gradient along its course and therefore shows various channel patterns (of which five were chosen for intensive measurements). It also has easy access via the newly constructed A9 road and is only visited occasionally by hillwalkers. The River Feshie in the Cairngorms, Scotland, has a different channel pattern and is more active. It has detailed background information (particularly of discharge and channel changes) since 1976

readily available (R.I. Ferguson, personal communication, 1987) and is in a private estate only accessible to limited personnel. The Lyngsdalselva in Norway is highly active and therefore little time was needed to see significant changes. Again there would be no human interference with scientific equipment and a large labour force was available courtesy of the British Schools Exploring Society 1984 expedition, to help with data acquisition.

Previous gravel-bed river research, although geographically widespread, has tended to be dominated by research groups working on a particular river using their own preferred methods and analysis. The problem with such focused research is that it has been difficult to disentangle real differences between river types from apparent ones due to methodological inconsistencies. The work reported here aims to overcome this problem by using identical methods, equipment, personnel and analysis. Such standardisation was rigorously applied throughout the study period so that reliable comparisons and cross-referencing between different channel patterns could be made.

With a standardisation of data collection and three rivers with seven different selected channel patterns this study can reliably add to the current documentation of gravel-bed river behaviour.

2.1.2 Allt Dubhaig

The Allt (= river) Dubhaig is an unregulated tributary of Loch Garry at Drumochter in the Tayside Region of the Scottish Highlands. Its source is the Allt Coire Dhomhain (Grid ref. NN 602 746), which flows eastwards before sharply turning southwards to take the course of the Allt Dubhaig

(Fig. 2.1). The Allt Dubhaig drains a catchment area of 13.5 km^2 up to the gauging station, underlain dominantly by metamorphics of the Moinian assemblage. River-bed pebbles of this rock type have an average density of 2540 ± 39 kg m^{-3}. The mountainous boundaries of the catchment rise up to 975 m a.s.l., while the reaches studied follow a valley floor of between 420 and 440 m a.s.l. The river flows over glacial till and several steep undercut terraces can be observed in the headwaters, whilst the lower stages flow through hummocky moraine characteristic of this part of the Scottish Highlands. Limited sediment is provided from terrace collapse and erosion in the headwaters and the rapid drop in stream gradient downstream prevents erosion of the hummocky moraine. Several abandoned bank edges and scars show that the river has been reworking the morainic drift of the valley floor since the last major glaciation of the area during the Loch Lomond readvance (Sissons 1974).

The catchment is devoid of trees but has a full cover of grass, heather, and other short vegetation. Since the Dubhaig is located in a mountain environment, snow accumulation in the winter and snowmelt in the spring, together with the cold temperatures have a considerable affect on the discharge and behaviour of the river. During the winter months the river freezes over with up to 0.5 m of ice, so rendering the river inactive. Field observations show that this ice almost freezes to the bed surface so that any subsequent rainstorms or initial thawing of snow result in rapid over-ice flow at an unusually high bank level. During one particular storm the ice-blocked river led to almost overbank flows with very high velocities. The full impact of this behaviour needs further investigation.

During the autumn and winter following prolonged frontal rainfall, in the

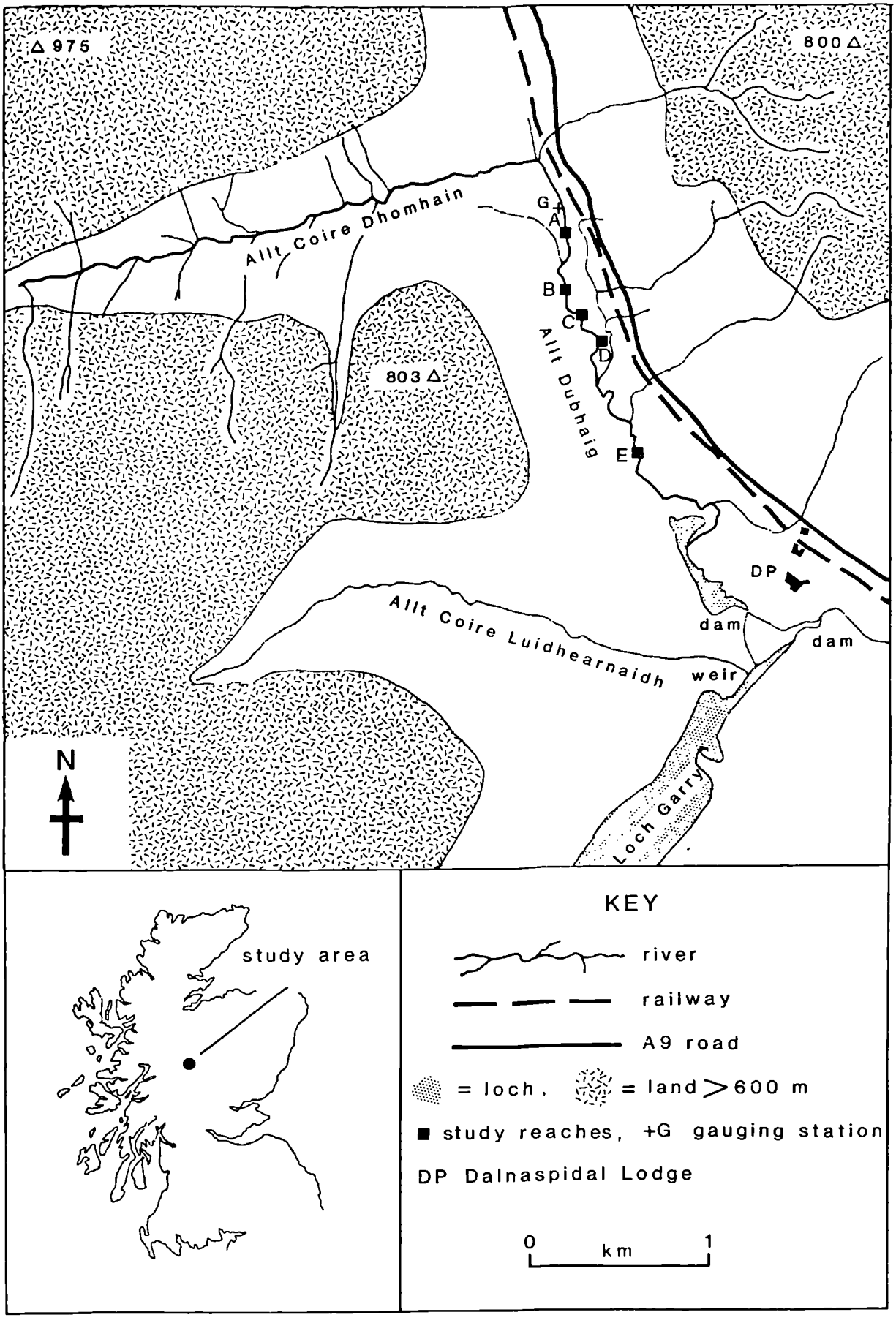

Fig. 2.1 Location of the Allt Dubhaig and the five study reaches.

spring with diurnal snowmelt peaks, and following convective storms in the summer, frequent flooding can occur (see 2.2.1). During the 27 months of observations (from October 1983 to January 1986) no consistent weather pattern emerged; the first winter was cold and had above average amounts of snow, the second winter was very cold but had little snow, while the third winter was similar to the first and had snow into late May. The summer of the first year was warm and dry but the second summer was exceptionally wet with many storms and persistent frontal rainfall.

The Dubhaig has no significant tributaries or interferences from man-made structures so the discharge downstream is constant. However there is a rapid decline in slope downstream (and therefore stream power) which results in several channel patterns of different form. These patterns were identified and five reaches termed A, B, C, D, and E, were selected for investigation (see Fig. 2.2). Their relation to slope change is shown in the longitudinal profile (Fig. 2.3) where Reach A has a slope of 0.021 dropping to 0.004 in Reach E.

For each reach a surveying network was set up to enable cross-sections to be relevelled at regular intervals, and planimetric maps to be produced (see 2.2.5). The benchmark network varied according to the channel pattern, being parallel to the channels in the cases of braided or single channels (reaches A, B, and E), but following the bank edge for curved channels (reaches C and D). Care was taken to keep the cross-sections perpendicular to the channel which involved having up to three different origins for cross-sections when the channel meandered (reaches C and D). More details concerning the surveying technique are given in 2.2.5.

The general appearance and benchmark network for the five reaches is shown

Fig. 2.2 Aerial photographs taken on 30.7.71 showing the five study reaches of the Dubhaig and the general transition from divided-meandering-straight channel pattern downstream (courtesy of B.K.S. Surveys Limited).

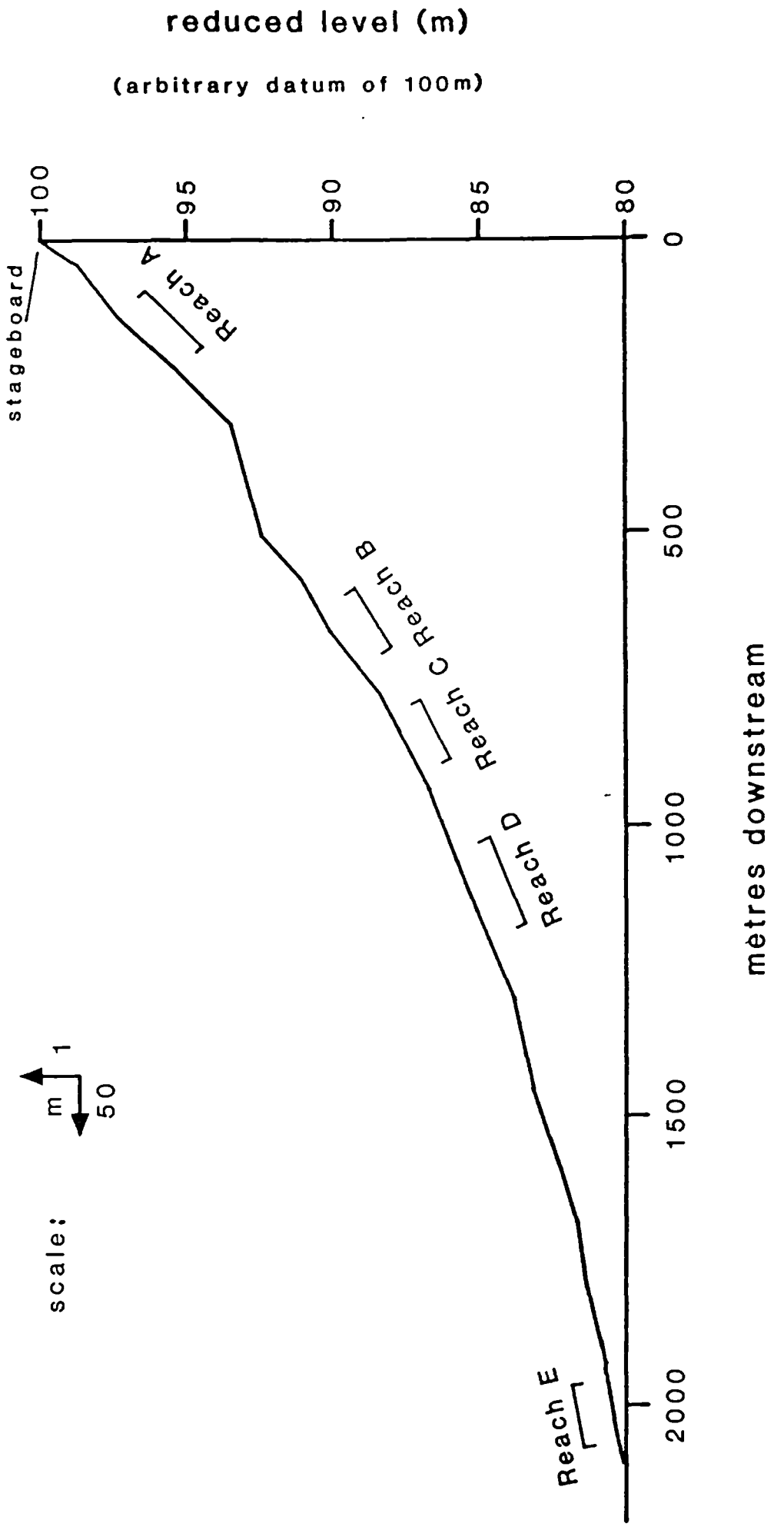

Fig. 2.3 Longitudinal profile of Allt Dubhaig from the gauging station above reach A down to reach E (closing error of 4 cm).

in Figs. 2.4a-e. All five planimetric maps were surveyed at the beginning of the research period, and subsequent changes are described in 5.2. Reach A (Fig. 2.4a) is characterised by rough turbulent flow through a poorly defined pool/riffle cycle between A1 and A3 which then diverges onto a broad riffle between A3 and A4 before flowing either side of a medial bar centred on A5. The channels both go through a pool/riffle cycle before the right hand channel plunges down a steep riffle to join the more placid left hand channel at A7. The combination of the two channels at A8 results in a return to rough turbulent flow as seen at A1. The eight cross-sections were set up at 10 m intervals and all levels were reduced to an arbitrary datum of 4 m at A1.

At a further 450 m downstream the Dubhaig becomes rather unstable and assumes a more braided pattern (Fig. 2.4b). The assorted bar formations of Reach B did not change their positions dramatically during the study period and there was no reoccupation of the relict channel which curves around the left hand side of the floodplain. The reach begins at B1 with a convergence of flow from a diagonal riffle into the talweg which runs parallel to the right bank edge. The deep pool starting here stretches down to B4 where the flow diverges onto the next riffle. Beyond B4 the flow converges through another deep pool before dividing into a complex series of convergent/divergent zones associated with the mid-channel bars between B4 and B7+. The seven cross-sections were spaced at 15 m intervals and all levels were reduced to an arbitrary datum of 3 m at B1.

Reach C is about 100 m downstream of Reach B and marks a transition from the divided channel patterns of reaches A and B, into the lower gradient and resulting meander formation of reaches C and D. Reach C has seven cross-sections which spread out radially from three benchmarks on the

(a) Dubhaig Reach A

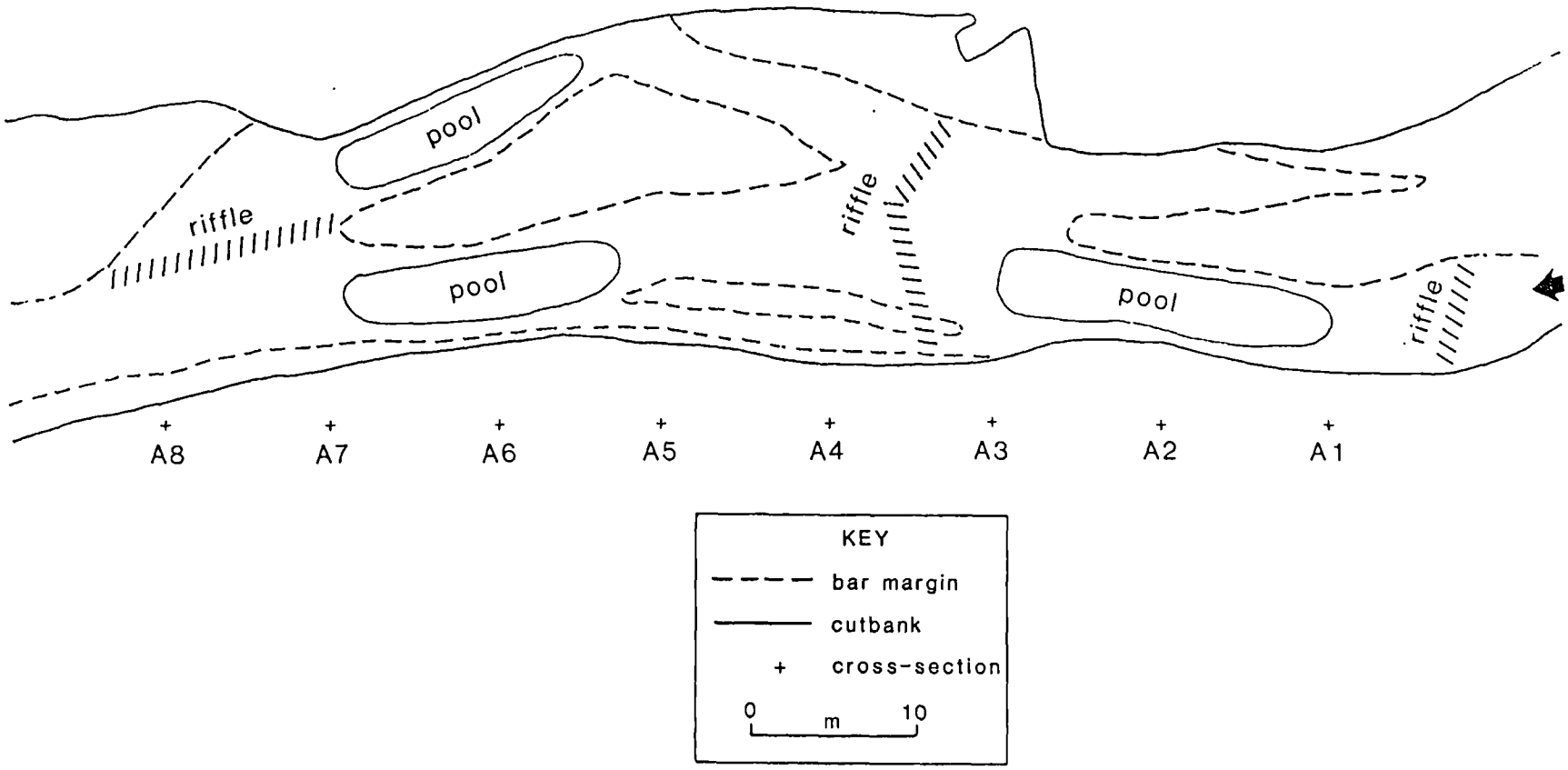

Fig. 2.4 Planimetric maps of the five study reaches surveyed between March and May 1984 together with their pool/riffle cycles and cross-section benchmarks: (a) Reach A (b) Reach B (c) Reach C (d) Reach D, and (e) Reach E.

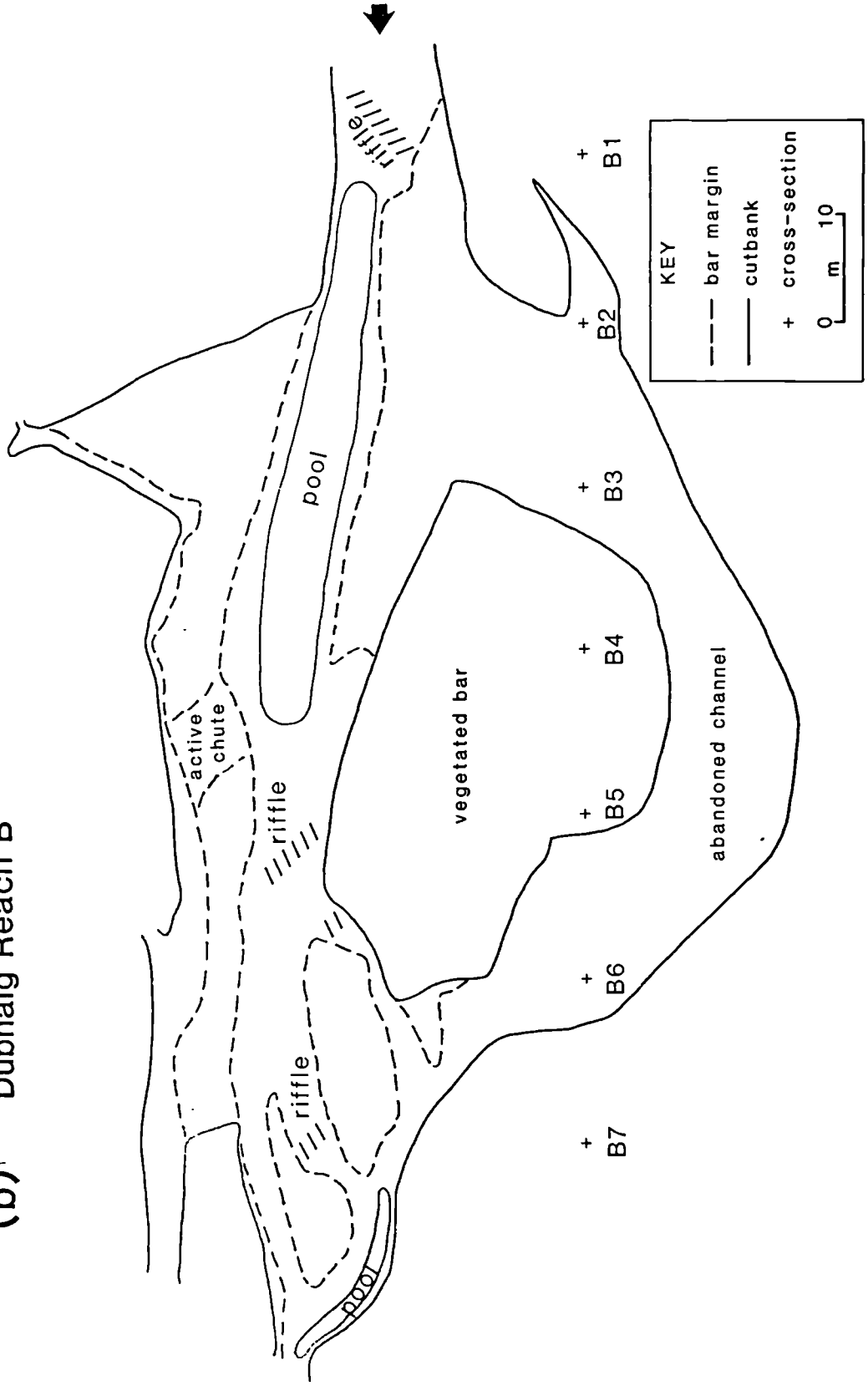
(b) Dubhaig Reach B
pool
riffle
active chute
riffle
vegetated bar
abandoned channel
pool
B1
B2
B3
B4
B5
B6
B7
KEY
bar margin
cutbank
cross-section
0 m 10

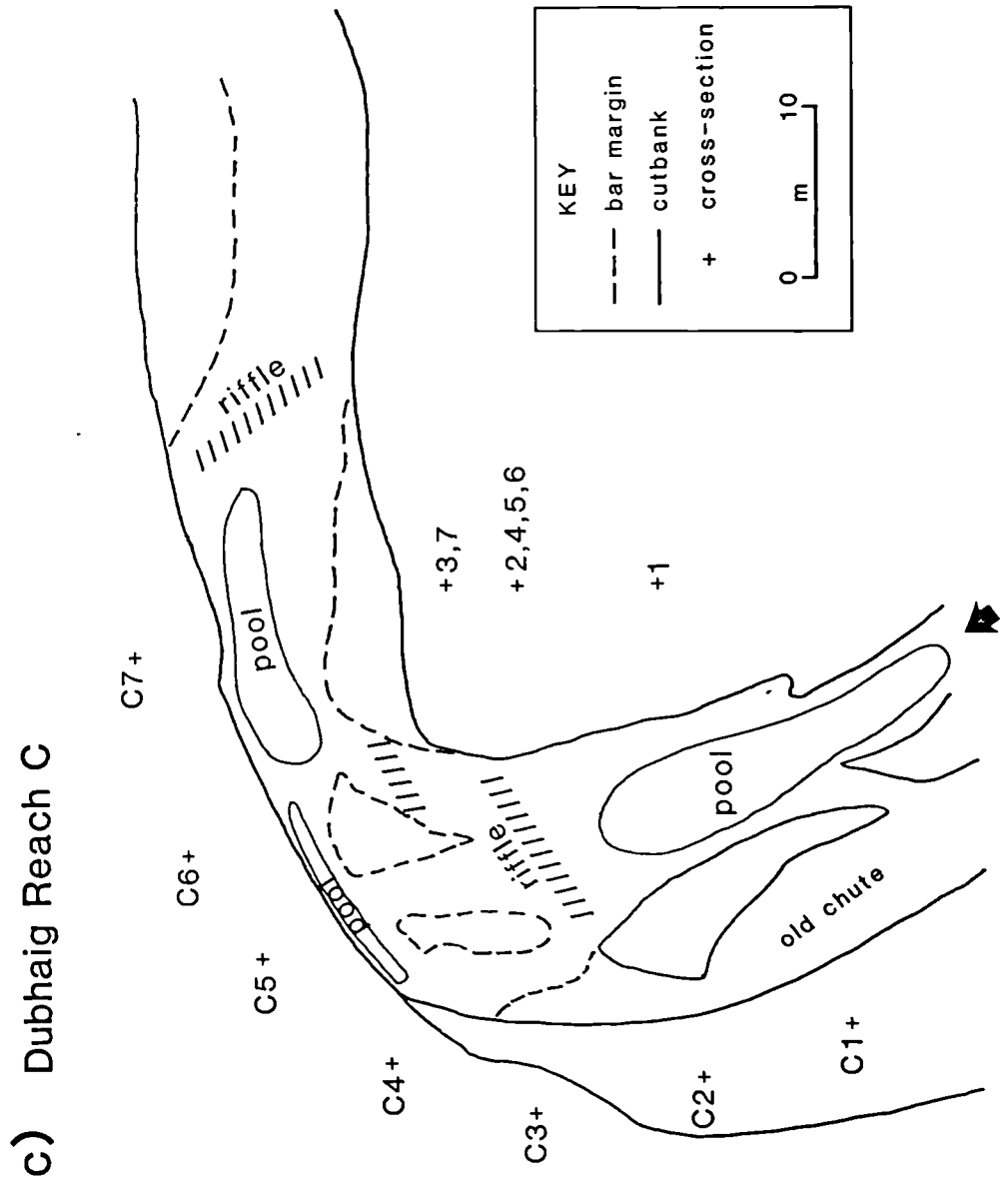
(c) Dubhaig Reach C
KEY
bar margin
cutbank
cross-section
0 m 10
riffle
pool
riffle
pool
old chute
C7+
C6+
C5+
C4+
C3+
C2+
C1+
+3,7
+2,4,5,6
+1

(d) Dubhaig Reach D

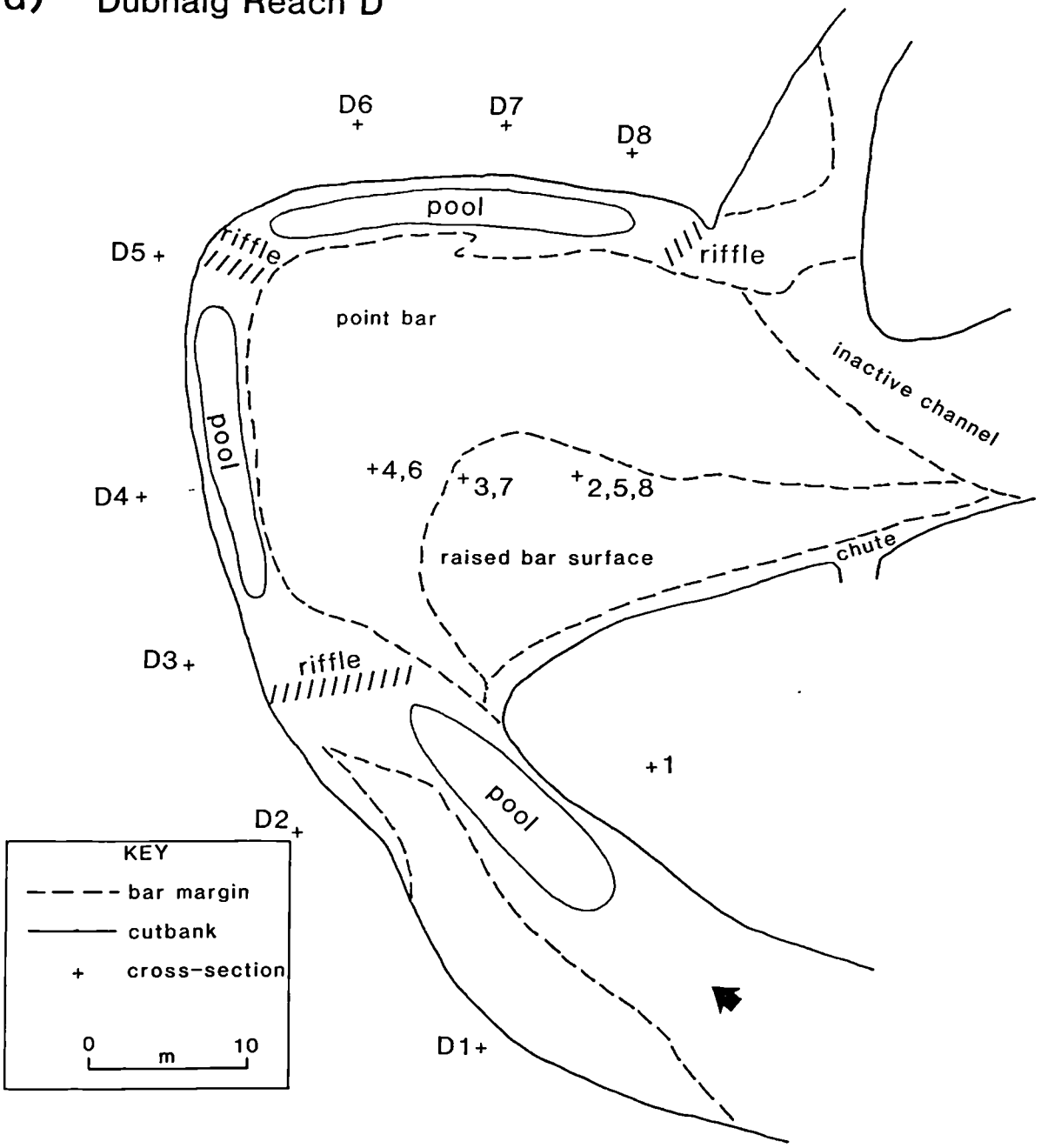

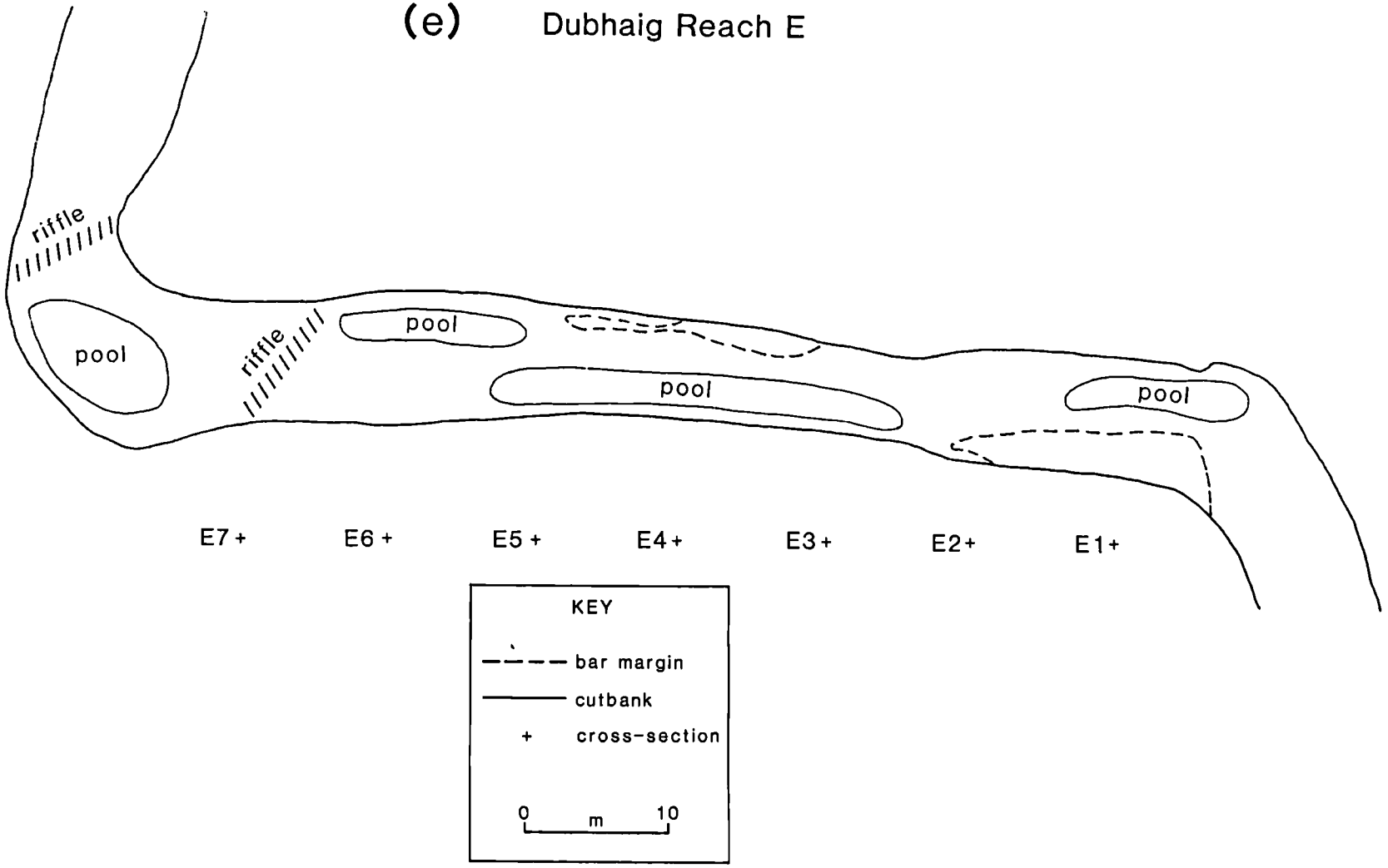
(e) Dubhaig Reach E
riffle
pool
riffle
pool
pool
pool
E7+
E6+
E5+
E4+
E3+
E2+
E1+
KEY
bar margin
cutbank
+ cross-section
0 m 10

inner vegetated point bar (Fig. 2.4c). The arbitrary datum of 3 m was chosen for the benchmark C1 to which all levels were reduced. The reach has a clear pool/riffle sequence which leads onto and around the outer remnants of the point bar. This bar is dissected and separated from the inner point bar by a fast and shallow chute. The channel then resumes its pool/riffle sequence as it diverges onto the next bar unit.

At Reach D the gradient drops sufficiently to allow the channel to develop the classic meander and point bar morphology of many lowland gravel-bed rivers. The eight cross-sections perpendicular to the channel were reduced to the arbitrary datum of 3 m at D1 (Fig. 2.4d). The general flow pattern follows pool/riffle cycles around the point bar and takes the left-hand channel beyond section D8.

Reach E is much further downstream where the very gentle gradient results in several reaches of almost straight channel separated by isolated bends. The channels are vaguely reminiscent of Smiths' (1983) anastomosing rivers with the channels having well vegetated banks with slight levees that separate the channel from backwater swampy areas. The channel has little emergent gravel even at low flow (Fig. 2.4e) and a subdued pool/riffle sequence. The flow starts from a deep pool at the head of the reach beyond E1 and then alternates from the left hand side to the right of the channel before emerging as a riffle at E7. Seven cross-sections spaced 10 m apart run parallel to the bank edge and are reduced to an arbitrary datum of 3 m at E1.

2.1.3 River Feshie

The River Feshie is a tributary of the Spey and drains the western

Cairngorm Mountains in the Scottish Highlands. Since 1976, R. I. Ferguson (Stirling University) and A. Werritty (St. Andrews University) have monitored and documented channel changes and bar development of the Feshie (Werritty and Ferguson 1980, Ferguson and Werritty 1983). A description of the Feshie's catchment can be found in Ferguson and Werritty (1983). Fig. 2.5 shows the general location of Glenfeshie and the study reach. Briefly, the Feshie drains an area of 107 km^2 up to the study reaches, mostly underlain by Moinian schists lying at 700-1000 m a.s.l., although the north-east part on the Cairngorm granite batholith rises to 1265 m (mean density of channel material is 2600 $\pm$ 6 kg m^{-3}). The basin is bisected by a deep glacial trough through which the river flows, before turning north at about 400 m a.s.l. into the wider, lower part of Glenfeshie. The lower course of the river is confined locally by bedrock and post-glacial terraces, but in three reaches it is free to migrate laterally and is actively reworking outwash gravels (Ferguson and Werritty 1983). The work reported here is concentrated on the uppermost braided reach near Glenfeshie Lodge, termed the 'tree reach' by Ferguson and Werritty (1983) (Grid ref. NN 844 926, see Fig. 2.5). Here the river has a steep gradient (averaging 0.009) and together with frequent floods, can actively rework the non-cohesive gravels.

The part of the Feshie in the tree reach was termed a "wandering gravel river" by Ferguson and Werritty (1983), whereby it has moderately divided channels which are wide and shallow, flanked and locally divided by expanses of bar gravel, but which lack the degree of channel division characteristic of many proglacial braided rivers (see Fig. 2.6). The tree reach can switch channels and create new deposition and scour zones quickly and frequently, so often rendering planimetric maps of channel position out of date. Despite major channel switching during the 31 month study period the general appearance of the tree reach as surveyed on 2/4/84 is shown in Fig. 2.7. Thw two reaches chosen for closer

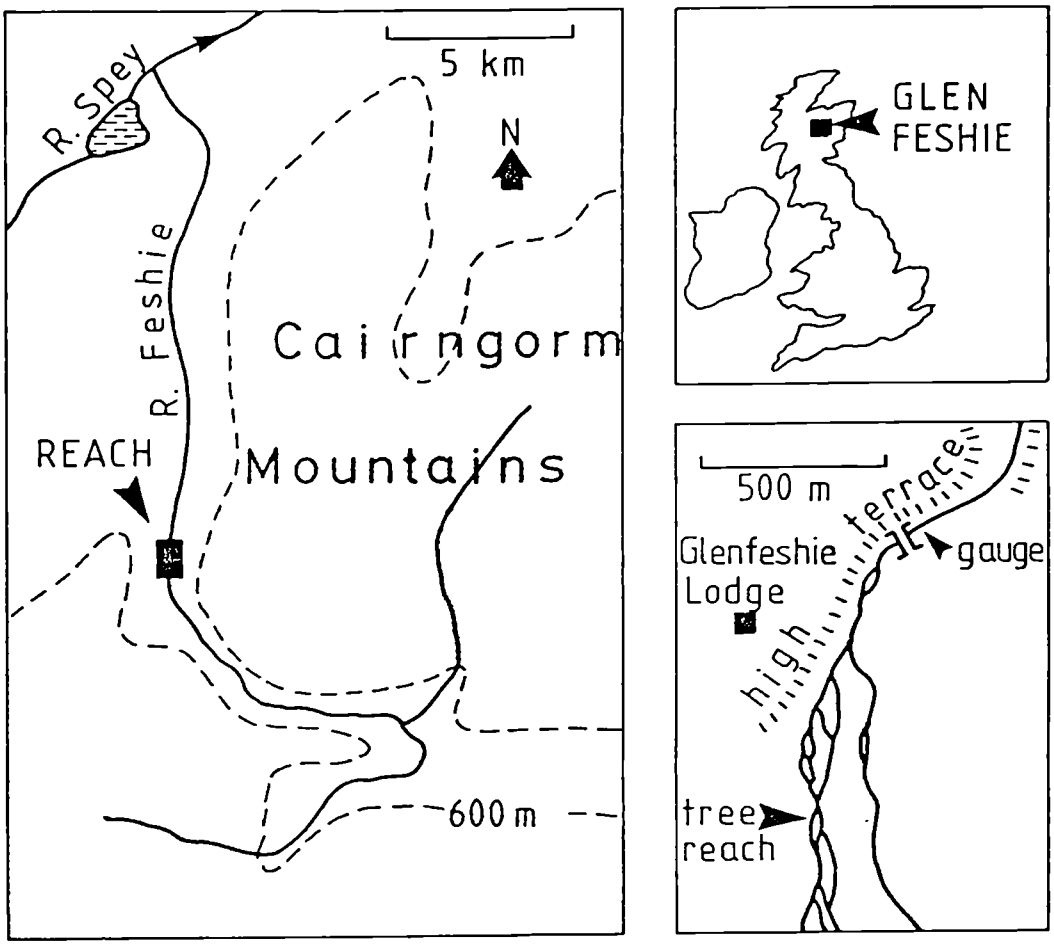

(from Ferguson and Werritty (1983))

Fig. 2.5 Location of Glenfeshie and the 'tree reach' which contains the sub-reaches studied in detail.

Fig. 2.6 Aerial photograph of the tree reach taken in August 1986 showing the locations of the two reaches reported on here and the reaches currently under investigation by Ferguson and Werritty.

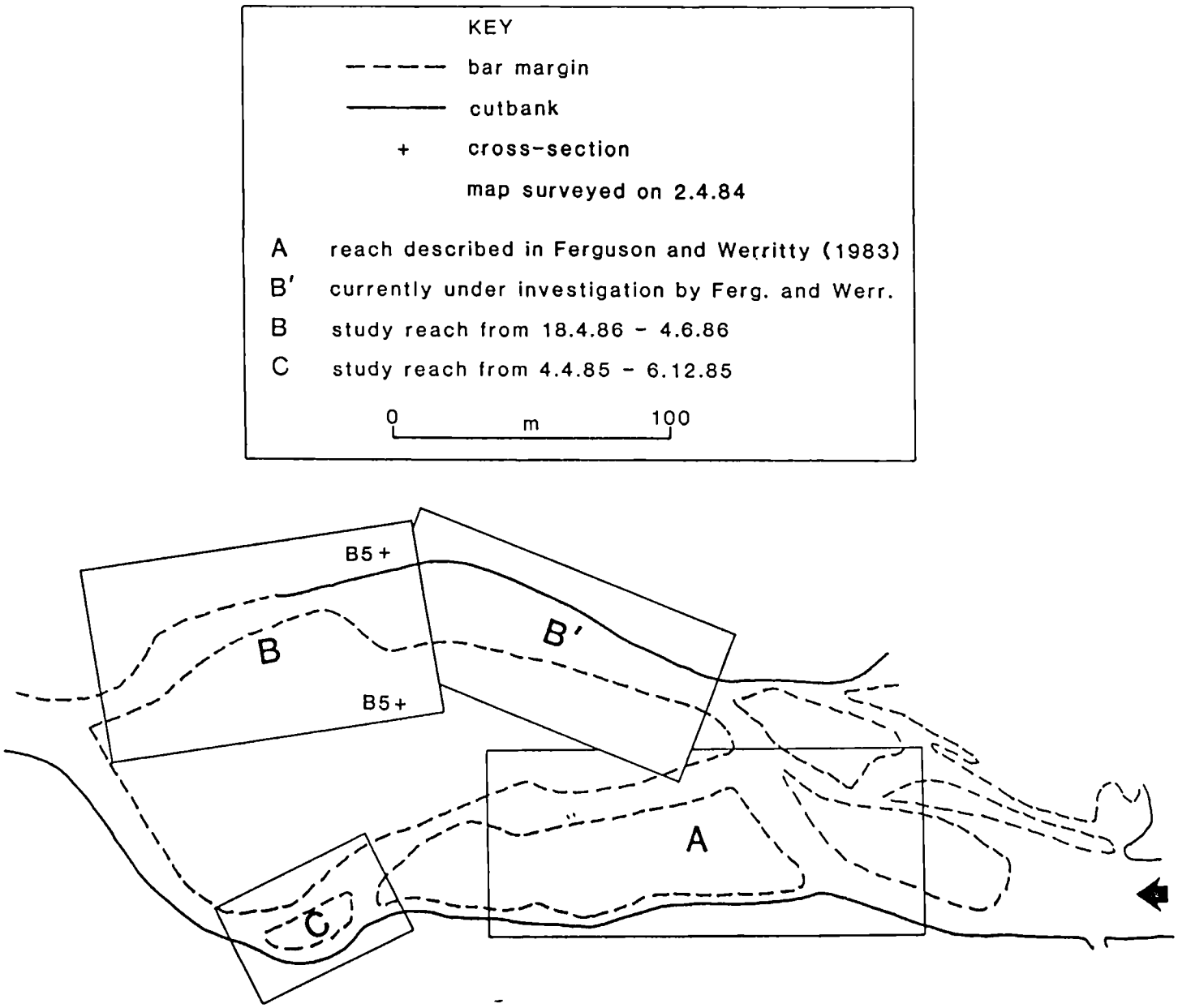

Fig. 2.7 Planimetric map of the tree reach showing the locations of the study reaches reported on here and the reaches being investigated by Ferguson and Werritty.

investigation (termed B and C) and the reach monitored since 1976 by Ferguson and Werritty (termed reach A) are superimposed on the base map in Fig. 2.7. The work reported here in reach B is only for cross-sections downstream of B5 (plotted in Fig. 2.7) although measurements of longer-term channel changes (including the four upstream cross-sections) are being taken by Ferguson and Werritty as part of a separate project.

During the measurement period the Feshie switched its position with a series of major avulsions (and blocking of channels). The channel changes in reach A for the years 1976-81 were reported by Ferguson and Werritty (1983) and the study here concentrates on reaches B and C. Reach C on the west side of the floodplain had eight cross-sections set up at approximately 10 m intervals and perpendicular to the channel. These were surveyed between 4/4/85 and 6/12/85 - the last survey quantifying the affects of an avulsion to the east side of the floodplain which left reach C abandoned and dry. The general appearance of the reach is shown in Fig. 2.8a. The head of the reach is dominated by a wide diagonal riffle with a steep avalanche face between C1 and C3 which leads into a deep scour pool following the bank edge from C1 to C5. As the flow diverges out of the pooltail at C5 it divides around the medial bar centred on C7 and then recombines to form a single arcuate channel for about 200 m downstream. The amount of flow moving through either distributary around the medial bar depends on the stage (see 5.3.2) with the right-hand channel more important than the left-hand channel at low flow and vice versa at high flow.

Reach B (Fig. 2.8b) was surveyed along the new channel's position after reach C had been abandoned. Seven cross-sections spaced approximately 15 m apart were set up perpendicular to the channel and surveyed at the beginning and end of the snowmelt season of 1986 (March to June). The cross-sections were reduced to the arbitrary datum of 3 m at a station on

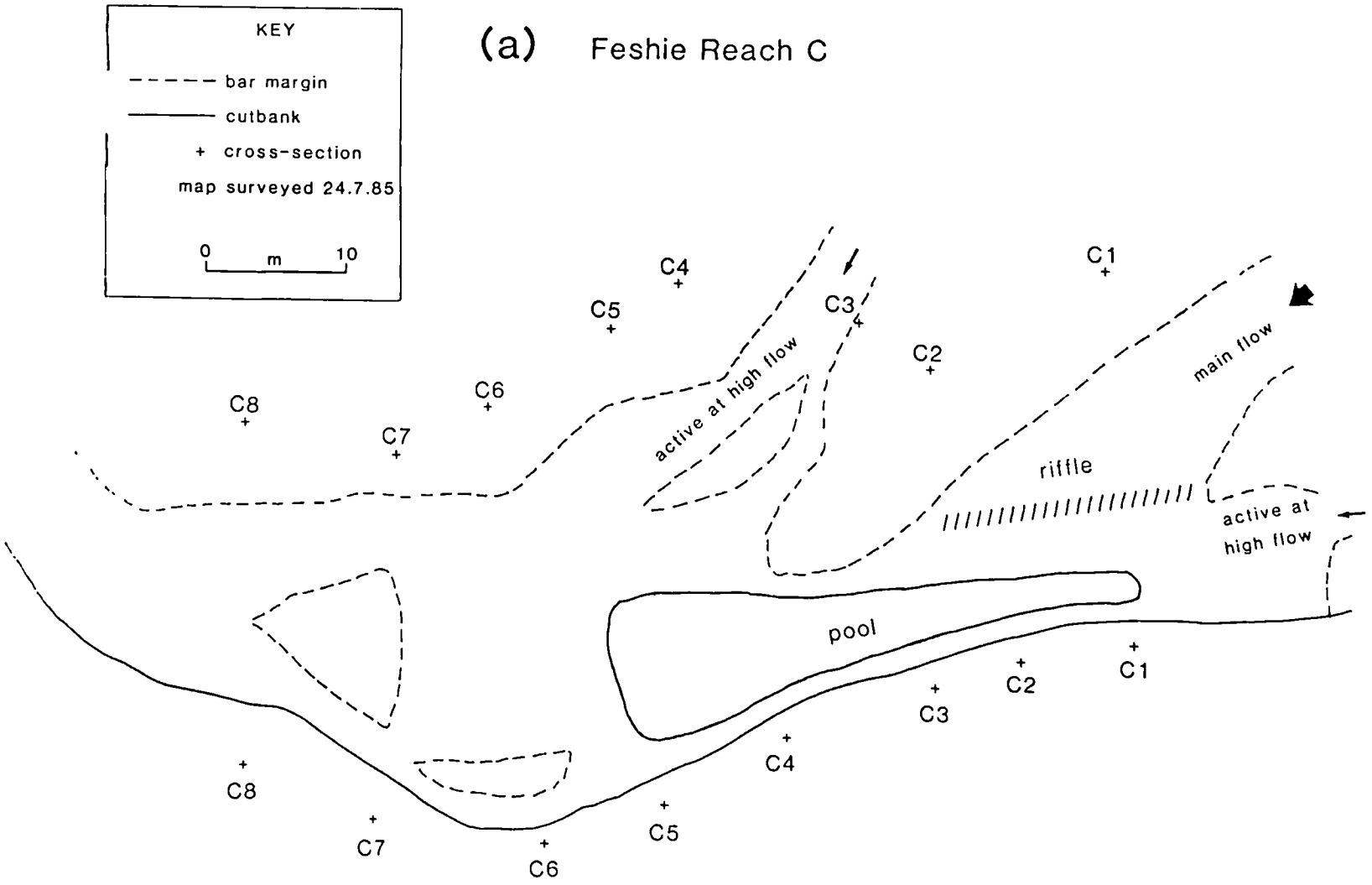

Fig. 2.8 Planimetric maps of the Feshie study reaches (a) reach C, and (b) reach B.

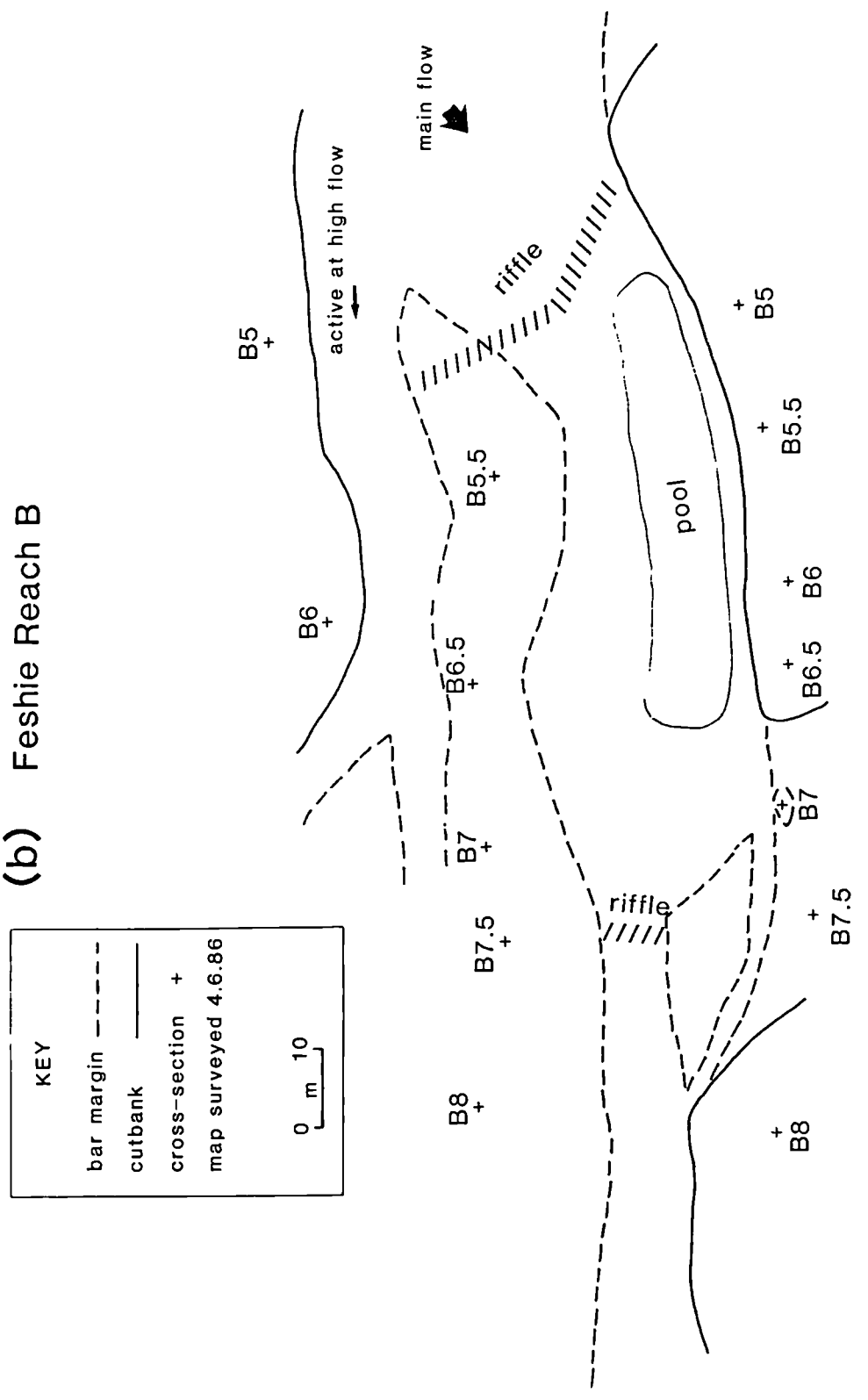
(b) Feshie Reach B
KEY
bar margin
cutbank
cross-section +
map surveyed 4.6.86
0 m 10
B5
B6
B6.5
B7
B7.5
B8
B5.5
active at high flow
main flow
riffle
pool
riffle
B5
B5.5
B6
B6.5
B7
B7.5
B8

the left bank of the floodplain originally used by Ferguson and Werritty (likewise for reach C). Reach B was very similar to reach C showing a clear pool/riffle cycle (which is one of the reasons it was chosen - see 3.1). The main flow spreads itself across the wide riffle at B5 before plunging down a steep avalanche face and into the scour pool between B5 and B6.5. At low discharges the flow diverges out of the pooltail and then converges from B6.5 onwards to run down a steep narrow riffle centred on B7.5. This single channel leads onto the next bar system 70 m downstream.

2.1.4 Lyngsdalselva

The Lyngsdalselva (elva = river) flows into the Lyngen Fjord 320 km north of the Arctic Circle in Norway (Fig. 2.9). The catchment of 22.8 km^2 above the study area is bordered by mountains rising up to 1830 m a.s.l., while the river flows along a valley floor at about 200 a.s.l. With most of the catchment area being of such high terrain, most of the precipitation falls as snow and accumulates on the mountains and glaciers. The work reported here was conducted in the summer months of July and August 1984 during which snow still fell on the mountains, but melting during hot, sunny days and intense rainfall events could lead to rapid runoff over the compact and impermeable ice and rocks. Near sea level on the valley floor however, no snow fell during the five weeks of work and temperatures always remained above freezing.

The river is fed by several corrie glaciers and two valley glaciers, the latter partly nourished by icecaps on the highest mountains in Arctic Norway. The glaciers have been retreating for a century, exposing an abundant supply of sediment of all sizes with very little vegetation cover. Bedrock is mainly iron-rich gabbros with some dunite (mean density of channel bed material was relatively high at 3093 $\pm$ 34 kg m^{-3}). As

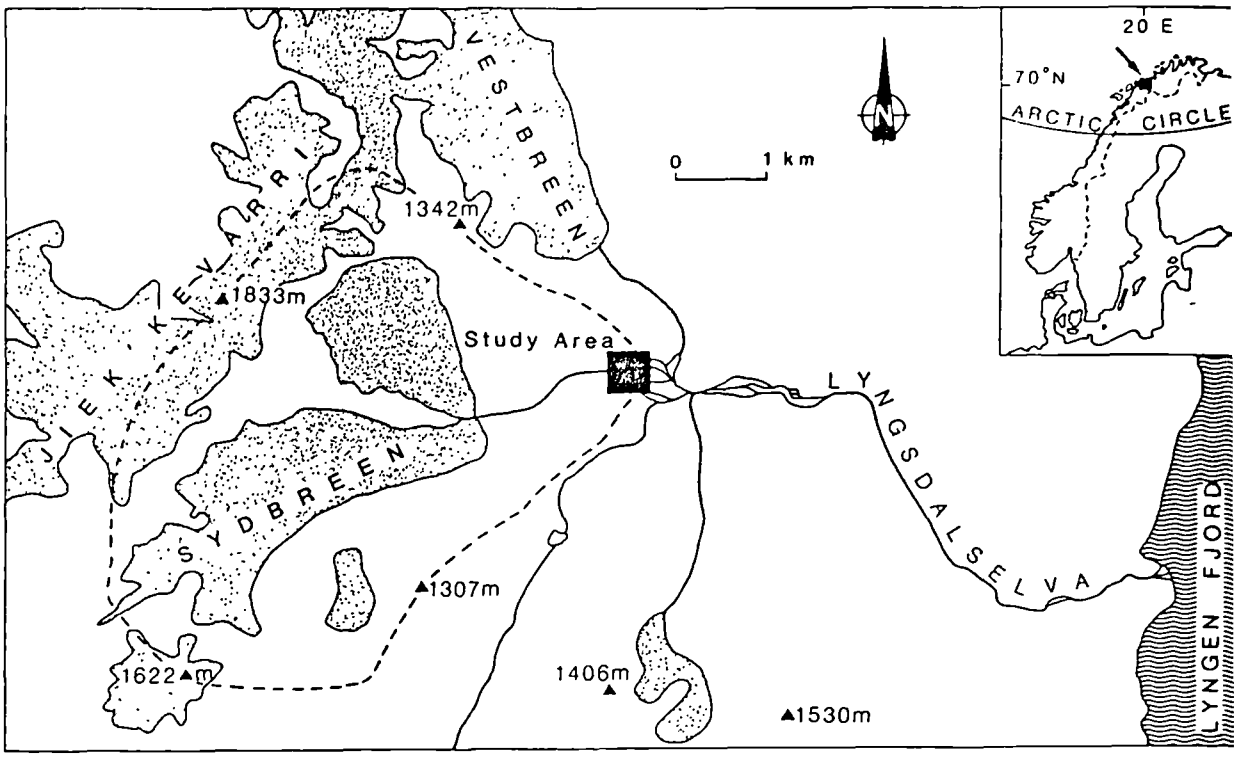

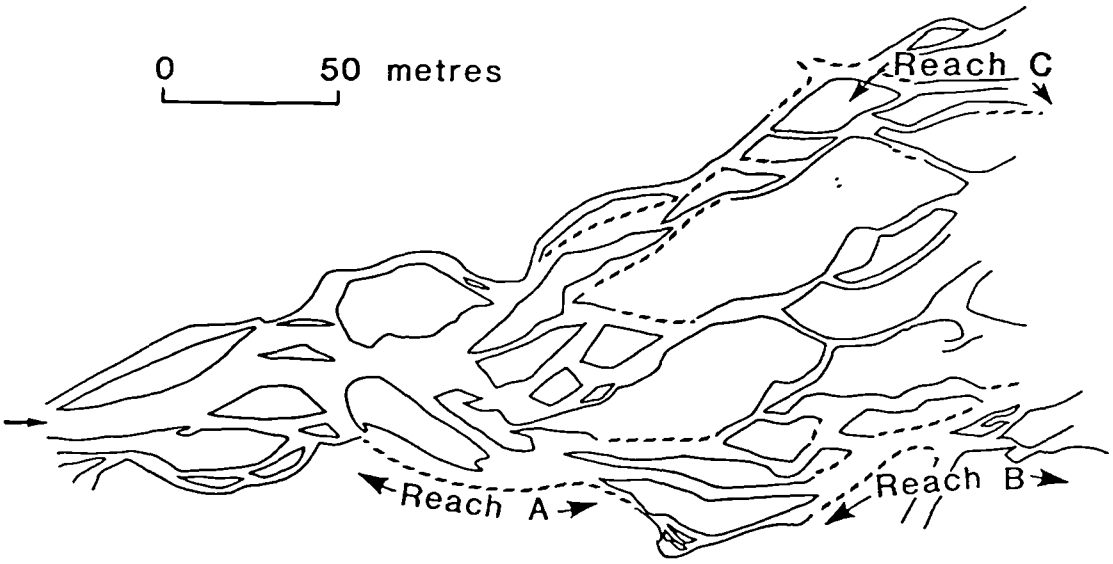

Fig. 2.9 Location of the Lyngen Peninsula and study reaches.

expected in a proglacial environment, high concentrations of fine suspended sediment were present throughout the study period.

For the first 1.5 km of its course from the Sydbreen glacier snout (Fig. 2.10) the river traverses recently deglaciated bedrock and coarse till in a generally single channel of mean gradient 0.059. It then abruptly splits into several channels, the gradient drops to about 0.025, and the channel becomes braided on a classic outwash plain that extends 2 km downstream. These channels then recombine into a single torrent as the river cuts its way through bedrock on its way to the Lyngen Fjord.

Three reaches of the braided section were chosen for intensive study, termed A, B, and C. Reaches A and B were monitored from 24 July to 10 August, but after being abandoned during a major flood and avulsion on 7 August, work concentrated on Reach C of the new main channel, on the opposite side of the floodplain.

Reaches A and B (Figs. 2.11a-b) each had 12 benchmarks set perpendicular to the channel and reduced to an arbitrary datum of 2.0 m at section A12. Reach A was dominated by a medial bar which provided a single-divided-single channel cycle (mean gradient 0.022), as compared to Reach B which was essentially a single channel (though with some low relief mid-channel bars) bordered by freshly trimmed avalanche fronts and bank edges (mean gradient 0.028). Reach C (mean slope 0.024) on the northern margin of the braided area had seven cross-sections set perpendicular to the channel (Fig. 2.11c). The head of the reach had a brief splitting of the channel around a small medial bar, but then followed a straight course before diverging onto the next bar system near C7.

All three reaches are part of the classic proglacial meltwater river

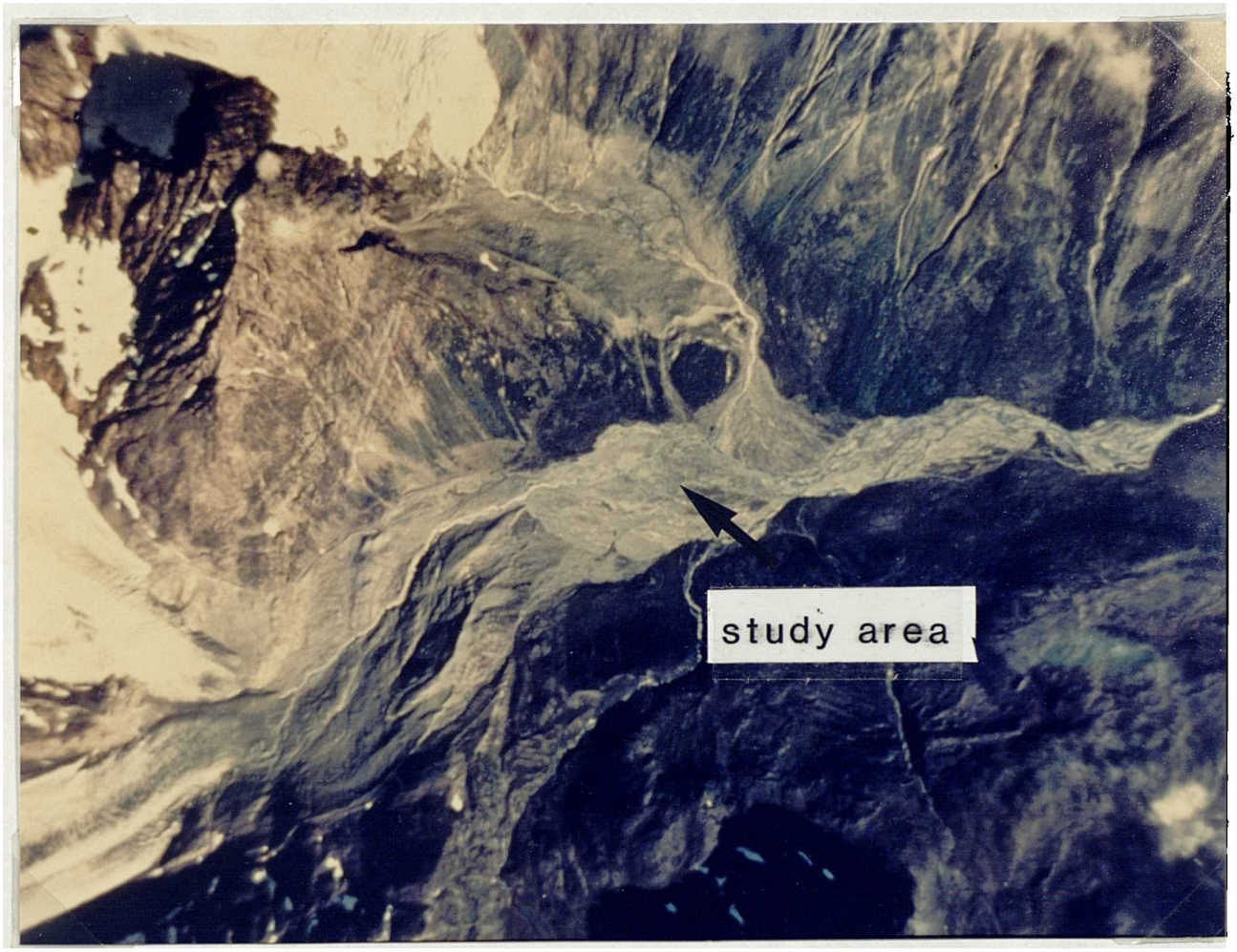

Fig. 2.10 Aerial photograph of the Lyngsdalselva taken on 18.8.77 (photo courtesy of F.W.A.S., Norway). Note the retreat of the glacier in Fig. 2.9 since 1977.

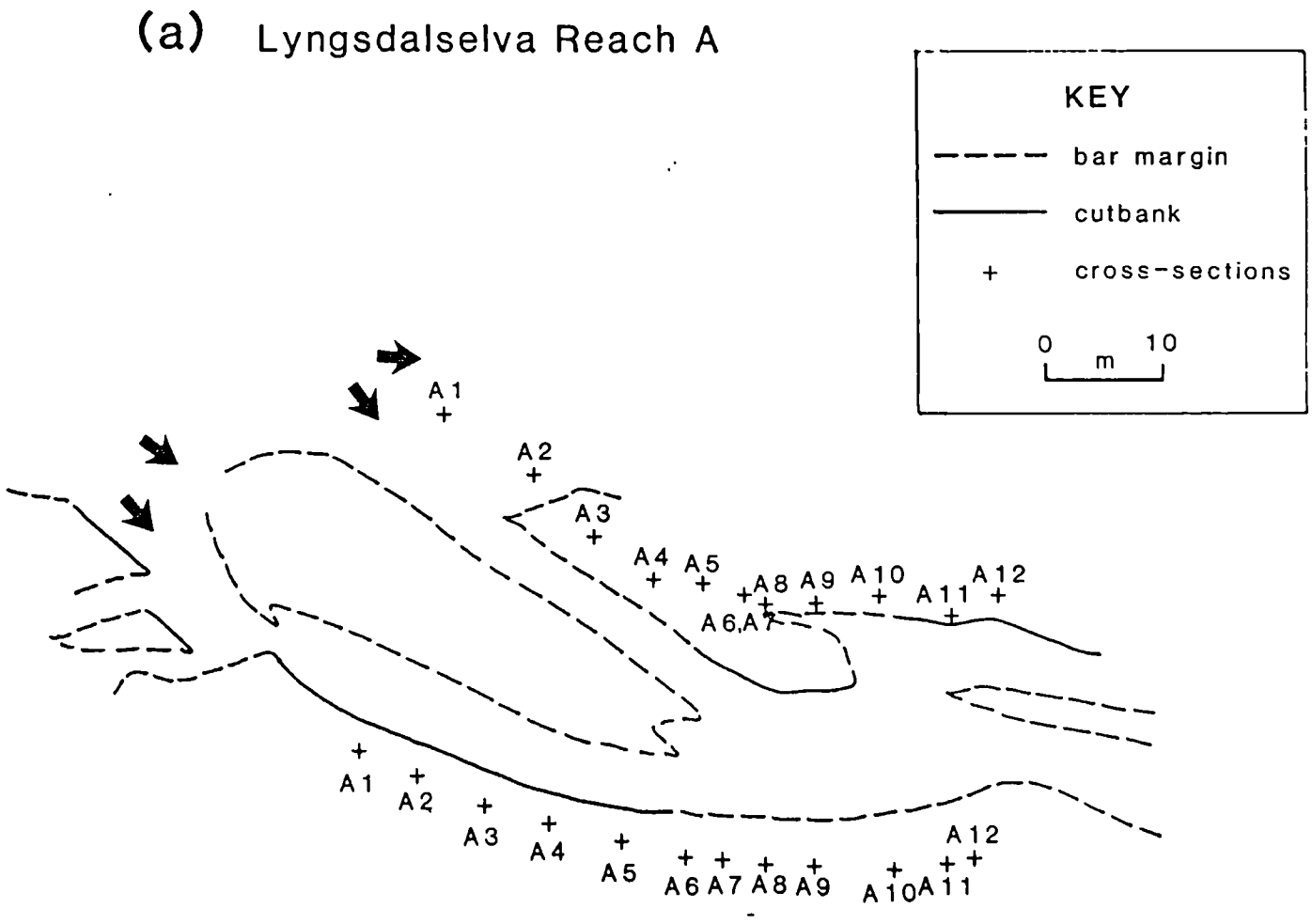

Fig. 2.11 Planimetric maps of the Lyngsdalselva study reaches (a) reach A surveyed 29.7.84 (b) reach B surveyed 29.7.84, and (c) reach C surveyed 9.8.84.

(b) Lyngsdalselva Reach B

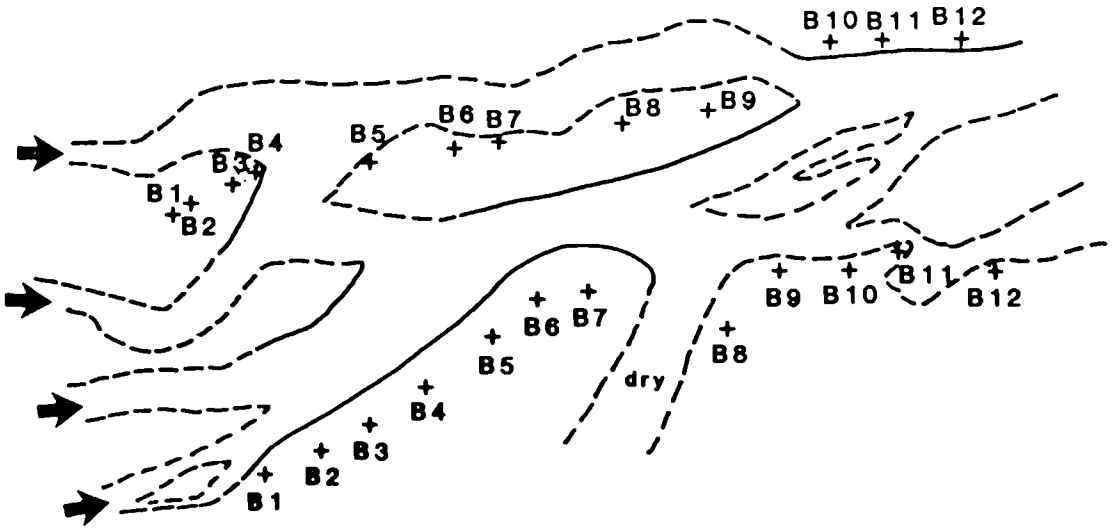

(c) Lyngsdalselva Reach C

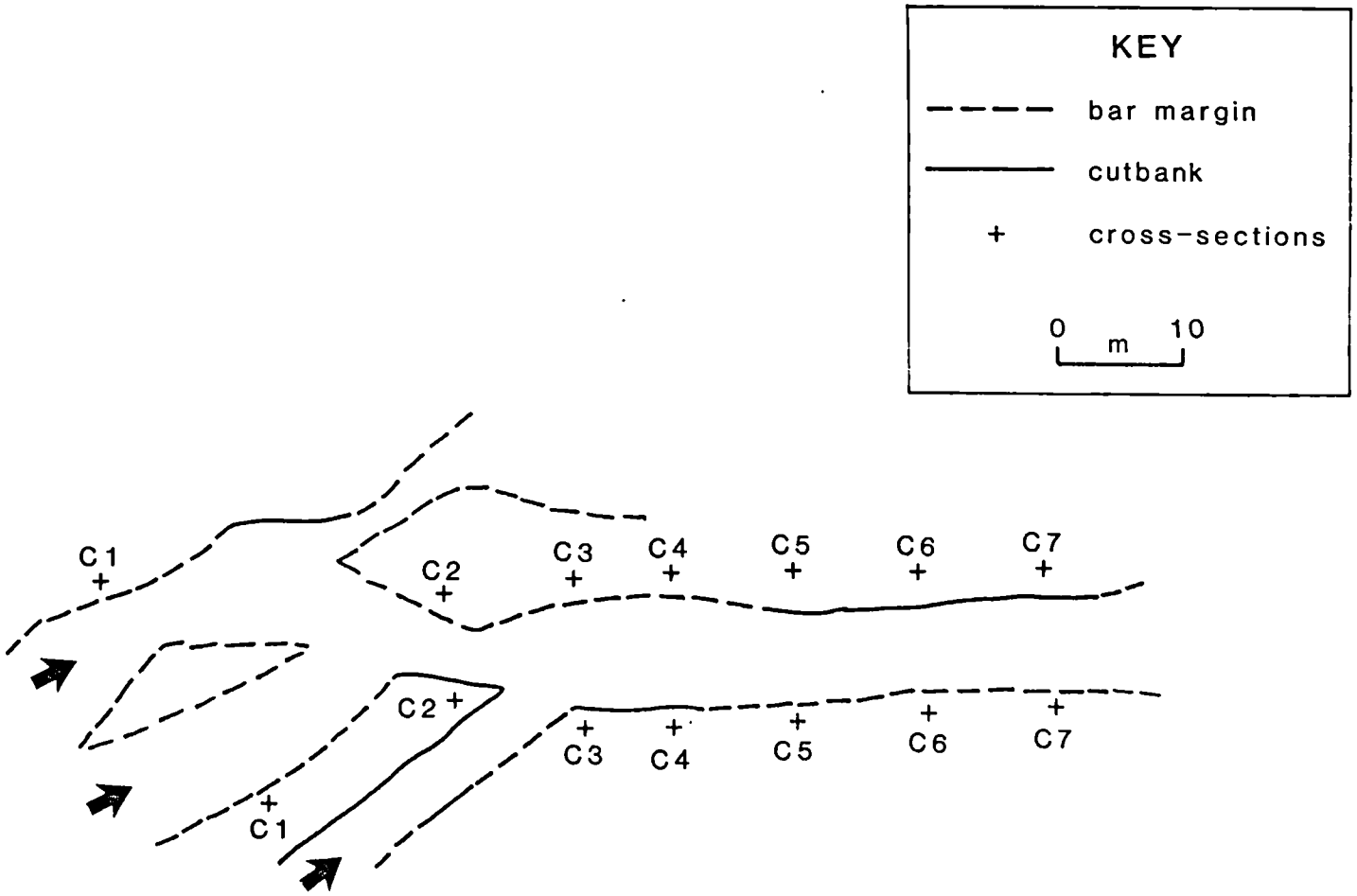

environment with the characteristic abundant supply of coarse and fine sediment, a broad valley floor of reworked sediments, multiple channels and a hydrological regime giving prolonged competent flows which enable significant quantities of material to be moved. Although this river pattern is highly braided it provides an interesting comparison to a few Scottish and Welsh rivers braided today, but also to many British rivers that must have been braided in the closing stages of the last glaciation.

2.2 Field Measurement Techniques

2.2.1 Discharge

Various methods and instruments can be used to measure the discharge of rivers and the eventual choice of the method is dependent both on the type of river to be gauged and the accuracy required for the study. In the case of the three rivers studied, three independent techniques were used to log water fluctuations and corresponding changes in discharge. The discharge figures were not used in direct hydraulic calculations for any of the three rivers, but an indication of discharge was needed during measurements and sampling. The methods used therefore reflected these needs together with being suitable for the respective river pattern.

The Dubhaig above Reach A has a single channel, steep vegetated bank and coarse boulder edges, and is no more than 10 m wide at bankfull. With no tributaries downstream and a stable channel with bedrock occasionally protruding on the channel floor, a site 68 m upstream of Reach A was chosen for a gauging section. The gaugings of discharge using a current meter at 0.2 and 0.8 depth were linked to changes in water level by a stageboard and a Bell and Howell pressure transducer connected to a Grant Squirrel data logger, situated a further 52 m upstream. No stilling well was used but the transducer was fitted in a sheltered area and had an

electronic high frequency filter to stabilise the output. The logger can record changes in water level to a resolution of 3 mm up to a maximum water depth above the pressure transducer of 0.75 m (far greater than the banktop height). Batteries linked in series provide power to keep the logger running for 30 days. Recordings were taken at 30 minute intervals, and with a linear calibration of millivolt readings on the logger to water level readings off the stageboard, a rating curve was constructed. Although the logger system was not installed and working until 15/3/85, previous current metering enabled a rating curve to be set up from 23 gaugings (which included gaugings after installation to check the rating curve was not changing). Current metering was undertaken at stage heights (H) varying between 15 cm (14/6/84) and 50 cm (29/11/84) with respective discharges (Q) of 0.19 and 4.8 $m^3 s^{-1}$. No correction factor was required to the stageboard heights and the equation

$$Q = 10^{-4.03}.H^{2.77}$$

was fitted to the relationship with a standard error of estimate (s) of +14%, -13%. Bankfull discharge is estimated at 6 $m^3 s^{-1}$ (almost constant for all reaches) and the highest recorded discharge was 9.3 $m^3 s^{-1}$ on 3/12/85. The pressure transducer/Squirrel logger system proved to be very reliable despite extreme temperatures and a large variation in water levels.

The flow duration curve (Fig. 2.12) for data between 5/3/85 and 13/12/85 (before the channel froze again) shows that the estimated bankfull discharge was exceeded for a total of 0.3% of the record (which represents 21 hours during nine separate floods). The mean discharge for the 10 months of data was 0.93 $m^3 s^{-1}$ which was exceeded 31% of the time.

A record of stage on the Feshie has been kept by Ferguson and Werritty

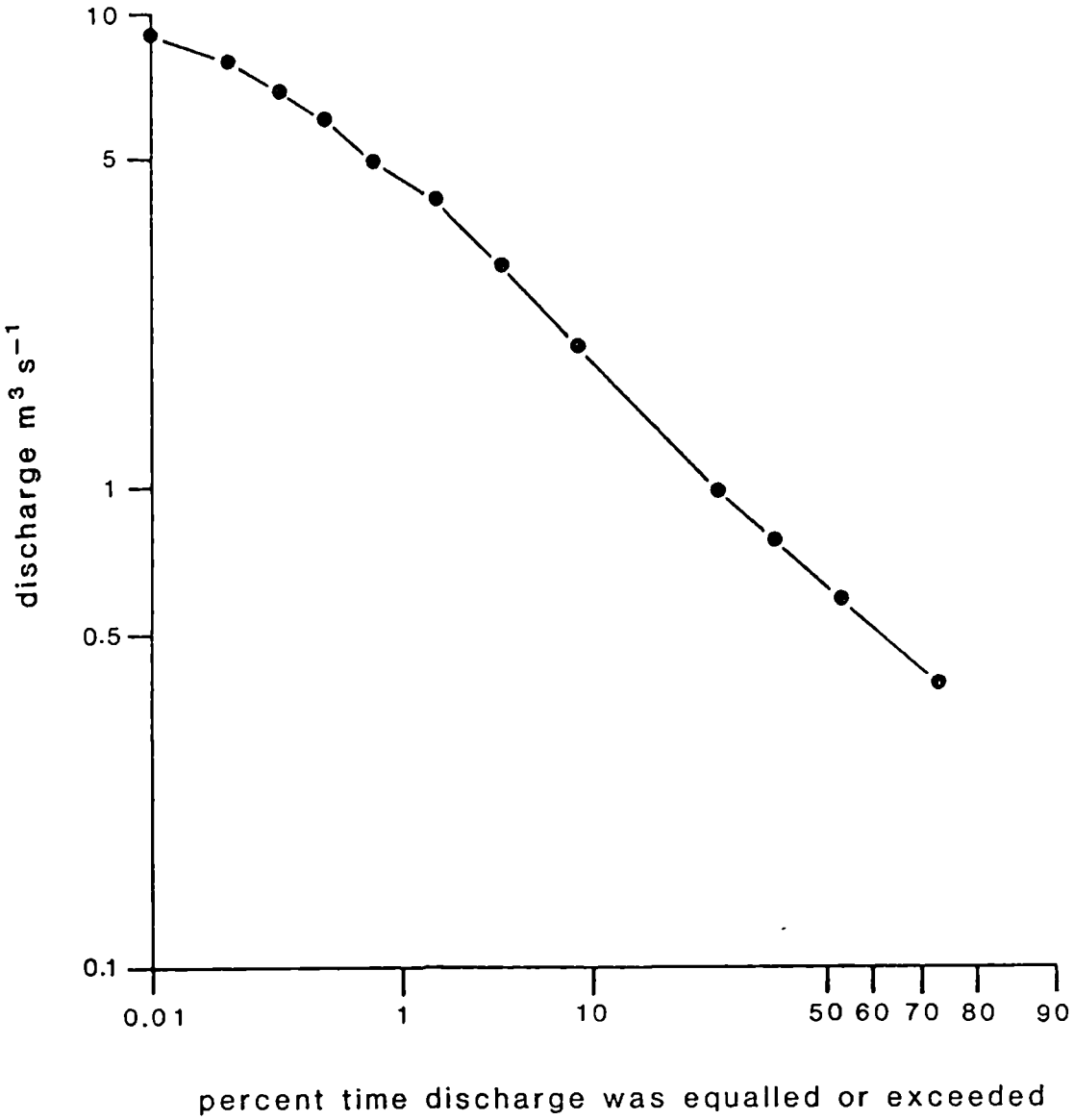

Fig. 2.12 Flow duration curve for Allt Dubhaig from 0.5 hourly discharge data between 15.3.85 and 13.12.85.

since 1978. An autographic water level recorder was installed at a partly confined section 1.1 km down from the Tree Reach (see Fig. 2.5). A well defined rating curve was set up in 1978-1981 by current metering discharges up to 20 $m^3 s^{-1}$ from an adjacent bridge. However, following a large flood in September 1981 the rating curve changed and so work during the study period concentrated on re-establishing a new rating curve by additional gaugings. By an iterative process minimising the standard error of estimate, the best fit correction factor to the stageboard height (H, in cm) was applied and the resulting new rating curve had an equation of

$$Q = 10^{-2.95}.(H + 32)^{2.17} \quad \text{with } s = +13\%, -12\%$$

The new rating curve was regularly checked by gaugings ranging from 1 to 25 $m^3 s^{-1}$. Ferguson and Werritty (1983) report that the bankfull discharge is estimated to be between 20 and 30 $m^3 s^{-1}$ and records from 1978 to 1981 show that three floods exceeded 100 $m^3 s^{-1}$ and 51 floods exceeded 20 $m^3 s^{-1}$. During the 31 month study period up to 2/5/86, 31 floods exceeded 20 $m^3 s^{-1}$ with the largest recorded flood estimated to be about 69 $m^3 s^{-1}$ on 23/9/84.

The record of discharge was not complete during the study period due to instrument failure, and two periods of information were lost from November 1983 to April 1984 and from October 1985 to early January 1986. During these times several overbank floods occurred. By comparison with the hydrological records of nearby rivers, the snowmelt season of 1984 seemed particularly significant with many high flows following a marked diurnal cycle. During the winter of 1985/6 (when reach C was being monitored) an overbank flow occurred which left a clearly defined trash line near the gauging station. By surveying the height of the trash line compared to the stageboard the flood's magnitude was calculated as 89 $m^3 s^{-1}$. In

January 1986 the chart recorder was replaced by a more reliable pressure transducer/logger set up identical to that installed in the Dubhaig.

As described in 2.1.4, the Lyngsdalselva study area was located on a braided section of the outwash plain downstream of a steeper single channel. A temporary stageboard was fixed to a large boulder in the single channel and the stage was recorded visually at the beginning and end of the day but more regularly during obvious changes in discharge and stage related hydraulic measurements. Discharges were estimated using an approximate rating curve fitted to 12 gaugings by the salt dilution method over stage heights (H) from -2 cm to 29 cm. This defined a rating curve of

$$Q = 10^{-2.98}.(H + 30)^{2.13} \quad \text{with } s = +18\%, -15\%$$

The rough bed and hazardous wading conditions prevented current metering of the gauging section, but gaugings of several of the main channels were undertaken as a check on the salt dilution method. Background information on rainfall and air temperature was collected at a station alongside the braidplain.

The discharge varied with weather conditions in expected ways. It varied little from about 4 $m^3 s^{-1}$ in the generally dull but dry weather of late July when temperatures rarely exceeded 18° C. More pronounced diurnal peaks, from about 5 to 7 $m^3 s^{-1}$, occurred in the sunnier conditions of early August when glacier melting accelerated with maximum temperatures approaching 25° C. The flow was highest of all, peaking at 8.1 $m^3 s^{-1}$, on the night of the 7-8 August following 7 mm of rain in a 90 minute thunderstorm at the end of a hot day with high meltwater discharge. Thereafter the discharge progressively dropped as the temperatures fell (a mean daily maximum of 11° C for the next 21 days), glacier melting

virtually ceased, and rainfall was replaced in most of the drainage basin by snowfall not contributing immediately to runoff. The lowest flow recorded was a discharge of about 1 $m^3 s^{-1}$ on 29 August at the end of the study period.

2.2.2 Velocity and shear stress

Shear stress (drag force per square metre of bed) and velocity were measured using a modified Braystoke current meter system with four 5 cm diameter impellers on a single wading rod connected to a multichannel revolution counter controlled by a 30 second timer (see Fig. 2.13). The use of four impellers on one rod reduces the time needed for each profile and ensures an accurate spacing of measurements at exactly the same lateral and longitudinal position. The logarithmic profile commonly known as the "Karman-Prandtl law of the wall" (cf. Yalin 1972)

$$u/u_* = 1/\kappa . \ln(z/z_0)$$

(where u is the time-averaged longitudinal velocity measured at height z above the bed and κ is von Karman's constant, taken as 0.40) was fitted by least squares allowing the bed shear stress $\tau = \rho u_*^2$ (ρ being the water density and u_* the friction velocity) to be estimated from the slope of the line. The equations of Wilkinson (1984) were used to calculate the standard error of each estimate of shear stress where the standard error of the gradient of the fitted logarithmic profile, Sm, is given by

$$Sm = \frac{1}{\sqrt{(n-2)}} . \frac{\sigma y \sqrt{(1-r^2)}}{\sigma x}$$

where σx = standard deviation of the x data values (velocity), σy = standard deviation of the y values (log height), r = the correlation coefficient between the x and y data values and n = the number of current

Fig. 2.13 The Braystoke current meter array and multichannel counter used to measure velocity profiles to estimate bed shear stress. Note: in use the current meter propellers would be more closely spaced at the bottom of the shaft.

meter impellers. The standard error for the shear stress estimate, $S\tau$, is then given by

$$S\tau = 2 u_* \rho K Sm$$

The vertically-averaged mean velocity (v) at each site was estimated by integrating the fitted profile up to the full water depth, which is equivalent to measuring velocity at 0.63 depth. Stream power per unit bed area can then be calculated as the product τv and, like τ and v, refers to a point rather than a cross-sectional average. This is an important distinction since most previous studies reported in the literature have relied upon a cross-sectional or reach average value for shear stress. This is conventionally calculated using the Du Boys equation

$$\tau = \rho g R S$$

(where τ is the bed average shear stress, g is the acceleration due to gravity, R the hydraulic radius and S the water surface slope). This relies on cross-sectional or reach average values for R and S when clearly they vary on a local scale according to the bed geometry and spacing of pools and riffles, bar structures and so on. If conditions are too hazardous to current meter or the magnitude of peak flood discharge is being estimated from trash lines, then the Du Boys method of estimating shear stress is the only option open. However, in the case of the work reported here the competence of the river was usually represented as a point instantaneous value, reflecting the maximum ability of the flow to entrain sediment at a specified point. This could then be related to at-a-point estimations of bedload transport.

Using velocity profiles to obtain measurements of shear stress is not necessarily trouble free. Indeed this method has seldom been adopted in

gravel-bed rivers (see for example Hein (1974), Bathurst et al. (1979), Southard and Middleton (1985)). Two major difficulties are encountered when velocity profiling in gravel-bed rivers with coarse heterogeneous bed material. Firstly, the current meter shaft must be placed on the 'assumed' (see later) bed and avoid being perched on, or hiding in the wake of, larger particles. This was left to the discretion of the person holding the current meter array, who would spend a few moments 'feeling' the bed surface before an appropriate position for measurement was chosen. Clearly this is crucial for shear stress estimations since misplacement would lead to anomalously low or high velocity gradients.

Following from this is the difficulty in defining the true zero height for velocity profiling. As shown earlier, the shear stress was measured assuming z to be the height of velocity measurement above the bed. However as Fig. 2.14 shows, in coarse bed material there is usually significant intergravel flow beneath the current meter base, and therefore a problem concerned with selecting a bed surface or horizontal zero plane that represents the surface of the bed to which all impeller heights are relative. As Fig. 2.14 shows, in the case of z_1' the height of the impeller should not be taken as the height above the current meter base (or surface grain), but the height above the zero plane (where z = 0). Thus the earlier equation is oversimplified and should be written

$$u/u_* = 1/\kappa . \ln((z+d)/z_0)$$

where d is the 'zero-plane displacement' (that distance below the current meter base to the assumed bed surface). For a direct solution of this equation a value of d needs to be obtained in the field. Herein lies the difficulty, since not only is it impossible to define such a clear zero

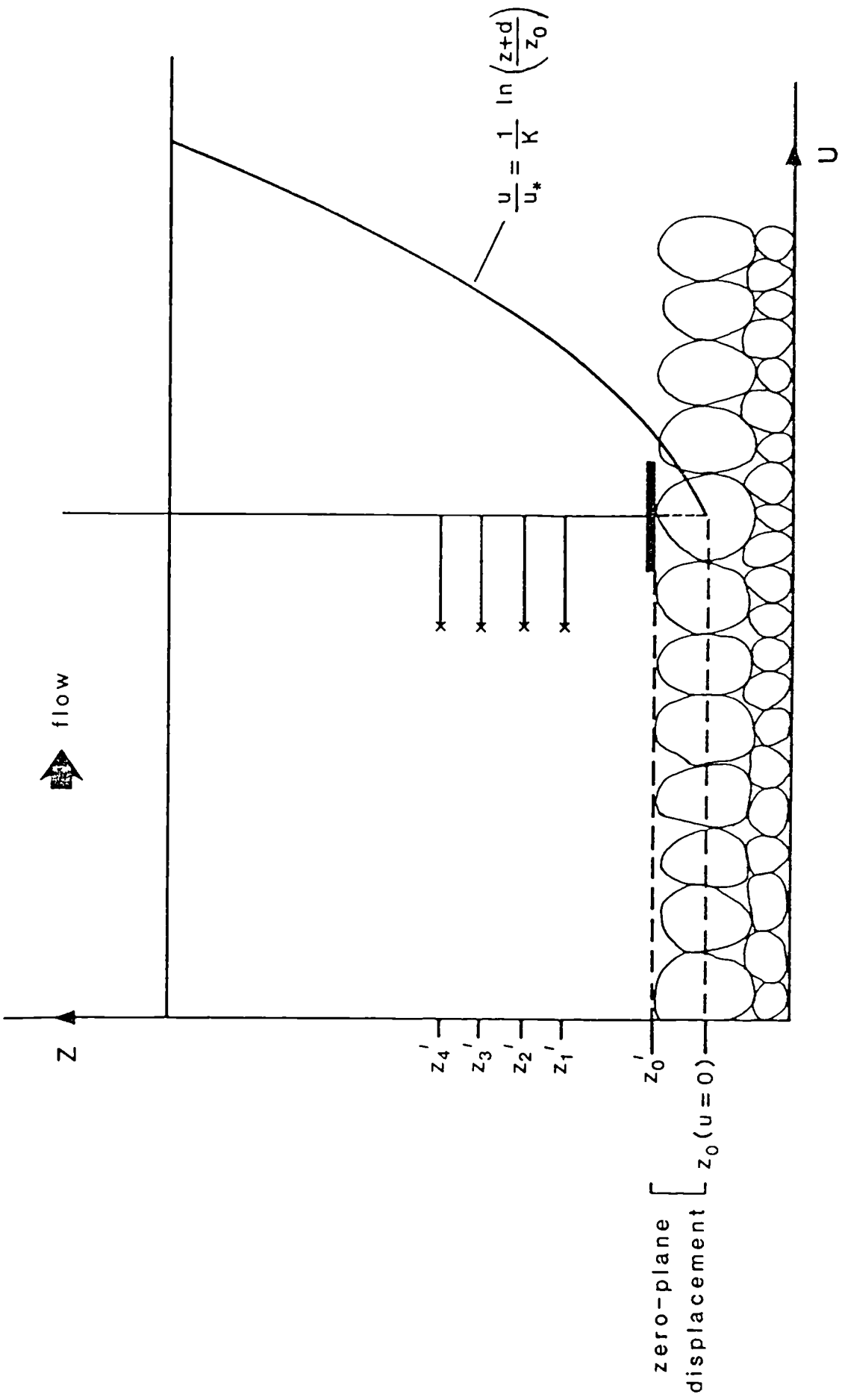

Fig. 2.14 Schematic diagram showing the 'assumed' and true zero plane of velocity (the difference being the zero-plane displacement).

plane, but also it would vary according to bed geometry, discharge and grain size; for example through pools and riffles.

Other studies have been directed towards finding a solution for d either indirectly, or using laboratory simulated conditions. The problem is similar to that which microclimatologists face using logarithmic wind profiles above crops where the suitable zero plane is neither the soil surface nor the top of the plants but somewhere in between (Cowan 1968, Stanhill 1969, Riou 1984). Hydraulic engineers and geomorphologists (Jackson 1981, Van Rijn 1984, Southard and Middleton 1985) have given some indication of the location of the zero plane with respect to the bed grain size, which is similar to the result used for crops with respect to crop height. Riou (1984) found his work agreed with other microclimatologists, and recommended the location of the zero plane to be 0.3 h below the top of the crop, where h is the height of the crop. Jackson (1981) gives a review of the findings of studies conducted up to 1974 and concludes that the value of d varies between 0.2 and 0.4 of the diameter of surface grains. This presents another problem, since most workers state a value for d relative to the surface grains. In coarse heterogeneous material which is poorly sorted, it is difficult to choose a grain size that represents the surface size. The problem is simplified in the work of microclimatologists who assume a horizontal crop surface, while others have worked in simulated conditions or sand-bed rivers with little bed relief. The only work available expressing d in terms of a grain size statistic is the work of Van Rijn (1984) who used a value of d equivalent to 0.25 D_{50} (D_{50} being the grain size of the bed surface that 50% is finer than). With the uncertainty in the value of d and the problems involved applying such a correction in coarse and spatially variable bed material, the method used in the work reported here relied upon correcting for d at each site of measurement.

This technique depends heavily upon the law of the wall. Strictly the law of the wall is only valid in the lower 15% of the flow depth (Schubauer and Tchen 1961, Task Force 1963). If the plot is not linear it can often be linearised by adding a small increment to each propeller height, which corresponds to the zero-plane displacement.

Despite the simplicity the method's drawback is that it should only strictly be used in deep flows. Since the top impeller in the current meter array can only be set at a minimum height of 25 cm (because of the impeller diameter and cable fittings) then a water depth of at least 160 cm is required before it can be assumed that there is a logarithmic change in velocity with height in the profile measured. However not all workers are in full agreement with this rigid restriction on the use of the law of the wall. Yalin (1972) has showed using an empirical analysis "that there is no reason..... that the log distribution should not be valid up to the free surface" whilst both Dietrich (personal communication, 1985) and Southard and Middleton (1985) stated that though there is no physical reason to expect the log law to hold true to the water surface, empirically any deviations are insubstantial. Indeed Southard and Middleton (1985)note that most hydraulic equations assume that there is a logarithmic increase in velocity to the water surface (for example when gauging discharge). The problem is greatest particularly close to the bed due to the protrusion of sediment, and near the water surface due to eddies, where there may be a distortion of the velocity field. With careful positioning of the current meter array however these factors can be minimised. For the purpose of the study here the velocity measurements were taken as close to the bed as possible (the lowest impeller was usually at 7 cm above the bed) and following the arguments of Yalin (1972), Dietrich (personal communication, 1985), and Southard and Middleton (1985) the velocity profile was taken as being logarithmic up to

the water surface.

The strategy used to correct for the zero-plane displacement and calculate the shear stress was aided by a computer programme. All velocity profiles were replicated at least three times to average out macroturbulent fluctuations and the number of revolutions entered into the computer. The programme then averaged these readings, converted them to velocity, and plotted the velocity profile. If the profile was obviously kinked in a convex-upwards way (and the corresponding standard error of the shear stress estimate was high) implying a correction for the true zero plane was needed, the programme had the option to enter various values of d. Once the profile was straightened the shear stress was recorded. This method was both quick and consistent and seemed to give realistic values when compared to the field conditions. Furthermore the computer programme included an estimate of the roughness height, Z_o (which is the intercept on the y axis) and if the corrected profile was substantially different from the known bed roughness (taken as near the D_{50}) the shear stress estimate was discarded. Notably most of the velocity profiles approximated a logarithmic increase in velocity from the current meter base and no correction at all (over 90% needed) for the zero-plane displacement (examples are given in Appendix C).

In addition to shear stress, a more rapid indication of spatial differences in flow strength and direction for a reach was obtained using a single current meter close to the bed. Both the Braystoke and Ott current meters were used for this purpose, the latter being preferred due to its lightness and portability. All 'bed velocity maps' were constructed from velocity readings at 6 cm above the bed as proposed by Hein and Walker (1977). The direction of bed velocity was either inferred from spitting into the flow or measured using a compass and piece of string tied to the current meter impeller. The near-bed velocities are

also a guide to the spatial distribution of shear stress which is proportional to the square of velocity at a fixed height if vertical velocity profiles are logarithmic and roughness height constant.

2.2.3 Bedload transport

Different methods of varying sophistication and precision have been used to measure bedload movement (see Gomez (1987) for a comprehensive review of these). Up to the early 1970s, crude bucket or basket samplers were used to gain an insight into the instantaneous at-a-point bedload transport rate (see for example Fahnestock (1963)). Despite their advantageous large capacity which can retain a wide range of particle sizes they have a poor trapping efficiency which is not constant and can be as low as 30% (Engel and Lau 1980). A more serious consideration of the problem of trapping bedload was given in the late 1960s and led to the installation of large-scale constructions. In 1969 a vortex-tube bedload sampler was installed on the Oak Creek (Klingeman and Milhous 1970, Klingeman et al. 1979) which ejected the passing load from the channel bed and permitted a continual or intermittent sampling of the total bedload with trapping efficiency close to 100% for coarse sand and larger particles. Further work in 1973 led to the installation of a conveyor belt system on the East Fork river (Leopold and Emmett 1976) which again sampled full width bedload movement and could cope with loads as great as 150 kg min^{-1}. Although such large and expensive constructions provided excellent data on the frequency and magnitude of total bedload transport and the size distribution of the transported sediment, their immobility meant they were of little use if more intensive information was required on the spatial distribution of bedload possibly in rapidly changing flow conditions. To overcome this and provide a portable apparatus, Helley and Smith (1971) designed a pressure-difference sampler with a 7.62 cm square sampling orifice leading to a 0.25 mm mesh collecting bag, which could be

hand held or suspended from a cable across the channel. Emmett (1980) has since shown that this has a 100% sampling efficiency for sediment sampled in the size range 0.5-16 mm, while Hubbell (in press) reported that although it is 100% efficient for sizes up to 32 mm, as the transport rate exceeds about 1.5 kg m^{-1} s^{-1} this efficiency drops markedly and the sampler overestimates the finer sediment sizes.

Most of the work reported on bedload movement in the 1970s was undertaken using either these fixed installations or Helley-Smith samplers, and was dominated by studies on sand/gravel bed rivers in the U.S. These mechanical sampler devices have also been installed and reported on for the Torlesse in New Zealand (Hayward and Sutherland 1974, Hayward 1979) and in the Virginio Creek in Italy (Billi and Tacconi in press). However the mechanical bedload samplers have several sampling difficulties particularly in coarse bed streams. Adequate contact with the stream bed during sampling is difficult to achieve at flood stage, a representative sample of cobbles and pebbles is very heavy and hard to manage, and large sampling constructions may disturb the flow and modify transport rates near the device. A new technique was therefore needed, which prompted the work of Ergenzinger and Custer (1983), and Reid et al. (1984) on electromagnetic tracing of pebble movement. The idea relies on the principle that when a permanent magnet passes over an iron-cored coil of wire a measurable electrical current is generated. By using either naturally magnetic pebbles or impregnating artificial pebbles with ferrite rods, the movement of individual clasts can be monitored via a transmitting coil buried in the channel bed. Although the equipment suffers from the same drawback as the mechanical samplers in that it is limited to individual sites, as well as being expensive, restricted to small channel widths, and vulnerable to high flows, it has provided some of the most intensive bedload entrainment information through flood events ever reported (Reid et al. 1984).

The work reported here was limited by both time and finances, so a method was needed that was well used and documented in the literature, inexpensive, quick and portable, and which gave a reliable estimate of spatial variations in bedload transport. For this purpose the Helley-Smith sampler was favoured, using the conventional 7.62 cm square orifice fixed to a wading rod and hand held on the river bed for between 30 seconds and 10 minutes, depending on the flow conditions. Sampling was either alongside the current meter array or at the same point immediately before or after velocity profiling, so that the bedload transport rates could be related to the shear stress acting on the bed. The bedload samples therefore represented at-a-point bedload transport rates rather than an average for the whole channel width. The bedload samples were oven-dried, sieved at 0.5Ø intervals, and weighed to determine total transport rates, individual sieve fraction transport rates and grain size distributions.

Bedload samples were replicated if there were anomalously low or high bedload catches, but in order to give an indication of spatial variations in transport rate as flow conditions changed rapidly, often only one sample per measurement site was taken. This could introduce inaccuracies into the results particularly if bedload transport travels in pulses as suggested by Emmett (1975), Reid et al. (1985), and Hubbell (in press), but provisional bedload sampling showed that the samplers could trap reliable duplicate sets of bedload samples (both in weight and size distribution) so that bedload pulses must either have been infrequent or non-existent in the three study rivers.

Further problems occur when sampling in coarse bedded rivers. Although the Helley-Smith sampler is 100% efficient for sizes up to 32 mm, no calibration results are available for any larger sizes (Hubbell in press).

As the sampler's nozzle is only 7.62 cm square, firstly the efficiency must decrease rapidly as the diameter of pebbles approaches this size, and secondly any coarser material will not be sampled. Although an enlarged Helley-Smith was constructed with a 15.2 cm square sampling orifice it was found that the original sampler was both easier to handle and in most cases trapped all the sizes moving. Material coarser than 72 mm only appeared to move in peak floods, and could be detected by inspecting the grain size distributions of the bedload, which were clearly truncated.

Sediment movement was also measured indirectly using marked pebbles. This approach has been commonly adopted (for example Laronne and Carson (1976), Thorne and Lewin (1979), Leopold and Emmett (1981), Leopold and Emmett (1984)) and involves introducing marked pebbles into the bed and tracing their movement after flood flows. A technique that labels natural sediment by enhancing its magnetic remanence through an artificial diagenetic heating process has been developed by Arkell et al. (1983). Unfortunately the mineral composition of the pebbles from the study areas is not the same as those used by Arkell et al. (1983) and provisional tests of the method proved unsuccessful. Instead, the more popular and inexpensive method of painting and numbering individual clasts was favoured.

The size distributions of the pebble tracers were partly matched to that of a Wolman (1954) sample of the bed (truncated at 22 mm) carried out over the relevant area, but also to a size range representing the coarser fractions of the bed surface. The selection of pebbles from the channel was random to obtain a truly representative range of shapes and particle geology. The pebbles were painted a distinctive yellow colour using gloss paint, which proved to be durable but much cheaper than the conventionally used road-lining paint. Each pebble was numbered, weighed and measured (a, b, and c axis). The pebbles' shape parameters were computed using the

formulae of Krumbein (1941) for sphericity, $(c^2/ab)^2$, and Cailleux (1947) for flatness, ((a+b)*100/2c). The experimental design for the pebble tracers varied for each river investigated, but followed the same routine whereby the pebbles were inserted at known positions and subsequently re-mapped tacheometrically after a flood event (see 2.2.5).

For the Dubhaig a total of 2574 pebbles were inserted in the five study reaches. The pebbles were traced through four flood events with the number of pebbles inserted in each reach varying for each flood. Initially up to 290 pebbles were inserted in reach A, over 120 in reaches B to D, and 85 in Reach E, but since the number of pebbles recovered decreased after the first two floods another 60 pebbles (in sets of five 0.5ϕ classes coarser than 22 mm) were inserted in each reach. The pebbles were placed in the channel bed surface layer either by removing a similar stone size and replacing it with the marked pebble, or by stepping on the tracer to force it into the bed structure. This procedure is very important since recent work has shown the entrainment of sediment is greatly influenced by its bed packing characteristics and protrusion (see 4.1 for a review of these works).

Pebble tracing in the Feshie was undertaken during the winter of 1985 in reach C and in the snowmelt season of 1986 for reach B. In Reach C two groups of 100 pebbles in sets of five 0.5ϕ classes coarser than 22 mm were seeded into the surface layer at 0.5 m intervals across the barhead and bartail of the active medial bar between C7 and C8. Because of the narrowness of the bartail the second group of pebbles were inserted in three separate lines 3.5 m upstream, along, and 1 m downstream of C8. Different colours were used to differentiate between the two bar units. Upstream a set of 100 pebbles were placed at C1 (riffle), C3 (poolhead), and C5 (pooltail) and their movements were analysed as part of an undergraduate dissertation (Brewster 1986). A Wolman (1954) count

dictated the five most common size classes to represent the sizes of both tracer experiments. In Reach B 379 pebbles spanning seven 0.5ϕ classes were seeded in sections B5, B6, and B6.5. Their positions were resurveyed at the end of the snowmelt season in June, six weeks later.

Pebble tracing was also used on the Lyngsdalselva. Three inputs of a total of 188 pebbles were inserted in Reach A on the rise, peak, and falling stage of a major flood. Since the river was bankfull these were simply thrown in at a known section at the head of the reach. A further 255 pebbles were seeded in the bed and on a medial bar at the head of Reach C and their downstream movement measured eight days later during a period of low discharge.

Only a brief outline of the tracer experimental designs are given here and a much more detailed discussion of the numbers, sizes, and weights of pebbles inserted, the exact positions of implacement, and the discharge variations throughout the tracing periods is given in Chapters 3-5.

The inadequacy of all pebble tracing experiments is that they yield no data that pinpoints the actual incidence of motion during a flood wave. In addition it may be an oversimplification to assume that the displaced particle has moved at peak discharge. However, since recovery rates were exceptionally high in most cases (see 3.2 and 3.3), and pebbles were resurveyed frequently enough to ensure their movement could be isolated to just one flood event, the data does provide valuable information on the direction and proportion of particles moving and their individual transport rates.

2.2.4 Sediment size distributions

Characterisation of alluvial material is important. Bed surface material

affects resistance to flow and provides the material to be transported as bedload. The size distributions of surface and subsurface material enter into competence and sediment transport calculations (Chapter 4) and hence into the consideration of channel form and stability. The orientation of imbricated pebbles on bar surfaces gives some indication of flow patterns during flood discharges (Chapter 5). It is therefore important to investigate the spatial and vertical variation in sediment properties of channel beds and depositional units, both within reach and between different channel patterns.

The size and grain size distribution, shape, and orientation of channel sediments were investigated using three sampling techniques well documented in the literature. To provide the grain size variation both down-bar and vertically, bulk samples were taken of surface and subsurface bar sediments. Recently this sampling technique in coarse bedded rivers has been under review and stringent conditions suggested to ensure representative sampling (Mosley and Tindale 1985, Church et al. in press).

The sampling method started with the selection of a bar which best reflected the character of the reach and which appeared to have been recently active (so as to minimise the effect of winnowing out of fines). Tapes were laid out both down and across the bar to give a network of possible sampling locations. Depending on the size of the bar and spatial variation in surface grain size, a number of sampling sites were selected in close proximity (usually not more than 3 m apart). These were randomly selected except that inputs of fresh material, boulder and sand tails, and pebble clusters were avoided. The sites were then excavated around an area of approximately 1 m^2 to the base of the coarsest exposed stone (which was usually removed first and its imprint noted). As Church et al. (in press) note, this task is remarkably difficult because of the irregular occurrence of large stones, but this problem was tempered with

the aid of an entrenching tool and trowel. Most workers accept that the surface layer is one grain deep (for example Klingeman and Emmett 1980, Gomez 1984), so excavating to the largest surface particle's depth seems reasonable. Since individual clasts were often very large, all pebbles coarser than 16 mm were sieved in the field using a combination of a handtape, template, 16 mm sieve and a spring balance and bucket. The remaining sediment was classed as the subsurface sample and was sampled to a depth of at least twice the diameter of the largest stone.

The size of sample taken and number of samples needed to truly represent a site has been a focus of considerable attention. As Mosley and Tindale (1985) conclude, a single bulk sample gives an estimate of the true population "which is at best inaccurate and at worst meaningless." They showed that from a 854 kg sample, approximately 100 kg was needed to provide an accurate determination of mean grain size. This sampling procedure followed the recommendation of Church et al. (in press) who proposed that the sample size should be defined by the weight of the largest clast in the sample - this should not exceed 0.1% of the total sample weight for sizes up to 32 mm, 1% to 128, and 5% to 256 mm. They found that these requirements were fulfilled with samples typically weighing 150 to 350 kg. With the high demand on labour, resources, and time these sampling restrictions are clearly difficult to follow. The policy adopted therefore was to take a sample which when sieved for pebbles greater than 16 mm left a sample size that filled a large bag (usually weighing about 10 kg). Depending on the coarseness of the sediment, this generally led to a total sample weight of between 15 kg and 60 kg.

The spatial variability of bulk material presents another problem. Mosley and Tindale (1985) found that 228 and 50 bulk samples were needed to estimate the mean grain size to ± 10% and ± 20% respectively of the true

value. Again the logistics involved in taking so many samples are not viable for this study, but since only general indications of spatial variation were required the procedure outlined above was sufficient. Besides surface and subsurface sampling, undifferentiated bulk samples of both layers were taken of common sedimentary units of the floodplain. These were simply shovelled into a bag after field sieving all coarse sizes.

All bulk samples were oven or air-dried and sieved for 15 minutes at 0.5ϕ intervals down to 4ϕ (0.063 mm). The weighed sieve fractions were entered into a computer programme which converted them into percentages and plotted them in the form of a histogram and cumulative frequency graph. In most cases only the D_{50} (median) value was used to characterise the grain size of the sediment sample (where D_{50} represents the size that 50% of the sample is finer than). The same laboratory and analytical procedure was also used to process all the Helley-Smith bedload catches (>0.25 mm). 113 bulk samples and 72 bedload catches from all three rivers were sieved and processed.

The other technique used to characterise the size of channel sediments was pebble counting. This took place on the channel bed and partially submerged bars where bulk sampling was impracticable. Although Kellerhals and Bray (1971) noted that different methods of selecting material for size analysis led to non-equivalent results, they showed that grain size statistics from pebble counting and bulk sampling needed no conversion and were equivalent. The results from the two different methods can therefore be compared. The random walk technique (Wolman 1954) was used whereby the sampler looks away from the bed and picks up the pebble directly below the tip of the toe of his boot. 100 pebbles were selected in this way, which is well above the minimum number required to represent the median size (Wolman 1954, Bray 1972, Hey and Thorne 1983). The pebbles were either

passed through a template or had their b-axis measured and then grouped into 0.5ø classes. Since the grain size distributions should be restricted to those portions of the total size range that have been sampled representatively, the samples were truncated at 8 mm as recommended by Church et al. (in press).

To provide information on palaeocurrent directions during infrequent and high magnitude floods when bar surfaces are overtopped, the dip directions of well imbricated pebbles were measured using a compass. This method has also been successively employed to reconstruct flow directions by Rust (1972), Boothroyd and Ashley (1973), and Thompson (1986). Sites with pebbles showing clearly defined b-axis directions were chosen at a random distance apart and marked. The bearings of five pebbles were taken relative to magnetic north and then averaged and corrected to provide a bearing from the surveying benchmark lines. Each measurement site was later surveyed so that their locations could be superimposed onto a base map. Imbrication directions were only determined for bars in reaches A to D on the Dubhaig.

2.2.5 Surveying

Planimetric maps and point fixing, channel cross-sections, and gradients were surveyed using Kern GKO-AC and Zeiss automatic levels with accompanying 4 m staffs. The surveying methods used were identical for all three rivers in association with the benchmark networks described in 2.1.

The surveying of changes in height to produce cross-sections always began by taking a height reading onto the respective benchmark datum point for the reach. This allowed all subsequent heights to be reduced to a common datum and repeated surveys to be superimposed. The level was then either

turned 90° from the survey line or directed along the line of section defined by pegs on the far bank. In the case of cross-sections less than 50 m long, a metal tape was stretched across the section and held tight by two arrows. For longer cross-sections the distance was measured using tacheometry (see later). The staffman would move at predetermined intervals placing the staff next to the tape, communicating the distance to the observer. The staffman used the following criteria for taking a height reading: (a) at 1 m intervals across the floodplain and every 0.5 m in the river channels; (b) at bank tops and bottoms and water edges; (c) at the deepest part of the channel, the highest part of the channel bed and bars and any sharp changes in elevation (such as rising out of the channel onto a bar); (d) at any other significant points such as vegetation boundaries, the edges of relict channels, distinctive grain size changes and so on. The observer would read the heights on the staff to an accuracy of 1 cm by rounding up or down to the nearest even number. This method prevents a consistent bias inherent from following a simple 'rounding up or down' approach.

The procedure for producing maps and fixing points of interest was different and used both the horizontal circle and the three stadia lines. In a level, the parallactic angle is held constant by using the Reichenbach recticule stadia lines. The difference between the upper and lower stadia line readings onto the staff multiplied by 100 is then equal to the distance from the staff to the level. In addition, the stadia lines are at such a distance apart that the differences between the upper stadia and the middle stadia, and the lower and middle stadia are equal. Hence, when a distance reading was recorded the middle stadia was also taken to check any possible observation errors.

A map is produced using the principle of tacheometry which is the use of a distance and angle to define a point. The level was usually set up at a

surveying pin (although this is not necessary) and directed to a benchmark of known position. The horizontal circle was set to 0° so that all subsequent bearings were relative to a fixed line. The surveying would then consist of the staffman following a previously planned route, placing the staff at locations of interest. The technique of tacheometry was also used for mapping specific points such as benchmark controls, pebble tracers, imbrication direction sites, grain size sampling points, and used in conjunction with the middle stadia height readings to determine slopes. The angle readings were usually taken to the nearest 0.5° and the stadia lines to the nearest 1 mm. Fig. 2.15 shows the possible errors involved in surveying a fixed point to such accuracy. Since the staff could only be read to the desired accuracy for distances up to approximately 110 m, more than one control station was sometimes required but the bearing and distance relative to the original benchmark zero was recorded and compensated for in subsequent calculations.

The methods for measuring height and distance can both contain significant errors. The main problem encountered is defining the representative surface heights and outlines of the channel bed, bar and banks. The rivers have characteristically coarse material and bank erosion leads to turf collapse into the channel. Placing the staff on any of these obstructions could therefore lead to height errors of up to 0.5 m. To overcome this, any large boulder protruding out of the bed surface was deliberately avoided by positioning the staff on either side. However, since turf blocks in the channel had a considerable effect either in protecting the bank from further erosion or diverting the flow, they were always included in the channel surface topography. Bank edges were often difficult to define since they often had bevelled tops and undercut bottoms. To combat this, as many readings as possible were taken close to the bank top to pick up its concavity and then the bank bottom was taken as being directly below the edge of the vegetated top. This had

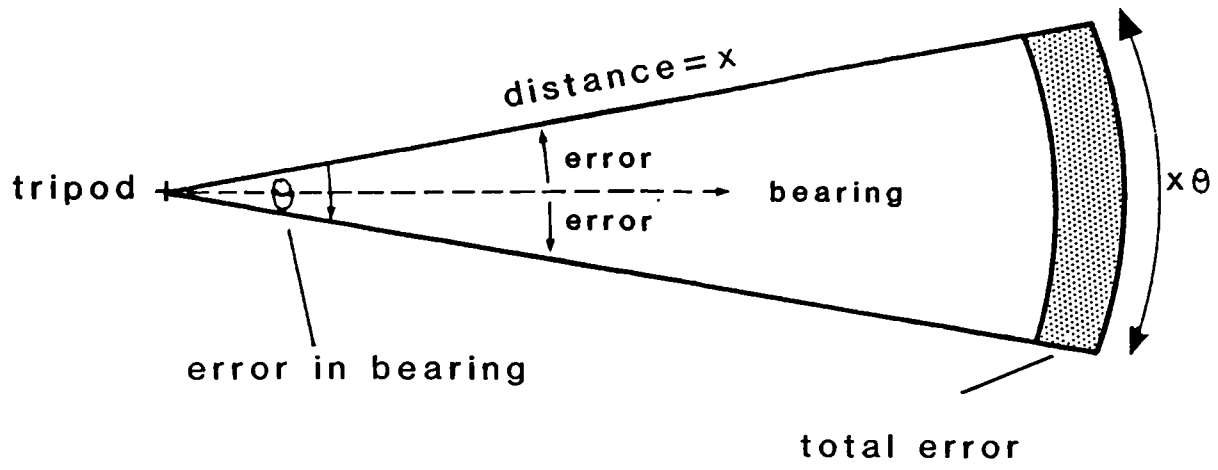

With a bearing error of ±0.5°

horizontal error = ±x. (2π.(0.5°))/360

$\simeq \pm x/120$

for example at 100 m distance there is a horizontal error of ±0.8 m

With an error in the upper and lower stadia reading of ±1 mm

error in distance = $\pm(\sqrt{1^2 + 1^2})/10$ metres

= ±0.14 m (constant for all distances)

If stadia readings taken to ±5 mm for long distances:

error in distance $\simeq$ ±0.7 m

Fig. 2.15 Error margins in tacheometric surveying.

consequences for both cross-section and planimetric surveying. Again, using the same staffman each time helped to avoid inconsistencies in the surveying results.

Besides height irregularities, the measurement of distance was also important to enable cross-sections to be superimposed to pick up differences in channel width, position and height over time. In the case of cross-sections, every effort was made to keep the metal tape as tight as possible and distances were read to centimetre accuracy. When using tacheometry, care was taken to place the staff on short flat vegetation or a large stable pebble to avoid the sinking or rising of the staff leading to inconsistent stadia readings.

The field surveying data was processed and plotted using the computer statistical package MINITAB and the graphics package GINO. Data could be quickly transformed either into reduced levels for cross-sections or Cartesian coordinates for planimetric maps and plotted with a pen plotter linked to the mainframe computer.

The magnitude of channel change during a specific time period was quantified using a combination of a HIPAD digitiser linked to an Apple II computer and a modification of the prism formula (Fig. 2.16). For each reach the cross-sections from successive dates were superimposed and the locations of deposition and erosion identified. Each block of erosion or deposition for every cross-section was than digitised to give areas of channel change (m^2). The zones with a consistent mode of channel change downstream were identified (e.g. a strip of bank erosion of bar aggradation) using both the cross-sections and planimetric maps, and the prism formula was used to calculate the volume of change for each zone (m^3). The formula used was modified so that it would take into account a pair of non-parallel cross-sections (see Fig. 2.16). The volume of

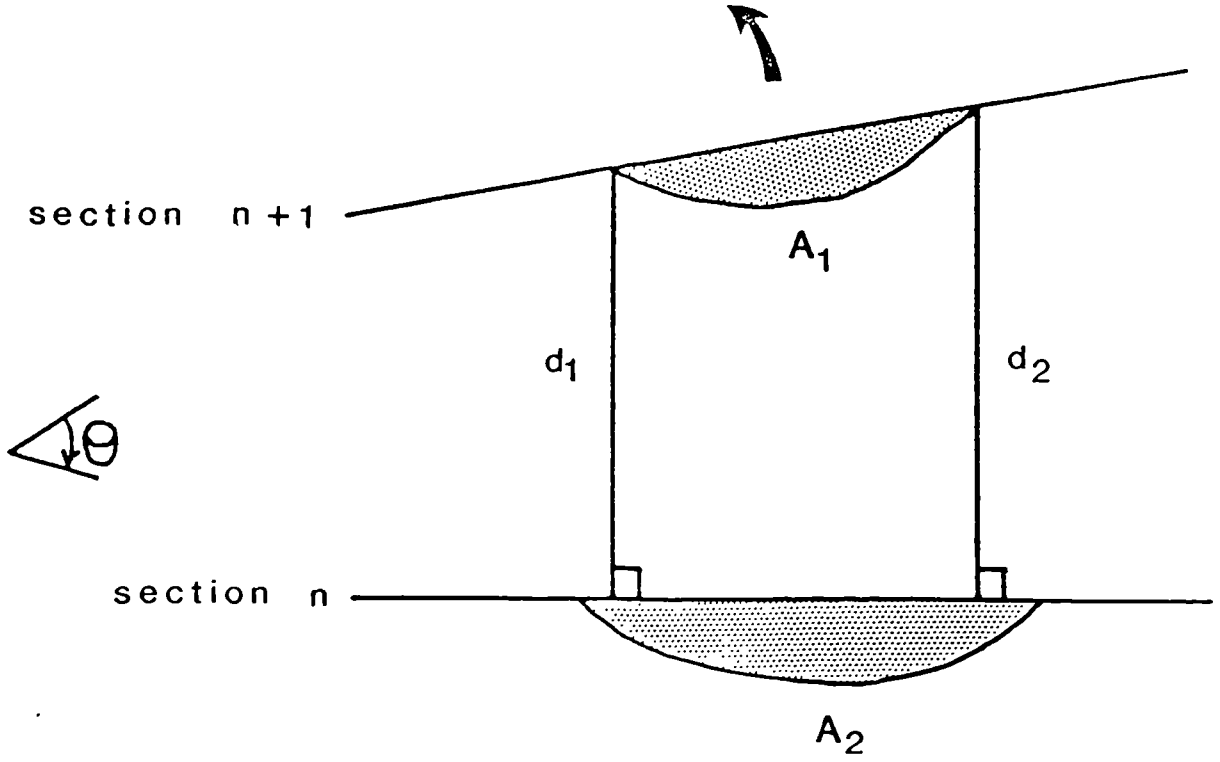

Assuming a linear rate of change in width and mean depth downstream:

$$\text{Volume} = (d_1 + d_2)/2 \ * \ (A_1 + A_2 + \sqrt{A_1.A_2})/3$$

where if sections are non-parallel $A_1 = A_1.\text{Cos}\theta$, and

A_1 = Area of downstream cross-section change

A_2 = Area of upstream cross-section change

d_1 = Perpendicular distance between successive cross-sections on left bank

d_2 = Perpendicular distance between successive cross-sections on right bank

θ = Angle by which the cross-sections are non-parallel

n = Number of cross-section

Fig. 2.16 The prism formula used to calculate the volumetric changes in channel geometry between successive time periods.

channel change in the reach could then be expressed in terms of a net erosion or deposition of sediment.

3 POOL/RIFFLE HYDRAULICS

3.1 Introduction

The discussion in 1.3 showed that the fundamental morphologic and functional component of gravel-bed rivers is the pool/riffle unit. Previous work has shown that these units are generally easily recognisable (especially at low flow), are at a regular spacing apart, and are important in maintaining the nonuniform geometry and development of channel patterns. The formation of pools and riffles is one of the mechanisms for attaining dynamic equilibrium of the stream system (Leopold et al. 1960, Yang 1971, Keller and Melhorn 1978) and may be a primary determinant of meandering (Leopold and Wolman 1960, Leopold and Langbein 1966, Richards 1976a, 1978). The presence and form of the pool/riffle topography varies with channel pattern (Bridge 1985, Thompson 1986), being most dominant and obvious in meandering channels (Bluck 1971). Here the deep pools are wrapped around the bends where they scour beneath the concave bank, at and past the apex of the bend, while the riffles are generally located on the straight sections representing a diagonal continuation of one point bar into the next on the opposite side of the channel. This simplified case of channel meandering can have many variations (Brice 1974) and if the bend is of sufficient amplitude, multiple sets of pool/riffle units may form within it (Keller 1972a, Lewin 1972). In straight or gradually curving reaches the presence of alternate sidebars can determine the pool/riffle spacing (Leopold 1982), but also the riffles can form as central features around which the flow divides (Richards 1976b). In braided channels the multi-bar system is a reflection of the complex flow pattern where the pool/riffle sequences are

often ill-defined and replaced by long "runs" (Mosley 1983) with rough turbulent flow which then diverges onto barheads. As discussed in 1.3 however there is no strict classification of channel patterns and often a combination of all pool/riffle forms can be found in a reach with its unique bed, bank, and bar morphology.

The pool/riffle unit has a major effect on flow geometry (and therefore bedload competence and capacity) which often changes from low to high stage (Keller 1971, Andrews 1979, Lisle 1979, 1982). At low discharges the pools are comparatively deep with a low water surface gradient and are a stark contrast to the steep water surface gradient and shallow water of the riffles. Hence at low flow the near-bed velocity and shear stress and therefore competence is greater over riffles than through pools. This has consequences for sediment movement with the coarsest sediment likely to be moved off the riffles into the deep pools where it can often be covered by winnowed out finer material (c.f. Hack 1957). As the discharge increases it has been generally accepted that the bed velocity/shear stress hierarchy between pools and riffles converges (Richards 1976a, Bhowmik and Demissie 1982) and may even reverse (Keller 1971, 1972b, Andrews 1979, Lisle 1979, 1982, Hirsch and Abrahams 1981, Campbell and Sidle 1985). As the stage increases the water surface gradient and depth contrast is drowned out and the shear stress increases through the pools at a greater rate than in the riffles. This increase may continue to a point where the shear stress through the pool becomes greater than that through the riffle and the cross-over in hydraulic properties commences. This is commonly known as Keller's 'velocity-reversal' hypothesis (Keller 1971, 1972b).

Under these conditions, the coarsest material being transported through pools is likely to be deposited on riffles, and since deposition on

riffles tends to occur at higher discharges than in pools, the riffle sediments are coarser than pool sediments. This difference in sediment size has been observed by many workers (for example Leopold et al. 1964, Keller 1971, Church 1972, Richards 1976b, Hirsch and Abrahams 1981, Bhowmik and Demissie 1982) although these differences are often not significant statistically (Milne 1982). The spatial variability of sediment sizes, the recent history of discharge events and the sampling method used to characterise the bed material can all confuse any perceived relationship.

Despite its simplicity and widespread usage in the literature the reversal in hydraulic properties envisaged by Keller has only been supported by two other sets of hydraulic measurements. Andrews (1979) measured changes in the discharge, width, and depth and from the principles of hydraulic geometry calculated the mean velocity for 11 cross-sections of the East Fork, U.S. A pair of 'typical' pool and riffle sections were selected by Andrews (1979) to show that there was a convergence and cross-over in mean velocity at a discharge of 14 $m^3 s^{-1}$ (61% of the bankfull discharge) with the pool having a much greater velocity at high flow. This was supported by other measurements of the changes in cross-sectional geometry with the pool-like sections scouring and riffle-like sections filling when discharges exceeded bankfull stage. Lisle (1979) also working on the East Fork showed that calculations of the mean shear stress (using the Du Boys formula) for a pool/riffle sequence in discharges from 6 to 34 $m^3 s^{-1}$ (bankfull was 22 $m^3 s^{-1}$) converged, crossed, and then diverged as the discharge increased with the rate of increase in the pool being the greatest. The data of Andrews (1979) and Lisle (1979) above the cross-over threshold strengthens Keller's (1971) hypothesis which had depended upon extrapolation of previous trends at lower discharges.

However their results should be treated with some caution since they are from the same river (and so may be site-specific), do not include any direct measurements of the flow strength, use mean values (oversimplifying the spatial variation in hydraulics), and in the case of Lisle (1979) show considerable scatter about the trend lines (which are fitted by eye).

Several workers are not convinced that the pool shear stress ever reaches a point where it exceeds the riffle shear stress. Richards (1976a) compared the hydraulic geometries of two pairs of adjacent riffles and pools and showed that the velocity through pools and riffles became "less differentiated" at high flows but whether there is a reversal "still requires further demonstration." However as Andrews (1979) notes Richard's observations were limited to a relatively small range of discharges and hence the mean velocity through the riffles was always greater than it was through the pools. Bhowmik and Demissie (1982) agreed that the shear stress in pools increases faster than at riffles with increasing discharges, but state "there is no evidence or reason why it will be greater at a pool than at a riffle for higher discharges". Furthermore they argue that if Keller's reversal does occur then the coarser material should be expected at the *pools* not the riffles. At high discharges the shear stress is supposedly greater in the pools and therefore only coarse lag material will remain in the pools whilst all the finer gravel is transported from the high shear stress pool zone to the lower shear stress riffle area. However since most workers agree that riffles are coarser than pools, Bhowmik and Demissie (1982) argue that the bed material sorting must therefore take place at low flows when the difference in shear stress between that of a riffle and a pool are greatest.

This line of thought is also followed by Teleki (1972) in a critical discussion of Keller's (1971) paper. Teleki used an empirical analysis to show that the pool velocities could never exceed riffle velocities if the Froude number ($Fr = v/(gd)^{0.5}$) was less than one (i.e. subcritical flow) although the hydraulics could be different with supercritical flow (Froude number greater than one). Since all of Keller's (1971) data is for subcritical flow Teleki (1972) argued that the bed sorting must therefore take place at low flow when the riffle velocities were higher than the pool. In his reply to this criticism Keller (1972b) referenced the flume work of Simons and Richardson (1966) to show that the formation and maintenance of the pool/riffle unit is probably independent of the Froude number and although it is doubtful that Dry Creek ever experiences supercritical flow it "does not appear to affect whether or not there may be velocity reversal in the pools and riffles." Keller (1972b) concedes that he "cannot prove conclusively that there is a velocity reversal" and that "the lack of observations at higher flows weakens the argument" but states that "the work of other authors and numerous field observations... suggests that a velocity reversal where pools with low bottom velocity at low flow become areas with fast bottom velocity at high flow is quite probable."

The hydraulic adjustments in pools and riffles are therefore still open to considerable debate. The matter is further complicated by the lateral and longitudinal variation of velocity distribution within the pool/riffle units (which may change at different rates with increasing discharge), and as mentioned earlier, the differences in the prominence and form of the units in different channel patterns.

In order to test Keller's hypothesis and to see whether it can be extended to different channel patterns, bed grain size, and selected subunits of the pool/riffle cycle an experimental design was set up mainly in the

Dubhaig (five reaches), but also on a smaller scale in the Feshie (two reaches). For each reach investigated a pool/riffle unit was identified and divided into four subunits: poolhead, midpool, pooltail and riffle. The riffle was easily recognisable at low flow with its characteristically steep water surface gradient and rough turbulent flow through occasional protruding boulders. The selection of the subunits within the pool however was more subjective depending on both the depth of water and field observations of the bed geometry and flow speed and direction. The midpool was always located at the deepest part of the talweg at low flow, but the site of the poolhead and pooltail varied according to the distance of the riffle up and downstream. The pooltail in particular can be much longer than the poolhead and the whole pool geometry can take on a shape very similar to a cross-section through a typical meander bend. In such circumstances the poolhead and pooltail were located about halfway between the riffle and midpool.

Measurements were taken of both the hydraulics and bed competence for each pool/riffle subunit at varying discharge. Although the nature and detail of the experiments varied between the Dubhaig and Feshie, the measurements needed to quantify discharge, flow strength, and bed competence were all taken in an identical manner. These methods for logging discharge, velocity profiling to estimate shear stress, and pebble tracing were outlined in 2.2.1 - 2.2.3.

3.2 The Dubhaig experiments

The bulk of the work on the response of the pool/riffle unit to increasing discharge was undertaken in the Dubhaig. A pool/riffle cycle was selected in each of the five channel patterns A to E and the subunits labelled with pegs on the bank for relocation. The pool/riffle cycles were at the head of the reaches so that the tracer pebbles would tend to move within the

reach length (to provide some information on channel change as discussed in 5.2). At each of the 23 sites (reaches C, D, and E having both top and bottom riffle sites) shear stress measurements were taken in up to eight different discharges (0.50 - 9.3 $m^3 s^{-1}$, bankfull = 6 $m^3 s^{-1}$). The frequency of measurement depended on the flow conditions since on some occasions priority was given to Helley-Smith bedload sampling (see Chapter 4). In each case the time of measurement was recorded and this was subsequently linked to the 0.5 hourly logged discharge record.

To supplement the hydraulic measurements pebble tracers of different sizes were inserted in each of the riffle, poolhead, midpool, and pooltail subunits as explained in 2.2.3. These were traced through four floods (only three in reach E) for a total of 20 weeks. The hydrographs for the high discharges during each of the tracing periods are plotted and discussed in 4.6.4. The recovered pebbles were replaced in their original locations after two of the floods but the movement of pebbles in the second flood on 27/8/85 represents a cumulative distance and duration of discharge from the previous tracer experiment started on 6/6/85 (because the locations of the pebbles from the first flood on 27/7/85 were surveyed but they were not removed from the bed).

As briefly outlined in 2.2.3 the pebble tracer experiments (both for the Dubhaig and Feshie) involve several assumptions and uncertainties. As common in all tracing experiments it is usually assumed that the pebble tracers move at peak discharges. As the results in 4.3 and 4.4 will show however this is certainly not the case and different sizes of sediment can move at discharges much less than the maximum. For the analysis here it is also assumed that the distances of pebble movement represent a single travelling event, but in practice their movement probably entails a series of intermittent jumps. To complicate the analysis further, a pebble may move from the poolhead at a certain discharge (and shear stress) but to

initiate movement again (from say the pooltail) requires a higher discharge (due to the differential shear stress within pool/riffle sequences as will be discussed in 3.4). In addition, if the pooltail is finer than the poolhead, a pebble that is the D_{60} of the poolhead, when moved may become the D_{90} of the pooltail and therefore protrude more into the flow and increase its chance of entrainment. Despite these complications the pebble tracer experiments provide valuable information on the mean distance of travel from a source area, the sizes and amount of tracer moved and the flow direction during high discharges.

The pebble tracer data for each of the 23 pool/riffle subunits is summarised in a table of results for each reach (Tables 3.1 to 3.5). The percentage and mean distance of tracer movement provided the most useful results and are thus used to help interpret the accompanying hydraulic measurements. The mean distance of tracer movement was particularly informative and is used in preference to the percentage movement (which often did not differentiate between sites). Although the distance moved by bed material is not directly related to the local shear stress the magnitude of local flow strength does affect the initial momentum that is given to a pebble once it is dislodged from the tight interlocking structures typical of coarse heterogeneous bed material. Unfortunately the maximum size of pebble moved from each subunit gave no indication of the flow competence since in most cases all but a few pebbles moved and the only remaining pebbles were on the margins of the talweg (which reveals another uncertainty in the tracer experiments - the neglect of a lateral difference in shear stress).

For each reach and subunit of the pool/riffle cycle the shear stresses measured are plotted against discharge in a form analogous to a rating curve. Both variables were logged and 22 of the relationships were significant at the 0.05 level (the riffle site in reach B being the

exception). The decision to log the variables was based on three criteria: (1) some relationships had a hint of curvilinearity (particularly at the two extremes of the scatter), (2) a comparision of the r^2 values for an arithmetic and log-log regression of the 23 sets of data showed that the log transformation improved the r^2 value in 78% of the cases, and (3) the work of Keller (1971), Andrews (1979), and Lisle (1979) also used logged variables so the Dubhaig results would be directly comparable with their findings.

One problem with log transformation is that it stretches out the data points and is therefore sensitive to extreme values in the data distribution. In the case of reach E at low discharges the shear stress values were close to zero (the lowest recorded shear stress was 0.1 N m^{-2}) and though arithmetically the difference between readings of 0.1 and 1 N m^{-2} is small, on a log scale this is represented by a full log cycle (equivalent for example to a difference of 90 N m^{-2} (10 - 100)). The low shear stress estimates are prone to large errors (when represented as a proportion of the actual value) and therefore can alter the gradient or position of the linear regression line for the whole distribution. For example a reading of 0.1 $\pm$ 1 N m^{-2} means the point lies somewhere within a range of one log cycle but a reading of 1 $\pm$ 1 N m^{-2} does not lead to such a wide error margin in log terms. The log-log plot for reach E is particularly vulnerable to this effect so the arithmetic plot is used in 3.2.3 to interpret the hydraulic properties of the pool and riffle subunits (although the log-log plot is shown for comparison).

As in all the plots of shear stress versus discharge the relationships are only approximate given the limited number and range of the data points. However all reaches showed that there was a relationship (close to or almost linear when logged) between the at-a-point shear stress and discharge and therefore that general comments could be made about the

response of the individual subunits of the pool/riffle cycle to a change in discharge.

3.2.1 Reach A

Fig. 3.1 shows the plot for reach A (n= 8 in all cases) with the highest discharge when shear stress was measured being 9.3 $m^3 s^{-1}$ (the peak discharge of the 10 month record period and 153% of the bankfull discharge). The ratings for the pool subunits separate out in the order pooltail, midpool, poolhead, corresponding to a higher shear stress for a given discharge. Other things being equal this is what would be expected as the discharge rises as illustrated in Fig. 3.2.

The Du Boys equation $\tau = \rho gRS$ (which strictly should only be used for uniform flow) shows that the average shear stress is proportional to the depth-slope product (R being the hydraulic radius which is equivalent to the mean depth). As the stage rises the depth increases at a greater rate at the poolhead. Since ρ and g are constants and the water surface slope changes at a constant rate within the pool, the shear stress is solely a function of the change in depth and hence is greatest at the poolhead in high flows. This is simply an extension of Keller's (1971) velocity reversal hypothesis where the hydraulics of the pools and riffles change at varying rates as the discharge increases.

Fig. 3.1 shows a completely opposite hydraulic situation to that described by Keller and previously cited workers. In reach A not only is the shear stress in the riffle lower than in the pool at low discharges, but the rate of increase in shear stress is greater than that for the pool subunits. Hence there is a cross-over as envisaged by Keller (1971), but whereby at higher discharges the riffle has a higher shear stress not the pool. The explanations for this pattern can be found by looking carefully

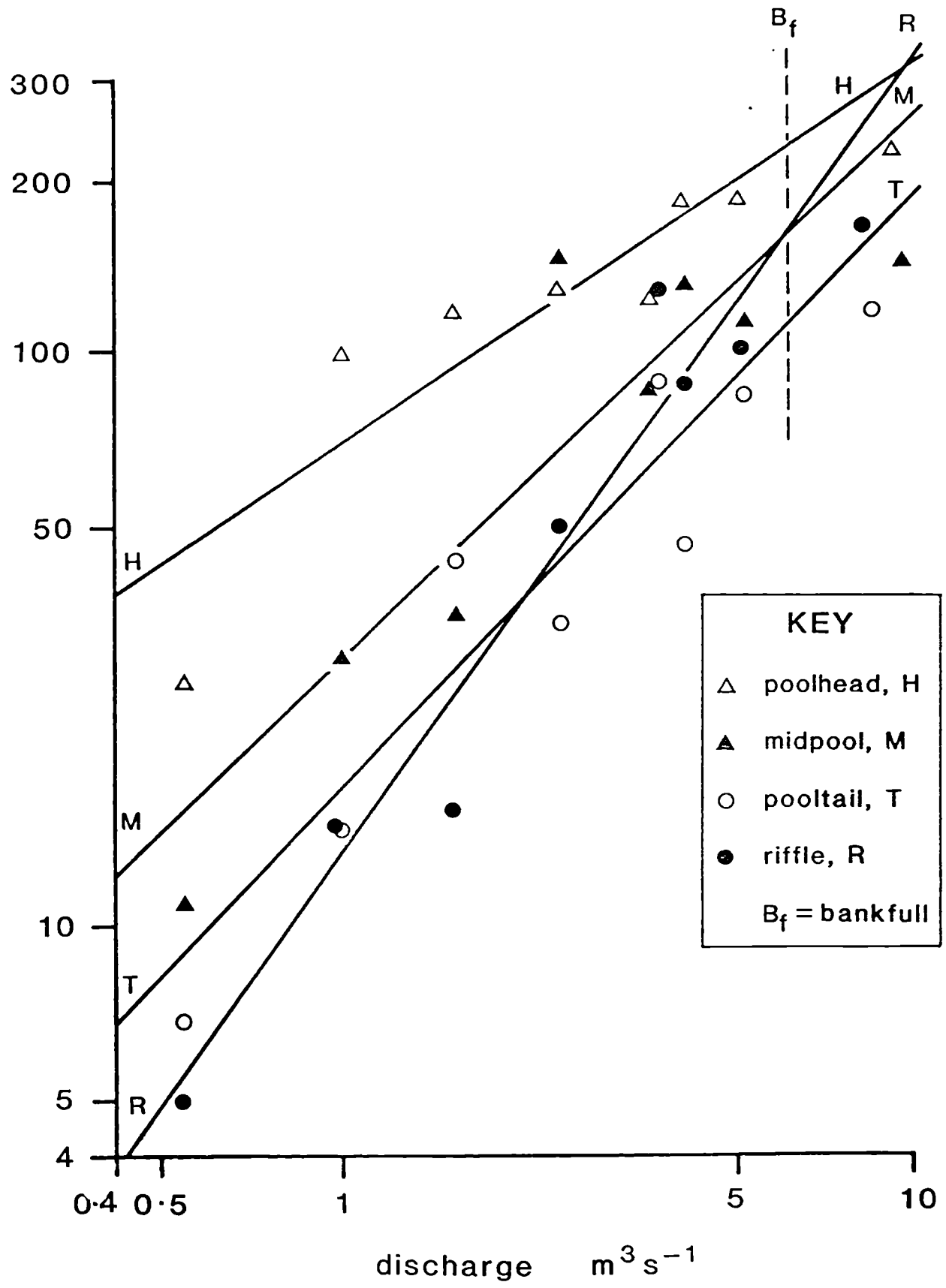

Fig. 3.1 Measured changes in shear stress with discharge for different subunits of a pool/riffle cycle in reach A of the Dubhaig.

from Du Boys $\tau = \rho g \bar{d} S$

ρ and g are constants, assuming S changes at a constant rate in the pool

$\tau = k.\bar{d}$

greatest change in $\bar{d}$ is at the poolhead (and therefore τ)

decreasing downstream to the riffle

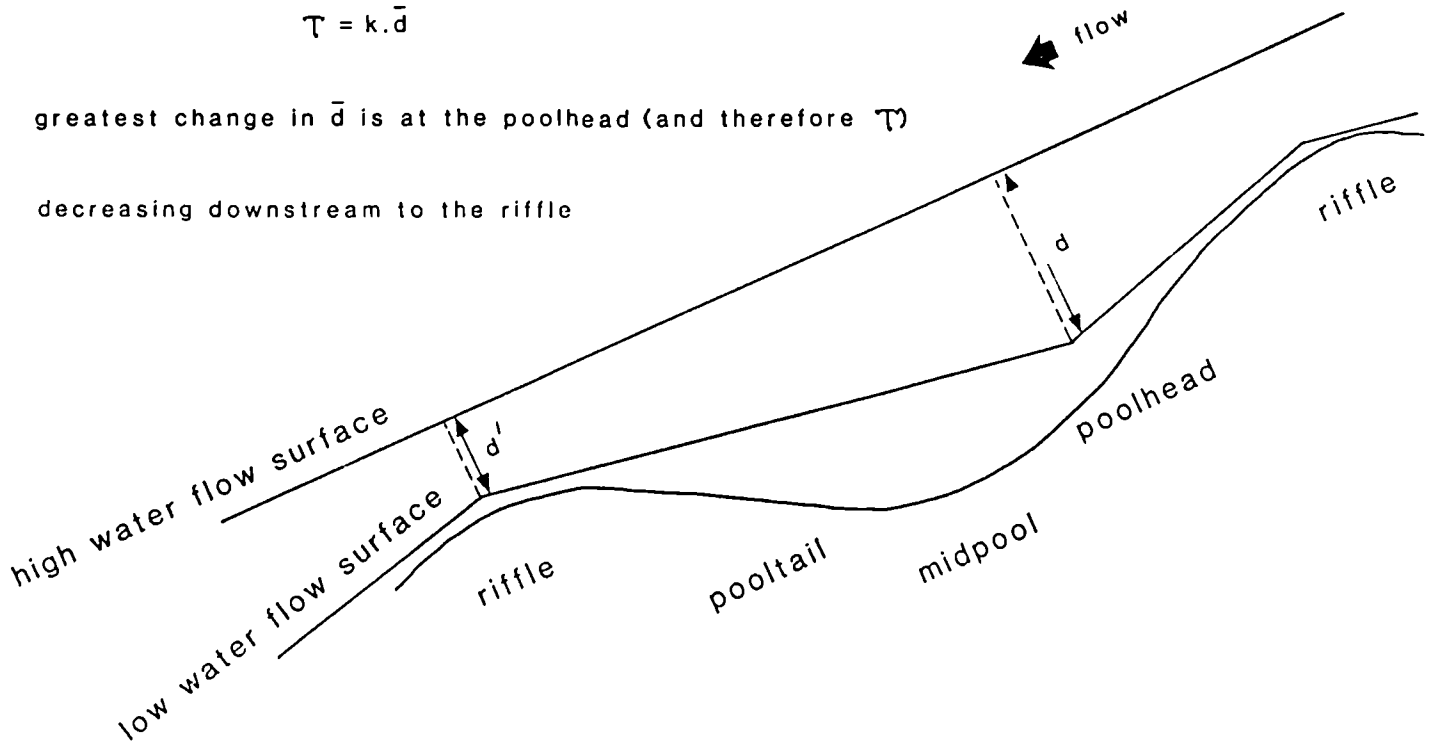

Fig. 3.2 Schematic diagram of different subunits of a pool/riffle cycle showing the expected changes in shear stress with increasing discharge (assuming that the shear stress is proportional to the mean depth).

at the site location. When the original measurement sites were chosen there was a lack of obvious pool/riffle sequences in reach A that would be active all year round. Presented with this limited choice the pool/riffle sequence at the head of the reach was selected. This was far from satisfactory since the pool and riffle were both confined within steep vegetated bank edges on their left side and coarse bar avalanche faces on their right. At low flows the shear stress measurements and field observations support the view that the convergence and channelisation of flow was more important in the pool than the riffle. The wider riffle (7 m) was able to accommodate the low flow without increasing the bed shear stress significantly, while the narrower pool (5 m) led to a convergence of flow and higher shear stress. In other words an increase in the discharge in the pool only leads to an increase in the depth and velocity whilst the width term in the equation $Q = w.d.v$ (where Q is the discharge and w the width) is a constant. In the riffle however all three terms are involved. This explains the discrepancy shown in Fig. 3.1 with the pool having a higher shear stress than the riffle at low discharges.

As the stage increases this hydraulic hierarchy changes. Firstly the riffle can no longer widen and therefore the bed shear stress increases substantially, and secondly the midpool and pooltail subunits begin to lose some of the flow by reactivating chutes and overtopping the bar on the right side of the channel that had restricted their flow at lower discharges (Fig. 3.3a). The pooltail particularly does not require a large increase in stage to enable it to overlap the adjacent bartail. As the discharge increases the midpool also overtops the bar and even more flow is lost to the channel now flowing on the right-hand side of this extended side bar (inactive at low flow). Meanwhile both the riffle and poolhead are confined within the bar and bank edges and only near peak discharges (here being 9.3 $m^3 s^{-1}$) do they eventually overtop the bank and bar and increase the area available for flow (see Fig. 3.3b). Thus at

Fig. 3.3 (a) Reach A of the Dubhaig during a flood of about 9 $m^3 s^{-1}$, views looking (a) upstream from A4 showing the occupation of the right-hand distributary (labelled Z) by flowing over the adjacent bar's tail and (b) upstream from A1 showing the overbank flow just above the riffle shear stress measurement site.

peak flow the riffle and poolhead are overbank (but still roughly within the channel as defined at low flow) and the midpool and pooltail overtop the bar to their right (but not the bank edge to their left as shown in Fig. 3.3a) and reactivate the chute (estimated to take approximately 20% of the flow at peak discharge).

Although this unusual hydraulic situation was not originally planned in the experimental design it serves to illustrate that Keller's velocity reversal hypothesis does not always apply in every pool/riffle cycle and channel pattern. This is particularly true in divided channel systems (as in reaches A and B) which are themselves associated with ill defined pools and riffles, but have further complications introduced by the presence of bars and chutes which are active at higher discharges. Further evidence to verify the findings in reach A is described in 3.3 for reach B of the Feshie.

The hydraulic measurements in reach A are strongly supported by the pebble tracer results summarised in Table 3.1. The high shear stress at peak discharge for the poolhead and riffle shown in Fig. 3.1 is reflected in the distances of tracer movement - a mean distance of 17 m for the riffle and 13 m for the poolhead (of those moved). The lowest shear stresses during high flows are in the pooltail and the tracers here moved the lowest mean distance - only 6.8 m. If it is assumed that the majority of pebbles move near the peak discharge (although there is some size and shape selection as will be shown later in Chapter 4) then the distance of travel seems to correlate well with the flow strength. The unusual hydraulic situation in reach A resulted in the riffle having both the highest percentage and the furthest distance of pebble movement which is consistent with the shear stress measurements but the opposite of Keller's hypothesis.

Table 3.1 Dubhaig reach A pebble tracing results and bed grain size for different subunits of a pool/riffle cycle.

Site	Subunit	D_{50} mm	No. Inserted	% Recovery	% * Moved	Mean dist. moved of all pebbles m	Mean dist. moved of those moved m
1	Riffle	113	208	59	67	11	17
2	Poolhead	122	183	63	57	7.6	13
3	Midpool	144	184	71	61	7.8	13
4	Pooltail	110	170	73	66	4.5	6.8

* Of those pebbles found.

The bed surface grain size did not match this hierarchy in shear stress and sediment competence as convincingly. Following the arguments of Keller (1971) that bed sorting takes place at high flows then it would be expected that the areas of high shear stress at peak discharge would be competent to move the coarsest material and would deposit them in the areas of low shear stress. For reach A this should result in the riffle and poolhead being finer than the midpool and pooltail. Table 3.1 shows that this is not so clear-cut despite the midpool being markedly coarser than any of the other subunits. The pooltail is surprisingly fine but this could be explained by the Wolman sampling of the pooltail infringing on the finer bartail area rather than keeping strictly within the low flow channel.

Finally it is interesting to note that Fig. 3.1 implies that the reversal in hydraulic properties occurs at a discharge of approximately 2 $m^3 s^{-1}$ for the pooltail, 6 $m^3 s^{-1}$ for the midpool and 10 $m^3 s^{-1}$ for the poolhead. These 'reversal discharges' can be compared with the results of Keller (1971), Andrews (1979), and Lisle (1979). Although Andrews and Lisle never looked at subunits within the pool/riffle cycle the midpool was probably taken as the representative pool site. As mentioned earlier Andrews (1979) found that the reversal in hierarchy between the pool and riffle was at about 60% of the bankfull discharge which is similar to the results of Lisle (1979) who found that it was between 50 and 90% of bankfull flow. Keller's original paper in 1971 used data from the centre of the pool and showed a velocity reversal at a discharge of 4.5 $m^3 s^{-1}$ which he stated had a recurrence interval of 1.2 years (he did not quote the bankfull discharge). In his 1972b paper Keller also plotted previously unpublished data for the bottom velocities of the "end of the pool" site versus the riffle. Although there is a slight convergence of the velocities, their similar gradients led Keller (1972b) to suggest that "the processes which may cause the reversal may dissipate at the end of

the pool."

As already discussed because of the local bed and bar topography in reach A the pool and riffle subunits do not match the Keller (1971) velocity-reversal hypothesis. Keller's work showed that the poolhead would be the first to experience a velocity reversal (the increase in velocity being greatest here) and the midpool then pooltail requiring progressively higher discharges before their velocities exceeded the riffle velocities (if at all). In the case of reach A the pooltail was the first to exceed the riffle velocities and the midpool then poolhead 'reversing' at higher flows. This is qualitatively the opposite of Keller's (1971) work but corresponds to the special hydraulic situation for reach A. Taking the midpool as an average of the pool sites the velocity reversal occurs at somewhere near bankfull discharge (which is equalled or exceeded 0.3% of the time) and is in the range suggested by Keller (1971), Andrews, (1979), and Lisle (1979).

3.2.2 Reach B

The hydraulic measurements in reach B are depicted below in Fig. 3.4. The shear stress measurements (n = 7) were taken in discharges up to 5.5 $m^3 s^{-1}$. As mentioned earlier there is considerable scatter of the riffle shear stress points (r^2 = 38%, calculated t = 1.8) so that the gradient and position of the regression line in Fig. 3.4 can only be taken as approximate. Despite this the riffle points plot much higher than most of the pool data points below about 4 $m^3 s^{-1}$ and the gradients of the riffle shear stresses lead to a cross-over of hydraulic properties with the pool subunits at around bankfull discharge. At high discharges the shear stresses of the pool subunits separate out in the order midpool > poolhead > pooltail. This is closely matched by the pebble tracer movements shown in Table 3.2 although the poolhead tracers again travelled the furthest

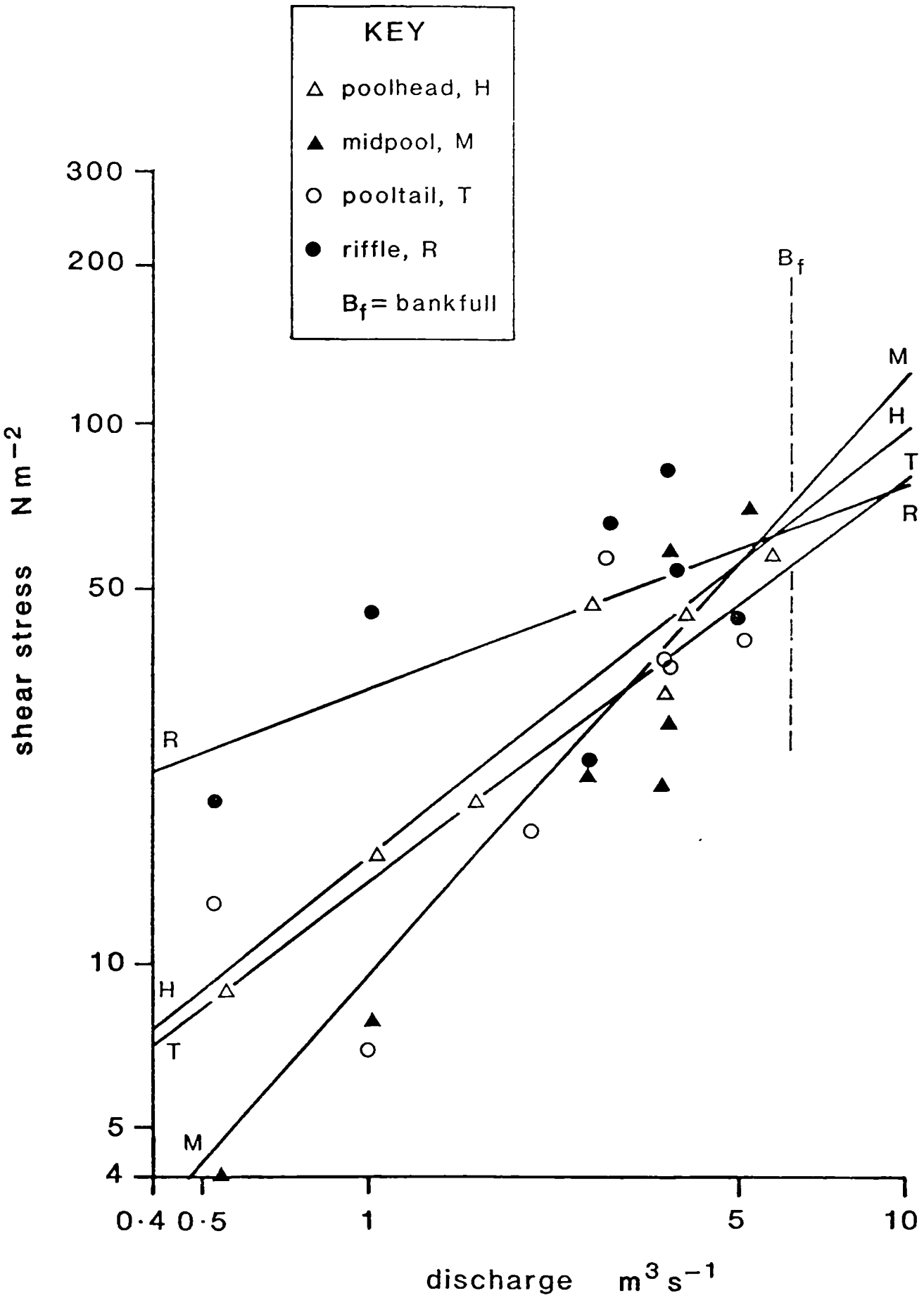

Fig. 3.4 Measured changes in shear stress with discharge for different subunits of a pool/riffle cycle in reach B of the Dubhaig.

Table 3.2 Dubhaig reach B pebble tracing results and bed grain size for different subunits of a pool/riffle cycle.

Site	Subunit	D_{50} mm	No. Inserted	% Recovery	% * Moved	Mean dist. moved of all pebbles m	Mean dist. moved of those moved m
5	Poolhead	75	114	60	65	18	28
6	Midpool	66	118	64	84	18	22
7	Pooltail	68	128	75	90	12	14
8	Riffle	87	128	72	70	7.9	11

* Of those pebbles found.

average distance. The riffle pebble tracers did not move as far as the tracers from any of the pool subunits lending further support to there being a velocity-reversal at high flows during which bed sorting takes place.

The percentages of pebbles that were moved during the four flood events show that the poolhead had up to 25% less movement than the other three subunits. This paradoxical situation whereby the poolhead pebbles travelled the furthest, but had the least percentage of movement can be explained by the low tracer recovery rate for the poolhead (60% compared to over 75% for the pooltail) which suggests that the missing pebbles were probably not buried at their original locations but had moved well out of the reach.

The grain size distribution of the surface bed material again shows the difference in competence between the pool and riffle units with the riffle considerably coarser than all the pool D_{50} measurements (i.e. a deposition zone for coarse material moved from the poolhead upstream) although the individual pool subunits do not separate out as clearly (probably because of the presence of lag material in the poolhead and the similarity between the ratings for each subunit as shown in Fig. 3.4).

3.2.3 Reaches C, D, and E

As described in 2.1.2, reaches C, D and E have channel patterns close to the conventional meandering and straight types described by Leopold and Wolman (1957). Reach C is a transitional form between a divided and single channel pattern but is similar to reaches D and E in that the pool/riffle cycle is much more obvious and easy to recognise compared to reaches A and B.

In reaches C to E shear stress measurements were taken at both the top and bottom of each riffle. As Fig. 3.5 shows for reach C, there is a clear difference in the magnitude of shear stress between riffle sites (which are only 5 m apart) but the rate of change is almost identical. This is also true for reaches D and E although the difference in the shear stress values are not as marked. The bottom of the riffle would normally be expected to have a greater shear stress than the top because the flow would have already gained momentum, but reach D shows that this is not always the case especially if the riffle diverges considerably downstream at low flow. Taking the mean position of the riffle sites Fig. 3.5 shows that for reach C there is a reversal in shear stress at about 3 $m^3 s^{-1}$ which is lower than the reversal discharge found in reaches A and B (but is similar to reach D whilst reach E is even lower as shown later). This magnitude of discharge was exceeded 3.8% of the time (about 14 days) so that there is plenty of scope for sediment movement from the pools if the shear stress reaches competent values (see 4.5).

In reach C at discharges around bankfull the pool subunits increase in shear stress in the order midpool < poolhead/pooltail. Table 3.3 shows that this pattern is generally followed by the tracer and grain size results. Again the poolhead is the dominant source of pebble movement with 80% movement (tracers moving double the mean riffle distance) and all the pool subunits moving pebbles further than the riffle. The pooltail which has the greatest rate of increase in shear stress with rising discharge has a high recovery rate of 89% but a surprisingly low mean distance of movement (only just more mobile than the riffle). The grain size distributions lend further support to the velocity reversal shown in Fig. 3.5 with the riffle much coarser than all the pool subunits and this time the pooltail much finer than the poolhead and midpool (suggesting that there is movement of coarse material from the pooltail at high discharges as implied from Fig. 3.5).

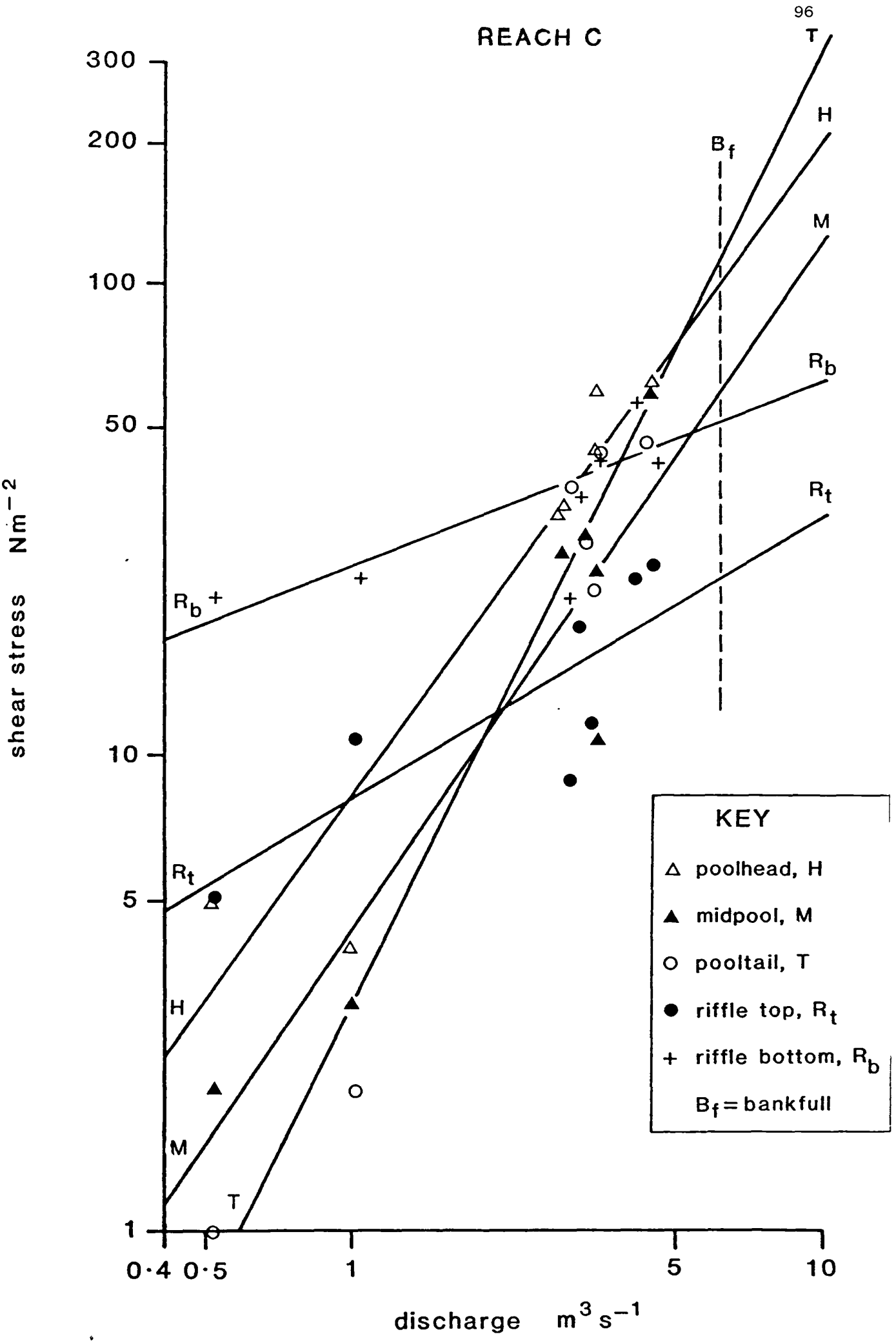

Fig. 3.5 Measured changes in shear stress with discharge for different subunits of a pool/riffle cycle in reach C of the Dubbaig.

Table 3.3 Dubhaig reach C pebble tracing results and bed grain size for different subunits of a pool/riffle cycle.

Site	Subunit	D_{50} mm	No. Inserted	% Recovery	% * Moved	Mean dist. moved of all pebbles m	Mean dist. moved of those moved m
9	Poolhead	64	104	68	80	23	29
10	Midpool	62	100	76	84	16	19
11	Pooltail	52	168	89	64	10	16
12/13	Riffle	70	150	66	67	10	14

* Of those pebbles found.

The hydraulics with changing discharge for reach D are shown in Fig. 3.6. The pattern is similar to that for reach C in that there is a reversal of shear stress at about 3 $m^3 s^{-1}$. At around bankfull discharge the shear stress in the different units increase in the order riffle top/bottom < midpool < pooltail < poolhead although all the pool subunits have a very similar rate of change of shear stress with increasing discharge. At low discharges both the riffle top and bottom are greater than all the pool subunits with the riffle top having higher shear stresses since the riffle has room to diverge downstream at low flow (and therefore spread the same amount of flow over a larger area which reduces the shear stress). The pebble tracer results complement the shear stress measurements with the distances moved from each of the pool subunits almost identical and all more than three times the distances moved by the tracers from the riffle (Table 3.4). The pooltail was the most efficient in moving coarse sediment with 93% of its pebble tracers moved and the joint highest mean distance of movement (although it had a low recovery rate of 47%). The riffle had a low recovery rate of 50% which together with the results of the distances travelled of those found, suggests that most of the riffle pebbles were buried in close proximity to their original locations.

The riffle was again much coarser than all the pool subunits suggesting that it was a depositional zone at high flows and also helping to explain the burial of tracers just discussed. The pooltail and poolhead were the finest subunits of the pool suggesting that they may be the main contributors of coarse sediment for the riffle at high flows (consistent with the shear stress measurements in Fig. 3.6).

Finally, the hydraulic measurements in reach E are shown in Figs. 3.7a-b. As discussed earlier because of the low shear stress values the hydraulic interpretations will be based on the arithmetic plot in Fig. 3.7a. The

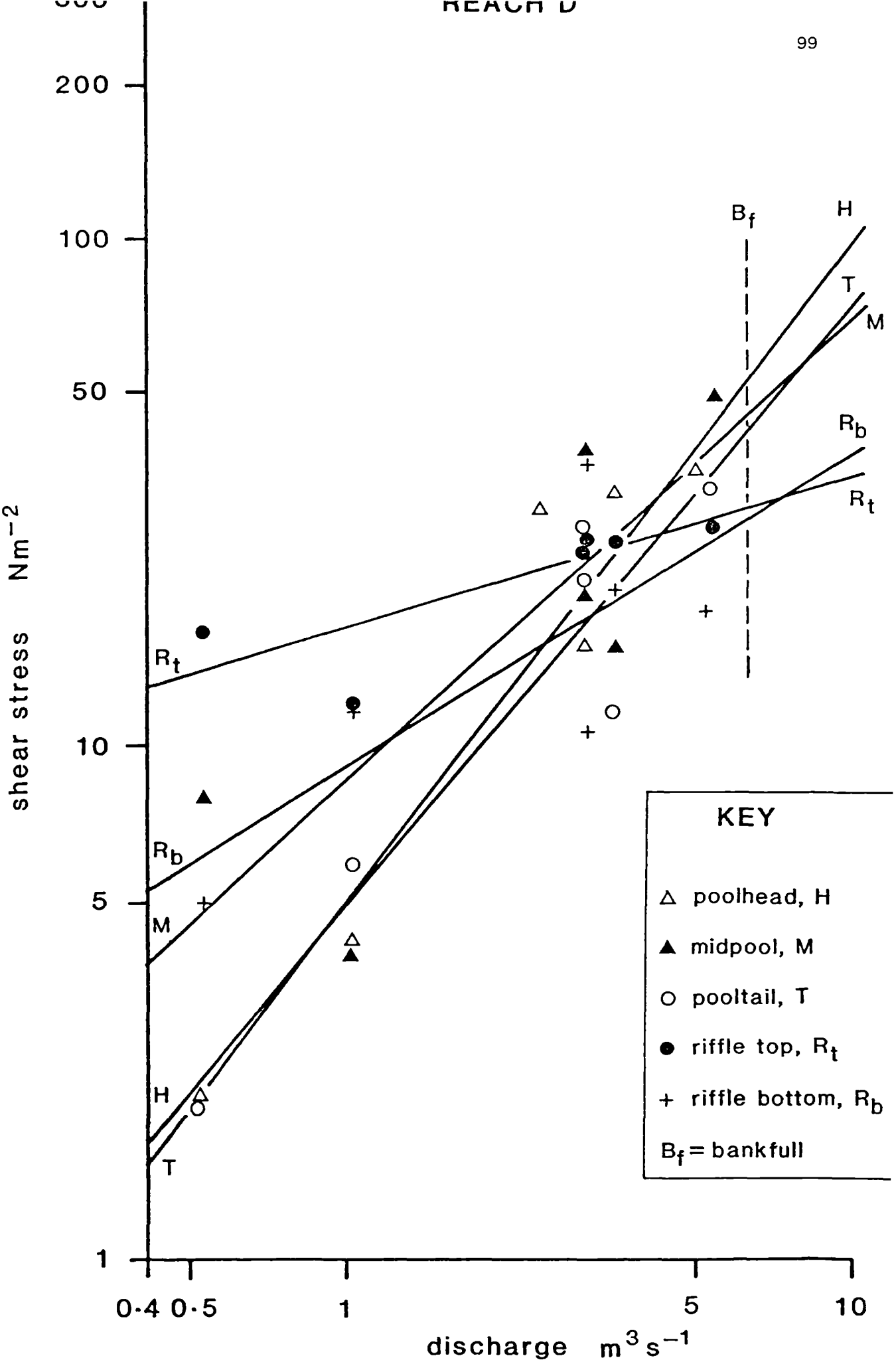

Fig. 3.6 Measured changes in shear stress with discharge for different subunits of a pool/riffle cycle in reach D of the Dubhaig.

Table 3.4 Dubhaig reach D pebble tracing results and bed grain size for different subunits of a pool/riffle cycle.

Site	Subunit	D_{50} mm	No. Inserted	% Recovery	% Moved *	Mean dist. moved of all pebbles m	Mean dist. moved of those moved m
14	Poolhead	63	121	76	79	14	18
15	Midpool	70	110	66	84	17	20
16	Pooltail	60	106	47	93	17	18
17/18	Riffle	78	116	50	74	3.9	5.3

* Of those pebbles found.

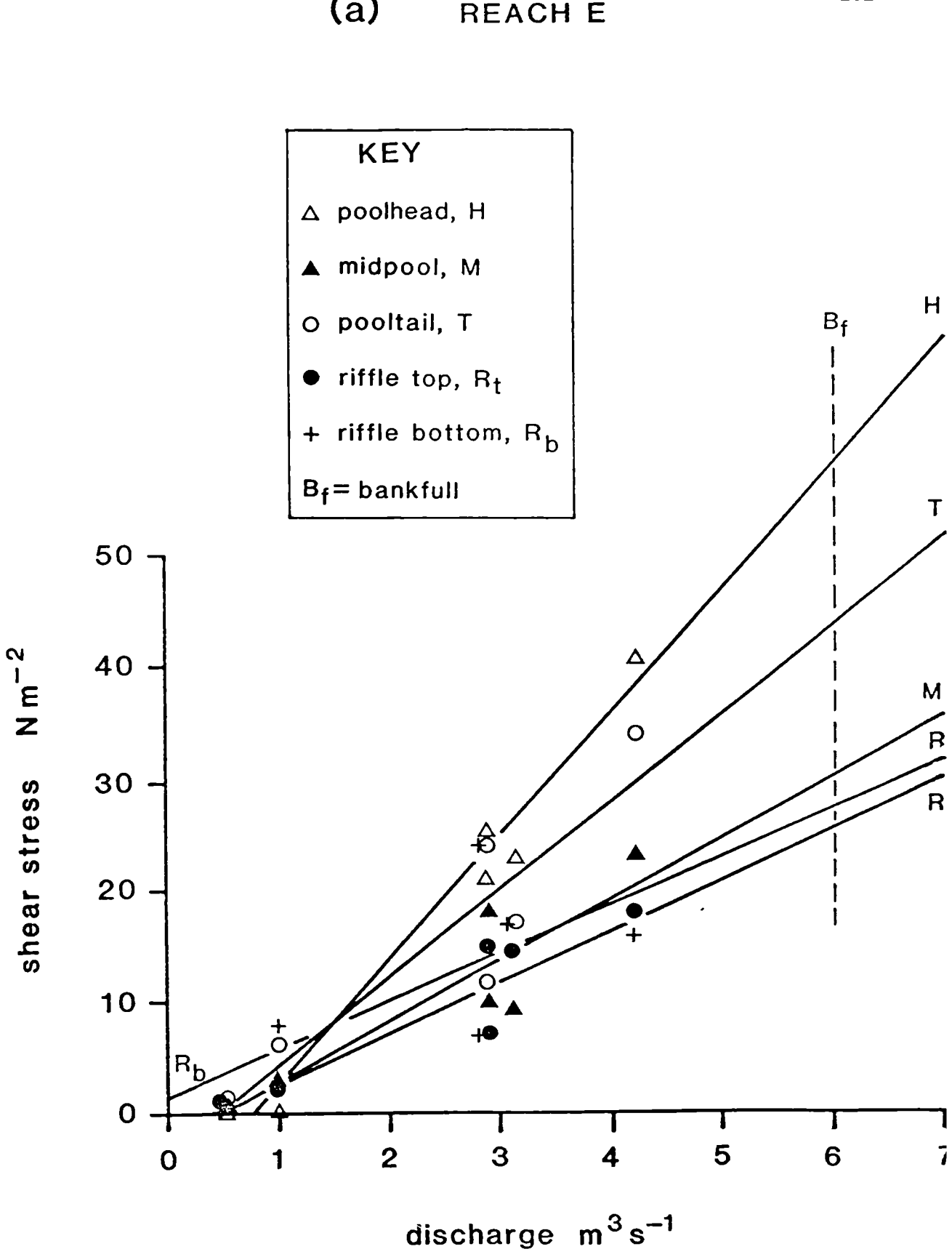

Fig. 3.7 Measured changes in shear stress with discharge for different subunits of a pool/riffle cycle in reach E of the Dubhaig (a) arithmetic plot, (b) logarithmic plot.

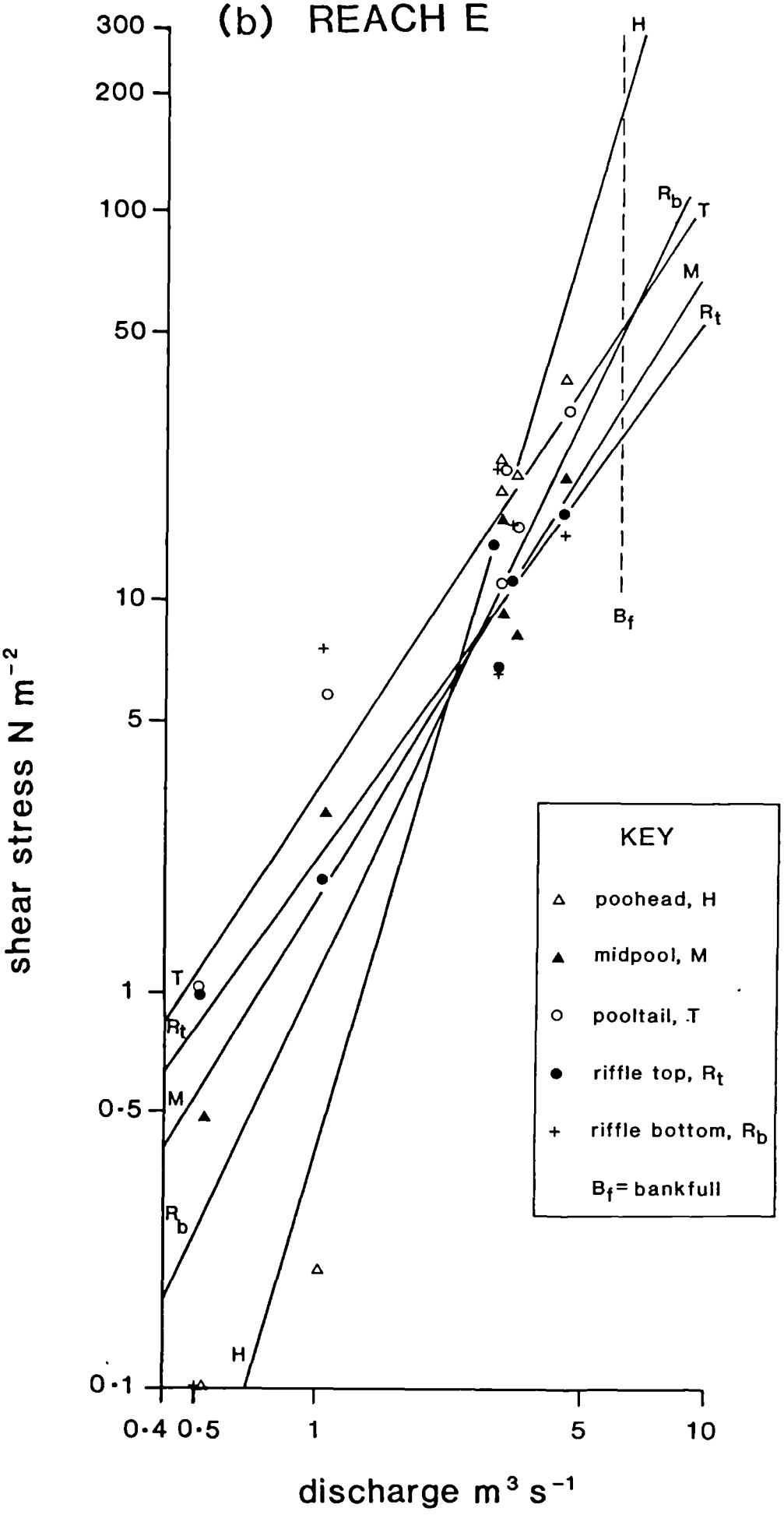
(b) REACH E
300
200
100
50
10
5
1
0·5
0·1
0·4
0·5
1
5
10
shear stress N m⁻²
discharge m³ s⁻¹
H
Rb
T
M
Rt
Bf
KEY
poohead, H
midpool, M
pooltail, T
riffle top, Rt
riffle bottom, Rb
Bf = bankfull

Table 3.5 Dubhaig reach E pebble tracing results and bed grain size for different subunits of a pool/riffle cycle.

Site	Subunit	D_{50} mm	No. Inserted	% Recovery	% * Moved	Mean dist. moved of all pebbles m	Mean dist. moved of those moved m
19	Poolhead	40	90	86	51	7.1	14
20	Midpool	40	88	90	60	6.0	10
21	Pooltail	40	85	91	57	5.8	10
22/23	Riffle	40	103	90	47	2.2	4.6

* Of those pebbles found.

gradients and intersections of the shear stress ratings for all the subunits however are reasonably similar for both plots in Figs. 3.7a-b with the poolhead clearly having the greatest rate of increase of shear stress with rising discharge and the riffle sites the lowest. The reversal in shear stress between the pool and riffle subunits is at around 1.5 $m^3 s^{-1}$ which is much lower than reaches A to D. The pebble tracer results in Table 3.5 again follow the trends in flow strength with all tracers from the pool subunits moving a greater distance than the riffle. The poolhead tracers moved the furthest (mean distance of 14 m) and the riffle the least (5 m). The percentage movement did not show a convincing pattern although the riffle moved the least amount out of all the subunits. The recovery rates were all very high (> 85%) reflecting the low shear stresses plotted in Figs. 3.7a-b and the size of the pebble tracers compared to the surrounding bed material (as discussed in 5.5.2). Since the bed surface grain size was fairly uniform, only one Wolman sample was taken (from the riffle with a D_{50} of 40 mm) so no comparisons can be made between the at-a-point shear stress measurements and bed roughness.

3.3 The Feshie Experiments

The work in the Feshie was on a much smaller scale than the Dubhaig and did not permit the construction of rating curves of shear stress and discharge. A pool/riffle cycle was selected in reach B (B5-B6.5) and reach C (C2-C6). The subunits in the pools and riffles were identified and located along the cross-section survey lines. In reach B the shear stress was measured on three occasions on 2/5/86 during a rising snowmelt discharge from 11 to 23 $m^3 s^{-1}$ (the latter close to bankfull). To supplement the hydraulic measurements, tracer pebbles had been placed at six locations two weeks prior to the snowmelt discharge. A total of 311 pebbles were placed in the riffle (B5), poolhead (B5), midpool (B6) and

pooltail (B6.5). An additional 68 pebbles were placed at two other locations - at section B6.5 in a backwater on the right-hand side of the channel, and on the top of a retreating bank at section B5 within 2 m of the water's edge.

The hydraulic measurements in reach C were very limited and confined to a single set of readings on 4/4/85 in a moderate snowmelt discharge of approximately 14 $m^3 s^{-1}$. A total of 300 pebble tracers were inserted in the riffle (C1), poolhead (C3) and pooltail (C5) in the summer of 1985 and traced through two flood events on 1/9/85 and 3/12/85 with peak discharges of 59 and 89 $m^3 s^{-1}$ respectively (see 5.3.2 for a discussion of these floods). The tracer results were analysed as part of an undergraduate dissertation (Brewster 1986).

The results for reach B are summarised in Table 3.6. Only the first and final set of shear stress measurements are included in Table 3.6 to highlight the differences between low and high stage (the middle set of readings are discussed in 5.3.1). The shear stress results show that at the lower discharge the riffle had the highest shear stress while the pool subunits decreased in flow strength downstream. An additional section B5.5 which was at the head of the long midpool had a shear stress of 49 ± 12 N m^{-2} at the lower discharge which complements this downpool decrease in flow strength. As the stage rises there is a cross-over of hydraulic characteristics with the riffle actually recording a lower shear stress than previously (Table 3.6). The poolhead and midpool still dominate the pool unit with the poolhead having the highest rate of increase in shear stress (31%) compared to the 25% increase in the midpool and 22 and 21% in the pooltail sites. The shear stress at B5.5 however was 75 ± 20 N m^{-2} at the bankfull discharge (a 53% increase) showing that the upstream end of the midpool was also an area of strong flow at high discharges. Notably the crossover takes place within the range of bankfull discharge as found

Table 3.6 Feshie reach B hydraulics, pebble tracer and bed grain size results for a site on the top of the floodplain margin and different subunits of a pool/riffle cycle

Site	Subunit	Early τ N m^{-2}	Late τ N m^{-2}	D_{50} mm	No. Inserted	% Recovery	% Moved ***	Mean dist. moved of all pebbles m	Mean dist. moved of those moved > 2.0 m m
5	Riffle	86*	66 ±12	62	73	89	62	3.3	5.7
5	Poolhead	53 ±6	69 ±12	87	116	6.0	100	73	73
5	Overbank	-	-	-	41	39	100	93	93
6	Midpool	36 ±8	45 ±10	68	68	32	96	85	89
6.5	Pooltail	32 ±4	39 ±7	54	54	41	46	49	55
6.5	Pooltail B'water	24 ±1	29 ±6	**	27	74	90	7.9	19

* Two propellers only

** Not measured

*** Of those pebbles found

for reaches A and B of the Dubhaig.

The explanation for the seemingly abnormal shear stress change in the riffle is linked to the earlier argument in 3.2.1 for reach A of the Dubhaig. In any channel that can increase its width with an increase in discharge Keller's (1971) hypothesis need not hold true. In the case of reach A in the Dubhaig, at a high discharge the pool overtopped a side bar to reactivate a chute on the opposite side of the channel and therefore any further increase in stage would spill over the bar into this new channel. The riffle in reach B of the Feshie is a much simpler example of this increase in cross-sectional area. The Feshie has been described by Ferguson and Werritty (1983) as a wandering gravel river with characteristic wide and shallow channels flanked and locally divided by expanses of bar gravel. At the head of reach B the diagonal riffle is up to 60 m wide with either end of the riffle bordered by low relief gravel bars. As the stage rises the flow simply broadens the riffle as compared to the flow in the poolhead which is confined by a semi-vegetated but uncohesive bank on its left side and a steep avalanche face of a long diagonal bar on its right. The increase in flow does not seem to increase the shear stress appreciably on the riffle (the drop in shear stress could easily be accounted for by the misplacement of the current meter on the third occasion), whilst the confined pool has a more rapid increase in shear stress since all the flow must come down approximately the same channel width. This situation reveals an important flaw in Keller's (1971) work and subsequent researchers who have assumed that the velocity reversal hypothesis holds true in all channel patterns. The two cases of reach A in the Dubhaig and reach B of the Feshie indicate that if the channel is allowed to freely migrate and re-occupy chutes and submerge bars, then little increase in shear stress can be expected at any point in the active channel with rising discharge.

Further evidence to support this idea comes from the pebble tracing results for reach B summarised in Table 3.6. The average distances travelled by the tracers were similar for all the pebbles found (moved or not) and those that had moved a distance greater than 2.0 m. Table 3.6 shows that of the six inputs of pebble tracers the riffle pebbles moved the least average distance, the midpool and poolhead both moved long distances, while the overbank pebbles moved the greatest distance. The pooltail moved the least distance out of all the pool subunits with the backwater pebbles not surprisingly only moving a few metres. The percentage movement from each subunit shows that all of the poolhead and overbank pebbles and 96% of the midpool tracers were moved. The pooltail backwater surprisingly moved 90% of its tracers but the mean distance of movement shows that this was only a small 'hop' or 'topple' of a few metres downstream. All these results are again consistent with the hydraulic measurements and the previous results described in 3.2 for the Dubhaig. The highest rate of increase in shear stress measured at bankfull discharge for the tracer sites was in the poolhead and excluding the overbank pebbles (discussed later) they moved the second highest mean distance. The low recovery rate of 6% (compared to 40% overall) however suggests that a lot of the pebbles may have either moved early on to be deposited and then buried, or that they have been moved well out of the study reach. The discussion in 5.3.1 supports either of these possibilities with both a rapid aggradation of a new bar at B6-B7 and strong convergent flow at B5-B5.5. The almost constant or slow rate of increase in shear stress on the riffle at discharges around bankfull was not strong enough to mobilise a great proportion of the bed and only the occasional pebble was moved (and a small distance). The large width together with the diagonal flow direction across the riffle ensured that the pebbles only moved a few metres and did not tumble down the avalanche face into the poolhead where the shear stress was much greater at a higher discharge.

The bed surface grain size does not reflect this pattern of tracer movement and flow strength as shown in Table 3.6. The poolhead is much coarser than the riffle and both are coarser than the other pool subunits. The reason for this became obvious during the Wolman sampling of the bed surface. As is common for streams running through valleys with deep infills of poorly sorted till, over time a coarse lag of boulders builds up where the finer material has been winnowed out. Despite the pool being more competent to move coarser material than the riffle at high discharges there are still some very large boulders that are only rarely (if ever) moved onto the riffle so they remain in the pool. Hence the pool can be coarser than the riffle.

Up to now the significance of the distance moved by the pebbles placed overbank at B5 has not been discussed. This result is very important and needs to be analysed in some detail. The pebbles were placed arbitrarily in a line stretching 2 m from the bank edge. The bank is a section through the right margin of an area of floodplain cut off when the river switched in 1976-77 (Werritty and Ferguson 1980). Despite the vegetation cover the banks are uncohesive (made up of relict bars) and readily collapse. Field observations during the snowmelt flood on 2/5/86 showed that the bank collapse is by a process of selective entrainment (or 'sapping') of the fine sand matrix at the water's edge. This leaves a loose pile of cobbles which then are easily entrained and cause the bank material above to collapse and enter the channel. During the six week period between the pebble tracer insertion and recovery, the bank at B5 retreated by 2.5 m so that all the tracer pebbles fell into the river. Once in the channel their protrusion relative to the surrounding bed material is much larger than the rest of the imbricated bed material and therefore they are easily entrained (c.f. Carson 1986 and section 4.1). The results in Table 3.6 show conclusively that these pebbles were more

available for transport than their other tracer counterparts which were seeded into the bed (all pebbles found moved a distance of at least 3.0 m and up to a maximum of 282 m).

The significance this result has for channel changes and bar development will be discussed in 5.5.2, but briefly it seems in rivers that have uncohesive banks, high stream powers and freely migrating channels, the major source of sediment for bar development is from the channel banks (which themselves are usually relict bars). This has also been observed by Baumgart-Kotarba (in press) for a similar wandering gravel-bed river in the Carpathians, Poland. The Dubhaig has well vegetated stable banks which release little sediment so the major source of material for bar development is from the reworking of the channel bed. As 5.4 will show though, the Lyngsdalselva with its characteristically loose bank edges can retreat up to 6 m in a single flood event which can lead to up to 1 m of aggradation immediately downstream. In retrospect similar pebble tracing experiments in different rivers and at various locations along the bank edge might have helped to pinpoint the sources of coarse sediment for bar development. Previous work reported in the literature using pebble tracers have always used pebbles inserted within the channel (excluding the study of Kondolf and Matthews (1986) using eroding dolomite riprap). If the banks are retreating rapidly, any pebble tracing programme or bar development study must take into account the differences in protrusion and therefore ease of entrainment of coarse sediment tumbling into the channel from bank edges. More work is needed in this area for rivers with different channel patterns, stream powers and grain size distributions of both the banks and bed material.

The study in reach C was very limited and can only be discussed in general terms. The shear stress measurements at the riffle, poolhead, midpool and pooltail were 34 ± 1, 122 ± 12, 46 ± 10, and 47 ± 5 N m^{-2} respectively at

a discharge of about 14 $m^3 s^{-1}$. If these results are representative (they were all replicated at least three times) then they suggest that the pool subunits had all exceeded the riffle shear stress at a discharge at well below bankfull.

The tracer results in this reach are briefly summarised in Brewster (1986). Unfortunately the midpool was not included as a tracer site and the report does not quote the mean distances of travel for each subunit. Despite this, Brewster (1986) states that in the two tracing experiments the poolhead pebbles moved the furthest, which again fits into the results from other reaches and channel patterns discussed previously and also the provisional shear stress measurements taken. Statistical analysis for both experiments showed that there was a significant difference (0·05 level) between the distances moved from the poolhead and both the pooltail and riffle, although there was no significant difference between the distance moved from the pooltail and riffle (Brewster 1986). The bed surface grain size follows the pattern found in reach B with the poolhead coarser than the riffle (due to coarse lag material) but both subunits much coarser than the pooltail.

3.4 Discussion

The results in 3.2 and 3.3 give sufficient information to tentatively put forward a general model of response of the pool/riffle cycle to a changing discharge. Altogether the Dubhaig and Feshie provided results from hydraulic measurements, pebble tracers and bed surface grain sizes for seven reaches. Of the six different channel patterns only reach A of the Dubhaig and to a lesser extent reach B of the Feshie deviated from Keller's (1971) velocity-reversal hypothesis. What seems clear is that divided and freely migrating channels have a complicated response to a change in discharge which can involve widening of the cross-sectional area

available for flow and therefore a lower than average rate of increase of shear stress. This would not alter the relationship between the rate of change of shear stress in the pool versus that in the riffle if both were allowed to increase their channel area simultaneously. However, in the cases of reach A in the Dubhaig and reach B of the Feshie the increase in stage is only allowed to spread itself over a larger bed surface area in one of the channel units, while the other is confined within steep bank edges or bar avalanche faces. This leads to a differential rate of increase in shear stress with the subunits containing the narrowest concentration of flow having the fastest rate of change. Despite this complication, the response of the pool subunits and riffle to an increase in discharge still follows a predictable pattern with the highest shear stress zones (confined flow) having the furthest mean distance of pebble tracer movement (and in most cases the highest percentage of movement).

This interrelationship between the flow strength and sediment movement is also present in reaches B, C, D, and E of the Dubhaig and reach C of the Feshie. The shear stress measurements in these reaches show that as the stage rises the riffle (initially at a high shear stress) increases in shear stress at a lower rate than the pool. Furthermore, within the pool the fastest rate of increase in shear stress is at the poolhead, decreasing in magnitude down-pool. All reaches show that there is a velocity (or shear stress here) reversal as first reported by Keller (1971) as the pool's depth increases to a point where its product with the slope is greater than that at the riffle (an assumption based on the Du Boys formula but supported by at-a-point shear stress measurements). The discharge at which this reversal occurs seems to be near or just below the bankfull discharge which is consistent with the results reported by Andrews (1979) and Lisle (1979). Since most of the shear stress measurements reported here were taken within the bankfull capacity it is unknown whether the pool/riffle hierarchy continues once the banks are

overtopped but it probably follows the pattern shown by Lisle (1979) with the pool/riffle shear stresses continuing to diverge above the bankfull discharge though at a lesser rate (or gradient) than the within-channel discharges.

Since most of the sediment is entrained at higher discharges in the Dubhaig (see 4.7) and Feshie then the riffle is less likely to entrain sediment compared to the pool. As the discharge approaches bankfull, all subunits of the pool are close to, or in some cases well in excess of, the shear stress in the riffle and the pool becomes the most important contributor of sediment with the poolhead the overall dominant channel subunit. The pools are scoured at high discharges and the coarse sediment is moved onto the riffles and bars which have lower shear stresses and are not as likely to move the pebbles. Hence the riffles are coarser than the pools (for the Dubhaig reaches B, C, D, and E, and reach C of the Feshie). There is some degree of bed material sorting within the pool with a down-pool coarsening from the finer poolhead (which has the highest rate of increase and magnitude of shear stress at high discharges and therefore scours the coarsest sediment off its bed) to the coarser pooltail (which is a lower shear stress zone at high discharges and therefore a depositional zone for the coarser sediment moved from the poolhead). All the ratings of shear stress and discharge show that the pool subunits increase at very similar rates and magnitudes of shear stress (a narrow band) so that the within-pool sorting can easily be masked by the spatial differences in shear stress (and further complicated by the presence of lag material that rarely moves). Furthermore the zones of high shear stress are more likely to erode the bank material (especially if it consists of uncohesive relict bar gravels as in the case of the Feshie) and therefore supply coarse sediment to replenish the scouring bed material. All these factors interact to complicate the formation of any definite spatial pattern in the pool bed grain size. Despite this a

general model of the response of the pool/riffle cycle to an increase in discharge can be put forward and is illustrated in Fig. 3.8.

The combined and averaged distances of pebble tracer movement for all five reaches of the Dubhaig also support this model with the mean distance of travel (whether of all those found, or just those moved) increasing in the order riffle < pooltail < midpool < poolhead (Table 3.7). Interestingly though the percentage movement from each subunit (and recovery rates) are very similar which suggests that the differences in shear stress between different subunits in the pool/riffle cycle do not affect the total amount of sediment movement (% moved) but do influence the distance travelled when the particles are eventually entrained (mean distance).

As the discharge increases and there is a reversal in hydraulic properties, the poolhead is usually the first to reach a competent shear stress that can move large sizes of material (assuming that they move at high discharges). The poolhead (and then in the order midpool, pooltail, riffle) pebbles would be the first to be released from the surface armour. Their protrusion would automatically increase to 100% of their surface area and they would begin to travel downstream. Since the poolhead pebbles would be entrained first they are exposed for a longer time in high competent shear stresses (even if these shear stresses are lower in other subunits where the pebbles may have moved to) and therefore have a better opportunity to travel further.

There are many variations within this general model. The hydraulic conditions and the nature of the bed upstream, the spatial variation in bed surface grain size, and the differences in geometry of the pools and riffles both within-reach and between channel types, all have an influence on the change in shear stress and sediment transport with rising discharge. Despite this the results in 3.2 and 3.3 put forward a set of

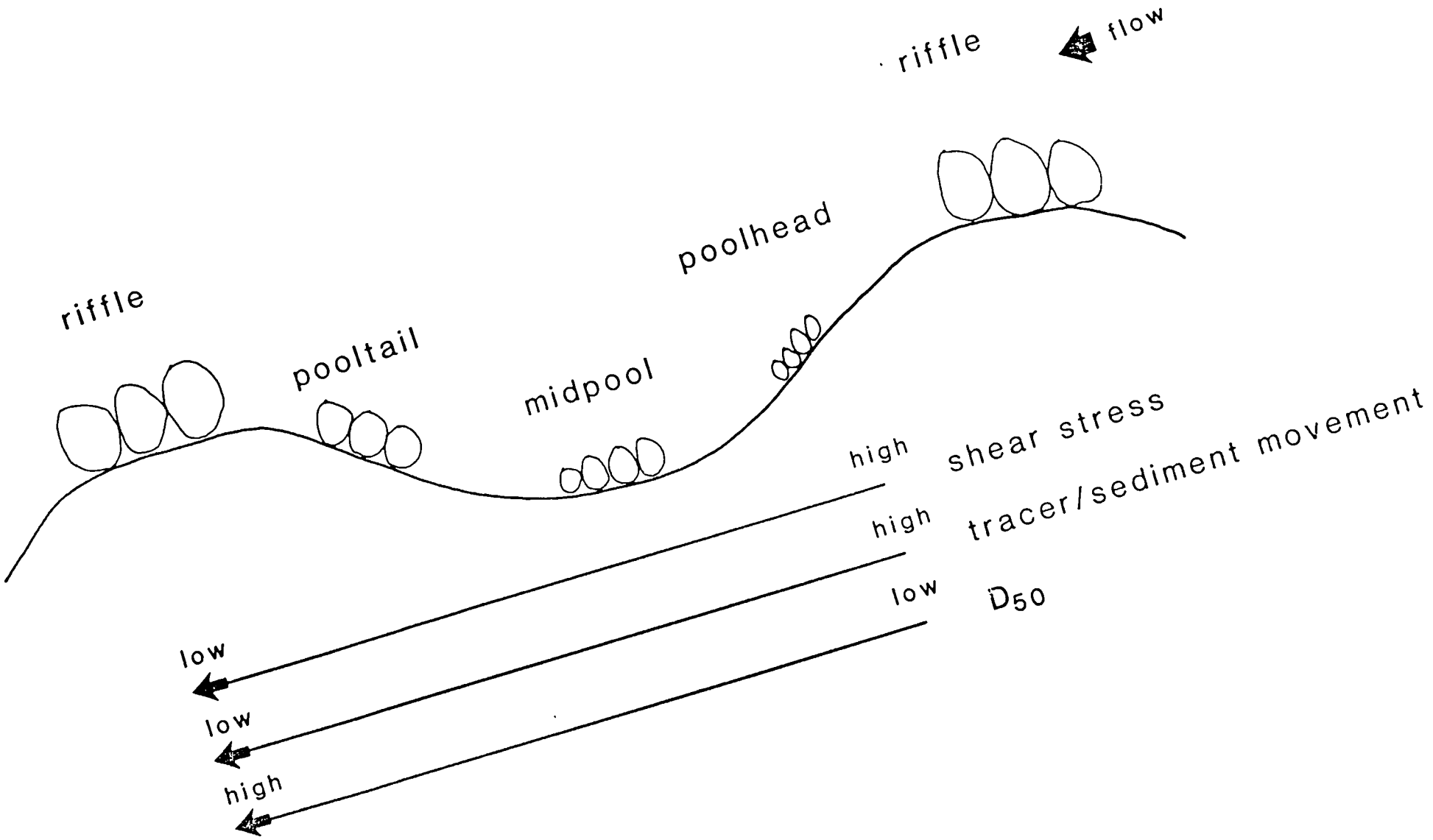

Fig. 3.8 General model of the hydraulics and bedload movement at high flows and the resulting bed grain size sorting for different subunits of a pool/riffle cycle.

Table 3.7 Summary of the pebble tracer experiments for each subunit of the pool/riffle cycle in the five reaches of the Dubhaig.

Subunit	No. Inserted	% Recovery	% Moved *	Mean dist. moved of all pebbles m	Mean dist. moved of those moved m
Poolhead	612	70	66	13	20
Midpool	600	73	73	12	17
Pooltail	657	76	62	9.2	15
Riffle	705	64	64	7.4	12

* Of those pebbles moved.

logical and consistent measurements that give overriding field evidence to support the model. Even when divided channels are considered, the bed D_{50}, tracer pebbles, and shear stress measurements are in the order shown in this model. For example, in reach A of the Dubhaig where the riffle is more competent than the pool at high discharges, the shear stress in the pool still shows a ranking according to the model of poolhead > midpool > pooltail, and likewise for the tracer pebble movement and in general the bed D_{50} (this time coarser in the pool not the riffle). The model is in agreement with the work of Keller (1971), Andrews (1979), and Lisle (1979) but extends their work to different channel patterns, shear stresses and grain size. The model seems to be satisfactory in both high discharges (above the reversal in shear stress which Keller (1971) never proved existed) and in coarse heterogeneous bed material where the entrainment of sediment is restricted by tight interlocking bed structures. The model also lends further support to the hypothesis of sediment movement explored in Chapter 4 by showing that bed sorting takes place at high discharges and that the selective entrainment of different sizes of material is the dominant mode of sediment transport for most of the flow conditions. Furthermore the results here show that the bed armour is rarely broken throughout the whole of the channel system. As the discharge rises the various subunits of the pool/riffle cycle reach competent shear stresses to mobilise most of the bed sediment at different rates and therefore the bed becomes increasingly spatially mobile (as well as more competent within each subunit) as the discharge continues to rise.

4 BEDLOAD TRANSPORT

4.1 Previous work

4.1.1 Introduction

The mechanics of bedload transport has been of interest to scientists for over two centuries. Descriptions of bedforms and their movement are recorded as far back as Du Buat in 1786. Throughout the 19th and early 20th century several investigators provided data and observations from field notes or simple flume experiments (see Mavis et al. (1935) and Mavis et al. (1937) for a discussion of these). In the mid 20th century these were replaced by theoretical and semi-empirical approaches to the problem of describing and predicting bedload transport. In more recent years, with the aid of sophisticated bedload trapping and monitoring mechanisms, direct field measurements have been incorporated into empirical formulae resulting in a general trend of convergence of thought reflected in several major papers in the past four years (for example Parker et al. (1982b), Andrews (1983), Carson (1986)).

The development of bedload transport theory incorporates many diverse studies over a long time-span. The research stems from various scientific disciplines, which can have complicated mathematical formulae. The discussion of this research will therefore only be limited to definitive works and briefly summarise their respective equations and theoretical background. Since the formulae introduce some new variables they are defined below.

4.1.2 Definitions of some hydraulic variables

Most of the theory of sediment transport involves variables or derived variables that frequently re-occur in many equations. To avoid inconsistency and to clarify each term so that they can be adequately substituted in the text by a symbol, four common definitions and formulae are listed below.

(1) Shear stress (τ) : Drag force per unit area acting parallel to the bed on a particle (N m^{-2}).

(2) Dimensionless shear stress (τ^*) : The ratio of the fluid forces keeping a particle in motion to the gravity force tending to keep the particle at rest. Shown by Shields (1936) to be equal to

$$\tau^* = \frac{\tau}{(\rho_s - \rho) g D}$$

where ρ_s and ρ are the sediment and water densities respectively, g the acceleration due to gravity, and D the diameter of the particle under consideration.

(3) Critical dimensionless shear stress (τ_c^*) : The dimensionless shear stress as defined above <u>but</u> at the point where the particle is just beginning to move (i.e. the critical or threshold condition).

(4) Dimensionless transport rate (ϕ) : After Einstein (1950), and is the ratio of the volumetric transport rate per metre width to the gravity forces tending to keep the particles at rest. Einstein (1950) expressed this as

$$\phi = \frac{i_b}{\rho_s \left(\left(\frac{\rho_s - \rho}{\rho} \right) g D^3 \right)^{0.5}}$$

where i_b is the mass transport rate per unit width.

Of the above definitions the dimensionless forms are more useful since they allow comparisons between variables without a consideration of units or scale. The work of Shields and Einstein is elaborated in 4.1.3 below.

4.1.3 The development of modern theory

Research on bedload movement has concentrated on three main areas of interest: (1) the threshold of sediment movement, (2) total bedload transport rates, and (3) size fractional transport rates. Since an understanding of the incipient motion of sediment particles underlies the principles of bedload transport rates, the previous work in this area will be discussed first.

If an experiment was conducted in an open channel with a given slope, uniform noncohesive material, and steady uniform flow, at very low discharges the material comprising the bed would be stationary. As the discharge increases it would reach a certain value when individual particles would begin to move. This condition is known as the *critical condition* or the condition of *incipient motion* of the sedimentary particles. This state is important to recognise and define since it is inherent in most bedload transport predictive equations. Despite its apparent simple interpretation the condition of incipient motion is ambiguous and has been used by many workers to represent different stages in the beginning of sediment transport. The problem centres around

defining what actually is the initiation of sediment transport - is it when a single particle first moves, a few particles move, there is general motion on the bed, or a limiting condition when the rate of sediment transport tends to zero? Some investigators, Einstein (1950) for example, do not accept that a distinct condition for the beginning of sediment transport exists; therefore Einstein did not use the concept of incipient motion in his analysis of bedload transport. The definition of critical motion is so fundamental to some studies of bedload transport that differences in results between workers can often be explained by these different interpretations of the beginning of sediment transport. This problem is highlighted below in a discussion of the development of the theory of bedload transport.

Many of the first measurements of sediment transport in the 19th and early 20th centuries attempted to describe the initial movement of a given size or weight of particle in terms of a critical velocity - either a competent mean velocity or bottom velocity (see Mavis et al. (1935) for a discussion of these). Hjulström's (1935) curve using mean profile velocity is particularly well known though the analysis was restricted to particles smaller than 100 mm with a strong bias to diameters less than 20 mm. These investigations provided some valuable information regarding the competence but as Garde and Ranga Raju (1977) point out, their data suffers from two defects: firstly, often the sediment is described only qualitatively and the true particle size is not given; secondly, in some cases the size is related to bed velocity but there is no mention of the height of the velocity measurement. In addition as Carson (1986) notes it is meaningless to specify a critical velocity for a channel bed of given particle size unless it is at a particle reference level *near* the bed or unless the mean velocity is corrected for the flow depth.

A more serious consideration of sediment movement was given by Gilbert (1914) in his flume study of sediment transport with varying gradient, discharge and grain size. By changing each of these variables one at a time he developed mathematical relationships to show that the stream capacity increases with steeper gradients, higher discharges and smaller calibre of load. Although the determination of the capacity or actual load of a river is not as simple as Gilbert (1914) assumed (since all his variables are interrelated and are also affected by stream width, depth and bed roughness), his study provided data which are still commonly used in modern sediment transport equations. In fact Gilbert was well ahead of his time and also contributed the first observations and measurements on the velocity reversal in pools and riffles (see Chapter 3) and the effects on the transport efficiencies of different size fractions of bedload when the size distribution of the total bedload is altered.

Gilbert's (1914) flume work considering the total bedload transport rate was followed by the classic works of Meyer-Peter and Müller (1948) and Einstein (1942, 1950) which are still popular among engineers today. From flume runs with sediment in the range 0.4 to 30 mm Meyer-Peter and Müller (1948) arrived at the relationship

$$\phi = 8(\tau^* - 0.047)^{3/2}$$

where ϕ is the dimensionless transport rate as defined in 4.1.2. This implies a zero transport rate (or critical conditions) at $\tau^* = 0.047$, which is remarkably similar to the earlier findings of Shields (1936) (as

discussed later), although Meyer-Peter and Müller were apparently unaware of Shield's results. Their work was carried out on different sets of uniform grain sizes and they found that the critical dimensionless shear stresses needed to set a particle in motion were the same, independent of the particle size.

Einstein (1942, 1950) was the first to attempt a semi-theoretical solution to the problem of bedload transport. His first relationship presented in 1942 did not include the effect of bedforms on bedload transport, but in 1950 he outlined a modified and more detailed solution to the problem which included a 'hiding function' to account for smaller particles needing a higher τ^* to set them in motion. This was calculated as a function of the ratio of the particle diameter to a characteristic particle diameter for the mixture (Einstein chose the D_{65} as his characteristic particle size). As stated earlier, Einstein disagreed that a critical condition for sediment movement exists and therefore he avoided using a critical shear stress concept in his bedload analysis. Instead, Einstein assumed that a particle moves only if the instantaneous hydrodynamic lift force exceeds the submerged weight of the particle. Once this particle is in motion, the probability of the particle being re-deposited is assumed equal at all points of the bed where the local flow would not immediately dislodge the particle again. Einstein assumed that the average distance travelled by any particle moving as bedload between consecutive points of deposition, would be constant - independent of the flow conditions, rate of transport and the bed condition. His bedload formula is complicated and is documented elsewhere (for example Yalin (1972) gives a detailed description) but fortunately Garde and Ranga Raju (1977) evaluate some coordinates for his relationship to enable the construction of the curve from Einstein's (1950) equation.

Although Einstein's (1950) formula is popular with engineers and the principles used in it are "sound and adequate" (Yalin 1972), there are

still several weaknesses in his analysis. The main problem arises from Einstein's assumption that there is a constant length of jump for each particle (for natural streams this distance was stated by Einstein to be approximately 100 times the diameter of the particle). As Yalin (1972) notes, there is no experimental evidence or theoretical explanation offered by Einstein (1950) to support the validity of this assumption and subsequent studies have disputed this idea. For a more detailed critical review of Einstein's (1950) work see Yalin (1972 p. 135-142).

Brown (1950) attempted to improve the Einstein (1942) calibration of ϕ against τ^* by transforming to a fully logarithmic plot (Einstein's relationship was semi-logarithmic). The so-called Einstein-Brown formula for $\tau^* > 0.1$ simplifies into a relationship of the form

$$\phi = 40(\tau^*)^3$$

As in the Einstein (1942, 1950) equations the flume data of Gilbert (1914) and Meyer-Peter et al. (1934) were also used by Brown (1950) to support his relationship (over a size range from 0.3 to 28.6 mm). At lower values of τ^* the 'linear' log-log extrapolation overestimates the actual transport rate since unlike the Meyer-Peter and Müller (1948) formula the Einstein-Brown relationship does not contain a threshold for the dimensionless shear stress.

Parker (1978) plotted the data from 278 gravel-bed channels (mostly flume) from the Peterson and Howells (1973) compendium and by fitting a line by eye arrived at the relationship

$$\phi = \frac{11.2(\tau^* - 0.03)^{4.5}}{\tau^{*3}}$$

This is very similar to the Meyer-Peter and Müller (1948) relationship both with its implied threshold of dimensionless shear stress of 0.03 and its simplification into a 1.5 power law at high transport rates. The relationship of Parker (1978) however does not have any gravel flume data points at $\phi > 0.02$ and only six points using artificial material with $\rho_s < 2.65$ at $\phi < 0.4$ (see Fig. 4.4 later).

The flume and semi-theoretically derived relationships of Meyer-Peter and Müller (1948), Brown (1950), Einstein (1950) and Parker (1978) were all obtained considering a bed with uniform sediment (or usually an amalgamation of results from several independent studies with beds of different grain size). Their equations predict the total bedload transport rate for a given dimensionless shear stress. However, with the exception of the revision by Einstein (1950), none of these equations considered movement from nonuniform or heterogeneous bed material which is common in gravel-bed rivers. Even the Einstein (1950) equation only corrects for the reduction of fluid flows on a particle owing to the presence of larger nearby particles and there is no allowance for the increased exposure to the flow of the coarsest particles (Misri et al. 1984). Furthermore the equations of Meyer-Peter and Müller (1948) and Parker (1978) indicate a threshold value for τ^* of 0.047 and 0.03 respectively regardless of particle size. These equations have since been used by engineers to predict sediment transport from mixed beds based on the assumption of a single representative value for particle diameter (usually D_{50}).

The first work on the initiation of sediment movement (or critical conditions) was published by A. Shields in 1936 using a series of flume experiments with bed material ranging, in different runs, from 0.36 to 3.44 mm. His aim was to determine τ_c^* for different particle sizes at

various particle Reynolds numbers defined by

$$Re = u_* D/\nu$$

where u_* is the shear velocity, and ν is the kinematic viscosity for the particle diameter D. For values of Re larger than 100 (the typical Re number in gravel-bed rivers is greater than 500), τ_c^* approached a constant value of approximately 0.06, i.e. there is no relationship between τ_c^* and D but a proportional τ_c-D relationship for a given fluid and sediment. This critical value represented an averaging of results from several flume runs with various materials of different densities and geometry. For decades this τ_c^* value was accepted and used extensively in palaeohydrologic investigations and engineering calculations, where the threshold of hydraulic conditions for the entrainment of particles larger than 2 mm in diameter was determined (for example Baker 1974, Baker and Ritter 1975, Bradley and Mears 1980, Maizels 1983).

Since Shields' experiments several investigations have reconsidered the threshold value of dimensionless shear stress and a large range of values of τ_c^* has been reported. As stated earlier Meyer-Peter and Müller (1948) indirectly imply a threshold of 0.047, while Chien (1956) summarised values of τ_c^* reported in results of nine different studies that ranged from 0.017 to 0.076. Neill (1968) observed that Shields' value for τ_c^* was on the high side and that the absolute lower limit for τ_c^* was approximately 0.030, while Church (1978) assembled data from numerous sources to show that values of τ_c^* varied from 0.02 to 0.12. Clearly then the work of Shields was oversimplified and some other factors must have been ignored in his analysis. Gessler (1965) and Neill (1968) discussed the difficulty of precisely defining the point at which particle motion begins as discussed earlier. Shields (1936) determined his τ_c^* value of 0.06 by measuring τ^* for different particle diameters through a range of

small transport rates and then extrapolating the relation back to a near-zero transport rate. Firstly as Vanoni (1975) notes, Shields did not actually go back to a truly zero transport rate but a negligible and measurable rate (the problem again arising from defining what the onset of bedload movement actually is). In addition Andrews (1983) suggests that even when dealing with a minute transport rate, when sand-sized particles begin to move, bedforms will develop which significantly increase the shear stress necessary to initiate particle motion (compared to the critical value for a flat bed). Also Paintal's (1971) experimental study of uniform and graded gravel revealed extremely small, but nevertheless measurable transport rates at values of τ_c^* many times lower than the 0.06 critical value.

The main limitation of Shields' (1936) work was that he never considered particle movement in a nonuniform size distribution of bed material. Although he used various materials with different densities he did not mix the particles, but conducted several runs with each sediment type and size. This critical value for sediment movement was then assumed by later workers to be similar for mixed beds with different sized particles. Recent work has shown that this is not the case. Work by Church and Gilbert (1975), Fenton and Abbott (1977), Parker et al. (1982b), Brayshaw et al. (1983), Carling (1983), Andrews (1983), Hammond et al. (1984) and others has shown that the bed material size distribution can affect the forces acting on a given particle by (1) hiding relatively smaller particles in the turbulent wake of relatively larger particles, (2) larger particles having a greater surface area protruding into the flow therefore exposing themselves to more fluid force, and (3) larger particles needing less force to start them rolling over smaller particles compared to smaller particles rolling over larger ones. These three conditions are shown in Fig. 4.1.

Fig. 4.1 An example of the complex bed structures that can form in coarse heterogeneous bed material which can enhance or restrict the movement of different size fractions. Note the tracer pebble trapped in the centre of the cluster.

The effect of nonuniform bed material therefore can explain why the reported critical dimensionless shear stress values vary around Shields' (1936) value of 0.06. This recent work in heterogeneous bed material (typically of sand-gravel bedded rivers) culminated in two important reports by Parker et al. (1982b) and Andrews (1983). Using data collected by Milhous (1973) in Oak Creek, a small gravel-bed stream in Oregon, Parker et al. (1982b) developed an empirical relation between τ_c^* and particle size for a nonuniform bed material. This relation was computed for 12 particle sizes from 0.6 to 89 mm by assuming a very small, but non-zero transport rate (similar to Shields (1936)), and regressing τ_c^* for each particle size, with the particle size expressed as a ratio of the median diameter of the subsurface material. The computed relation was

$$\tau_{ci}^* = 0.0876\ (D_i/D_{50})^{-0.982}$$

with $r^2 = 0.9997$ and particles in the range $0.01 < D_i/D_{50} < 1.65$

The exponent -0.982 implies that the value of τ_c^* varies almost inversely with the particle size. This means that the effect of large particles protruding into the flow and fine sediment being sheltered nearly compensates or cancels out the effect of the respective particles' weights. The exponent is close to a value of -1, which would imply that all particles would be entrained at the same shear stress and thus discharge, at a given location (i.e. all the particles would have equal mobility). If the exponent was close to zero this would mean that the work of Shields (1936) can be extended to mixed bed material and τ_c^* approaches a constant value (maybe 0.06). The relationship between the exponent or what will be termed the 'hiding factor' (where the hiding factor is -b) and τ_c^* can be more easily visualised by a rough sketch (Fig. 4.2). Shields' line of thought would be represented by a horizontal line

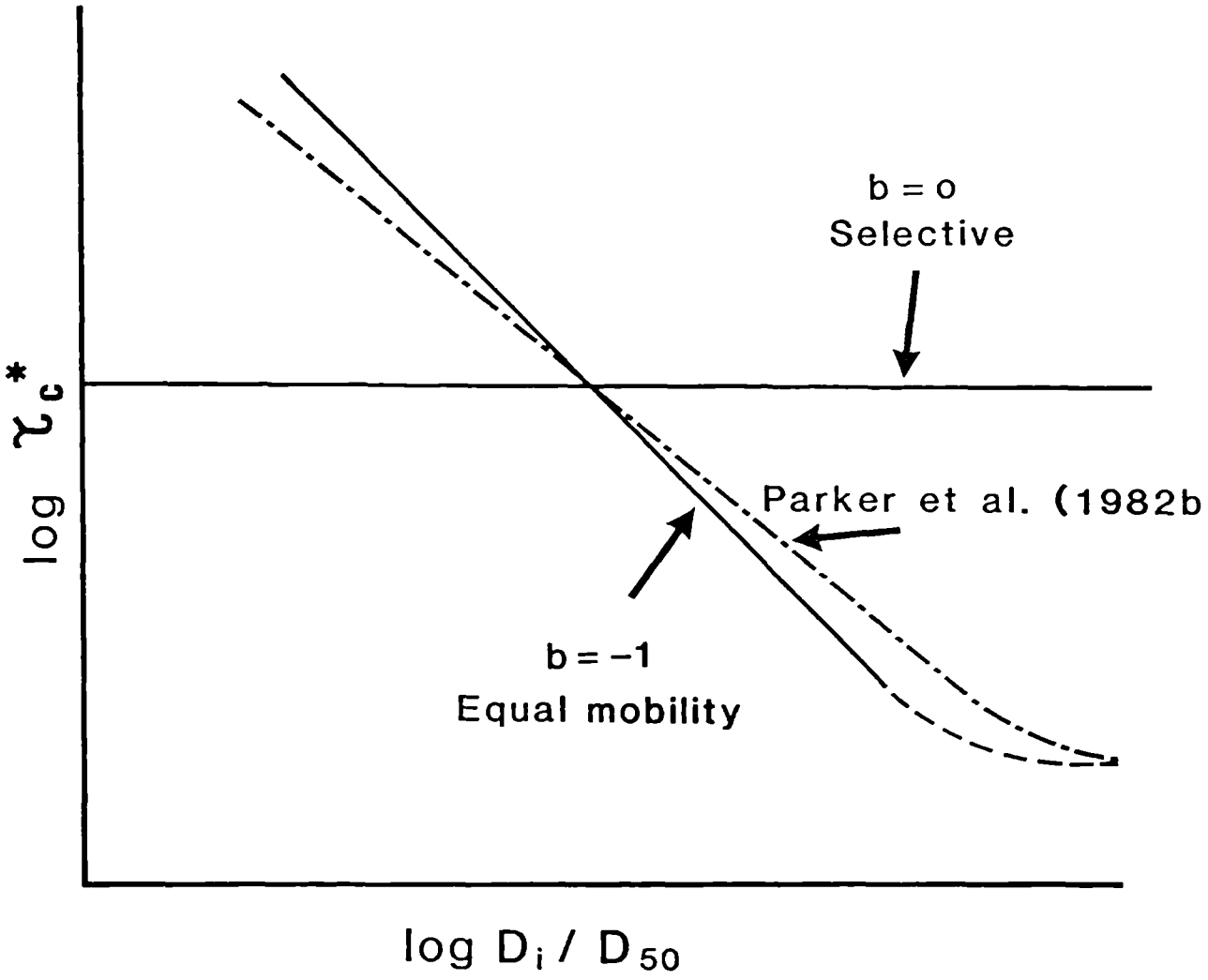

Fig. 4.2 Sketch showing the relationship between the hiding factor, critical dimensionless shear stress, and relative bed grain size.

(gradient of zero) whereas total equal mobility would be shown by a gradient of -1, that is for large sediment only a small τ_c^* is needed to start them moving (because they protrude into the flow and have greater pivoting angles) and for fine sediment a large τ_c^* is needed to entrain particles (since they are hidden both behind and beneath larger pebbles). Given that there is a slight deviation from a reciprocal relationship, Parker et al. (1982b) suggest that there is still scope for some selective transport although the bed particles would be entrained within a narrow range of shear stress, or discharge at a given river cross-section and therefore their equation would plot slightly flatter than the idealised equal mobility line (shown as a dashed line in Fig. 4.2).

The research of Parker et al. (1982b) was supplemented by Andrews (1983) working on the East Fork, Snake and Clearwater rivers (U.S.) which have natural self-formed channels. Rather than using the transport rates of individual size fractions to derive a relationship between τ_c^* and D_i/D_{50} as Parker et al. (1982b) report, Andrews (1983) looked directly at the competence of the flow using the largest particle trapped by Helley-Smith bedload sampling. His computed relation

$$\tau_{ci}^* = 0.0834(D_i/D_{50})^{-0.872}$$

with $r^2 = 0.98$ and particles in the range $0.3 < D_i/D_{50} < 4.2$

is remarkably similar to that of Parker et al. (1982b) (especially when considering that a different approach was used) and again suggests that in heterogeneous bed material most particles are entrained in a relatively small range of shear stresses.

Criticisms of this research methodology are scarce, partly because the

work is so recent and has not been tested elsewhere (though see 4.3 and 4.4), but also since this line of thought seems to be growing in popularity among fluvial geomorphologists. Carson and Griffiths (1985) note that since the relationship of Parker et al. (1982b) and Andrews (1983) depends on the definition and measurement of the subsurface bed material, it is not easily used. The problems and errors involved in sediment sampling in coarse bed material are discussed elsewhere (2.2.4) but are sufficient to limit the relationship's applicability to other rivers with beds of different grain size. Carson and Griffiths (1985) also question the logic of defining the critical stress for mobilising material in a gravel armour in terms of the *subsurface* median particle size. This topic is discussed in more detail in 4.3. The analysis of Andrews (1983) is particularly vulnerable to criticism since it depends heavily on the accurate measurement of bedload transport and shear stress. Carson (1986) notes that Andrews' (1983) calculations rely on the definition of threshold conditions for motion corresponding to a transport rate of about one particle in the largest size fraction collected in a sample, every minute, per metre channel width. As Carson (1986) states this is not the "idealised 'onset of motion' normally envisaged." Furthermore similar to Parker et al. (1982b), Andrews (1983) computed the shear stress using the Du Boys formula with the depth taken as the flow depth in the zone of maximum bedload transport within any cross-section. This may lead to an exaggeration of the shear stress values and certainly oversimplifies the spatial pattern of shear stress across a channel (see 2.2.2).

Finally the analysis of Parker et al. (1982b) was conducted in a small channel with flume-like geometry, peak discharges only up to 3.4 $m^3 s^{-1}$, and low to medium transport rates, while Andrews (1983) worked in larger channels but still with medium transport rates (the magnitudes of the transport rates are discussed in 4.7.2). These simplified conditions may

therefore limit their results only to rivers with similar characteristics. A full discussion of these two important works is presented in 4.3 to 4.5.

An alternative approach to predicting bedload movement was put forward by Bagnold (1977, 1980) stemming from his earlier work (Bagnold 1956, 1973). Instead of using a method based on tractive stress as in the forementioned studies he developed an approach based on unit stream power. His 1977 paper utilised flume data from Williams (1970) and field data from the East Fork, Snake and Clearwater rivers. As Carson (1986) notes despite these rivers having a bimodal bed material distribution (mixed sand-gravel beds) Bagnold (1977) derived his relationship only for sand-bed material. By examination of the submerged mass transport rates per unit width (i_s) and excess unit stream power, Bagnold (1977) proposed the relationship

$$\frac{i_s}{(W-W_c)} = 1.6\left[(W-W_c)/W_c\right]^{0.5} . (D/d)^{0.67}$$

where W is the unit stream power in kg m^{-1} s^{-1} and W_c the critical value of W for bed motion. Since i_s refers to the submerged mass this needs to be increased by $\rho_s/(\rho_s-\rho)$ to convert to dry mass (such as for dry sieve samples). In 1980 Bagnold revised his 1977 work empirically by the inclusion of the flume data of Gilbert (1914). At constant excess unit power and flow depth Bagnold (1980) found that the transport rates varied inversely with particle size. The resultant relationship when calibrated with Williams' (1970) flume sand data provided the equation

$$i_b = 0.0033(W-W_c)^{1.5}/(d^{0.67} . D^{0.5})$$

where i_b is the dry mass transport rate per unit width and is in kg m^{-1} s^{-1}. From Bagnold's (1977) work levels of sediment transporting

efficiency can be defined with 100% efficiency represented by

$$W = i_s \tan\alpha$$

where $\tan\alpha$ is a friction coefficient between the saltating mass and the bed taken by Bagnold as having a value of 0.63. These lines of efficiency have since been used by Hayward (1979) and Klingeman and Emmett (1982) to describe their transport rates in the Torlesse and East Fork respectively. Recently Carson (1986) has argued that the efficiency lines have no unique plot since they depend on excess unit power ($W - W_c$) and the locus of efficiency lines depends on the value of W_c with different curves (not lines). However W_c only has a significant effect on the $W - W_c$ relationship at low stream powers and so linear efficiency lines are acceptable for the range of powers reported in 4.2.

A confusion arises in Bagnold's work from the units he uses to describe stream power. This is discussed by Emmett (1982) following a personal communication from R.A. Bagnold. As Emmett (1982) points out both sides of Bagnold's (1980) equation involve the gravity acceleration (since weight and power are force units). Bagnold argues that the insertion of gravity on both sides of the equation is merely pedantic and therefore he drops the gravity term and expresses both quantities in mass units. This is how Hayward (1979), Klingeman and Emmett (1982) and Reid and Frostick (1986) plot their results. However, in the case of the work reported here the stream power is defined as the rate of application of stress to unit bed area and measured by the product of τv (see 2.2.2). In this case stress implies force and can only be expressed in Newtons so that the gravity acceleration cannot be cancelled out and still appears on one side of the equation. Hence the stream power values in W m^{-2} are larger by a factor of 9.8 than previously reported results and in order to make a

comparison with other work the stream powers used here must be divided by 9.81 (or moved by approximately one log cycle). This is important to bear in mind for the discussion in 4.2.

From this brief summary of the development of modern bedload theory it has been emphasised that there are problems with many of the traditional and often relied-upon predictive equations developed in simplistic conditions and involving numerous assumptions. Ackers and White (1973) provide a useful review of these earlier developed relationships by comparing the performance of these equations against actual case studies. Unfortunately most of the data used by Ackers and White (1973) to test these relationships was from flumes and sand-bed rivers. Of the only two field studies involving gravel material the τ^* ranged from 0.04 to 0.1 indicating conditions that only marginally exceeded the threshold for movement of the bed material (Carson 1986). Despite these limitations Ackers and White (1973) reported that only the Einstein-Brown (1950) equation (and a lesser known Rottner (1959) equation) proved tolerable in predicting total bedload transport rates (the Meyer-Peter and Müller (1948) and Einstein (1950) were two of the poorer estimators).

The understanding of bedload transport in gravel-bed rivers is currently undergoing a major change and questioning the validity and predictive powers of these traditional equations developed in some cases up to 50 years ago. In the past four years a new line of thought has come to the forefront attributable to the work of the Parker and Andrews teams (U.S.). This research has only been suitably reinforced by field data from seven rivers (some with a high sand content in the bed material). Much more bedload data is needed to test these new ideas in different environments, channel patterns and hydraulic conditions. Such a broad range of data was collected for all seven channel patterns of the Dubhaig, Feshie and Lyngsdalselva by direct bedload sampling using a Helley-Smith sampler and

indirectly using pebble tracers.

4.2 Total transport rate results

In order to compare the results both between sites and with previous work all the Helley-Smith bedload samples were processed and analysed in an identical manner. A total of 72 bedload samples were taken but uncertainties concerning the size distribution of the local bed material limited their use in some of the different analyses shown in 4.2 to 4.4.

The bedload data is interpreted using three approaches (1) total transport rates of bedload, (2) transport rates for individual size fractions involving what is termed here the 'Parker method', and (3) a direct investigation of the competence using what will be called the 'Andrews method'. The analysis of total transport rates is virtually self explanatory (and has been discussed in detail in 4.1.3) but the Parker and Andrews methods involve more complicated computations and so are discussed in more detail in their respective sections.

The discussion in 4.1.3 showed that there are two popular methods for examining the relationship between the total bedload transport rates and the fluid force transporting them. The transport rate in kg m^{-1} s^{-1} is often plotted against the dimensionless shear stress, τ^*, or the stream power, W (in W m^{-2}). Both approaches are used below to compare the Helley-Smith bedload transport rates for the Dubhaig, Feshie and Lyngsdalselva with the predictive equations described in 4.1.3 to see whether (1) their equations hold true with real field data, (2) they help to describe sediment movement in coarse bedded rivers, and (3) the relationships are consistent for different rivers with various channel patterns, grain size and hydraulic characteristics.

A preliminary analysis of the 72 Helley-Smith transport rates showed a set of consistent relationships but with a lot of scatter. By using a series of cutoffs of the trapped sediment however (at 0.25, 1, and 2 mm) it became apparent that the total transport rates could possibly be including some fine suspended load. Some of the Lyngsdalselva bedload samples were particularly prone to this especially the 8 and 12 August bedload samples from reach A which were taken after a major avulsion and bed disturbance on the 7 August. To avoid any distortion of the transport rates (and reduce the scatter) only sediment coarser than 2 mm was included in the computations. This leads to one of the Dubhaig samples (5/12/85, sample SS16) not being used so only 71 data points are included in the analyses below. The transport rates (greater than 2 mm) for all the three rivers vary over six orders of magnitude from 0.000001 to 2.2 kg m^{-1} s^{-1} with corresponding shear stresses from 6 to 406 N m^{-2} and powers of 5 to 938 W m^{-2} (the highest stream power measured was 1110 W m^{-2}). A full description of all the bedload data is given in Appendix A.

For comparison with the work of Meyer-Peter and Müller (1948), Brown (1950), Einstein (1950), and Parker (1978) the Einstein transport rates, ϕ were calculated for each sample using the formula outlined in 4.1.2. Following Parker (1978) the D_{50} of the surface bed material was used to represent the grain diameter, D. The choice and accuracy of this D_{50} value has an important influence on the position of the data points in the y axis direction since the Einstein equation involves a division by the D value raised to the power of 1.5. This explains the discrepancy between the analysis here and that for individual size fractions in 4.3 (which plots with much higher dimensionless transport rates when using the geometric mean of the sieve sizes for D). The dimensionless shear stress was also computed, again using the bed armour D_{50} as the representative grain size D in the formula outlined in 4.1.2.

Fig. 4.3 shows the 71 samples plotted on log-log scale with the curves from the work of Meyer-Peter and Müller (1948), Brown (1950), Einstein (1950) and Parker (1978) superimposed. For comparison Fig. 4.4 shows the plot from Parker (1978) for the 278 gravel-bed flume data from Peterson and Howells (1973) (notice the different scaling of the two axes). The immediate impression is that the field data in Fig. 4.3 plots along the same trends but below that suggested by previous workers (excluding Einstein-Brown see discussion below). The equations of Meyer-Peter and Müller (1948) and Parker (1978) both steepen at low transport rates as their implied threshold τ^* is approached. The field data in Fig. 4.3 follows this steep trend although there is a slight departure at very low transport rates. These are the previously mentioned samples from reach A of the Lyngsdalselva and represent different conditions of sediment availability due to the widespread disturbance of the bed and rapid aggradation and infilling of the channel. There is only a hint of curvilinearity in Fig. 4.3 as ϕ approaches values in excess of 0.01 but higher values of ϕ are needed to confirm this. The Einstein-Brown relationship is the only equation that is totally unsatisfactory overestimating the transport rates at low τ^* in both Figs. 4.3 and 4.4. As mentioned in 4.1.3 this is because the Einstein-Brown equation $\phi = 40(\tau^*)^3$ does not include a threshold for τ^*. Carson (1986) reports that the Einstein-Brown equation has been used in many engineering projects in New Zealand but it must be recognised that it is only valid for $\tau^* > 0.1$ (i.e. where the other curves flatten out to a slope of approximately 1.5). Data from Parker (1978), Andrews (1984) and Carson (1984) show that gravel-bed rivers only attain values of $\tau^* > 0.1$ relatively infrequently. Field evidence from the Dubhaig, Feshie and Lyngsdalselva confirm this and support Carson's (1986) conclusion that the Einstein-Brown equation may "simply be inappropriate" for use in gravel-bed rivers.

The most striking feature of Fig. 4.3 is that the field data for all three

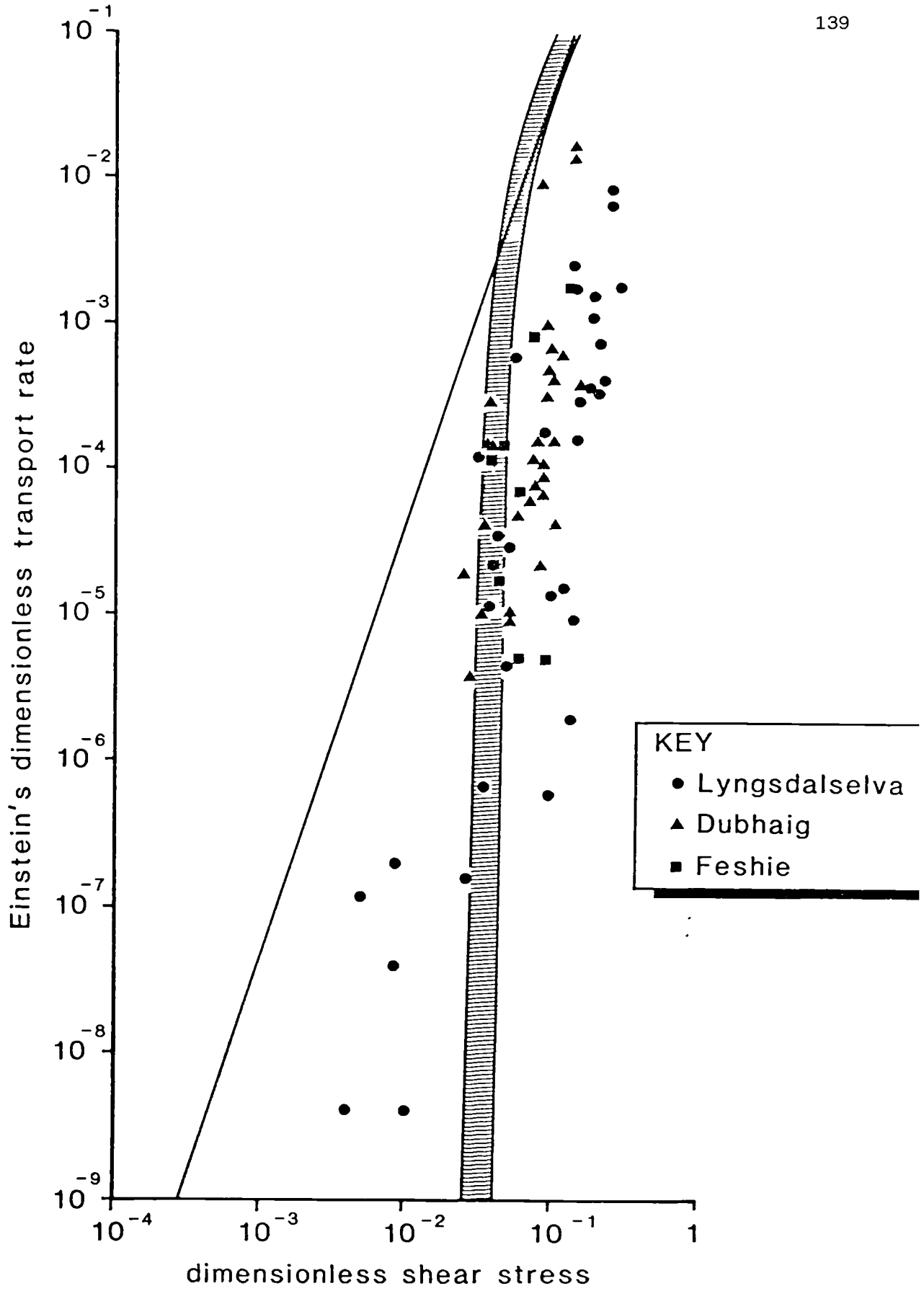

Fig. 4.3 Einstein's dimensionless transport rate (for sediment greater than 2 mm) plotted against dimensionless shear stress for 71 Helley-Smith catches from the Dubhaig, Feshie, and Lyngsdalselva. The single line represents the Einstein-Brown equation and the shaded area the locations of the Meyer-Peter and Müller, Einstein, and Parker curves.

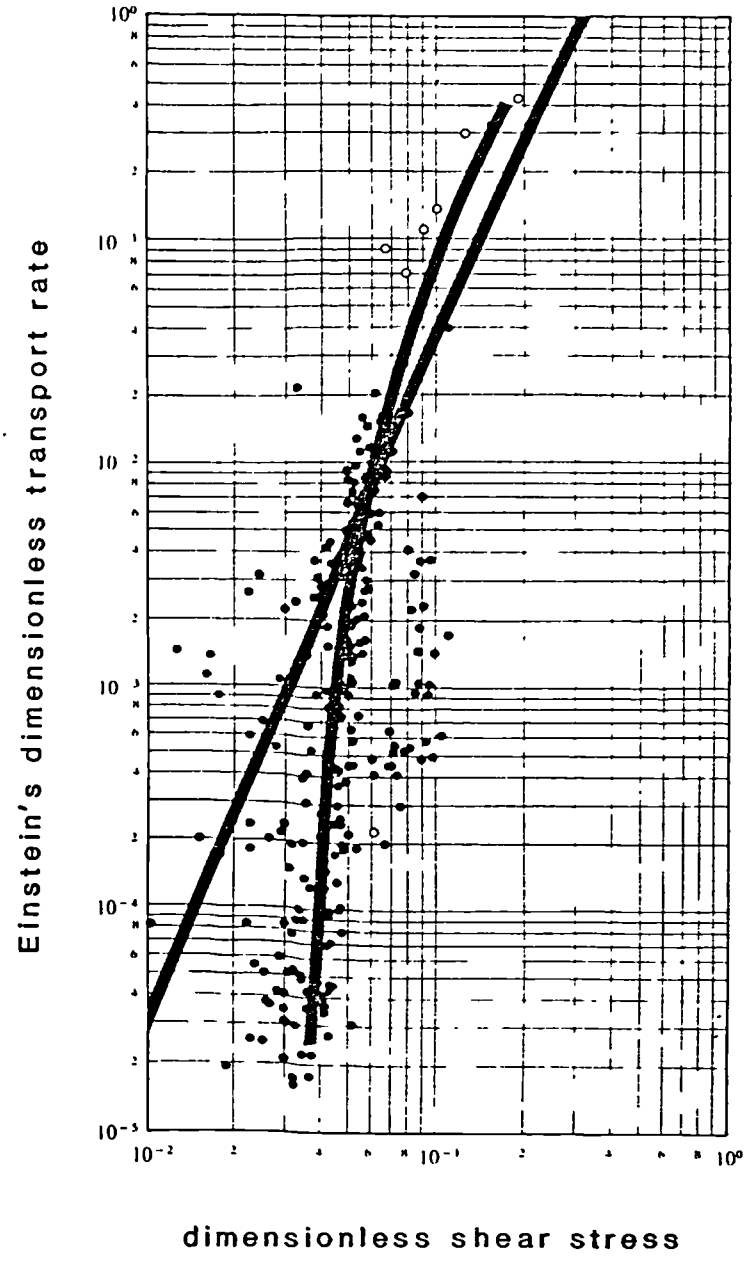

Fig. 4.4 Plot of Einstein's dimensionless transport rate against dimensionless shear stress from Parker (1978) with the Einstein-Brown line and Parker's own predictive curve superimposed.

rivers plots well below what should be expected using the relationships from previous work. This discrepancy of between approximately one and two log cycles is crucial in helping to understand the processes operating in rivers with coarse heterogeneous bed material. As discussed in 4.1.3 the relationships of Meyer-Peter and Müller, Einstein, and Brown were derived using either a theoretical basis or in flumes with runs using scaled down homogeneous material, often spherical and with no bed structures (spatially or vertically). Parker (1978) reported that he used the gravel-bed channel flume results of Peterson and Howells (1973) but did not quote the sediment size range (although it must have been limited). Though the laboratory has certain scale limitations which are difficult to overcome, the relationships derived are still a vast simplification of the situation present in real field conditions (particularly of coarse bedded rivers). Recent literature has shown that the transport of a pebble can be greatly influenced by its protrusion, shape, imbrication and bed packing characteristics and the degree of hiding and protection either behind or beneath larger pebbles (Fenton and Abbott 1977, Church 1978, Parker et al. 1982b, Andrews 1983, Brayshaw et al. 1983, Carling 1983, Hammond et al. 1984, Zhenlin and Komar 1986 and others). Bed structures such as the "clusters" described by Brayshaw et al. (1983), the imbrication of particularly ellipsoidal pebbles as described by Zhenlin and Komar (1986), the presence of a coarse armoured layer protecting the underlying fines reported by Bray and Church (1980) and others, and the effects of larger pebbles protruding into the flow while also providing shelter in their wake for finer material, all combine to affect the availability of certain size fractions in a mixed coarse bed. It is therefore not surprising that the field data for the three rivers plotted in Fig. 4.3 do not match the earlier flume, theoretical, and semi-empirically derived relationships which ignored these factors. Similar results are obtained for the size fractional transport rates and this topic will be discussed in more detail later in 4.3.

More recently work has concentrated on trying to derive a bedload equation for gravel-bed rivers in terms of stream power. As discussed in 4.1.3 Bagnold (1977, 1980) was the first to derive a total bedload transport equation based on flume and sand-bed channel data. Subsequent work has produced a comprehensive data base with the studies of the gravel-bedded Snake and Clearwater rivers (Emmett 1976), the sand-bedded East Fork river (Leopold and Emmett 1976, 1977) and the gravel-bedded Turkey Brook (Reid and Frostick 1986) providing data from rivers with a wide variation in channel width, grain size and discharge. The data collected in the Dubhaig, Feshie and Lyngsdalselva not only add to this data base but provide transport rates and shear stress values much higher than previously reported for less powerful and less active rivers (with transport rates all less than 0.2 kg m^{-1} s^{-1}).

The broad range of transport rates and shear stresses gives the opportunity to compare the three rivers' data to those of previous workers. Bearing in mind the discussion in 4.1.3 on the units of power and bedload transport, the data is plotted in Fig. 4.5 in a similar form to Bagnold (1977) with the lines of mechanical efficiency superimposed. As in the earlier analysis, plots of total transport rates > 0.25 mm and > 1 mm were constructed but had more scatter so transport rates are for all sediment coarser than 2 mm. The differences between a sand and gravel plot (> 0.25 mm) and gravel plot (>2 mm) will be shown later. Fig. 4.5 shows that the transport rate increases as almost the cube of stream power, with only a hint of the convexity that would be expected if transport rate depends on excess power over a Shields type threshold for the modal size as proposed by Bagnold (1977). The steeper than-linear trend implies an increase in transport efficiency as the discharge (and stream power) rises. At high stream powers the efficiency reaches above 1% as in previous studies of gravel transport (for example Klingeman and

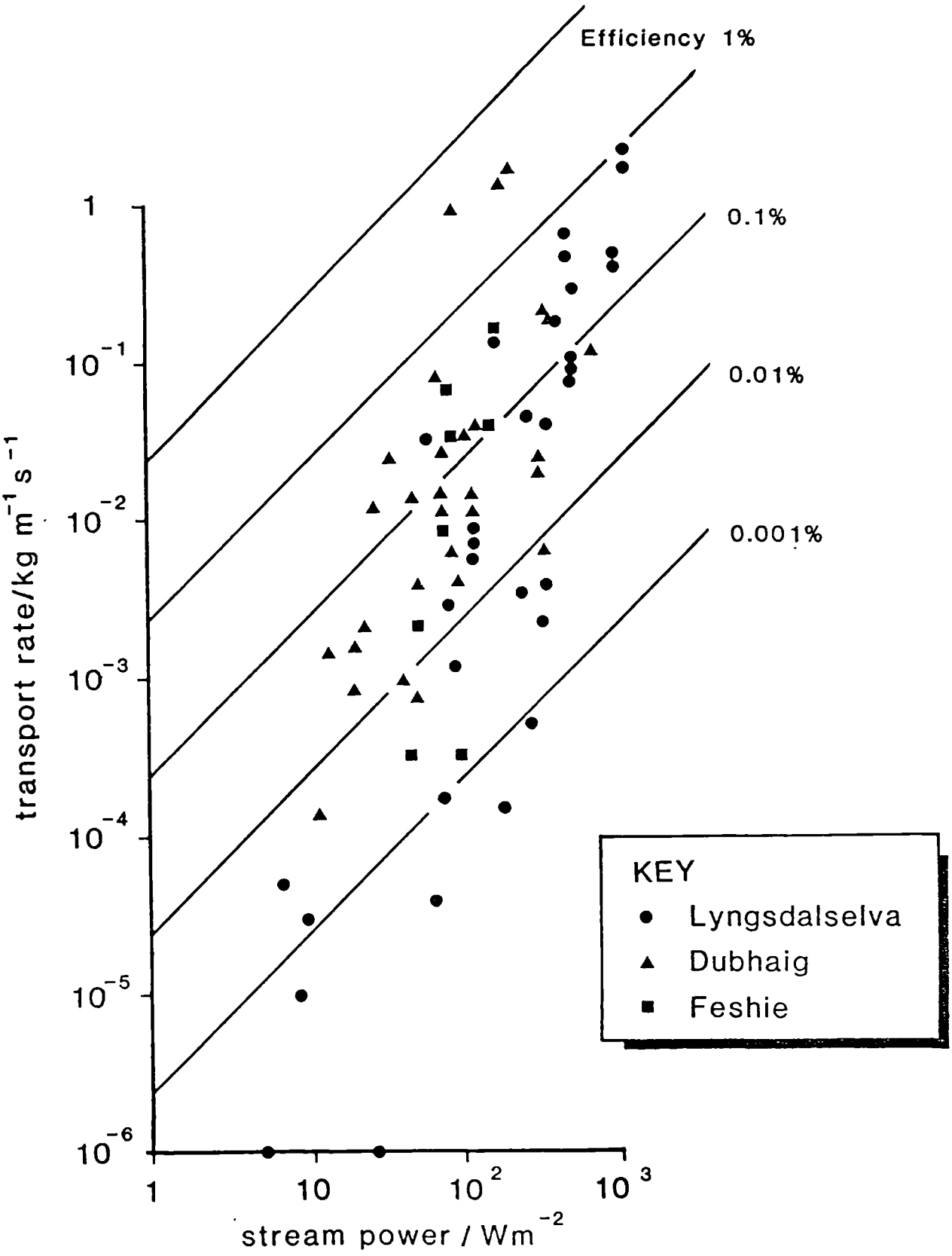

Fig. 4.5 Bedload transport rate per unit width (greater than 2 mm), as dry mass, plotted against stream power per unit bed area for 71 Helley-Smith samples from the Dubhaig, Feshie, and Lyngsdalselva.

Emmett 1982).

When the bedload transport rates are converted to immersed weight in kg m^{-1} s^{-1} as described in 4.1.3 and plotted alongside previous work on bedload transport rates as cited and presented in Reid and Frostick (1986), the Dubhaig, Feshie and Lyngsdalselva bedload appears to lie on a similar gradient to three of the four rivers (see Fig. 4.6), with the increase in transport rate again best approximated by the cube of stream power. This supports the suggestions of Reid and Frostick (1986) that there may be a common response of rivers to changes in stream power.

The East Fork data was included by Reid and Frostick (1986) so that a comparison could be made between the predominantly sand-bed East Fork and the other gravel-bed rivers. As Reid and Frostick (1986) note the East Fork bedload data plots both higher and to the left of the gravel-bed streams (and also the data from the Dubhaig, Feshie and Lyngsdalselva). They attribute this to the greater proportion of fine sediment present in the bed material and claim that the ranking of East Fork > Clearwater > Snake > Turkey Brook according to the amount of fines in the bed agrees with a similar ranking for the median values of percentage efficiency. This implies that a river with finer bed material is more efficient in sediment entrainment and transport.

This can be explained again by the sediment availability and how coarse bedded rivers manage to restrict the movement of certain sizes of sediment through hiding, sheltering, imbrication and in bed structures. The situation is similar to the Einstein plots discussed previously where the theoretical data using fine sediment in controlled laboratory experiments differed by over a log cycle from the inefficiently transported bedload samples from gravel-bed rivers.

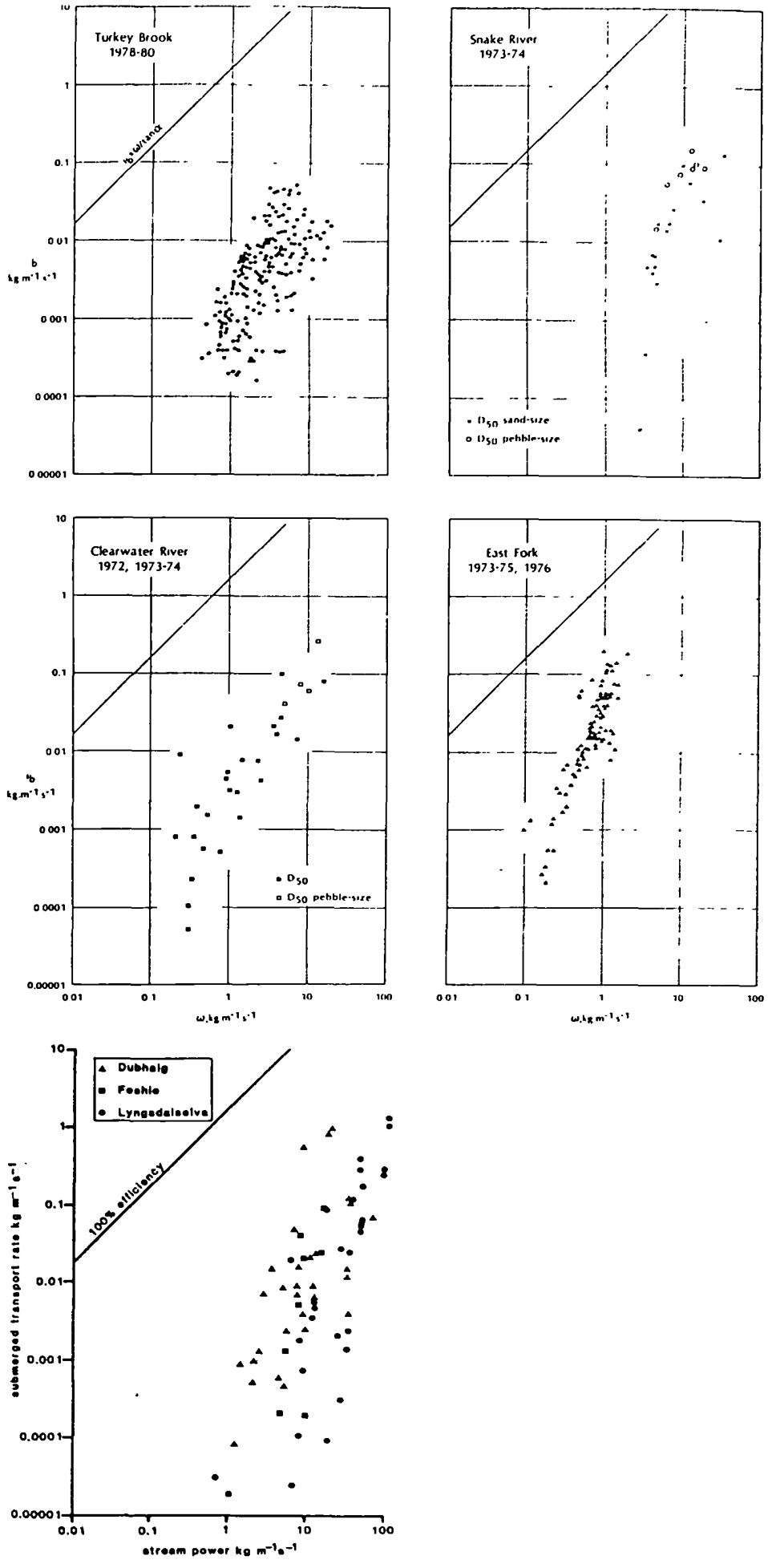

Fig. 4.6 Plots of bedload transport rate (as submerged mass) and stream power (in kg m^{-1} s^{-1}) for four different rivers after Reid and Frostick (1986) compared to the converted Helley-Smith transport rates (greater than 2 mm) and stream powers from the three rivers reported on here. Note that only transport rates greater than 0.00001 kg m^{-1} s^{-1} are plotted.

To understand the processes operating in gravel-bed rivers and to give further support to the earlier arguments for transport inefficiency, but also to show that this efficiency can increase as the discharge or shear stress increases, the Lyngsdalselva bedload samples are plotted as an example since they represent the widest measured range of transport rates and shear stresses. Fig. 4.7 plots the 33 bedload samples taken from three reaches during the five week study period. The samples are labelled according to the flow conditions they were taken in with (1) 'flood' samples being the only bankfull conditions, (2)'other' samples being the high to average meltwater flows, and (3) 'next day' referring to the day after the 'flood' samples were taken when due to an avulsion the original sampling area had been reduced to a very low flow.

Looking at the gravel only plot (Fig. 4.7, right) there is a clear separation of the samples by flow conditions with the efficiency increasing as the discharge increases. The efficiency changes over three orders of magnitude from the 'next day' to the 'flood' samples. This increased efficiency in flood conditions can be explained in terms of sediment availability along the same lines as the earlier arguments. Generally as the shear stress increases a greater range of sizes can be transported and therefore a greater proportion of surface grains are available for movement. If the entire surface layer is broken (as it was during the 'flood' bedload sampling period) then all sizes of the surface and subsurface are available and are transported en masse. Depending on the sampling time and bed conditions during a flood a state can be reached whereby all sizes can move regardless of their weight, size or position in the bed. The rapid rise in efficiency in Fig. 4.7 is therefore explainable by the change in sediment availability - nearly all sizes available for movement in the 'flood' but only the occasional breach of the armour and selective transport in the meltwater and low flows at other times. This will be elaborated on in 4.5.

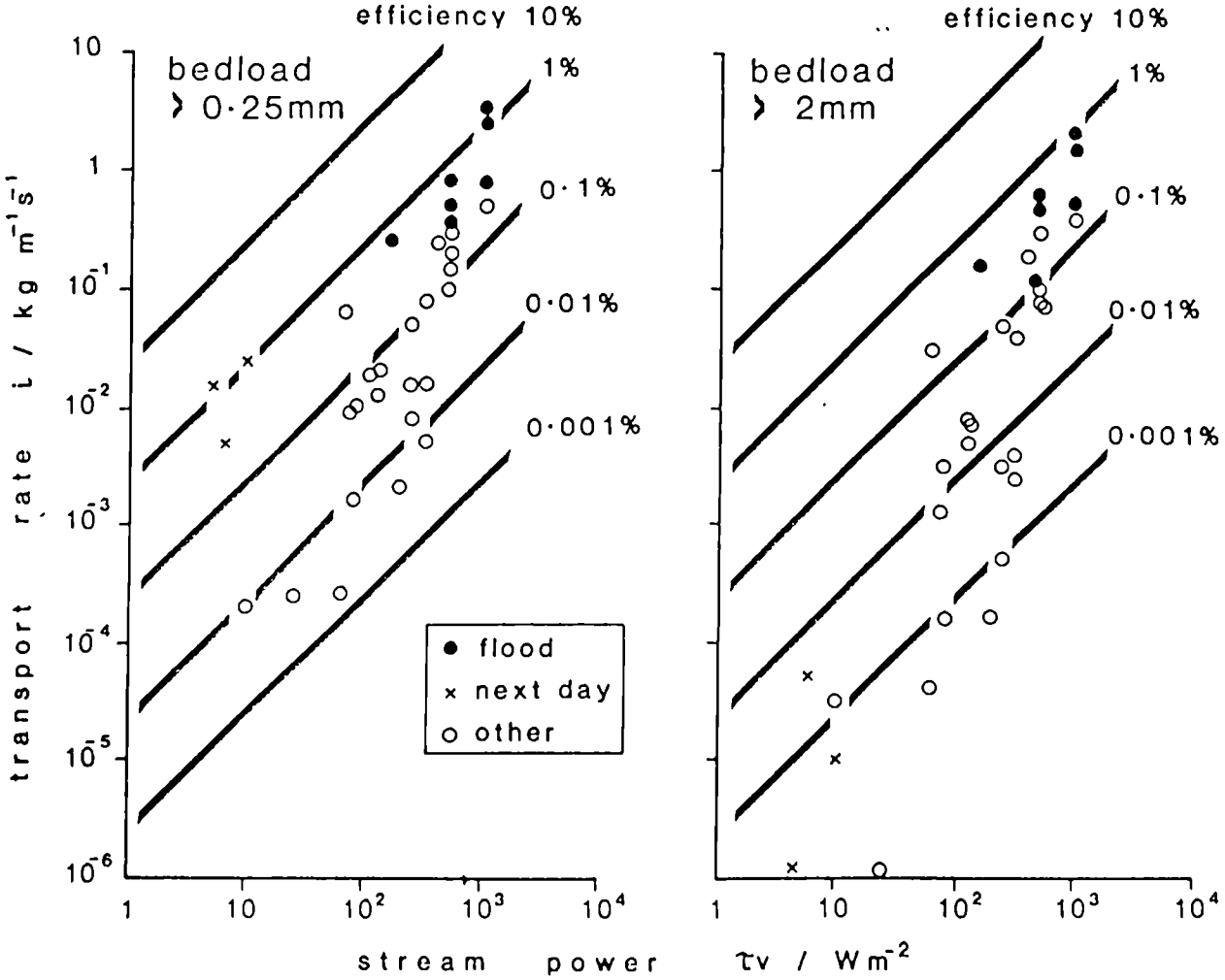

Fig. 4.7 Bedload transport rate as dry mass plotted against stream power for the 33 Lyngsdalselva Helley-Smith samples for all sampled sizes (left) and for gravel only (right).

Sediment availability also helps to explain the difference between the two plots in Fig. 4.7. Fig. 4.7 (left) shows that transport was also efficient on the 'next day' when despite very low discharge and stream power following avulsion on the falling stage of the previous night's flood, the transport rates were relatively high. Comparisons of the two plots in Fig. 4.7 however shows that the bedload was almost entirely sand-sized material. It was probably deposited from suspension on the falling stage of the flood, had not yet infiltrated into the gravel framework, and was being reworked as bedload. Subsequent low flow samples did not show abnormally high transport rates, which suggests that highly mobile falling stage deposits of fine sediment were shifted to more sheltered positions within a few days. This has important implications for interpreting bedload data since variations in sediment availability or the physical nature of the bed such as those just described, can distort the results of a Einstein or Bagnold-type analysis. This is also true for the Parker and Andrews methods described in 4.3 and 4.4.

Despite the problems in measuring bedload transport and shear stress in gravel-bed rivers the results reported for total transport rates are relatively consistent. Transport in gravel-bed rivers is inefficient compared to their sand-bed counterparts and this inefficiency can be visualised by plotting transport rates against some measure of flow strength (shear stress, power etc.) An analysis of total transport rates shows that the often relied-upon traditional equations derived for fine or uniform bed material do not predict the bedload transport in gravel-bed rivers. The reason for this discrepancy is that in heterogeneous bed material the availability of different sized particles is determined by several interrelated factors involving the discharge, shear stress, and the grain size, stability and physical structure of the bed. The Bagnold analysis in Fig. 4.7 shows that with an increase in discharge more sizes

are available. For a closer investigation of the response of various size fractions of the bed to changing hydraulic conditions an analysis similar to that reported by Parker et al. (1982b) was followed as shown below.

4.3 Fractional transport rates

This approach adapted from that first reported in Parker et al. (1982b) is complicated involving new notation and formulae. In order to understand and interpret the results the methodology must be carefully explained. Since the Parker type of analysis now forms a firm part of the theory of bedload transport his approach is closely scrutinised but also simplified (where possible) so that a researcher with a broad background in the subject area can understand and use it.

4.3.1 Methodology

All bedload samples were sieved at 0.5ϕ intervals and the transport rates in kg m^{-1} s^{-1} were calculated for each size fraction. Only fractions coarser than 1 mm were included in the analysis (Parker et al. (1982b) used fractions > 0.6 mm) since the hydraulic conditions affecting very small particles on a rough stream bed and the possibility that the very fine material may be transported as suspended load can introduce considerable scatter into the results. The fractional transport rates were re-expressed into Einstein's dimensionless form outlined in 4.1.2 using the geometric mean of the bounding sieve sizes as the representative diameter of each size fraction. As Parker et al. (1982b) note, the transport rate of each size fraction is a reflection of the amount (or percentage) of that size fraction available in the bed. For example, if 20% of the bed grain size distribution is in the 45 - 64 mm fraction but only 2% in the 1 - 1.4 mm fraction then with equal mobility the probability that the coarser material will be moved is ten times greater

than that for the finer sediment. Therefore a correction factor needs to be applied to the calculated Einstein transport rates (which is then also inherent in further computations). Parker et al. (1982b) suggest this correction should be based on the size distribution of the subarmour layer, not the surface armour since their observations show that the bedload size distribution is typically much closer to that of the subarmour than of the armour. However they do admit their choice of the subarmour is "somewhat arbitrary" and there is "an ambiguity" concerning the use of either the armour or subarmour.

Andrews and Parker (in press) in a review of their earlier work discuss the role of the armour (or "mobile pavement" as they describe it) and subarmour in active coarse bedded rivers and using flume and field data show that the surface armour is a regulator that acts to nearly equalise the mobility of grains contained in the substrate. As a consequence of this regulatory role they state that the size distribution of the bedload "should in the mean (for example annual) approximate that of the substrate" (Andrews and Parker in press). Since the Dubhaig, Feshie and Lyngsdalselva bedload is only from a few floods the D_{50} of the bedload is not representative of all high flows. However the mean D_{50} of the bedload for each reach or sampling site was always considerably less than the average D_{50} for the subsurface of the bed material. This may reflect spatial and temporal variations in bedload transport, the narrow range of bedload sizes that the Helley-Smith can sample, but also that Andrews and Parker (in press) may have underestimated the role of the surface armour in protecting the finer sediment below in the subsurface.

Their hypothesis that the armour is always in place, even during transport events in which almost all sizes of sediment are found in the bedload may not always be true. Although even during large floods the motion of gravel is sporadic, so that at any given time only a small fraction of the

surface grains are actually in motion, unlike the 'mobile armour' of Andrews and Parker, the surface can be destroyed by the transport of gravel (to be reformed later over a long time span). Personal experiences in rivers in Scotland, Norway and U.S.A. have indicated that the armoured layer is only rarely broken and there are few opportunities for the subsurface to be entrained, but on one such occasion during a rainflood in the Lyngsdalselva it did seem that the bed was totally mobile, there was a free interchange between surface and subsurface, and the armour was destroyed to reform during a prolonged low flow spell.

It seems therefore that both the 'mobile armour' hypothesis first put forward by Parker in 1980 (whereby all sizes exchange grains with the bedload) and the "static armour" explanation of workers such as Bray and Church (1980), Carling (1981), Klingeman and Emmett (1982) and Gomez (1983) (where only small grains are entrained until a flood destroys the surface layer) are both applicable to describing the sediment movement in gravel-bed rivers. The analysis used here acknowledges that the mobile armour hypothesis is the best explanation for understanding sediment movement in gravel-bed rivers in the majority of cases, but reflects current opinion that the surface armour of the bed is more important in determining the size of the material available for transport. Hence the subsequent calculations in the Parker method (and Andrews method in 4.4) use the size distribution of the surface sediment to represent the sizes available for transport. This is in contrast to Parker et al. (1982b) and Andrews (1983), but takes into account the role of the armour in restricting sediment movement from the subsurface (a compromise between the mobile armour and static armour explanations). On the occasion when the flood destroyed the armour layer in the Lyngsdalselva, the samples were corrected for the size distribution of the sediment available for transport in the subsurface.

The Einstein dimensionless transport rates for individual size fractions (ϕ_i) were corrected for the percentage by weight of bed material in each fraction (f_i) by multiplying ϕ_i by $1/f_i$. This involved an estimation of the total size distribution of the surface (and subsurface in the case of the Lyngsdalselva) bed material. Table 4.1 shows the average percentage size distributions (by weight) derived from bulk sampling on the seven reaches of the three rivers. The sampling strategy employed varied for each river and is briefly outlined below since it affects the confidence attached to the results for each river.

As mentioned in 2.1.2 the Dubhaig has a rapid change in slope which in turn helps to explain the downstream changes in channel pattern. Complementing this change in slope is a downstream decline in sediment size so that the size distribution of the channel bed material had to be measured for each study reach. Bulk sampling was undertaken as outlined in 2.2.4 with the number of samples reflecting the apparent spatial variation in surface size distribution. The samples were taken on partially or wholly emergent bars (all active) so that they provided a close approximation to the channel bed material size distribution. The samples were averaged to give a total weight in each size class for each reach and the percentage coarser calculated for each size fraction (see Table 4.1). The D_{50} was computed from grain size plots of the averaged total weights. Table 4.1 also shows the percentage of the total weights that the Helley-Smith can sample. It is interesting to note that for Reach A this represents 28% of the surface sediment which rises to 92% in Reach E. Similarly the Helley-Smith sampling range in the Feshie varies from 33% to 76% of the channel bed surface, and from 39% to 51% of the Lyngsdalselva surface and subsurface bed material. Although this appears to be a problem (as discussed in 2.2.3) it must be assumed that the relationship between flow strength and the sediment size entrained remains consistent for all sizes. Thus, the sampling of only part of the total

Table 4.1 Average bed material grain size distributions for the Dubhaig, Feshie, and Lyngsdalselva that are used throughout the bedload transport analyses.

Fraction	Dubhaig (surface) % in fraction					Feshie (surface) % in fraction				Lyngsdalselva % in fraction	
mm	A	B	C	D	E	5	5.5	6	6.5	Surf.	Subs.
1.0	0.3	0.8	0.4	0.5	1.0	0.2	0.1	0.3	0.3	1.5	2.3
1.4	0.4	0.9	0.4	0.5	1.5	0.4	0.2	0.4	0.3	1.3	2.1
2.0	0.4	0.9	0.2	0.6	2.0	0.6	0.2	0.1	0.3	1.2	2.0
2.8	0.6	1.2	0.3	0.9	2.8	1.0	0.2	0.3	0.6	1.2	2.0
4.0	0.7	1.3	0.4	1.2	3.1	1.1	0.3	0.6	1.0	1.2	2.0
5.6	0.9	1.9	0.7	1.9	4.1	1.9	0.5	1.3	1.9	1.6	2.8
8.0	1.1	2.7	2.0	3.0	5.4	2.3	1.5	2.0	3.4	1.9	3.4
11	1.6	4.6	5.4	5.2	8.1	2.9	2.0	3.5	8.0	2.6	4.8
16	2.0	6.0	8.1	6.8	11.3	1.6	3.0	8.5	10.3	3.3	5.2
22	3.6	10.3	13.7	12.8	17.8	3.2	11.1	17.1	21.2	5.7	6.1
32	5.0	13.3	18.2	16.2	18.9	4.7	23.2	23.1	18.3	6.9	8.3
45	11.1	18.2	18.5	17.8	16.4	13.3	22.0	17.7	10.3	10.7	9.5
Sampled weight kg	408	129	106	126	18	30	25	22	15	151	114
D_{50} mm	98	46	41	42	23	87	50	38	33	69	43
% in * H-Smith range	28	62	68	67	92	33	64	75	76	39	51

* Percentage by weight of sediment > 1 mm.

size distribution available for transport is in effect a subsample which is comparable to the total pattern of sediment movement (if this was possible to sample given the size of Helley-Smith that would be needed). Information regarding particularly coarse sediment movement was gained by the use of pebble tracers as discussed in 4.6.

The character of the bed material in the Lyngsdalselva was sampled in a similar way as in the Dubhaig, but fewer samples (although much larger in weight) were taken. The samples were taken at three sites on bars which were created during the rainflood on 7 August but were exposed by avulsion a few hours later so that there was no opportunity for fines to be winnowed out by moderate flows. The grain size distributions differed between sites but were pooled to give an average composite grain size curve.

The bed material of the Feshie was sampled using a different approach to obtain a grain size distribution that was both similar to the actual *channel* bed sediments and the local variations in bed size. Sampling was undertaken at low flow with the aid of a large bucket and entrenching tool. The largest stone in the surface was removed by hand and the depth of its imprint roughly noted. The rest of the surface sediment was scraped away with the entrenching tool and caught in the bucket laid horizontally on the surface downstream. This was frequently emptied to allow sediment to accumulate on the bucket floor - a process resembling Helley-Smith sampling of bedload. Once the surface was removed, the subsurface was scooped out with the bucket, taking care to keep all the fines when removing the bucket from the water. To gain an insight into the within-reach variation of surface sediment size this technique was applied at each bedload sampling site. The sediment availability correction factor used in the derivation of ϕ was therefore different for each sampling site - probably the most representative of all the rivers.

Once adjusted for the bed availability, Einstein transport rates for individual size fractions (n = 12 i.e. 1 - 1.4, 1.4 - 2.0 mm etc.) were converted to a special term Parker et al. (1982b) put forward, W_i^*, which is another dimensionless bedload parameter defined as

$$W_i^* = \frac{\phi_i}{(\tau_i^*)^{1.5}}$$

The τ_i^* are calculated using the formula outlined in 4.1.2. using the geometric mean of the bounding sieve sizes to represent D_i and the shear stress computed from velocity profiles for τ . Parker et al. (1982b) justify their use of W_i^* instead of ϕ_i since at low values of ϕ_i plots of ϕ_i versus τ_i^* tend to be very steep, whereas plots of W_i^* versus τ_i^* are not so steep making the job of determining an empirical relation from the data somewhat easier. Parker et al. (1982b) also justifies W_i^* on the grounds of no spurious correlation through D_i; however, τ_i^* is now on both sides. For the analysis used here both plots and computations using ϕ_i and W_i^* were undertaken and the results and conclusions proved to be identical regardless of the parameter used. For direct comparability however, the Parker et al. (1982b) term W_i^* will be used on all the bedload data.

A visual impression of the relationship between W_i^* and τ_i^* is obtained by plotting the logs of the two variables against each other for separate size fractions (assuming a constant D_{50} for all the samples, see later). Recalling the discussion of previous work on bedload transport in 4.1.3, if the work of Shields (1936) is correct, then the size of sediment transported should be proportional to the shear stress measured at the bed i.e. $\tau_{ci} \propto D_i$. However, if the work of Parker et al. (1982b), Andrews (1983), Andrews and Erman (1986), and Andrews and Parker (in press) is closer to explaining sediment movement in coarse heterogeneous bed material, the relative size of the sediment is important and at a certain

shear stress all sizes are available for transport i.e. $\tau_{ci}^* \propto D_i^{-1}$ where large sediment only requires a small τ_i^* to start them moving (because they protrude into the flow) and for fine sediment a large τ_i^* is needed to entrain particles (since they are hidden both behind and beneath larger pebbles). On a plot of W_i^* versus τ_i^* for individual size fractions Shields' line of thought would ideally be represented by a single line with all sizes superimposed on top of each other while the Parker pattern would be a clear separation of points with the larger sizes to the left of the plot and smaller sizes to the right. This is best illustrated by the plot used by Parker et al. (1982b) from 22 bedload measurements in the Oak Creek (Fig. 4.8).

Although their data is slightly unrepresentative in that it was obtained at very low flood discharges, from a flume-like channel using an average bed shear stress derived from the Du Boys equation, uses a single D_{50} value for the channel subsurface, and has very low transport rates, the plot shows the separation of different size fractions according to that expected if Shields work is inapplicable in nonuniform mixtures and there is not a constant τ_c^* for different particle sizes.

This can be showed empirically by assuming that the different grain sizes collapse, at least approximately, into a series of parallel lines (some of which are plotted on Fig. 4.8 according to the results reported in their paper). If a low reference value W_{ri}^* is arbitrarily chosen (the 0.002 value for W_{ri}^* reported in Parker et al. (1982b) is also used here) and the reference dimensionless shear stress for each size, τ_{ri}^* is read off the plot, a log-log regression between τ_{ri}^* and D_i/D_{50} leads to a relation

$$\tau_{ri}^* = a\left(D_i/D_{50}\right)^{-b}$$

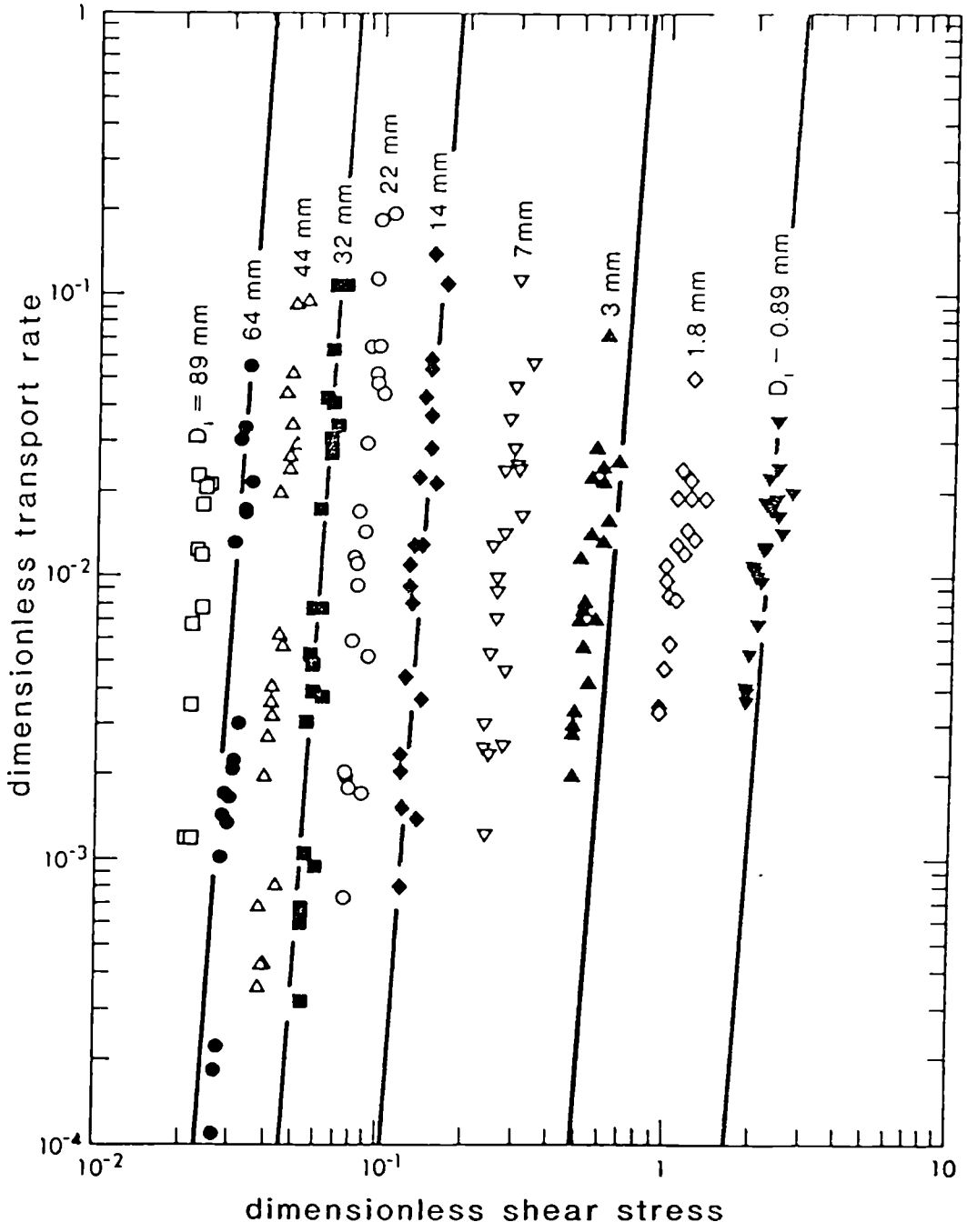

Fig. 4.8 Plot from Parker et al. (1982b) showing the separation of different size fractions of Oak Creek bedload when plotted as dimensionless transport rate, W_i against dimensionless shear stress. For clarity only a few example regression lines are superimposed onto the plot (calculated from the equations presented in their paper).

where -b, the hiding factor, is an exponent describing the influence of the relative size of material on its entrainment. A value of zero indicates a constant increase in the size of a particle entrained (relative to the surrounding material) with shear stress (i.e. Shields' work can be used in heterogeneous bed material) and a value of 1 shows that the size of material relative to the surrounding material has such a strong effect on its entrainment that τ_c is independent of D_i. The constant a is also important in that it is the reference critical shear stress, τ^*_{r50} associated with the D_{50} of armour or subarmour (whichever is used).

A problem with the plot of Parker et al. (1982b) is that they use (and assume) a constant D_{50} for all size fractions in all areas of the channel. Although their data was collected using a vortex sediment ejector extending the full width of the channel there must still be some spatial variability in the D_{50} of the subsurface (either horizontally or vertically). More importantly when data is obtained from different reaches and different local pool/riffle units (as reported here), a plot such that of Parker is irrelevant unless plotted for each reach of constant D_{50} value. For example the D_i = 1 - 1.4 mm relative to a D_{50} of 20 mm is larger and protrudes more when compared to a D_{50} of 120 mm. Therefore only when a constant D_{50} is used for the reach (such as the Lyngsdalselva) is a visual plot with D as the third variable of any advantage, otherwise D_i/D_{50} must be used. However to be consistent and to enable visual comparisons between the Dubhaig, Feshie, and Lyngsdalselva, the Lyngsdalselva samples were converted and grouped according to the D_i/D_{50} ratios used for the Dubhaig and Feshie data.

Likewise an alternative approach from that of Parker et al. (1982b) needs to be applied to obtain a relationship between τ^*_i and D_i/D_{50}. Rather than reading off τ^*_{ri} at a given W^*_{ri}, a log-log multiple regression using W^*_i,

τ_i^* and D_i/D_{50} gives an equation which can be rearranged, and substituting W_{ri}^* = 0.002, will give a relation identical to that of Parker et al. (1982b). Since the transport rates and shear stresses are both subject to error (see 2.2.2 and 2.2.3) the bisector of the forward and inverse regressions is used (Mark and Church 1977) which takes into account the residuals in both the y and x direction. The results and a discussion of their implications for sediment transport studies is presented below.

4.3.2 Results

The analysis of total transport rates in 4.2 showed that when the Einstein dimensionless transport rates were calculated and plotted against the dimensionless shear stress for 71 of the Helley-Smith samples there was a discrepancy in the transport rates of between one and two log cycles with that expected if the traditional bedload transport predictive equations are correct. There are two problems with this type of analysis for total transport rates : (1) the ϕ values are very low since the D_{50} of the bed surface is used (raised to the power of 1.5) in the Einstein equation and therefore the points correspond to the almost vertical parts of the predictive equations, and (2) the ϕ and τ^* do not show any effects that the different size fractions of the transported material might have on the overall transport rate.

As part of the Parker method described in 4.3.1 the Einstein dimensionless transport rates and dimensionless shear stresses have to be calculated for each size fraction of each sample. These can then be used to supplement the earlier findings in 4.2 and see whether there is any relationship with the predictive equations (at a higher ϕ) and if there is any size separation with τ^* as described in 4.3.1. The data for the three rivers are plotted in Figs. 4.9a-c with the regression equations, r^2, s value, t-ratio, and number of points, n, shown in Table 4.2. Only the 17

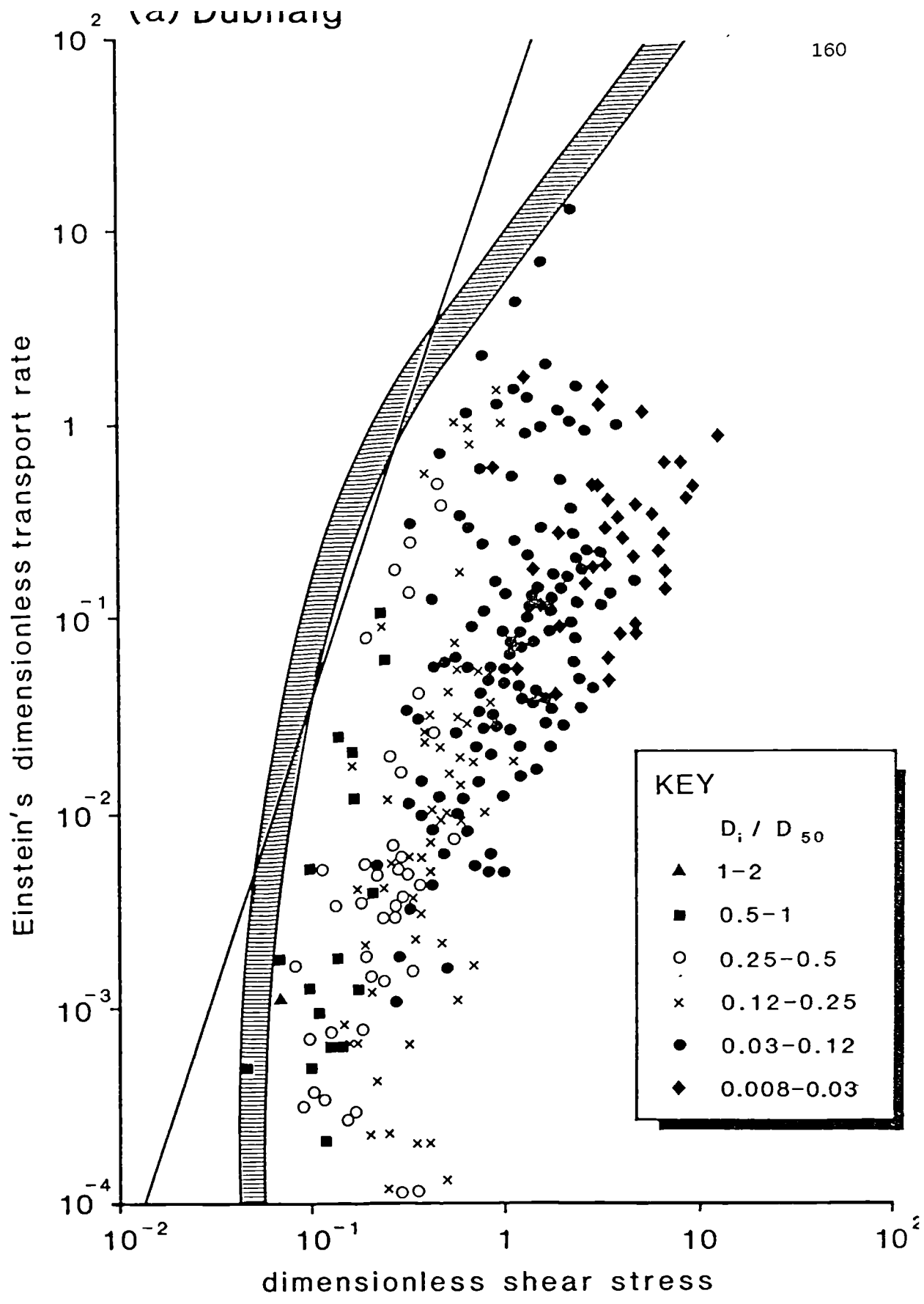

Fig. 4.9 Einstein's dimensionless transport rate against dimensionless shear stress for individual size fractions grouped according to the ratio of their mean geometric sieve size relative to the local surface D_{50} (or subsurface D_{50} in the case of the Lyngsdalselva flood samples). The three plots are for the (a) Dubhaig (b) Feshie, and (c) Lyngsdalselva, where the single line represents the Einstein-Brown equation and the shaded area the locations of the Meyer-Peter and Müller, Einstein, and Parker curves. Note that for clarity the two smallest D_i/D_{50} ratios represent four fractions.

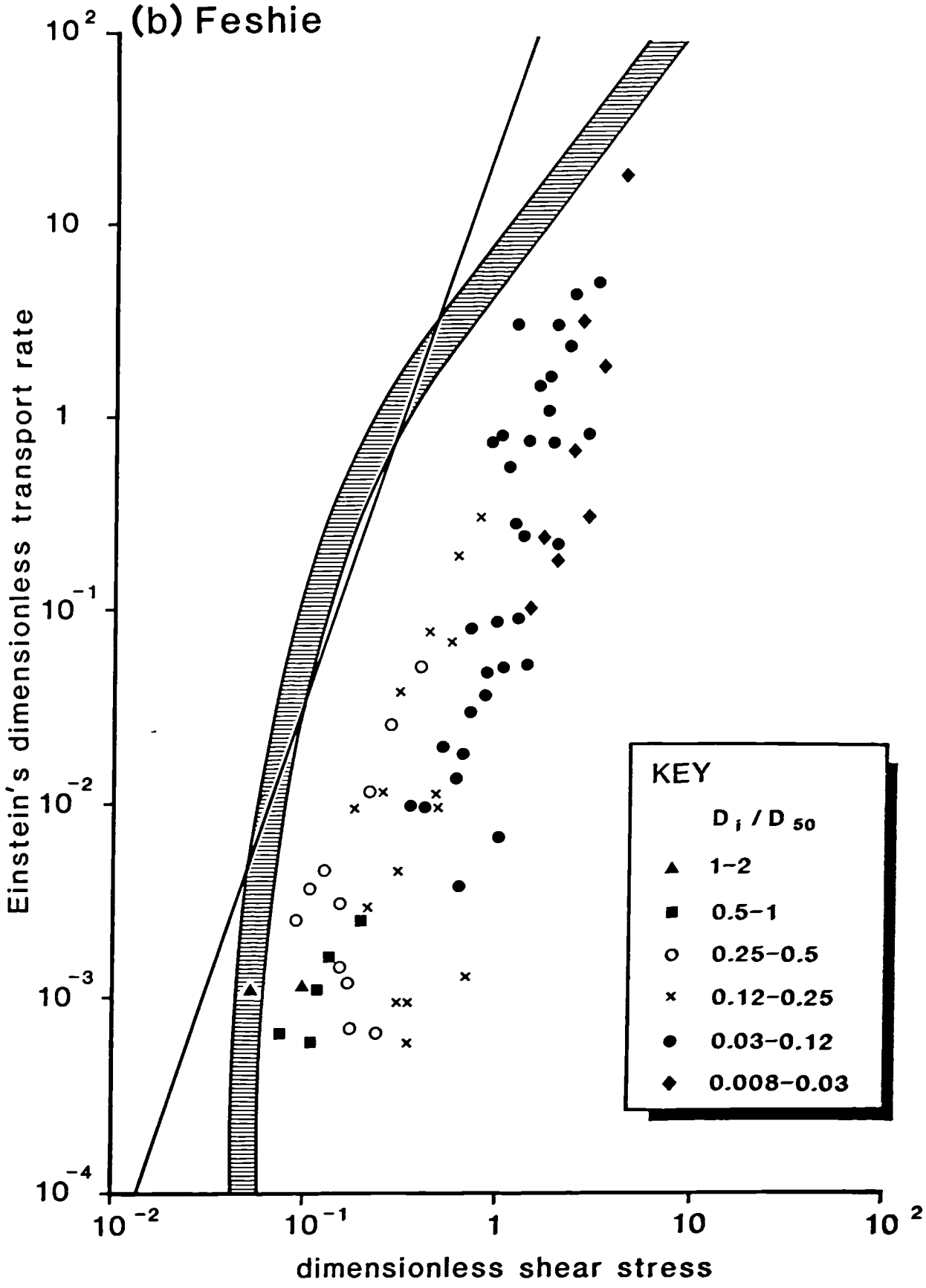
(b) Feshie
Einstein's dimensionless transport rate
dimensionless shear stress
10^2
10
1
10^{-1}
10^{-2}
10^{-3}
10^{-4}
10^{-2}
10^{-1}
1
10
10^2
KEY
D_i / D_{50}
1–2
0.5–1
0.25–0.5
0.12–0.25
0.03–0.12
0.008–0.03

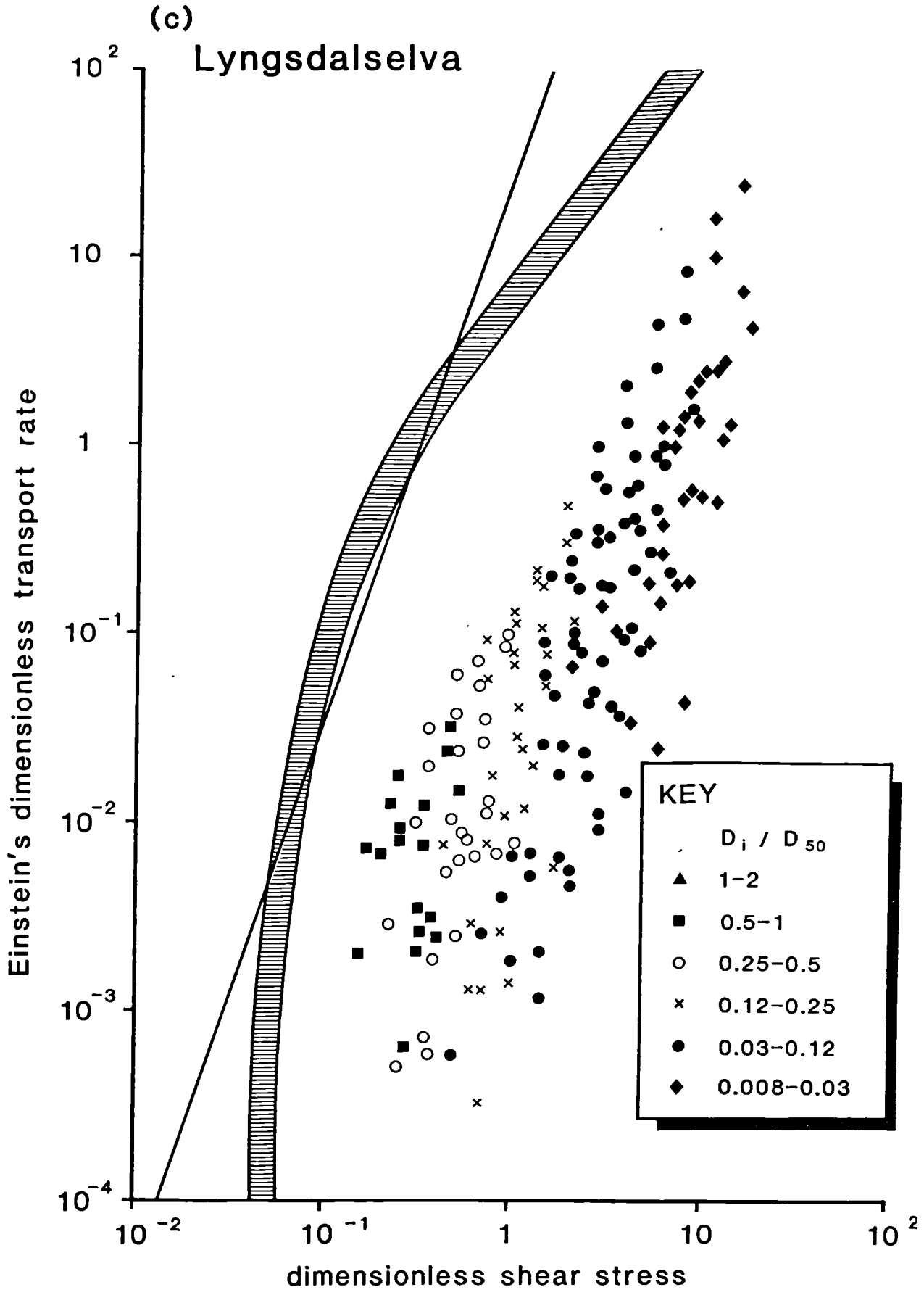
(c)
Lyngsdalselva
Einstein's dimensionless transport rate
dimensionless shear stress
KEY
D_i / D_{50}
1-2
0.5-1
0.25-0.5
0.12-0.25
0.03-0.12
0.008-0.03

Table 4.2 Regression equations of Einstein dimensionless transport rate against dimensionless shear stress for individual size fractions (with corrected intercept) for the Dubhaig, Feshie, Lyngsdalselva, and all the data combined.

Data	n	Regression equation	s	calc. t	r^2 %
Dubhaig	281	$\phi_i = 0.25\tau_i^{*1.8}$	0.79	18*	54
Feshie	73	$\phi_i = 0.34\tau_i^{*2.3}$	0.59	15*	77
Lyngsdalselva	180	$\phi_i = 0.066\tau_i^{*1.7}$	0.62	18*	65
All rivers	534	$\phi_i = 0.18\tau_i^{*1.7}$	0.74	27*	58

* Significant at the 0·05 level.

pre-avulsion bedload samples from the Lyngsdalselva are used in the size fractional analyses because of uncertainties in the bed material grain size and the differences in sediment availability before and after the flood of 7/8 August (see 4.2). Because of the large amount of scatter the intercept was multiplied by the correction factor of $\exp(2.65s^2)$ from Ferguson (1986).

As Figs. 4.9a-c and Table 4.2 show there is a considerable scatter of the data (indicated by the s values) although the relationships are highly significant at the 0.05 level. This is not surprising when considering the problems associated with current metering and Helley-Smith sampling (2.2.2 and 2.2.3) in coarse bedded rivers. Despite the scatter it must be remembered that the plots for each river are actually composite plots using data from different reaches with different sized bed material (although they are all corrected for the percentage available from the bed for each size fraction for every reach). Unfortunately conditions only permitted one day's bedload sampling and shear stress measurement in a competent flow in the Feshie and the plot only represents a total of eight samples.

Hidden behind the scatter the data do follow the trends described earlier in 4.2. Despite their being a hint of curvilinearity at low transport rates, regressions of the lines for each river all have gradients close to, but slightly steeper than, 1.5. This is a similar gradient to that of the predictive curves of Meyer-Peter and Müller (1948), Einstein (1950), and Parker (1978). Since the transport rates are lower, the regression lines are much steeper for each river, representing that part of the traditional curves before linearity is achieved. However, the general gradient of about 1.7 is still close to that suggested by earlier workers. It may be recalled that this 1.5 trend of the Einstein plots is also used in the work of Parker et al. (1982b) who recommended a conversion from ϕ_i

to W_i^* (by dividing ϕ_i by τ_i^* to the power of 1.5) to allow the data to separate out more satisfactorily and show the steepening of transport rates at little above the threshold.

A comparison of Figs. 4.9a-c shows that the three rivers all plot in a very similar position relative to the superimposed curves of traditional work. This discrepancy of between one and two log cycles has been explained in 4.2 by the inefficiency of sediment transport in heterogeneous bed material. It was argued that the bed structure and variation in sediment size leads to a restriction of particle entrainment with the fine material requiring a higher τ^* because they are hidden and trapped. In contrast the coarser particles need a lower τ^* since they protrude and have smaller pivoting angles. Figs. 4.9a-c show this clearly when the transport rates are separated into different size fractions. The coarser fractions plot to the left (small τ^*) and the finer fractions to the right (high τ^*) with clear boundaries between each size fraction. To some extent this is a function of the change in D in the formula $\tau^* = \tau / (\rho_s - \rho)gD$ since for each sample τ, ρ_s, ρ, and g are the same for all fractions. However the fact that for each individual size fraction all the samples plot along similar parallel trend lines (as in a Parker plot) shows that there is a consistent pattern in each river. Furthermore in the cases of the Dubhaig and Feshie where the bedload samples are from different reaches there is still a regular pattern for all size fractions.

It is also interesting to note that the three rivers have similar threshold values of τ_i^*. Although the lowest value of τ_i^* regardless of particle size does not necessarily represent critical conditions i.e. just when the particle is beginning to move, it does give some indication of the lower limit of τ_i^* (which should be just above the τ_{ci}^* limit). The values of the smallest τ_i^* were 0.046, 0.053, and 0.155 for the Dubhaig, Feshie, and Lyngsdalselva respectively which also fall into the range

suggested by previous workers cited in 4.1.3 (the Lyngsdalselva τ_i^* was as low as 0.006 in post-flood conditions, but this and other points are not used in Fig. 4.9c since the bed conditions and grain size were unknown).

The plots of ϕ_i against τ_i^* demonstrate that there is a complex series of processes operating in gravel-bed rivers which need further investigation. The Einstein plots show that the entrainment of gravel is not as efficient as the theory claims it should be, so how can this inefficiency be explained and quantified? As discussed earlier in 4.3.1 the Parker method looks at the transport rates of individual size fractions and assesses whether there is any size selective transport or whether all sizes have an equal chance of being entrained. The hiding factor in the relation of τ_{ri}^* to D_i/D_{50} that is arrived at using the Parker method is in effect a scale of transport possibilities from 0 to 1 representing the degree of restriction of particle movement. A hiding factor between 0 and 1 corresponds to a general situation whereby some fines and smaller pebbles are hidden and prevented from moving, while larger pebbles protrude into the flow and move, but in some of the cases their weight cancels out their chance of entrainment. The varying proportions of selective and equal mobility of particles are sandwiched between a hiding factor of zero at the one end (where larger particles will only move of the fluid force increases) and a hiding factor of 1 at the other (where all sizes move regardless of their weight, size or shape). With a rise in discharge (and shear stress) over a particular bed a hiding factor of zero would mean progressively coarser particles move, but with a hiding factor of 1 nothing moves at first until a 'threshold' condition is reached and all sizes move. In terms of efficiency, with a hiding factor of 1 a bed is less efficient at low flows, but more efficient at high flows (once the threshold has been crossed). In this way the hiding factor can be used to quantify the outcome of the processes operating in coarse heterogeneous bed material.

The results from a detailed Parker analysis for individual rivers and all the data combined are given in Table 4.3 while Fig. 4.10 shows an example of the data plotted on a Parker-type diagram. As an example to help explain how Table 4.3 was derived, the calculations involved for the Lyngsdalselva will be followed through in detail. It was decided that several 'cutoffs' could be employed on the data to see if they altered the results or made them statistically significant. The four cutoffs chosen were (a) all the data regardless of size or position on the plot, (b) W_i^* greater than 0.01, i.e. a minimum but significant transport rate, (c) D_i/D_{50} > 0.1, i.e. excluding very fine material with coarse surrounding bed material, (d) τ_i^* < 1, i.e. only bedload as dictated by the suspension criterion implied by Bagnold (1966). The data for the 17 bedload samples that were taken before a major channel avulsion were compiled as discussed in 4.3.1 and plotted in Fig. 4.10. The overall impression from Fig. 4.10 is that there is a definite separation of points from low to high τ^* according to size (which is not surprising since it is identical to the earlier Einstein plot of the same data in Fig. 4.9c but without the 1.5 gradient). A forwards multiple regression for all the data gives an equation of

$$W_i^* = 0.249\,\tau_i^{*1.448}\left(D_i/D_{50}\right)^{1.378}$$

with s = 0.52, r^2 = 30%, n = 180 (both predictors significant at the 0.05 level). By setting W_i^* to 0.002 and rearranging, the hiding function can be obtained

$$\tau_{ri}^* = 0.0357\left(D_i/D_{50}\right)^{-0.952}$$

However, since measurement error is present in both the transport rate and

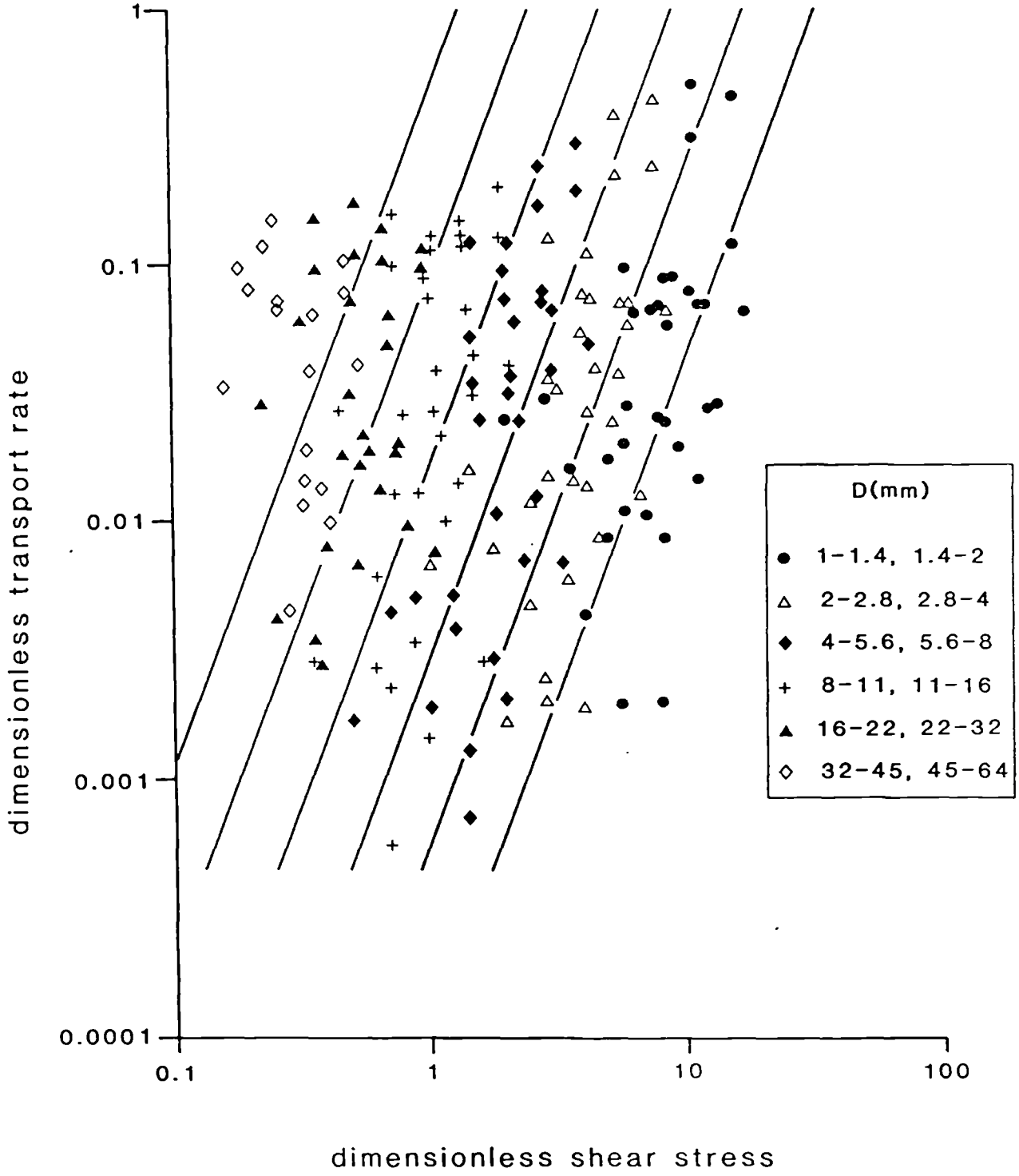

Fig. 4.10 Dimensionless transport rate, W_i^*, plotted against dimensionless shear stress for individual size fractions of the 17 Lyngsdalselva pre-avulsion Helley-Smith samples (compare to Fig. 4.8). Regression lines are superimposed from the calculations shown in the text.

shear stress it is just as valid to work from the inverse multiple regression

$$\tau_i^* = 0.515\, W_i^{*0.204} \left(D_i/D_{50}\right)^{-0.890}$$

with s = 0.20, r^2 = 84% (both predictors significant at the 5% level) which gives a hiding function of

$$\tau_{ri}^* = 0.145 \left(D_i/D_{50}\right)^{-0.890}$$

Better still, the two regressions can be bisected using the mathematical procedures outlined in Appendix B (R.I. Ferguson, personal communication, 1986) to obtain the hiding function

$$\tau_{ri}^* = 0.0868 \left(D_i/D_{50}\right)^{-0.920}$$

Because of certain constraints on the data some of the multiple regressions are untrustworthy and therefore are not included in the results in Table 4.3. The main reason for this is that ϕ increases so steeply with an increase in τ^* for each size fraction that the forwards regression can occasionally lead to fitting a horizontal line to the data (because the least squares regression minimises the residuals in the y direction and with a steep gradient the residuals are large). The N.A. symbol in Table 4.3 represents these unusable results.

The hiding factor calculated for all the Lyngsdalselva data is very similar to those calculated using different cutoffs. Table 4.3 shows that

Table 4.3 Hiding factors from Parker-type analysis on different sets of data from the Dubhaig, Feshie, and Lyngsdalselva.

Set of Data	All Rivers	Dubhaig	Feshie	Lyngsdalselva
All data[A]	0.75** n 534	0.65 n 281	0.67 n 73	0.92** n 180
W_i^* > 0.01[B]	N.A.	N.A.	0.75** n 42	0.94** n 136
D_i/D_{50} > 0.1[C]	0.71* n 274	0.75** n 149	0.84 n 35	0.99** n 90
τ_i^* < 1[D]	0.43** n 302	0.38 n 178	0.54 n 47	N.A.
τ_{r50}^*[E]	0.047	0.072	0.054	0.087

A > 1 mm
B Minimum transport rate
C Excluding fine material
D Bagnold's suspension criterion
E For all data > 1 mm (as above)

* Significant at the 0.1 level
** Significant at the 0.05 level

two other hiding factors are greater than 0.9 and significant at the 0.05 level although the cutoff of $\tau^* < 1$ does not give a usable result. Interestingly Table 4.3 shows that even when the $\tau^* < 1$ cutoff is employed for data from other rivers the hiding factor comes out appreciably lower in magnitude than that expected using other cutoffs. This together with the Einstein plots in Figs. 4.9a-c gives support to the suggestion that the fine sediment appears to follow the trends set by the coarser particles regardless of the τ^* and that any censoring of the data only serves to cloud any relationship that may exist. The Bagnold (1966) criterion for suspension may therefore be on the low side, especially in coarse heterogeneous material.

Table 4.3 also shows the τ^*_{r50} from the multiple regressions for each river and all the data combined (using no cutoffs). The τ^*_{r50} values of 0.072, 0.054, 0.087, and 0.047 for the Dubhaig, Feshie, Lyngsdalselva, and all three rivers combined respectively are very similar to the Parker et al. (1982b) value of 0.088 and Andrews (1983) of 0.083. The Lyngsdalselva is particularly interesting since it has hiding factors and τ^*_{r50} almost identical to that found by Parker et al. (1982b) and Andrews (1983). The τ^*_{r50} for the other rivers are still well within the range of τ^*_c suggested by previous workers discussed in 4.1.3 (for example Church (1978) assembled data with τ^*_c between 0.02 and 0.12) although τ^*_{r50} is not strictly equal to τ^*_c.

As stated earlier the Parker et al. (1982b) analysis was supplemented by Andrews (1983) using a different type of data and approach but arriving at a similar net result with a relation between τ^*_{ci} and D_i/D_{50} and a hiding factor represented by the exponent, -b. Hence the Andrews (1983) method and results will be described before a general discussion of the differences between rivers and implications for the mode of bedload transport.

4.4 Analysis of maximum size transported

4.4.1 Methodology

This method was first reported in Andrews (1983) and is based around the assumption that the τ^* computed for the largest particle travelling as bedload at a given discharge would approximate the critical value, τ^*_{ci}, as long as larger particles were present on the river bed. Most of the bedload samples used in this type of analysis described below were taken when some lag material was left on the bed, but it may be doubtful whether this applies to the Lyngsdalselva rainflood data. The averaging of results inherent in the Andrews method helps to overcome this problem and also the randomness of whether one brief Helley-Smith sample catches one of the critical-sized pebbles whose transport rate in number per unit width and time is presumably very low.

All bedload samples are grouped according to the size class of the largest particle present (D_{MAX}) and τ^*_{ci} calculated for that size class using the measured τ and geometric mean of the bounding sieves in the equation in 4.1.2. The series of values of τ^*_{ci} for various size classes are averaged ($\overline{\tau}^*_{ci}$ for every identical D_i/D_{50} ratio and a log-log regression determines the slope of the line or hiding factor. Again a b exponent near the value of 1 means that most particle sizes move within a narrow range of shear stress or have almost total equal mobility.

Following the work of Parker et al. (1982b), Andrews (1983) likewise derived his relationship using the ratio of D_i to the D_{50} of the subsurface material. Andrews (1983) does report that he attempted to use the surface bed material as the representative grain size, but the correlation coefficient and standard error of estimate for his data

indicated that the relationship was stronger using the subsurface material as characteristic of the river bed material. As discussed in 4.3.1 the surface bed material is preferred for use in the Parker method with the exception of the flood samples of the Lyngsdalselva. This same assumption is used in the Andrews method except that all the Lyngsdalselva samples are compared to the surrounding surface D_{50} to avoid inconsistency and the data plotting further to the right, so distorting the relationship. Only data with a D_{MAX} coarser than 5.6 mm was included in the analysis since it is unlikely that a D_{MAX} for any material finer would truly represent the flow conditions (given the sampling errors with such small material). A plot using all the data (39 points) supported this suggestion with a large scatter introduced by the finer samples.

The Andrews method is useful not only as a comparison to the Parker method but also since it allows all the data regardless of size differences in bed material to be plotted on one graph. It must be noted however that Andrews (1983) advocates an averaging of τ^*_{ci} which although it does not alter the computed relation, does improve the plot and scatter within the relation.

4.4.2 Results

The data from all the rivers are calculated and plotted according to the Andrews method as shown in Fig. 4.11 (64 bedload samples, 34 points, D_{MAX} > 5.6 mm). A log-log regression gives the relation

$$\overline{\tau^*_{ci}} = 0.0851 \left(D_i / D_{50} \right)^{-0.829}$$

with s = 0.22, r^2 = 57%

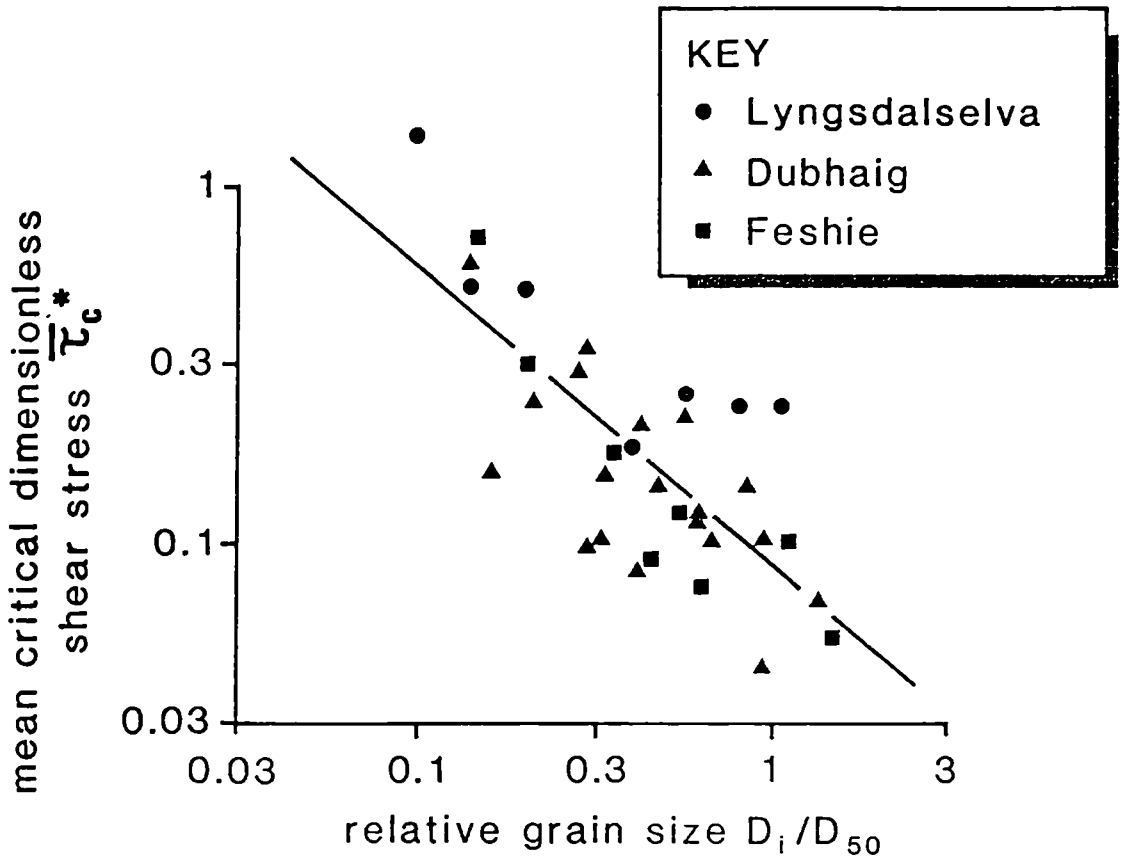

Fig. 4.11 Mean critical dimensionless shear stress plotted against relative grain size for all the Helley-Smith bedload samples from the Dubhaig, Feshie, and Lyngsdalselva.

Despite the scatter the relationship is highly significant (at the 0.001 level) and is similar to the hiding factor from the Parker method shown in Table 4.3. Also the τ^*_{csO} value of 0.085 falls into the range discussed previously and is remarkably similar to that reported by Parker et al. (1982b) and Andrews (1983). Since the averaging of τ^*_{ci} reduces the number of points for each river, individual regressions for each river are not reliable. However using the Dubhaig which has the largest amount of data available (19 points based on 31 bedload samples) the regression gives a hiding factor of 0.69 (s = 0.20, r^2 = 47%, calculated t of -3.9). Again the hiding factor is very similar to that found using the Parker method which for all the Dubhaig data is 0.65 and a cutoff excluding fine material is 0.75 (significant at 0.05 level). These results give further support to Parker et al. (1982b) and Andrews (1983) by showing that the Andrews and Parker methods give similar conclusions even though they use a different analytical approach to arrive at the relation. In addition Fig. 4.11 shows that all three rivers plot in the same range of τ^*_{ci} and D_i/D_{50} (i.e. all approximately on the same trend line) and thus must have similar hiding factors. This is backed up by Table 4.3 which shows that all hiding factors calculated by the Parker method are greater than 0.65 (excluding the $\tau^*_i < 1$ cutoff) with the significant relationships all greater than 0.75. Furthermore, the data for all the rivers together, with no cutoffs, gives a significant relation and a hiding factor similar to that for each river treated separately.

4.5 Discussion

Interpreting the results from 4.3 and 4.4 along the lines reported in Parker et al. (1982b) and Andrews (1983), leads to the conclusion that bedload transport in rivers with coarse heterogeneous bed material is not simply a case of larger particles moving as the shear stress increases. Larger particles increase their chance of movement by having smaller

pivoting angles and protruding into the flow. Conversely, the hiding of fine particles in bed structures and in the wake of, and beneath larger particles restricts their chances of being entrained. These two situations combine to give a state where the effect of the larger particles having a heavier weight cancels out with the problems that fine material have to become exposed to the flow and all the sediment regardless of size and weight has a near equal chance of being mobilised. Taken to its extreme and as reported in the recent paper by Andrews and Parker (in press) this situation can result in total equal mobility as expressed by a hiding factor of 1. Importantly though the results reported here show a hiding factor much less than 1, although certainly greater than zero which would imply total selective transport. This is in agreement with the analysis of Ferguson (in press) using almost the same Lyngsdalselva data but when correcting the samples for the percentage of sediment available in the *subsurface*. His conclusion that his data are closer to the equal mobility end of a spectrum of transport possibilities starting from constant Shield stress for all sizes at the other extreme seems to be borne out by the results found here. The hiding factor of 0.947 reported by Ferguson is similar to that found when some of the data is corrected for the bed surface size but is still much higher than that found in the Dubhaig and Feshie as shown in Table 4.3. The reasons for this discrepancy are discussed later.

Despite this it does seem that the recent work by the research teams of Parker and Andrews appears to be getting closer to qualifying the effects of the processes acting in gravel-bed rivers and that the traditional work of Shields (1936), Meyer-Peter and Müller (1948) and Einstein (1950) should no longer be used in any engineering or palaeohydrological computations involving sediment with a range of sizes.

The results from the Dubhaig, Feshie, and Lyngsdalselva lend further

support to recent criticisms of the Parker and Andrews work raised in discussions at the Pingree Park Workshop on "Sediment Transport in Gravel-Bed Rivers" in August 1985 (R. I. Ferguson, personal communication, 1985). If the results expressed in the papers of Parker et al. (1982b), Andrews (1983), Andrews and Erman (1986) and Andrews and Parker (in press) are correct (with hiding factors very close to 1) then this implies that there is almost total equal mobility that will be replaced by a return to no sediment movement when the hydraulic conditions drop below this 'threshold' of shear stress. But if the arguments of Parker and Andrews are followed and total equal mobility is possible with the mobile armour continually releasing all sizes of sediment to the flow until the shear stress drops below a threshold, then there would be no scope for any size selective transport and therefore there should be no down-bar or downstream fining. Their opinions on this are elaborated in 4.6.2 but are countered by the overwhelming evidence for selective transport observed by many fluvial geomorphologists. The results for the Dubhaig, Feshie and Lyngsdalselva reflect this, which can be shown either by the relationship between the shear stress and the D_{50} of the bedload (Fig. 4.12) or pictorially by an extensive grain size map of bar surfaces. (Fig. 4.13).

Fig. 4.12 and Table 4.4 show that there is a positive relationship (significant at the 0.05 level for each individual river) between the D_{50} of bedload and the shear stress i.e. that the median size of the bedload increases as the shear stress increases as traditionally assumed. Fig. 4.13 shows that there is ample evidence for both down-bar and downstream fining in the Lyngsdalselva. For example, at W at the head of the braiding reach the characteristic size is 277 mm, compared to 53 mm at X in the lower reaches, and on bar Y the size falls from 154 mm at the bar head to 70 mm at the tail. The selective transport implied by this is most likely a function of slope (which reduces by half from W to X), compounded by the overall divergence of flow from a single channel into

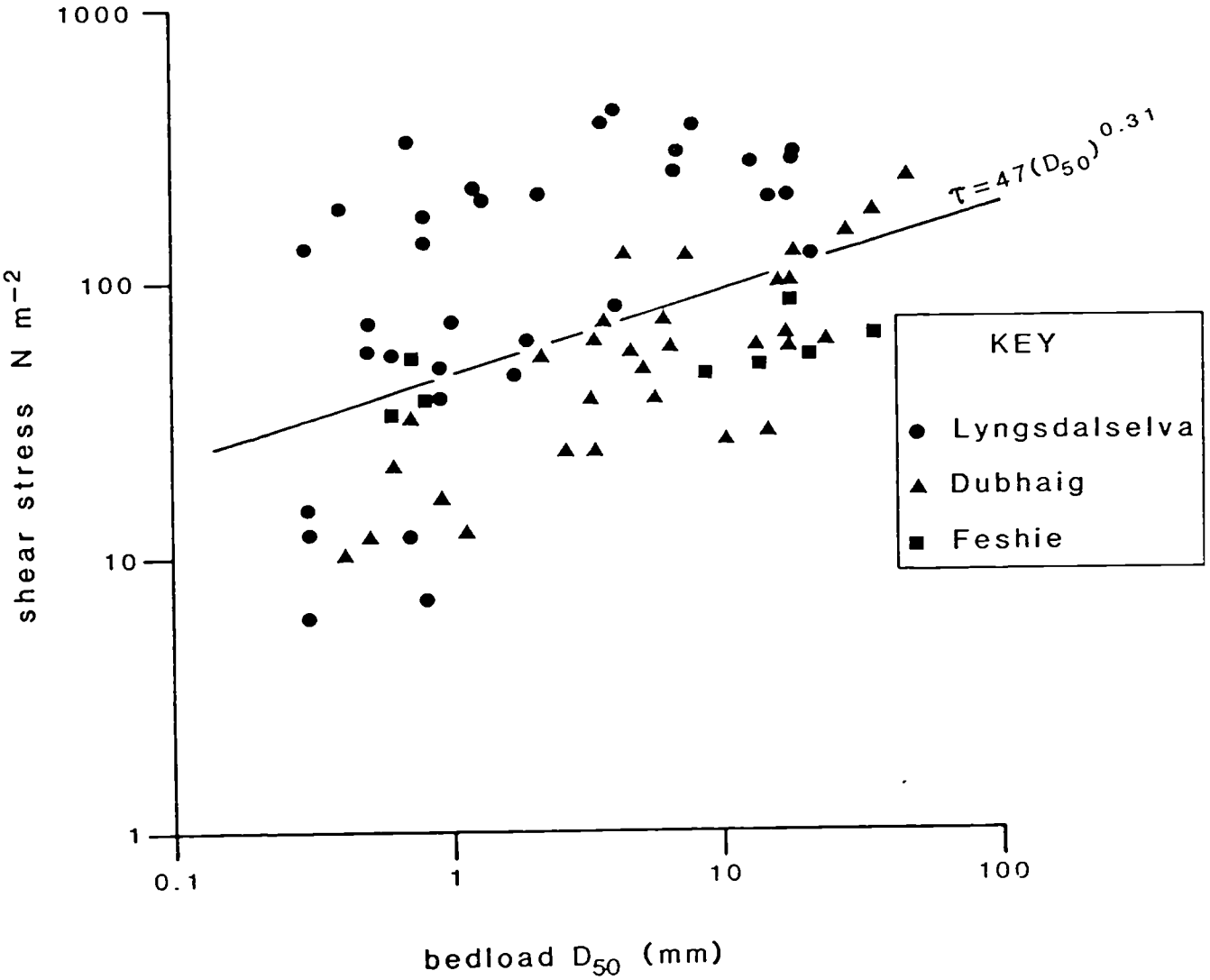

Fig. 4.12 Shear stress plotted against the bedload D_{50} for 72 Helley-Smith samples taken in the Dubhaig, Feshie, and Lyngsdalselva.

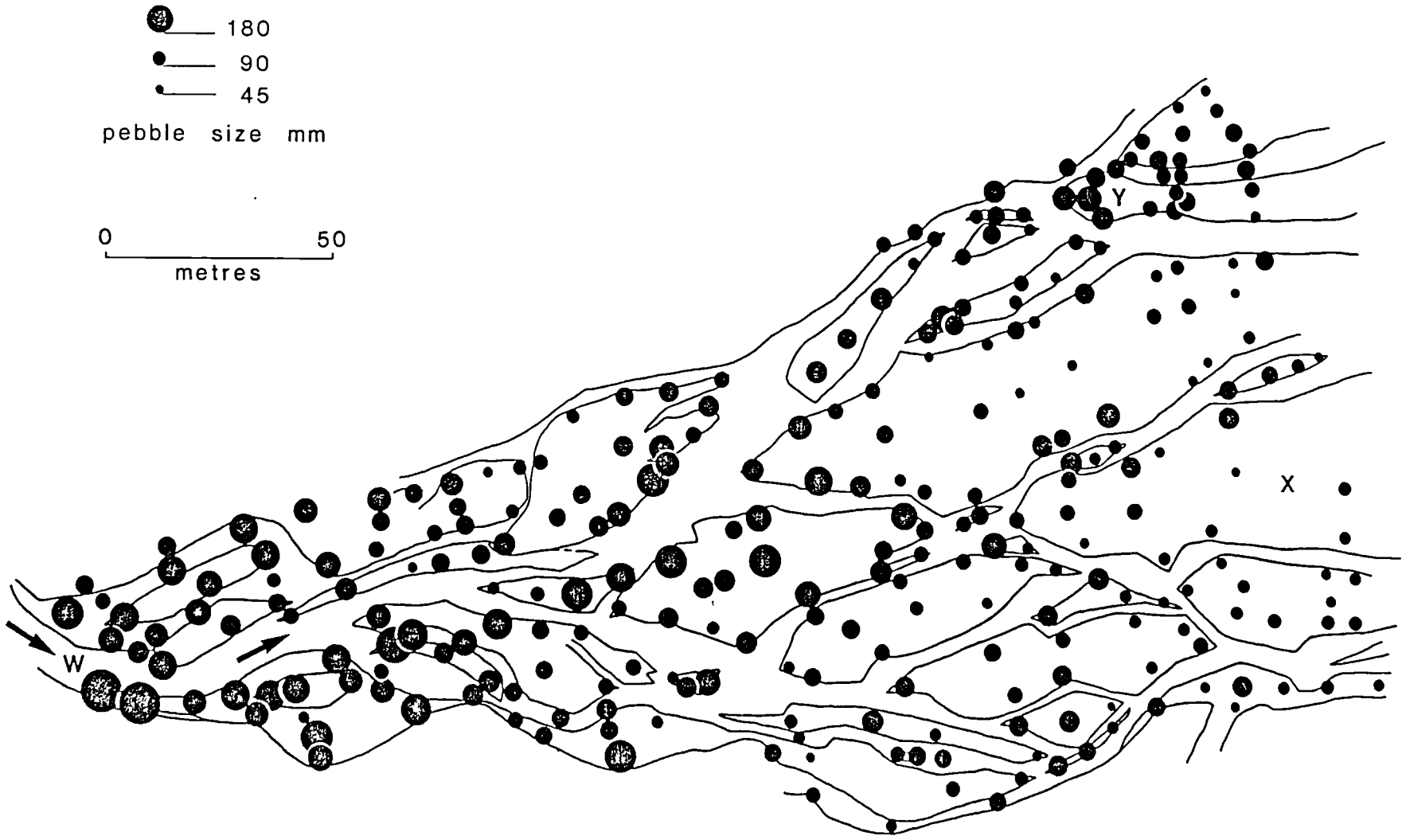

Fig. 4.13 Maximum surface grain size (mean b-axis of 10 largest clasts in 1 m²) on bars within the study area of the Lyngsdalselva.

Table 4.4 Results from log-log regressions of shear stress against bedload D_{50} for the Dubhaig, Feshie, Lyngsdalselva, and all rivers combined.

Data	n	Gradient	s	calc. t	r^2 %
Dubhaig	31	+ 0.50	0.22	7.1*	63
Feshie	8	+ 0.13	0.096	2.6*	53
Lyngsdalselva	33	+ 0.52	0.42	4.3*	35
All rivers	72	+ 0.31	0.40	4.2*	19

* Significant at the 0·05 level.

several distributaries as it enters the braided reach (see Ashworth and Ferguson (1986)). Likewise the Dubhaig has a 76% decrease in surface D_{50} in 2 km from Reach A to E, and the Feshie Reach B has a down-reach change in surface D_{50} from 87 to 33 mm over the 45 m from a poolhead to a pooltail. Therefore there must have been some selective transport in all three rivers which either enables smaller particles to be carried a longer distance or whereby the smaller sediment is winnowed out of the coarse bed structures and imbricated armour layers.

To summarise, the hydraulic processes operating in gravel-bed rivers are complex with a great spatial variability. The entrainment of a particle at any point on the bed is not simply a function of the magnitude of the force that the flow is inflicting on the particles. The bed structure and physical arrangement of the various sized particles can enhance or restrict movement of different sizes. Data from the Dubhaig, Feshie and Lyngsdalselva indicate that the movement of sediment is not simply a choice between equal mobility or selective transport, but in between both. Likewise sediment movement cannot be described solely by the 'mobile armour' or 'static armour' theory, but a combination of both. At low flows there is selective transport as fines are winnowed out of the surface matrix. During a flood as the discharge (and shear stress) rises this selective transport increases, with larger sizes moving, but also the occasional protruding boulder moving. With the structure of the bed altered and unstable, the pebbles surrounding these boulders are equally mobile together with the fines both in their wake and below in the subsurface. At peak flows (or when the shear stress approaches some sort of 'equal mobility threshold') all sizes are moved and there is a free interchange between the surface and subsurface. As the flow drops the threshold is crossed again and there is a return to selective transport with the intermittent movement of boulders. The coarse material stops moving and forms pockets of low shear stress for the finer material to

settle in. In addition it protects the newly formed or modified subsurface. Bedforms develop as other pebbles drop out of the flow and collide and interlock with the initial stationary boulder. Finally as the flow drops below the competence required to move any sizes of coarse material the fine sand element of bedload infiltrates the bed sediments. In the following days or suitable time span, the occasional moderate flow, which is not high enough to entrain most pebble sized material, selectively transports the fines and any loose material (which in turn may release the odd pebble into the flow). There is therefore a return to the selective transport experienced before the flood.

This picture of sediment movement is very general and needs a lot more work to substantiate it. However, the Parker and Andrews-type analyses both support the idea that there is considerable scope for selective transport. Similarly the bed may almost act like a mobile armour for most of the moderate flows as envisaged by Andrew and Parker (in press) but at low flows this is replaced by a winnowing static armour, and at high flows occasionally by a totally destroyed bed with all sizes from the surface and subsurface moving en masse. The bedload samples used in the analysis here (excluding those taken in the rainflood in the Lyngsdalselva) were all taken in conditions in the range between a static armour merging into a mobile armour i.e. there was some equalisation of mobility due to hiding and protrusion effects but also substantial selective entrainment. The pebble tracing results described below in 4.6 also support this.

Work by Proffitt (1980), Proffitt and Sutherland (1983) and Sutherland (in press) has suggested that static armours may actually be more common than mobile armours in gravel-bed rivers. Proffitt's (1980) flume work with nonuniform material showed that at a constant discharge a static armour can form chiefly by selective entrainment. Sutherland (in press) argues that the mobile armour of the Oak Creek may actually be an

unrepresentative example to be extended to all rivers since there may well be "sediment supply from upstream causing either a mobile armour or an overpassing situation." Indeed Parker et al. (1982b) test their semi-empirical relationship using data from four other rivers and found that it only reasonably predicted bedload transport rates in two of the cases. They concluded that their relationship (and theoretical background) "is questionable" when applied to large, low-slope gravel-bed rivers with large amounts of throughput sand. A further complication is introduced as a result of recent work by Reid et al. (1985) and Reid and Frostick (1986) in the Turkey Brook, U.K. They suggested that there actually may be no simple relationship between gravel transport rates and channel flow parameters. Reid et al. (1985) showed that there may be suppression of gravel movement rates at the peak of flood flows (precisely at the time when the rates, theoretically, should be expected to be at a maximum). Carson (1986) questions whether these results are not a peculiarity of the local flow in the vicinity of the sampler and suggests that sediment movement may consist of such long hop trajectories that it misses their bedload trap. Certainly their results "seem strange" (Carson 1986) and are not supported by the field observations in either the Dubhaig, Feshie or Lyngsdalselva.

The controversy concerning the widespread applicability of Parker's mobile armour theory to all gravel-bed rivers is not helped by the circular argument in the original report by Parker et al. (1982b). They carefully selected data that represented conditions when the armour was "broken" (they used a discharge of 1 $m^3 s^{-1}$ as the arbitrary dividing line). When discharges exceeded 1 $m^3 s^{-1}$ "bedload transport becomes governed by hydraulic conditions rather than availability" (Parker at al. (1982b)). Thus the analysis starts off with mobile bed conditions and finishes by proving that the armour is fully mobile!

Clearly then there is mounting evidence in the literature to suggest that the work of Parker et al. (1982b) and Andrews (1983) may be site-specific and that a mobile armour may only exist in a few river types. The discussion here suggests that a static armour and mobile armour can both be present in gravel-bed rivers. The dominance or presence of either bed morphology is a refection of the discharge and shear stress. As the discharge rises, selective entrainment from the static armour is gradually replaced by an equalisation of particle mobilities. If the bed is ruptured then all sizes become equally mobile. As the discharge decreases there is a return to the static armour and selective transport again plays a major role (although some particles are still hidden or protrude/pivot). The results of any Parker of Andrews-type analysis must therefore depend on the magnitude of flow and shear stress that bedload samples are taken at. If the hypothesis put forward from the data reported here is correct then sampling when the armour is totally mobile/broken would indicate a hiding factor of almost 1 and near total equal mobility. However, sampling at conditions in near peak flows (say at just bankfull) where there is bedload movement, but only occasional pulses or spurts of coarse sediment, should give a hiding factor of below 1 but still well above zero (the situation reported here). If bedload sampling was conducted at low flows (given the sampling time required to obtain any representative sample size) then this should give a hiding factor close to zero.

Evidence to support this comes from the differences in hiding factors between rivers as shown in Table 4.3. The table shows that the Dubhaig and Feshie have very similar hiding factors of around 0.7 whereas the Lyngsdalselva has a hiding factor of about 0.9; close to the 1 equal mobility state. The 17 bedload samples used in the Lyngsdalselva Parker method analysis were all taken in high meltwater flows or bankfull conditions. The transport rates and shear stresses are some of the highest ever measured and are at least an order of magnitude higher than

in previous studies (see 4.7.2). Personal observations support the idea that the transport conditions in the Lyngsdalselva were very different from the Dubhaig and Feshie. The bed felt much looser and there was considerable scour around measuring instruments, very large pebbles were striking the current meter shaft, and particularly during the rainflood the collision of large boulders was clearly audible. All these observations point to conditions close to equal mobility with a rupture of the armoured layer and all sizes moving. Hence the Lyngsdalselva data gives a hiding factor near 1 using a Parker-type analysis (similar to the results of Parker et al. (1982b) when the armour was broken). The Dubhaig and Feshie data however reflect conditions when the armour was still intact and although there was sporadic interchange into the flow from a type of mobile armour, selective entrainment still played an important role. Further support for this comes from the pebble tracer results which are discussed in detail in 4.6.

The Parker and Andrews analyses in 4.3 and 4.4 show that both the effects of protrusion of large particles and hiding of fine sediment can lead to a near equalisation of mobility which when assisted by a breaking of the armour layer can lead to all sizes of sediment moving within a narrow range of shear stress. Unlike previous work, the Dubhaig, Feshie and Lyngsdalselva data show that there is still plenty of scope for selective transport both as the stage rises towards a peak flow and then later in subsequent medium/low flows. The number of occasions when the armour ruptures and all sizes of sediment are available for transport is probably very few (see 4.7 for a quantification of this for the Dubhaig) so the transport possibilities for the bulk of the flow conditions are dominated by selective transport. This helps to explain the down-bar and downstream fining found in all three rivers. The balance between selective and near equal mobility transport is not clear-cut and while they probably merge into each other, they can also be present at the same time in a river bed

with its spatially diverse nature of the bed and wide variation in shear stress.

4.6 Supporting evidence from pebble tracer experiments

The Helley-Smith bedload results in 4.2-4.4 indicate that the probability of entrainment for a particle is not solely dependent on the particle's weight. At peak discharges bedload transport approaches equal mobility although there is still some scope for selective entrainment. In order to establish whether there is a substantial difference in mobility with size and shape, nine separate tracing programmes were carried out in the three rivers.

4.6.1 Background and methodology

The study here has the advantage over previous projects in that the bedload transport has been investigated both directly by Helley-Smith sampling and indirectly by pebble tracing. The tracer results can thus be used to test whether the earlier findings in 4.2-4.4 (based on a small sample of at-a-point bedload catches) are supported by long term tracer studies. Furthermore the pebble tracers extend the previous results since the pebble tracers are generally coarser than the sizes that can be trapped in the Helley-Smith.

Pebble tracers have been used by Leopold et al. (1966), Keller (1970), Laronne and Carson (1976) and Mosley (1978) to directly investigate the factors affecting the movement of coarse tagged particles. All the studies agree that there is either no or a very slightly negative relationship between particle weight and the distance moved. This is in agreement with the results in 4.3 and 4.4 which suggest that there is always a possibility for some selective transport, the magnitude of which

depends on the river discharge.

Recent work by Komar and Zhenlin (1986), Zhenlin and Komar (1986), and Wiberg and Smith (in press) has indicated that the mobility of particles in heterogeneous bed material is not only affected by the particle's weight but also by its shape and size. Using laboratory tests with sediment up to 50 mm Komar and Zhenlin (1986) showed that the movement of pebbles increases in the order imbricated < angular < smooth ellipsoids < spheres, due to the relationship between the particle shape and its pivot angle. While spheres truly pivot (and at a smaller angle), ellipsoids are well imbricated and can only slide out of position. In addition Zhenlin and Komar (1986) found that the pivoting angles decrease with increasing size so that large pebbles were more likely to stand upright and protrude into the flow, while smaller particles would be depressed and hidden within the bed armour. This latter finding is already inherent in the equalisation of mobility hypothesis but their work supplies the first measurements to confirm the assumptions of Parker and Andrews.

Pebble tracing was undertaken in reaches A-E of the Dubhaig, reaches B and C of the Feshie and reaches A and C of the Lyngsdalselva. The technique of pebble tracing is described in 2.2.3 whilst some of the experimental designs are described in 3.2 and 3.3. The results for reaches A-E of the Dubhaig and reach B of the Feshie are a combination of the measurements described in 3.2.1 and 3.2.2 for pebble movement in different subunits of the pool/riffle cycle. The Feshie reach C tracer experiments were outlined in 2.2.3 and consisted of two groups of pebbles inserted on the barhead and bartail of a mid-channel bar. The Lyngsdalselva experiments are briefly described in 2.2.3. In reach A 188 pebbles were inserted during the rainflood on 7 August. The pebbles were thrown in at A1; 50 at the flood peak (2200h), 50 on the beginning of the falling limb (0012h) and 88 at 0055h when the channel was shallowing (see 4.6.4). Their

positions were fixed the next day. Reach C of the Lyngsdalselva had 255 pebbles inserted at the head of the reach and were re-located after eight days of low meltwater flows. For all tracer experiments the pebbles' weights, sizes and shape factors were computed as described in 2.2.3 and linear regressions performed on the logged variables of distance (the dependent variable) and weight, sphericity and flatness.

A more in-depth analysis of pebble movement was undertaken by considering different size fractions (at 0.5$\emptyset$ intervals) and plotting the percentage and mean distance of movement for each size class. For the Dubhaig the tracer data was separated into the pebble movements through the four individual floods and together with the Lyngsdalselva results provide data on the change in mobility with increasing discharge.

4.6.2 Size and shape selective transport

The results from the linear regressions for the nine reaches are shown in Table 4.5. Since it is not possible to include zero movement with logged variables the regressions are only for pebbles that had moved. Looking firstly at the distance/weight regressions, Table 4.5 shows that in eight of the reaches there was a negative relationship (and generally very weak - the maximum sized exponent is -0.33), with a lot of scatter (r^2 very low) and three relationships significant at the 0.05 level. Interestingly the only reach that had a positive relationship (which indicates that heavier particles move <u>further</u>) was reach A of the Lyngsdalselva. This compares with the strongest negative relationship which is also in the Lyngsdalselva (reach C). Recalling the results and interpretations of bedload movement for the three rivers discussed in 4.5, the samples used in the Lyngsdalselva Parker method analysis were taken in different bed conditions than the other two rivers (including the peak discharge on 7 August when the bed armour was broken). The reach A pebble tracers were

Table 4.5 Results from log-log regressions* of distance moved of pebble tracers (dependent variable) and the tracer's weight, sphericity, and flatness (independent variables) for nine reaches of the three study rivers.

River/ Reach	N	Distance/weight			Distance/sphericity			Distance/flatness		
		b	r^2	t	b	r^2	t	b	r^2	t
Dubhaig										
A	301	-0.019	0.0	-0.29	-0.12	0.10	-0.51	0.08	0.0	0.36
B	258	-0.29	3.8	-3.2**	0.88	2.8	2.7**	-0.83	2.6	-2.6**
C	283	-0.032	0.0	-0.32	0.60	2.3	2.6**	-0.58	2.3	-2.6**
D	227	-0.32	3.8	-3.0**	0.41	0.80	1.3	-0.37	0.70	-1.2
E	174	-0.20	2.1	-1.9	-0.16	1.2	-1.4	-0.60	1.8	-1.8
Feshie										
B	112	-0.22	2.9	-1.8	1.1	4.4	2.2**	-1.1	4.3	-2.2**
C	118	-0.0041	0.0	-0.071	0.45	1.8	1.5	-0.43	1.7	-1.4
Lyngsdal'										
A	49	0.40	4.0	1.4	-0.014	0.0	-0.040	-0.16	0.10	-0.23
C	168	-0.33	7.5	-3.7**	0.52	1.8	1.7	-0.54	1.9	-1.8

* The exponent/gradient (b), coefficient of determination (r^2), and calculated t-ratio (t) from the regressions are given.

** Significant at the 0·05 level.

inserted during the 7 August flood and measured the next day so that their movement was solely during mobile bed conditions in a brief peak flood. If the interpretations in 4.5 from the Helley-Smith sampling are correct then the Lyngsdalselva approached equal mobility during this rainflood. The tracer results directly support this even indicating that the coarser particles were more mobile than their finer counterparts. This has also been reported by Wiberg and Smith (in press) who showed from a flume study that the coarser particles were the first to move from the bed armour. However caution needs to be applied here since only 40% of the pebbles were recovered and the highly turbid proglacial meltwater probably prevented the re-location of many pebbles which had moved well out of the abandoned and dry reach A into the active areas downstream. Also there could be possible bias since larger pebbles are easier to find.

Reach C of the Lyngsdalselva has the strongest inverse relationship between the distance moved and particle weight (calculated t of -3.7, significant at the 0.001 level). The 89% recovery rate had 119 pebbles still within 3 m of their initial locations but 137 pebbles having moved by up to 49 m. The discharge during the eight day tracer experiment was the lowest of the five week study period (see 2.2.1) but differed from the Dubhaig and Feshie in that it was still high and competent to move some of the bed material (the Dubhaig and Feshie moved most sediment in short-lived floods and the strong armouring of the bed prevented substantial movement at low discharges). The reach C experiment therefore represents flow conditions described in 4.5 as being well below the 'threshold' for equal mobility, and selective transport is the primary mode of bedload transport. The regression equations of distance and weight in Table 4.5 supports this and gives further evidence to the suggestion made in 4.5 that the type of sediment movement is strongly dependent on the discharge and stability of the bed.

The regression equations for shape and sphericity factors also show a definite pattern. The three relationships that were significant at the 0.05 level for distance moved and sphericity were all positive as were three other tracer experiments. In contrast the distance moved and flatness regression equations were strongly negative and significant at the 0.05 level in three of the nine reaches and only weakly positive in one reach. These sphericity and shape regression equations complement each other and show that the pebbles that were moved the furthest distance were generally spherical and triaxial ellipsoids, while the pebbles that travelled the least distance were platy or discoidal (i.e. small c-axis). This is in agreement with the previously described results of Komar and Zhenlin (1986). However, Laronne and Carson's (1976) tracer experiments and Carling's (1983) study of trapped bedload both reported that there was no consistent relationship between either shape or sphericity and the frequency and distance of pebble movement. Although Keller (1970) found that the shape factor (expressed as a c-a axis ratio) was not an important influence on bedload movement (significant in his two experiments at the 0.25 and 0.50 levels) he reported that there was a greater tendency for angular particles to move further than rounded particles. The results in Table 4.5 suggest that the distance moved of a pebble is only weakly dependent on its weight and form but nonetheless small, spherical, particles tend to move the furthest.

A direct quantification of the influence of a particle's size on the distance moved can be obtained by plotting the mean distance moved versus the b-axis of the pebbles. The tracer data for the experiments were grouped into 0.5ϕ intervals (the Lyngsdalselva reach A only had two different size classes present so is not used) and plotted in Figs. 4.14a-b with the size expressed as the geometric mean of the respective 0.5ϕ interval. For reach D of the Dubhaig in Fig. 4.14a the size class with peak distance moved (mean of 26.5 mm) is unrepresentative since only

(a)

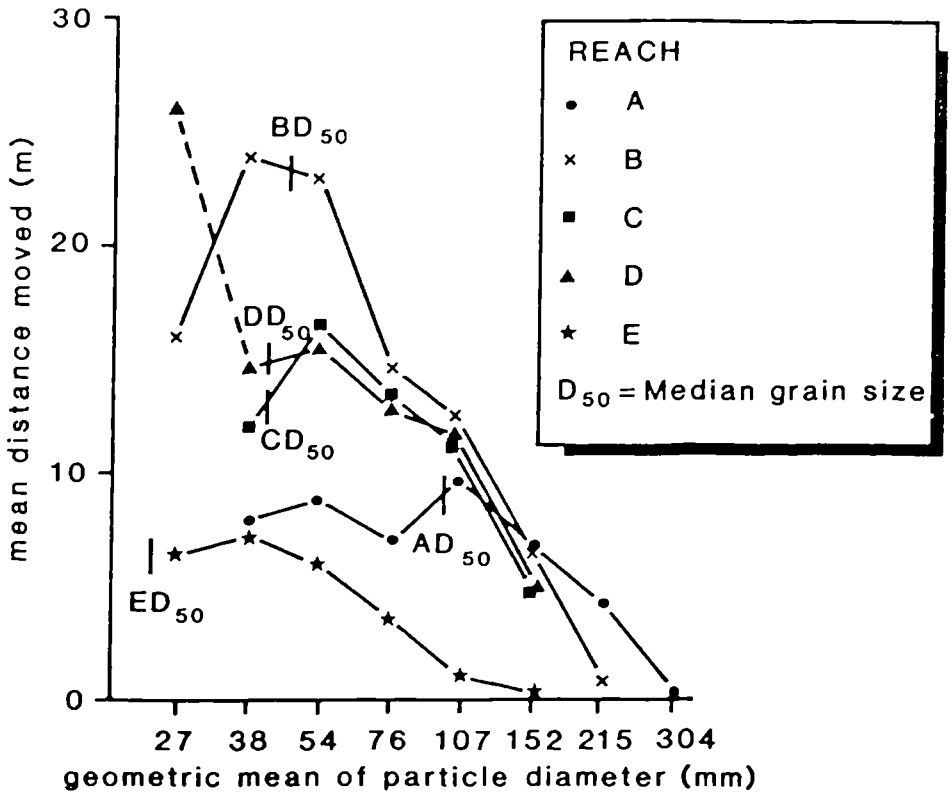

(b)

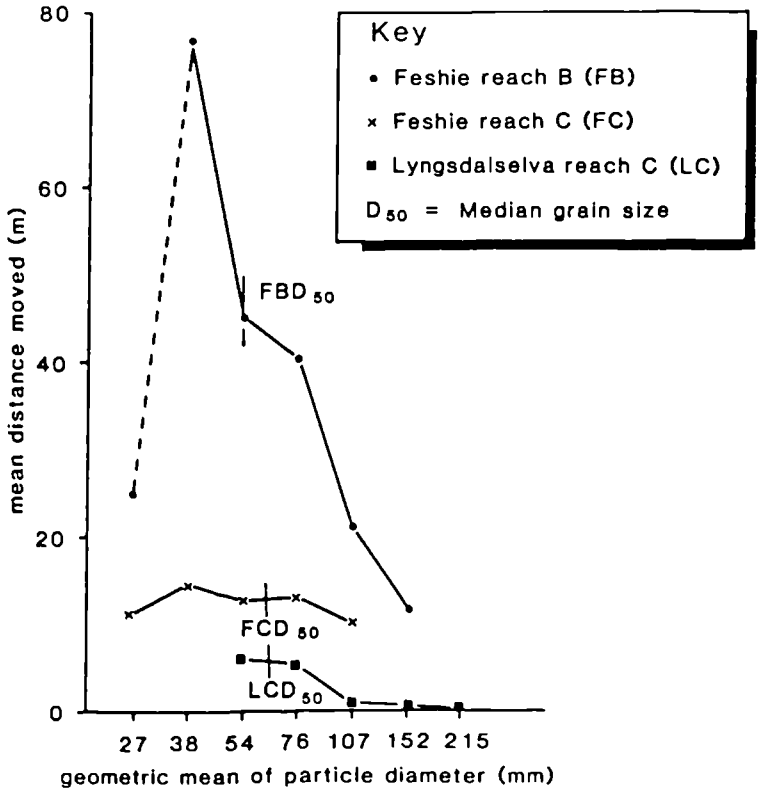

Fig. 4.14 Mean distance of pebble tracer movement for different size fractions (grouped in 0.5 phi sieve sizes) from tracer experiments in (a) reaches A-E of the Dubhaig, and (b) reaches B and C of the Feshie and reach C of the Lyngsdalselva.

one particle was inserted in that size range (and only moved on one occasion). Likewise only two pebbles were found in reach B of the Feshie in the 22 - 32 mm class (of 12 that were inserted). Excluding these two points, Figs. 4.14a-b show a similar pattern with the maximum distance moved in the size class, or just larger than, the median diameter. All eight reaches had their size class with the peak distance of movement within a 0.5 phi class of the D_{50} class. This is similar to the results of Meland and Normann (1969) (a flume study using sediment in the range 0.5 - 8 mm), Laronne and Carson (1976) and Mosley (1978) who all found overriding evidence to suggest that particles close to or just coarser that the D_{50} are the most mobile. This can be explained with reference to the equalisation of mobility hypothesis in that finer particles are trapped more easily between and beneath larger particles for long periods in flood flows and the larger ones are simply more difficult to keep moving (despite their greater exposure) because of their mass. As indicated by the results for reach B of the Feshie and reaches B and C of the Dubhaig this reduction of mobility in the finer and coarser-than-average fractions can be very marked. The trends in Figs. 4.14a-b support the regressions of distance and weight discussed earlier (and the Helley-Smith results discussed in 4.5) showing that there is some selective transport even if it is not of the finest grades.

A cautionary note should be added here since it should not be assumed that the pebble tracing results are directly comparable to the Helley-Smith results. Helley-Smith sampling traps bedload close to, or at, the point of entrainment. Hence the work of Parker and Andrews only applies to threshold conditions. This was used by Parker and Andrews at the recent Pingree Park Workshop previously mentioned to defend criticisms of their work when it was suggested that their results gave no explanation for the presence of downstream and down-bar fining (R. I. Ferguson, personal communication, 1985). They argued that although there is an equal chance

of entrainment of any size from the bed, this does not mean that there is equal mobility at the deposition stage i.e. their hypothesis encompasses both equal mobility at entrainment and then selective transport and deposition once the particles are moving. However, a growing opposition to this explanation maintains that their reasoning is inconsistent and there must be some selective transport from the bed to explain such obvious and large-scale sediment sorting observed by many workers in gravel-bed rivers (an opinion shared here by the author and also indicated by the analysis in 4.2-4.4). The pebble tracing results in Table 4.5 and Figs. 4.14a-b indicate that there is some selective transport of particles due to their weight, size and form but Andrews and Parker would argue that this could easily have occurred once the particles had been entrained. To see whether the trends for the distance of movement for different size fractions can be extrapolated to the point of entrainment the percentage movement of particles in different size classes are plotted for each reach. If Parker and Andrews are correct then different size classes for each reach should firstly join up in a horizontal line (i.e. have the same percentage of movement) and secondly show 100% movement (since all the pebbles should move once a threshold is crossed).

Figs. 4.15a-b shows the plots for all the nine reaches. Only the pebbles found are included since it is uncertain whether the missing pebbles were buried at their original locations (or elsewhere) or moved well out of the reach. In six cases the peak percentage of particles moved was within a 0.5 phi size class of the D_{50} class, but only three reaches had the most movement in the median class plus the next coarsest size (excluding reach A of the Dubhaig where there was 100% movement in the 22 - 32 mm range but only two pebbles were inserted in this class). When these results in Figs. 4.15a-b are compared with the mean distance of travel in Figs. 4.14a-b they show that there is a close similarity between the entrainment and deposition of different sized fractions. This is particularly true of

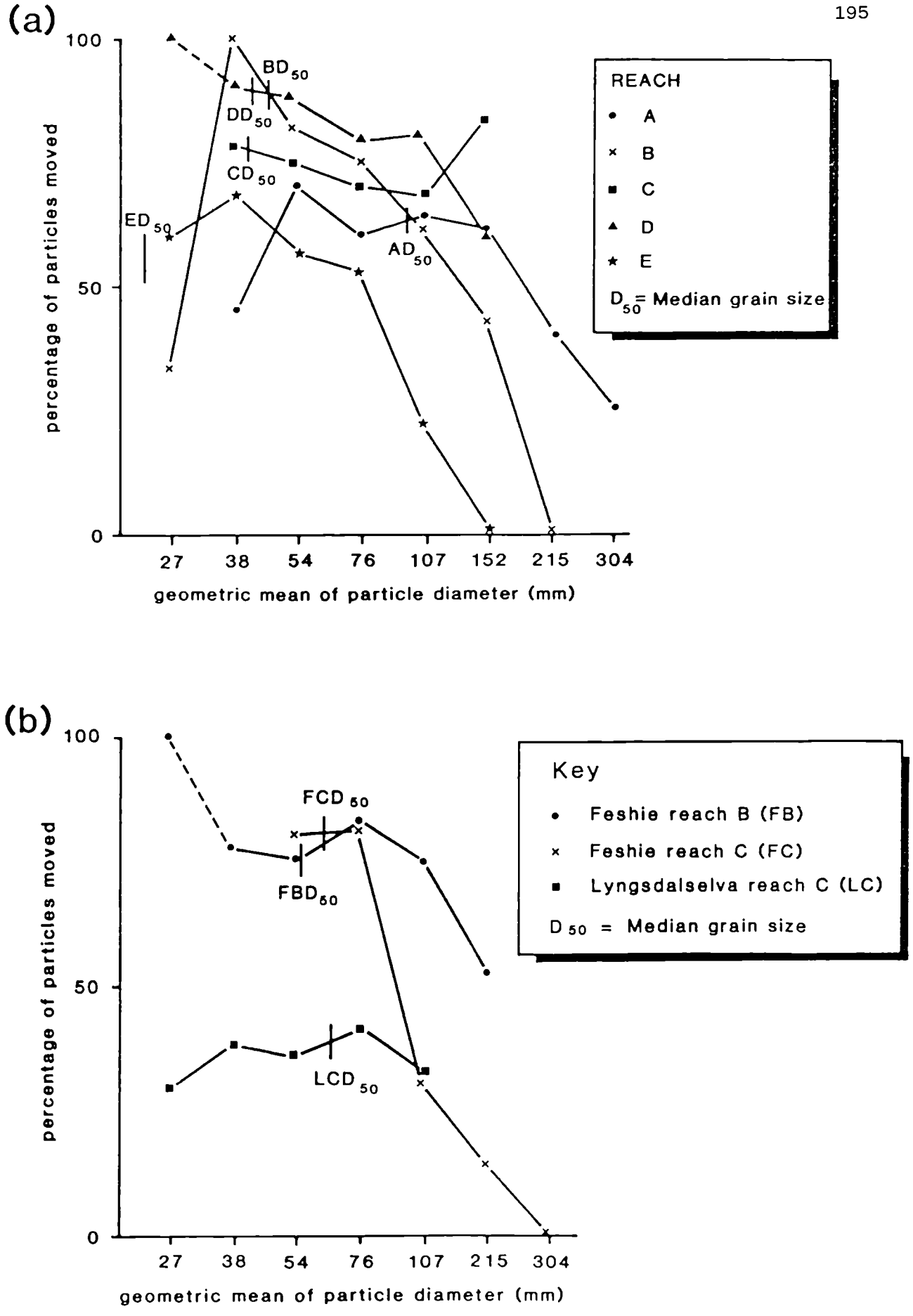

Fig. 4.15 Percentage of pebble tracers moved for different size fractions in (a) reaches A-E of the Dubhaig, and (b) reaches B and C of the Feshie and reach C of the Lyngsdalselva.

the coarser particles (> 90 mm) where there is a rapid drop in both the entrainment and distances moved, but the finer fractions also have limited movement. The flow is therefore selective both at entrainment and in transport and deposition.

4.6.3 Discussion and comparison to Andrews and Erman (1986)

These results form an interesting comparison to the Helley-Smith results in 4.2 to 4.4. Analysis of the bedload catches showed that there was scope for selective transport, but at peak discharges when the bed armour was broken (as in the Lyngsdalselva flood samples) all sizes of sediment were available and nearly equally mobile. During the bedload and tracer studies in the Dubhaig and Feshie, the shear stresses never reached high enough values to destroy the armour and thus transport all grades of sediment. This can be very generally inferred from looking at the shear stresses at the highest known discharges in the sampling period. For the Dubhaig the ratings of discharge and shear stress described in 3.2 can be used to compute the shear stress at the highest recorded discharge of 9.3 $m^3 s^{-1}$. The peak shear stresses are 286, 201, 190, 113, and 95 N m^{-2} for reaches A-E respectively. For the Feshie reach B the maximum bankfull shear stress was 82 N m^{-2}. These results compare with the three highest Lyngsdalselva shear stress measurements during the 7 August flood of 319, 364, and 406 N m^{-2} at various times and positions in the channel. Although the grain size, bed stability and supply and availability of sediment were different for each river it seems that the Dubhaig and Feshie need much higher flows than those observed before the whole of the bed is mobile.

The tracer results complement the Helley-Smith analysis for all three rivers. The Feshie and Dubhaig both show that there is more selective entrainment from the beds (and discharges) compared to the Lyngsdalselva.

With flows not competent to rupture the bed armour, the Dubhaig and Feshie tracers all show a weak but nonetheless consistent inverse relationship between the distance moved and the weight of the particles. The restriction of movement is particularly accentuated in the finer and coarser-than-average fractions with the smaller pebbles trapped or hidden in bed structures and the coarser boulders too heavy to move. However over time and with a wide range of flows it is possible to move all sizes of the bed. Even during the limited range of discharges in the Dubhaig, pebbles with b-axes up to 270 mm and weights near 16 kg moved during floods.

This work forms a useful comparison to that reported by Andrews and Erman (1986) who also combined Helley-Smith catches with pebble tracers to help interpret the mode of bedload movement. Figs. 4.16a-b shows their results with their 50 composite Helley-Smith samples following the trends reported in Andrews (1983) which reported a hiding factor of 0.87 (Andrews and Erman did not show an equation or hiding factor for their Sagehen Creek data, and in fact fitting a line by eye to their data suggests that the hiding factor was probably greater than 1). In Fig. 4.16b their pebble tracer data is plotted for two snowmelt floods in the same form as Figs. 4.15a-b earlier in 4.6.2. Unlike the Dubhaig, Feshie and Lyngsdalselva (and as found by other workers) Andrews and Erman's (1986) data do not show a decrease in the mobility of finer fractions and an increase in the transport of sizes close to the D_{50} of the bed. Their data is more reminiscent of the behaviour of the coarser fractions of the pebble tracers in Figs. 4.15a-b. There is a gradual decline in the mobility of the pebbles with increasing size although during the higher snowmelt floods in 1982, 40% of the particles with a mean diameter of 100 mm moved.

The snowmelt floods in 1982 also show that of the tracers that moved which were within the Helley-Smith sampling range (they used a 152 mm square

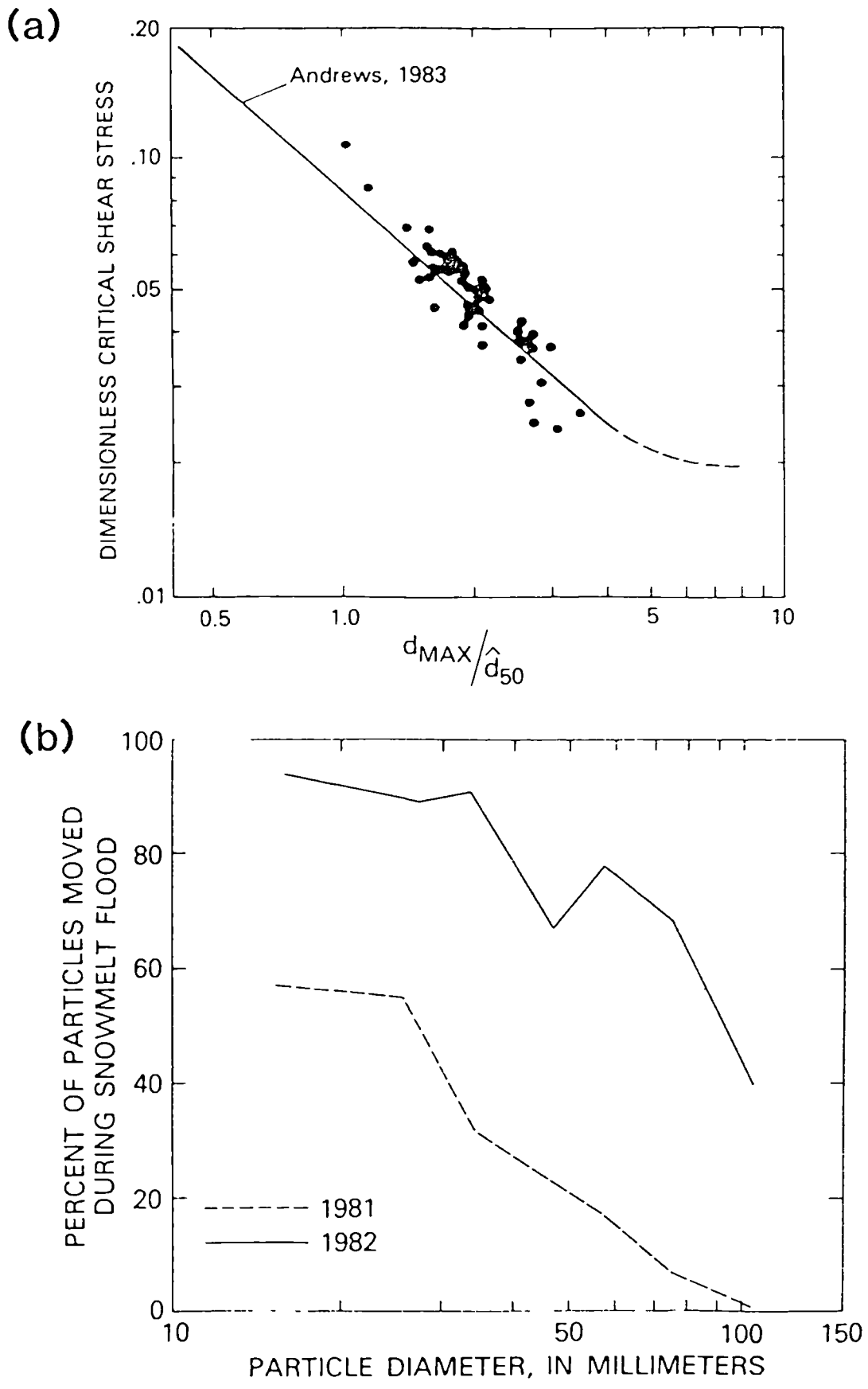

Fig. 4.16 Plots from Andrews and Erman (1986) of (a) mean dimensionless critical shear stress against relative grain size (see 4.11 for a comparison), and (b) percentage of pebble tracer movement for different size fractions during a snowmelt flood (compare to Fig. 4.18 later).

orifice) there was close to equal mobility expressed as the percentage of particles moved. In Sagehen Creek approximately 30% of the particles in the bed surface had an intermediate diameter larger than one half of the sampler's orifice (Andrews and Erman (1986)), but excluding these sizes Fig. 4.16b shows that the percentage of tracers moved in the higher flood are all within 30% of each other for different mean sizes. Using the interpretations expressed in 4.5, Andrews and Erman's (1986) Helley-Smith and pebble tracer data indicate that the sediment close to (or in this case just finer than) the bed armour D_{50} have an equal chance of being entrained in high flows. However the coarser fractions (greater than about two times the bed armour D_{50}) are still only selectively transported with the largest particles (relative to their surrounding material) rarely being moved. Andrews and Erman (1986) explain this paradox between their Helley-Smith catches and pebble tracers by showing that the bed is rarely totally mobile (the critical dimensionless shear stress needed to entrain the median bed particles in the Sagehen Creek is only equalled or exceeded on an average of 4.8% of the time). Their transport rates were "relatively small" but their pebble tracer results showed that nearly all sizes of bed particles can be transported even if few bed particles were entrained at any instant. Hence they argued that the bed surface was a mobile bed feature but was in equilibrium with the small transport rates involving nearly all sizes of material. Also despite the bed surface remaining unbroken, significant quantities of bed material of all sizes can be transported.

The arguments put forward earlier in 4.5 stressed the importance of understanding the bed and flow conditions during the bedload sampling (either Helley-Smith or pebble tracers). In Andrews and Erman's (1986) example of Sagehen Creek, Fig.4.16bclearly shows that the discharge from 1981 to 1982 does still not increase the mobility of the coarser fractions. The limited movement of the 100 mm particles mentioned earlier

only represent the D_{80} of the bed surface and undoubtedly sizes up to the D_{90} (130 mm) would have even less percentage movement. The Sagehen Creek data is similar to that for the Dubhaig and Feshie with selective transport for most of the flow conditions and equal mobility infrequently if ever achieved since the armour is rarely broken. The Helley-Smith samples from Sagehen Creek imply that there can be equal mobility in the finer fractions (especially close to or finer than the D_{50} of the bed surface), but these conditions should not be extended to include all sizes available in the bed. This contrasts with the Lyngsdalselva reach A bedload which showed that when the armour was ruptured all sizes were available for transport. The Dubhaig and Feshie Helley-Smith data showed that there was more scope for selective transport and this was explained by the bed being static and the discharge not high enough to rupture the bed armour. Andrews and Erman (1986) argue that their bed surface is a mobile feature since all sizes of sediment move (even if this is infrequent), but their pebble tracer data contradict this showing a rapid decline in the movement of fractions coarser than about 70 mm or the D_{60} of the bed. Hence the interpretations in 4.5 are returned to which suggest that the mode of bedload transport is a combination of selective and size or weight independent transport. The exact proportion of each type of transport is spatially variable but depends on the interrelationships of discharge, shear stress, bedload transport rates, grain size of the bed and the nature of the bed stability. A variation in any of these parameters can alter the type of bedload movement so that sampling in fluctuating spatial and temporal conditions can lead to obtaining a mixture of transport origins.

The results from all the pebble tracer data and the Einstein, Parker, Andrews and Bagnold-type analyses all point towards the need for a new set of hydraulic equations for gravel-bed rivers. The Parker and Andrews approaches seem to be the closest to arriving at a universal bedload

transport predictive equation but some of their arguments still need to be refined and modified. The traditional equations developed over 20 years ago are not applicable for describing sediment transport in gravel-bed rivers and therefore must be rejected. Instead more *field* data is required for various gravel-bed river channel patterns with different hydraulic conditions, grain size, sediment sources and pool/riffle nonuniformities. Only with this field data can the processes operating in gravel-bed rivers be properly understood and new equations put forward to help the predictive powers of hydraulic engineers.

4.6.4 Change in mobility with discharge

The increase in the availability of sediment with rising discharge has been discussed with reference to the Bagnold diagram of the Lyngsdalselva bedload in 4.2 and in the previous sections with the pebble tracer results. Only a brief synopsis will therefore be given here.

The high flows in the four tracing periods in the Dubhaig varied in magnitude and duration. The duration of discharge above 4 $m^3 s^{-1}$ and the peak discharge are given in Table 4.6 whilst the hydrographs for all the high discharges are shown in Figs. 4.17a-e. The hydrograph shape varied for each tracer experiment with the order of increasing importance for bedload transport being the July < November < August < December flood. The flows on 26-27 July maintained a moderate discharge for a long time period but as will be shown in 4.7 the discharge needs to be near to bankfull before it can move significant quantities and sizes of bed material. In contrast the November flood only had six hours of flow above 4 $m^3 s^{-1}$ but reached a peak discharge of 8.0 $m^3 s^{-1}$, hence it is ranked above the July floods. The highest and longest period of sustained competent discharge was in the December tracing experiment with nearly 40 hours of discharge above 4 $m^3 s^{-1}$.

Table 4.6 The Dubhaig pebble movements in the four tracing experiments with varying discharge.

Date surveyed	No. days pebbles in river	Duration of flow > 4 m^3s^{-1} hr	Peak Q m^3s^{-1}	Date of peak Q	Max. dist. moved m	Mean dist. moved		% moved
						All m	All > 0 m m	
30/7/85	55	13	5.1	27/7	50	4.8	11	48
29/8/85*	86	19.5	8.9	27/8	89	10	13	76
19/11/85	34	6	8.0	8/11	78	10	16	65
13/12/85	23	39.5	9.3	3/12	119	18	22	82

* Cumulative data which includes the previous flood's discharge and pebble movements (see 3.1 for explanation).

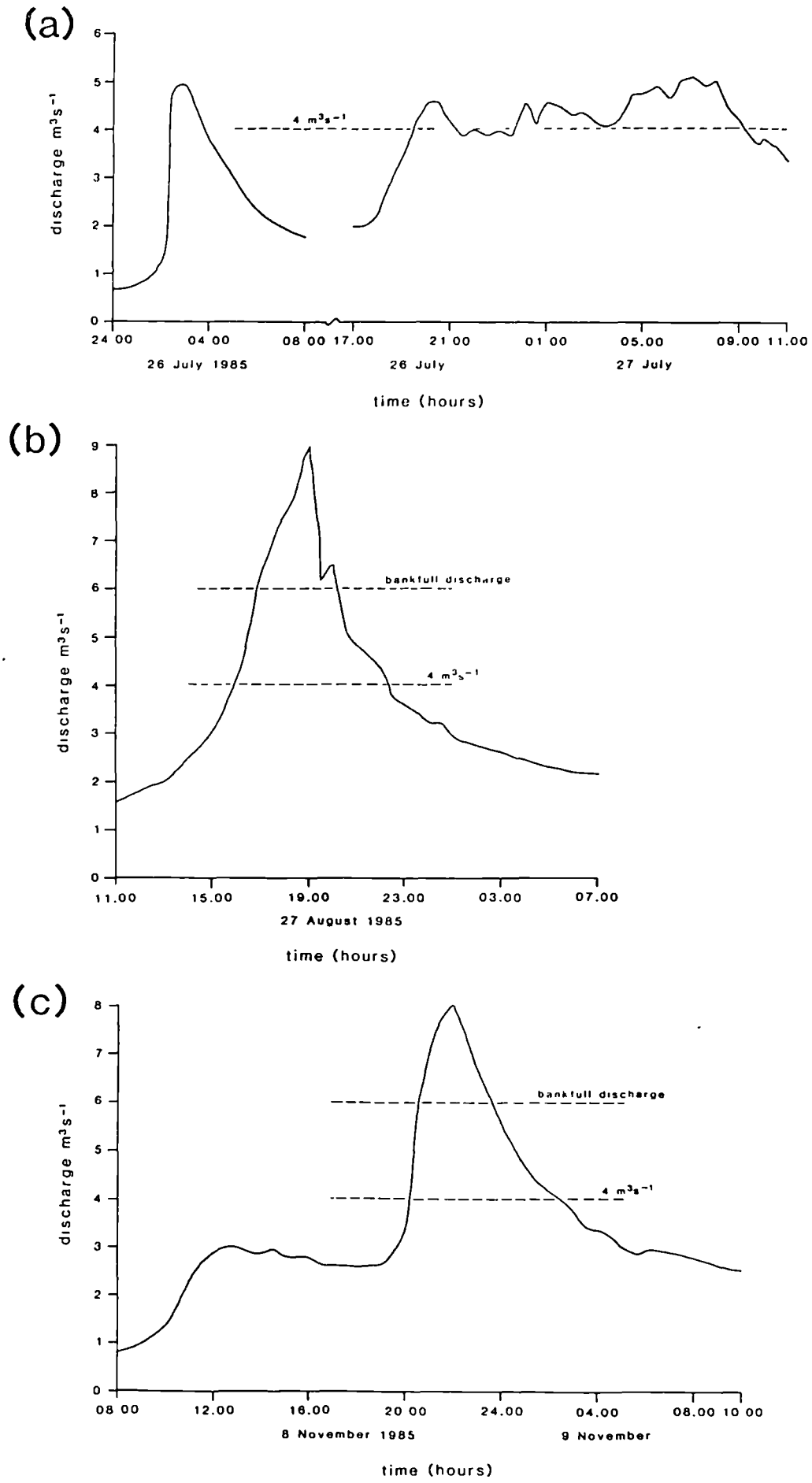

Fig. 4.17 Hydrographs for all the high flows during the four tracing experiments in the Dubhaig (a) on 26 July 1985 (b) 27 August (c) 8 November (d) 1/2 December (e) 3 and 12 December.

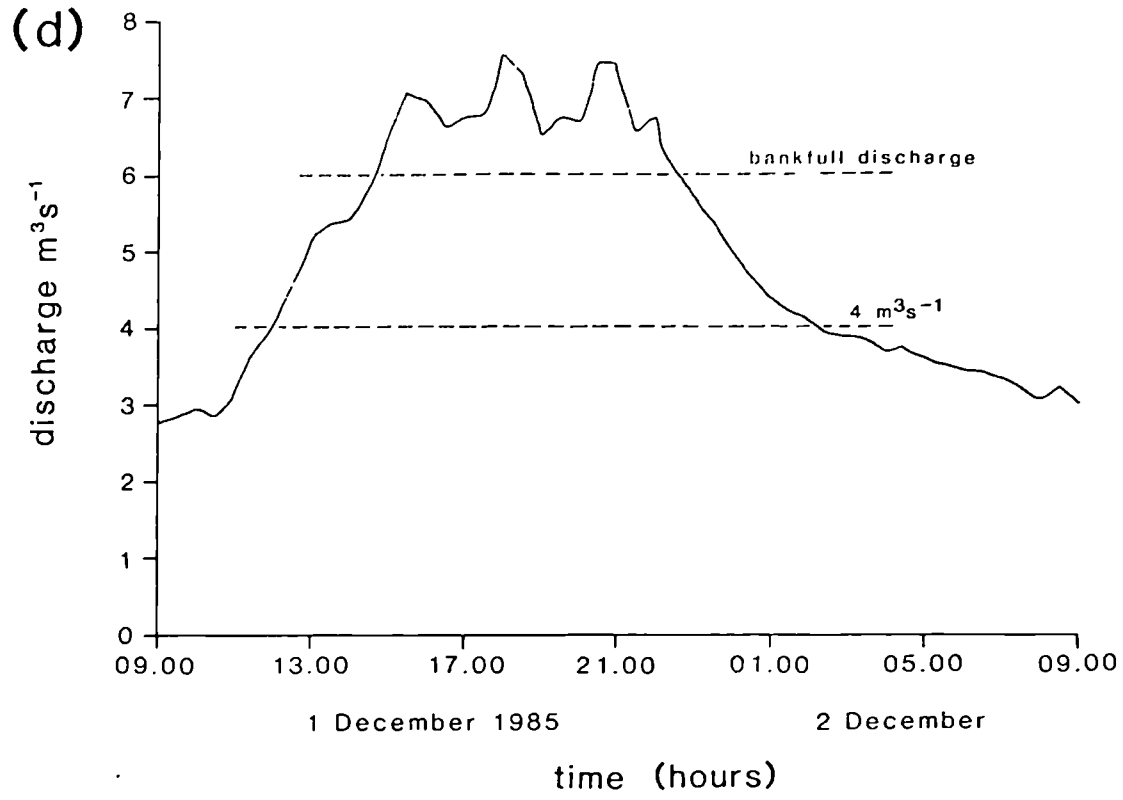
(d)
discharge m^3s^{-1}
bankfull discharge
4 m^3s^{-1}
0
1
2
3
4
5
6
7
8
09.00
13.00
17.00
21.00
01.00
05.00
09.00
1 December 1985
2 December
time (hours)

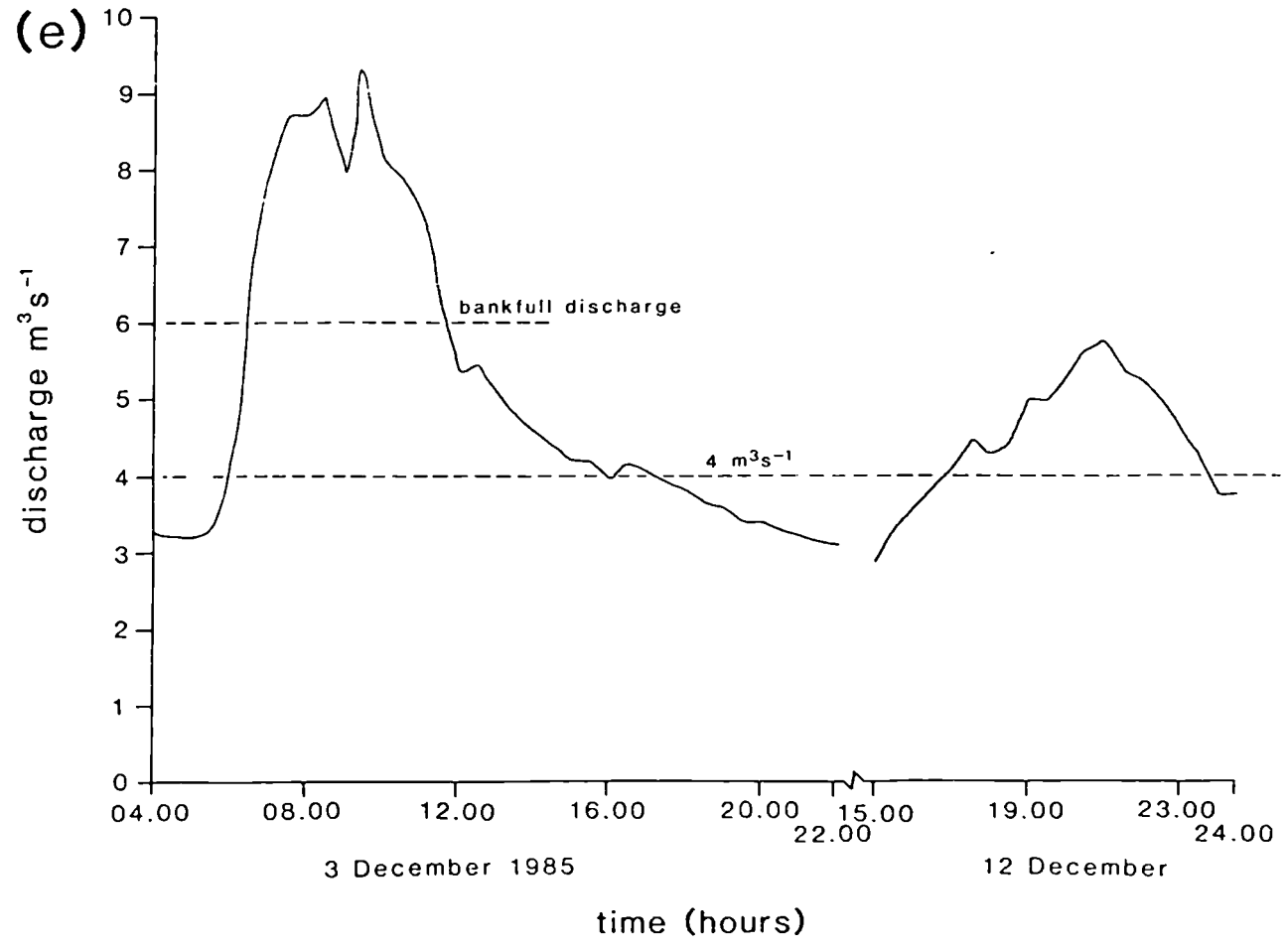
(e)
discharge m^3s^{-1}
bankfull discharge
4 m^3s^{-1}
0
1
2
3
4
5
6
7
8
9
10
04.00
08.00
12.00
16.00
20.00
22.00
15.00
19.00
23.00
24.00
3 December 1985
12 December
time (hours)

The response of the pebble tracers to these different discharges follows a predictable pattern with the maximum distance and percentage moved of pebbles matching the order of duration and magnitude of discharge expressed above (see Table 4.6). The change in percentage movement with increasing discharge was similar for all five reaches. Reach A is plotted as an example in Fig. 4.18. The percentage of entrainment of different sizes are offset according to the increase in the peak and duration of discharge but their slopes roughly follow the same pattern. The increase in the discharge is therefore accompanied by both a corresponding increase in the amount of sediment movement and the distance travelled. However, there is not a noticeable change in the availability of the different size classes of the pebble tracers. The coarser fractions are particularly insensitive to the increase in discharge (for example the August and December floods) giving further support to the earlier suggestions that the Dubhaig did not reach competent values to break the bed armour and equalise the availability and entrainment of all sizes of the bed.

The Dubhaig results form an interesting comparison to the Lyngsdalselva reach A tracer results taken during the flood on 7 August when the bed was fully mobile. Fig. 4.19 shows the location of the three inputs of pebble tracers superimposed onto the channel pattern after the avulsion on the 7/8 August (see 5.4.2.5). Of the first input of 50 pebbles only one was found (2% recovery rate), the rest having probably been transported and then buried. Of the second 50 inserted on the falling limb of the flood 15 were found (30%) mainly on newly-formed bars 35 m (A5-A7) and 50 m (A11+) downstream. Of the final 88 pebbles inserted when the channel was in the process of switching its course, 33 were recovered (38%) many close to where they were inserted and some up to 17 m downstream, but one at A11 in the group of pebbles from the second input. The first and second groups of pebbles were inserted when the armour was broken and there was

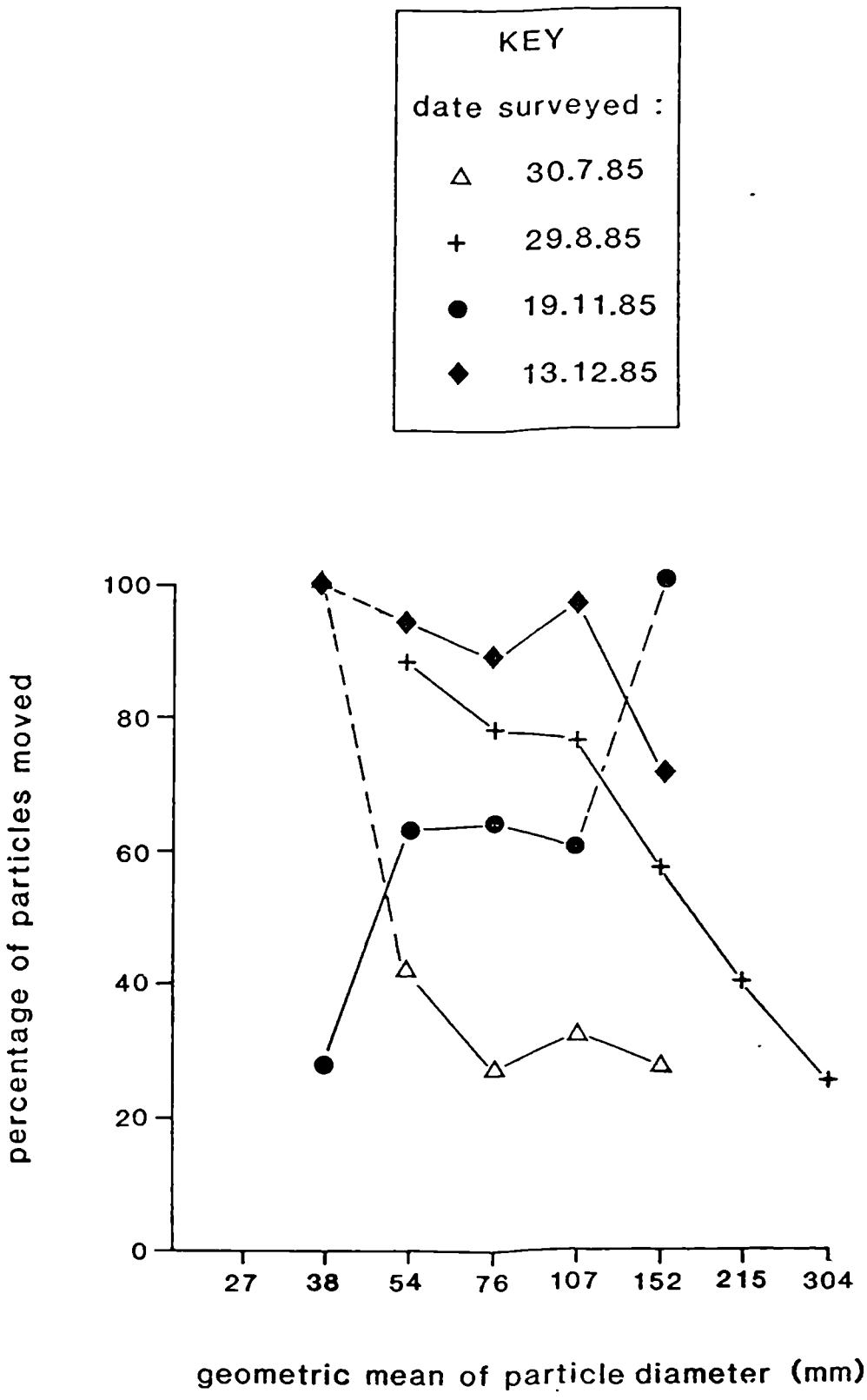

Fig. 4.18 Percentage of pebble tracer movement for different size fractions for the four tracing experiments (with varying discharge) in reach A of the Dubhaig.

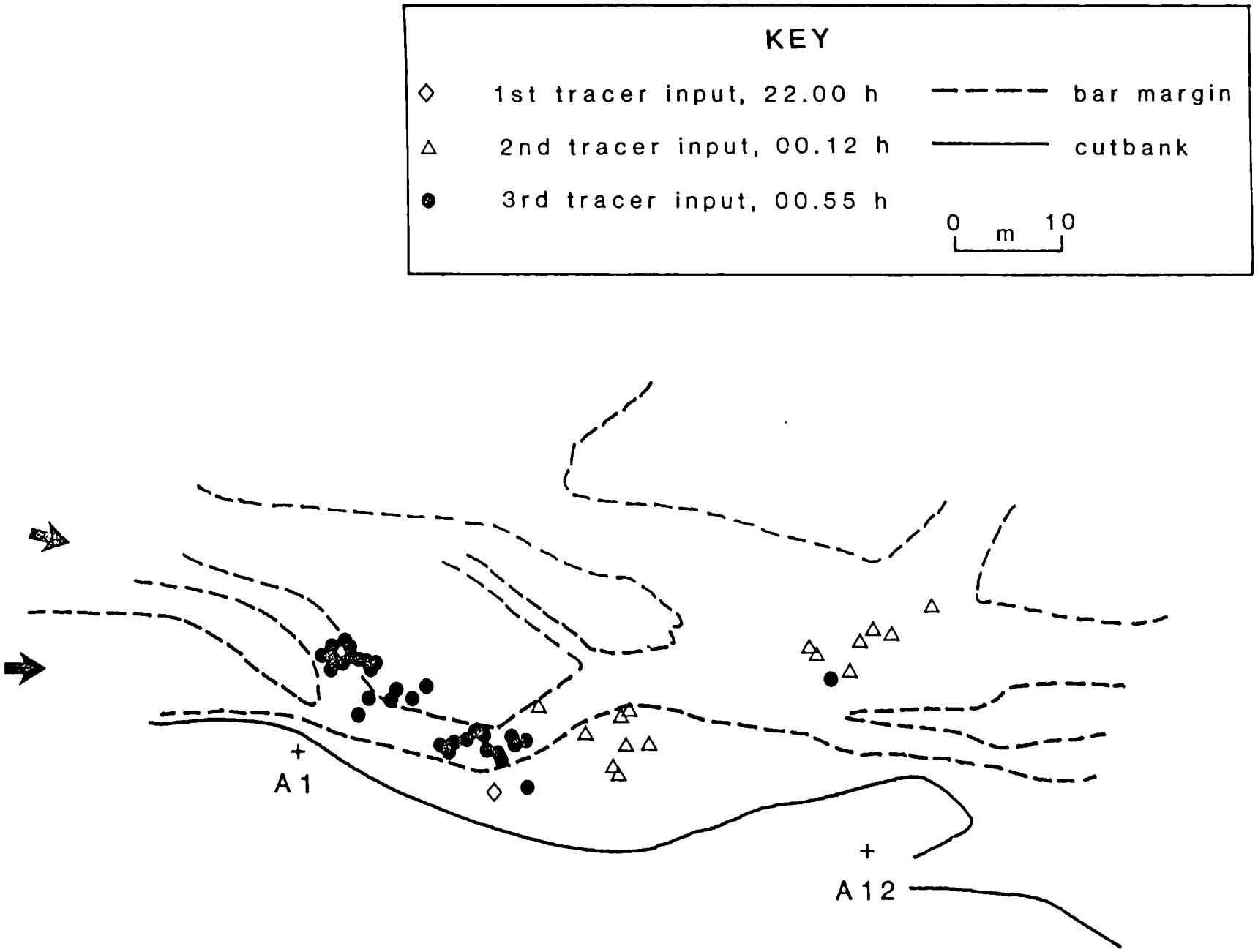

Fig. 4.19 Locations of the three pebble tracer inputs during the 7/8 August rainflood in the Lyngsdalselva.

rapid channel aggradation and bank erosion (see 5.4.2.5) while the third input was when the channel was shallowing and the armour was beginning to reform. The distinct concentrations of the tracers from different input times shows that there was a decrease in mobility with falling discharge (a pattern similar to the Dubhaig) but caution must be employed since there was only an overall recovery rate of 26%. All sizes were equally mobile and even the least mobile third input of tracers show a positive (though nonsignificant) relationship between the distance moved and weight (exponent of +0.37, $t = 1.3$, $n = 33$) suggesting that there was equal mobility as the channel was filling with sediment and no scope for selective transport once the channel had been choked and the main flow diverted. The Lyngsdalselva tracer results also show that when all sizes of sediment are available for transport the distances moved are dictated by the magnitude above the 'threshold' shear stress or discharge for equal mobility with the highest discharge moving all sizes the furthest.

4.7 Incidence of transport events - the case study of the Dubhaig

The bedload transport between 5/3/85 and 13/12/85 in the five reaches of the Dubhaig is investigated to help understand the temporal variations and the significance of transport events for the frequency and magnitude of channel changes and bar development. During this 10 month period a record of water discharge was taken at every 0.5 hour interval (see 2.2.1), and the 31 bedload samples taken during the four transport events (27/7/85, 2/10/85, 3/12/85, 5/12/85) could subsequently be linked to the respective discharge at the sampling time. Since only a limited number of bedload samples were taken, only general conclusions can be drawn about the frequency of bedload transport. Likewise, the short period of discharge data (effectively one year's record, since the river is frozen for the winter) may be misleading, especially when considering the wet summer of 1985, but still allows general inferences to be drawn about the flow

conditions necessary to initiate sediment movement. Unfortunately such intensive discharge data related to bedload sampling were not available for the Feshie and Lyngsdalselva, so the Dubhaig serves as a separate example for investigation, but may have wider implications for other rivers.

4.7.1 Methodology

The analysis uses methods, formulae, and data derived in earlier sections, chiefly in 3.2 and 4.1.2. Table 4.7 summarises the relevant statistics for the grain size distributions of the bed material and bedload. The mean of the surface D_{50} values for each reach was obtained by Wolman (1954) sampling for the 23 shear stress sites described in 3.2. This method was preferred to an average grain size distribution from bulk sampling of emergent bars since it is both quick, more representative of the local variations in bed roughness (bar/pool/riffles), and is still equivalent to the bulk sampling technique (Kellerhals and Bray 1971). The sampling of within-channel subsurface sediments is much more difficult and there is still no method available for use in coarse bedded rivers (Church et al. in press). Hence the grain size of the subsurface was characterised by a mean D_{50} value obtained from an active bar(s) of the reach. In addition to the bed material, the grain size distributions of the bedload were processed and computed to produce the D_{50} and maximum particle size (expressed as the mean of the relevant sieve sizes) for each sample, and then a mean for each reach (Table 4.7).

As stated in 2.2.1 the bankfull discharge for the Dubhaig was estimated from field observations as being about 6 $m^3 s^{-1}$(which is almost consistent for all reaches). The individual log-log regression equations for the ratings of shear stress versus discharge for each site (see 3.2) were used to estimate the shear stress at bankfull discharge (ordinary linear

Table 4.7 The size distributions and transport rates of the Dubhaig Helley-Smith bedload catches and comparisons with the sizes available for entrainment from the surface and subsurface bed material.

Reach	Reach surf. D_{50} mm	Reach subs. D_{50} mm	No. bedload samples	Bedload D_{50} mm	Surf.* D_x %	Subs.* D_x %	Bedload** D_{MAX} mm	Surf.*** D_x %	Subs.*** D_x %	Maximum transport rate kg $m^{-1}s^{-1}$
A	114	34	6	23	10	39	54	18	59	0.21
B	74	25	10	10	13	28	38	26	44	1.6
C	58	28	8	8	7	19	54	16	33	0.099
D	68	28	4	3	6	13	38	12	24	0.015
E	40	15	3	2	9	15	14	13	22	0.0044

* The equivalent percentage of material in the surface and subsurface bed material that is finer than the mean bedload D_{50} for the reach.

** D_{MAX} of bedload expressed as the geometric mean of the two bounding sieve sizes.

*** The equivalent percentage of material in the surface and subsurface bed material that is finer than the D_{MAX}.

regressions were used for reach E as explained in 3.2). This can then be put into the Shields (1936) equation shown in 4.1.2 (D = D_{50} surface), to give the dimensionless shear stress for movement of the median surface bed particle at each site. The mean of the 23 values, $\overline{\tau}^*_{BF50}$, therefore gives an average dimensionless shear stress for the reaches at bankfull discharge.

Recalling the results in 4.3 using an Parker-type analysis a relationship was derived for the threshold hydraulic conditions in the Dubhaig (for all data) of the form

$$\tau^*_{ri} = 0.0716\left(D_i/D_{50}\right)^{-0.654}$$

The τ^*_{r50} value of 0.0716 can then be compared to the $\overline{\tau}^*_{BF50}$ from the Shields equation to investigate whether the flow in the Dubhaig is ever competent to move up to the D_{50} of the surface.

4.7.2 Results and discussion

Results from the hydraulic computations show that the τ^*_{r50} and $\overline{\tau}^*_{BF50}$ are very similar. The τ^*_{r50} of 0.072 is higher than the previously reported values of 0.030 by Meyer-Peter and Müller (1948) and Neill (1968), and 0.031 of Andrews (1984) for the D_{50} of the bed surface. Andrews (1984) does not discuss the discrepancy between his 0.031 value and the τ^*_{c50} reported in Andrews (1983) of 0.083 but this might be explanable by the errors introduced by using the Du Boys equation as a cross-sectional average estimation of the shear stress. The τ^*_{r50} value of 0.072 reported here is consistent with the work reported by Parker et al. (1982b) and Andrews (1983) as well as the data from the Feshie and Lyngsdalselva shown in Table 4.3. More importantly the τ^*_i were derived using at-a-point

estimates of shear stress not cross-sectional averages. Thus they are accepted as being reasonably accurate and question the findings of the earlier cited work. The τ^*_{r50} compares with the $\overline{\tau}^*_{BF50}$ of 0.066 which is similar to the 0.051 average bankfull value of τ^* found by Charlton et al. (1978) in an investigation of 23 gravel-bed rivers in Britain (he also used the Du Boys equation to estimate the shear stress). In 10 out of 23 cases (43%), the τ^*_{r50} was equalled or exceeded by the bankfull discharge (which is 64% of the peak discharge measured), but by comparing the mean values, the $\overline{\tau}^*_{BF50}$ is just below the τ^*_{r50} indicating that on average, flows close to or above the bankfull discharge will mobilise all sediment on the bed surface up to the median particle size.

In the 10 month study period the bankfull discharge in the Dubhaig was equalled or exceeded for 0.3% of the time, which is 21 hours of flow and represents 9 different floods. This is within the range found by Nixon (1959) who found that the bankfull discharge was equalled or exceeded on average 0.6% of the time in 29 rivers in Britain (though with a big range). It seems likely, therefore, that the bed material in the Dubhaig is mobilised on an average of a few days per year and the stream is only competent to move sizes up to the median particle diameter of the bed surface in a few short-lived events. This has implications for the frequency of channel change reported in 5.2. If the Dubhaig can only move the majority of its bed material at discharges well above bankfull then the long periods of low flow (generally May to September) should show little channel change from the cross-sections and planimetric map surveys (see 5.2).

Further support for this temporal pattern in bedload transport comes from an analysis of the sizes of bedload moving in four high flows, three of which were between 3 and 5 $m^3 s^{-1}$, and one which peaked at 9.3 $m^3 s^{-1}$, but dropped to 3.9 $m^3 s^{-1}$. Table 4.7 shows the maximum diameter and D_{50} of

the bedload trapped and also the D_{50} and D_{MAX} of the bedload expressed as a finer than percentage of the surface and subsurface sediments (for example a D_{10} for the surface means that the average median bedload size for that reach has 10% of the surface bed material size distribution finer than it).

The results for different reaches show that only D_{50} sizes up to the D_{13} (reach B) of the surface and D_{39} (reach A) of the subsurface were being transported by these flows. Of the maximum particle sizes in the bedload samples, only sediment up to the D_{26} (reach B) of the surface and D_{59} (reach A) of the subsurface were trapped. Extreme caution has to be employed before interpreting these results since the samples are restricted by the small size range that the Helley-Smith can sample (< 76 mm). As described in 2.2.1, Hubbell (in press) has shown that the 100% sampling efficiency of the Helley-Smith drops markedly as sediment coarser than 32 mm is trapped. The maximum particle diameter in the bedload samples was coarser than 45 mm in two of the reaches and therefore may not be truly representative samples. Furthermore if sizes up to the D_{50} of the surface were moving, they could only be trapped in the Helley-Smith in four out of the five reaches (reaches A-E have a surface D_{50} of 98, 46, 41, 42, and 23 mm respectively). However, field observations while bedload sampling together with an inspection of the grain size distributions of each individual bedload sample shows that the coarsest sieve size was only represented by one or two pebbles and movement of large material was very infrequent (this can be assessed from the pebbles hitting the measuring personnel and the Helley-Smith sampler).

Given that it was not suspected that material coarser than 72 mm was regularly moving as bedload, the results of the above analysis are probably within the sampling efficiency of the Helley-Smith. Thus both the hydraulic geometry and bedload sampling results show that the Dubhaig

can only transport sizes up to the D_{50} of the surface bed material in flows close to or above bankfull discharge. This magnitude of discharge is rare and so bedload movement is limited to only a few events a year. Helley-Smith sampling in flows approaching and above bankfull discharge show that only sizes up to the D_{26} of the surface bed material are moved. However, only five out of the 31 bedload samples were taken in flows greater than 6 $m^3 s^{-1}$, so given the hydraulic calculations above, not even sizes up to the D_{50} of the bed surface would be expected to be entrained. To complicate this temporal pattern, there is a great spatial variability - not only in pool/riffle sequences (see 3.2), but laterally and downstream. If the sediment is better sorted then the relative bed relief is reduced and the importance of hiding and protrusion of sediment becomes less important in determining whether a particle will move.

Field observations throughout the 2.5 year study period gave no indication that the armoured layer of the five reaches was ever broken. This gives further evidence to support earlier conclusions that equal mobility is rarely achieved in these stable and strongly armoured gravel-bed rivers. The Parker analysis in 4.3 revealed a hiding factor of near 0.7 for all the 31 bedload samples of the Dubhaig which indicates that the armour was never totally broken during the Helley-Smith sampling period and selective transport was still prevalent together with the interchange of the occasional boulder from the surface armour.

Finally Table 4.7 shows the maximum total transport rates for each reach. The transport rates are in the range reported by previous workers (for example Andrews (1983) sampled bedload with transport rates between 0.002 and 0.07 kg $m^{-1} s^{-1}$ and Andrews and Erman(1986) between 0.012 and 0.10 kg $m^{-1} s^{-1}$) with the exception of reach B which had three samples with rates greater than 1.2 kg $m^{-1} s^{-1}$. This explains why reach B was transporting the coarsest surface bed material out of all the reaches but also shows

that there was probably no restriction on sediment entrainment for any of the sizes up to the maximum particle trapped by the Helley-Smith (the D_{26} of the surface armour).

5 CHANNEL CHANGE

5.1 Introduction

The preceding Chapters 3 and 4 have provided an insight into some of the channel processes operating in the Dubhaig, Feshie and Lyngsdalselva but have deliberately avoided any discussion of the effect these processes have on bar development and channel change. As outlined in 1.3 the cause and effect relationships in gravel-bed rivers are closely interlinked and a quantification of the change in channel geometry and position cannot be adequately discussed without reference to the channel hydraulics and bedload transport. The analysis below is therefore set out to describe the changes in each of the seven river channel patterns (nine reaches) of the three rivers beginning with a brief synopsis of the magnitude, frequency, and mode of channel change and then discussing the interrelationships with channel processes (at different discharges). The changes in each reach are discussed within their respective sections and an overall comparison between the different channel patterns is discussed in 5.5.

5.2 The Dubhaig

5.2.1 Measurement procedure

A brief description of reaches A-E of the Dubhaig and the surveying techniques and data analysis was given in 2.1.2 and 2.2.5. During the 21 month period of observation the five reaches were surveyed on five occasions. Since it was not possible to survey all the reaches in one day

the survey dates varied by a few days but in all cases there was no channel change in the intervening time period. The frequency of measurement was solely dependent on the incidence of channel change and was undertaken in March/April 1984, September/October 1984, March 1985, September 1985, and December 1985. The most active periods of channel change were usually during the autumn/winter months so the discussion below confines itself to the cross-sections for this period. The cross-sectional changes for the spring and summer months are briefly described in the text but are not plotted.

In addition to the surveyed channel changes the analysis for the five reaches in 5.2.2 - 5.2.6 also draws upon information from pebble tracers, bed velocity measurements and imbrication directions of pebbles on the exposed bar surfaces. These techniques are described in 2.2 and their results are superimposed on a base map (which also provides the locations of the cross-sections referred to in the text) at the beginning of each section. In the case of the pebble tracers either the movements during the highest flood are plotted (3/12/85) or if a large proportion moved out of the study reach, the tracer movements during the next most suitable high flood (see 4.6.4 for details of the tracing discharges) are used. The bed velocity maps were all measured at a discharge of 0.94 $m^3 s^{-1}$ which coincidentally is equivalent to the mean discharge and equalled or exceeded 31% of the time.

5.2.2 Reach A

The cross-sections from the most active time periods are shown in Figs. 5.1a-b and the tracers, bed velocities and imbrication directions in Fig. 5.2. The summer months of 1984 (March-September) showed little

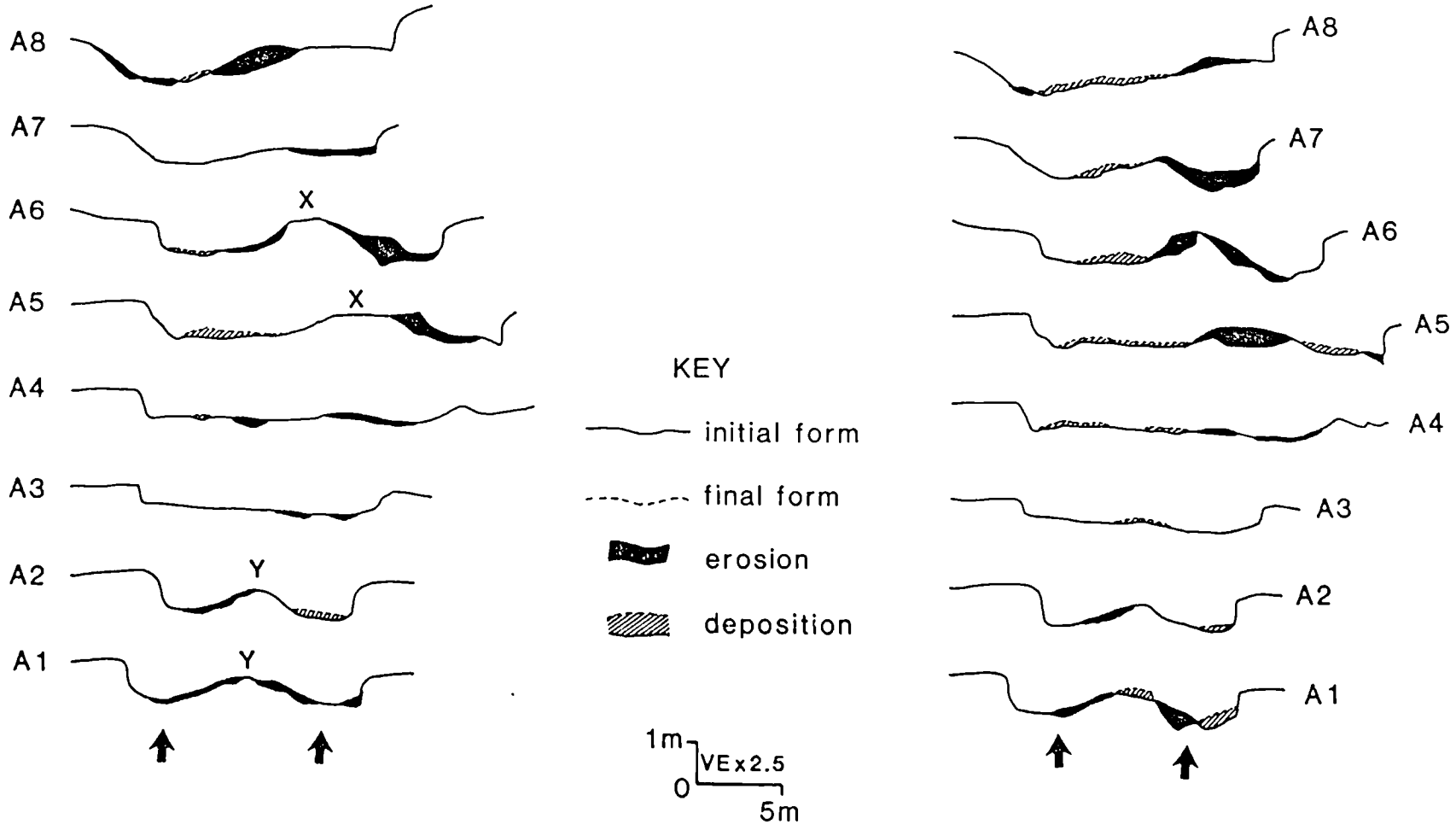

Fig. 5.1 Cross-sectional changes in the Dubhaig reach A from (a) 27.9.84 - 14.3.85, and (b) 13.9.85 - 11.12.85.

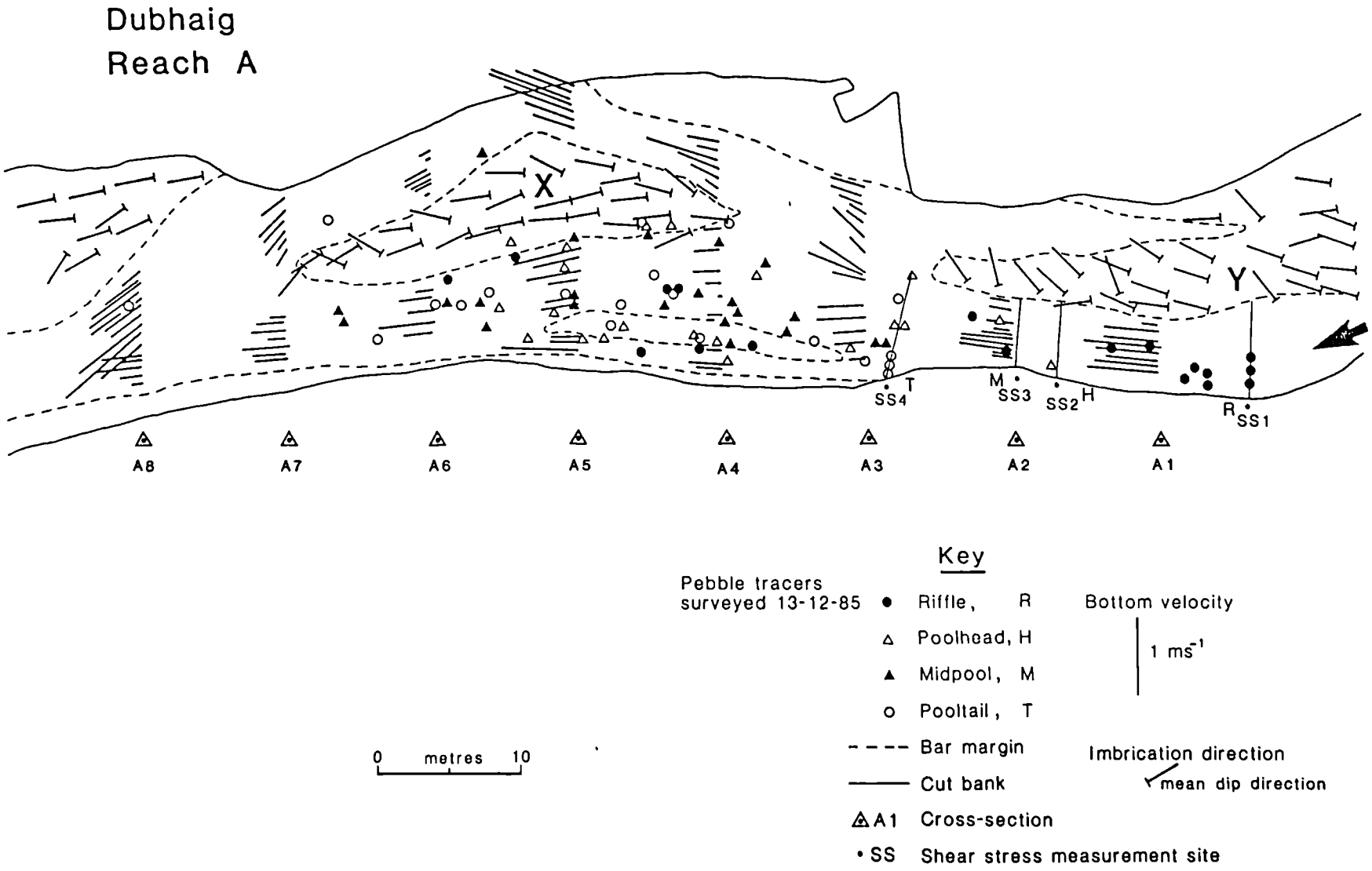

Fig. 5.2 Pebble tracer movements, bed velocities, and bar imbrication directions in reach A of the Dubhaig.

appreciable change (no erosion and only 3 m^3 of deposition) but the winter of 1984/1985 led to considerable scour of the reach. Using the prism formula described in 2.2.5 the total volumetric erosion for the eight cross-sections was 52 m^3 compared to only 9 m^3 of deposition. As Fig. 5.1a shows this erosion was concentrated on the right margin of the medial bar (labelled X) at A5 and also scour of the bed at A6. The riffle at A8 scoured by up to 50 cm which led to it translating about 5 m downstream. The small amount of deposition occurred as a thin veneer of sediment along the left flank of the medial bar at A4-A6. The overall picture was therefore of a growing dominance of the right-hand channel around the medial bar and an infilling of the left-hand branch of the diverging channel at A4.

The wet summer of 1985 (see 2.2.1) led to some limited channel change - up to 11 m^3 of erosion concentrated in the normally inactive right-hand channel at A1-A3 and 11 m^3 of deposition spread among many locations within the reach. The autumn months of 1985 were the most active in reach A with 64 m^3 of erosion and 38 m^3 of deposition. As Fig. 5.1b shows there was a trimming of the bar (labelled Y) at A1-A2 but the most significant change was the removal of the head of the medial bar at A5 and the scour of the tail at A6 (17 m^3 of material removed between A5 and A6). This strip of erosion continued into the right-hand channel at A7 where up to 40 cm of scour occurred. This erosion was partly offset by 6 m^3 of deposition between A1 and A2 of the right-hand channel and a broad strip of deposition up to 30 cm thick from A4 to A8. Fig. 5.3 shows the nature of the deposition in this area which involved pebbles with b-axes up to 200 mm (D_{93} of the surface armour) generally depositing as clusters or rolling up onto the bar to be left perched on the former surface armour. The overall change in the morphology of the reach can be seen by comparing

Fig. 5.3 Clusters and perched pebbles on the newly deposited bar surface (autumn/winter 1985) between A4 and A8 of the Dubhaig.

Figs. 5.4a-b. At low flow the left-hand channel around the medial bar (see Fig. 5.4a) is virtually abandoned and the river pattern has altered to a single arcuate channel confined within well vegetated steep bank edges (Fig. 5.4b). The downstream movement of the riffle at A8 can also be seen which has been replaced by an extension of the tail of the newly attached bar.

Interestingly the total volumetric change in the reach shows a net erosion of 66 m^3 so that the amount of sediment removed mainly from the medial bar was not compensated for by a growth of the bar near the left bank of sections A4-A8. Also during the 21 month study period there was no detectable bank erosion (both at the surveyed sections and field observations) so that channel changes were a direct result of the reworking of within-channel sediments and not supply related.

Fig. 5.2 shows the direction and strength of flow and coarse sediment transport at low and peak discharges. At low flow the near-bed velocities are strongest in the confined poolhead near A1 (up to 1.0 m s^{-1}) and the riffles on the right channel at A5 and at A8 (maxima of 1.3 m s^{-1}). This is in agreement with the Keller (1971) hypothesis for pools and riffles as discussed in 3.1 and the hydraulic measurements described in 3.2.1. During the flood of 3/12/85 (peak of 9.3 m^3 s^{-1}) and subsequent high flows all but three of the re-located pebble tracers moved down the left-hand channel at A4-A7 consistent with the cross-sectional changes for that time shown in Fig. 5.1b. The imbrication directions of deposited or realigned pebbles show the direction of the current (and presumably sediment movement) at higher discharges when the bars are overtopped. Fig. 5.2 shows that from upstream of A1 to A2+ the attached bar Y aggrades as the confined flow is replaced by diverging flow - the sediment

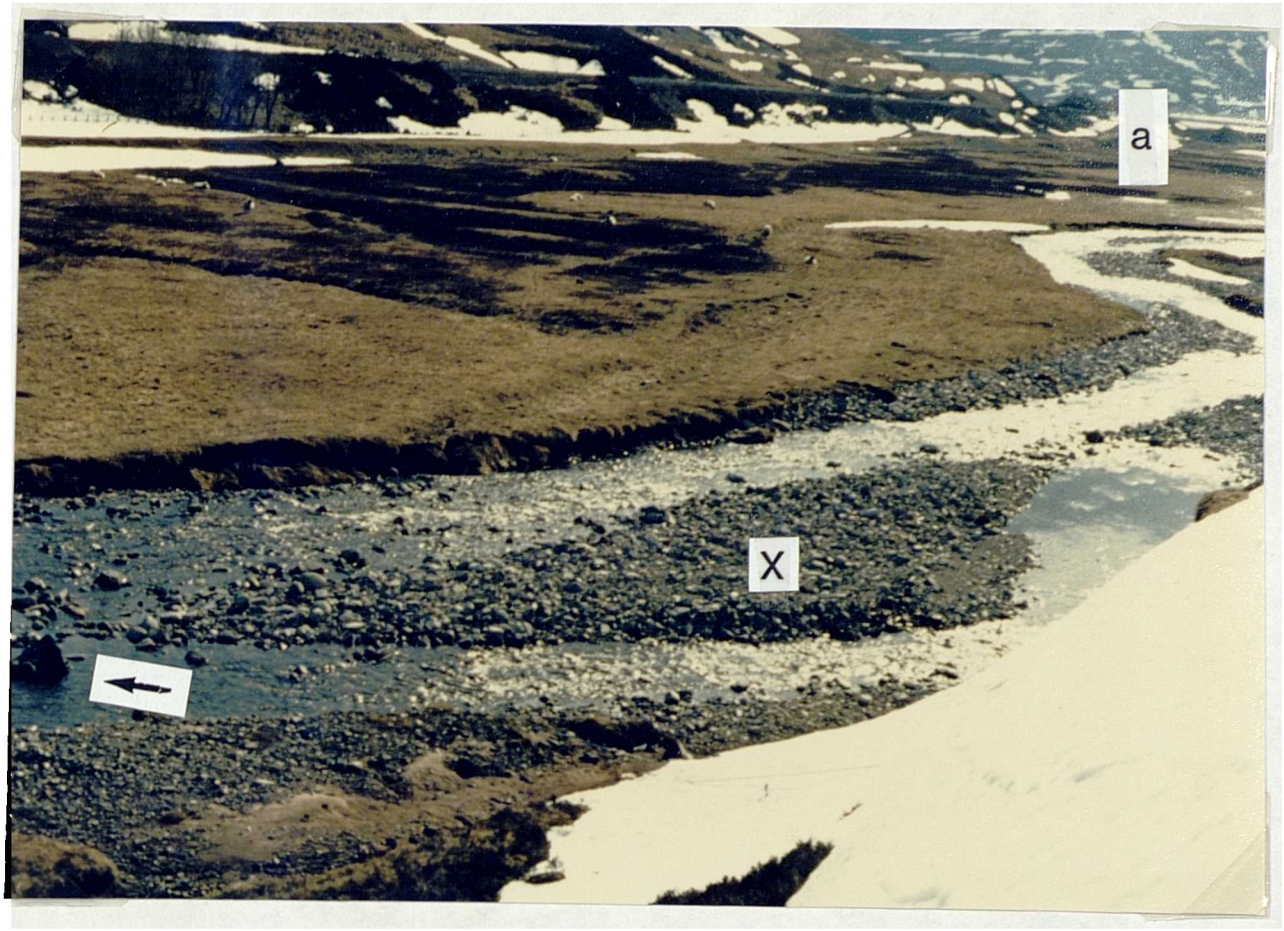

Fig. 5.4 Views from a nearby scarp looking down onto reach A of the Dubhaig showing (a) flow diverging around the mid-channel bar X (photo taken on 15.4.84) and (b) Infilling and abandonment of the left-hand channel around bar X after the autumn/winter floods of 1985 (photo taken on 13.12.85). Rock in the channel (labelled with an arrow) can be used to match up the two photographs.

presumably dropping out of the flow as the depth decreases over the bar top. A similar pattern can be seen at the head of the medial bar X where the divided channels at low flow (with their individual convergent zones) seem to be replaced by a broad divergence of flow at higher discharges.

It seems therefore that in reach A at low flow only local areas of confined flow and steep riffles are capable of modifying the channel geometry. At discharges close to 10 $m^3 s^{-1}$ (possibly the annual flood) the channel bed and bars are scoured and trimmed to create fresh but low and uniform relief bar features. At high discharges the flow pattern seems to change so that convergent zones at low flow become divergent zones at high flow. This reversal in flow pattern with increasing discharge will be explored further in 5.4.

5.2.3 Reach B

The cross-sectional changes over the two active autumn/winter periods for reach B are shown in Figs. 5.5a-b and a planimetric map of the reach in Fig. 5.6. The April-September 1984 period resulted in little channel change with no new deposition but 21 m^3 of erosion mainly along the edges of the long low relief bar (labelled W) on the right of the channel between sections B3 and B6. As Fig. 5.5a shows during the winter months of 1984/1985 this bar aggraded back to its former level together with a progressive growth of its avalanche face towards the right-hand bank edge. The right-hand distributary of the main flow here is inactive at low flow but infilled with up to 35 cm of deposition at B6 during the 1984/1985 floods. These winter flows were also responsible for the only channel widening in reach B in the whole of the study period. At B2 up to 3 m of erosion occurred where the channel flows down a diagonal riffle leading

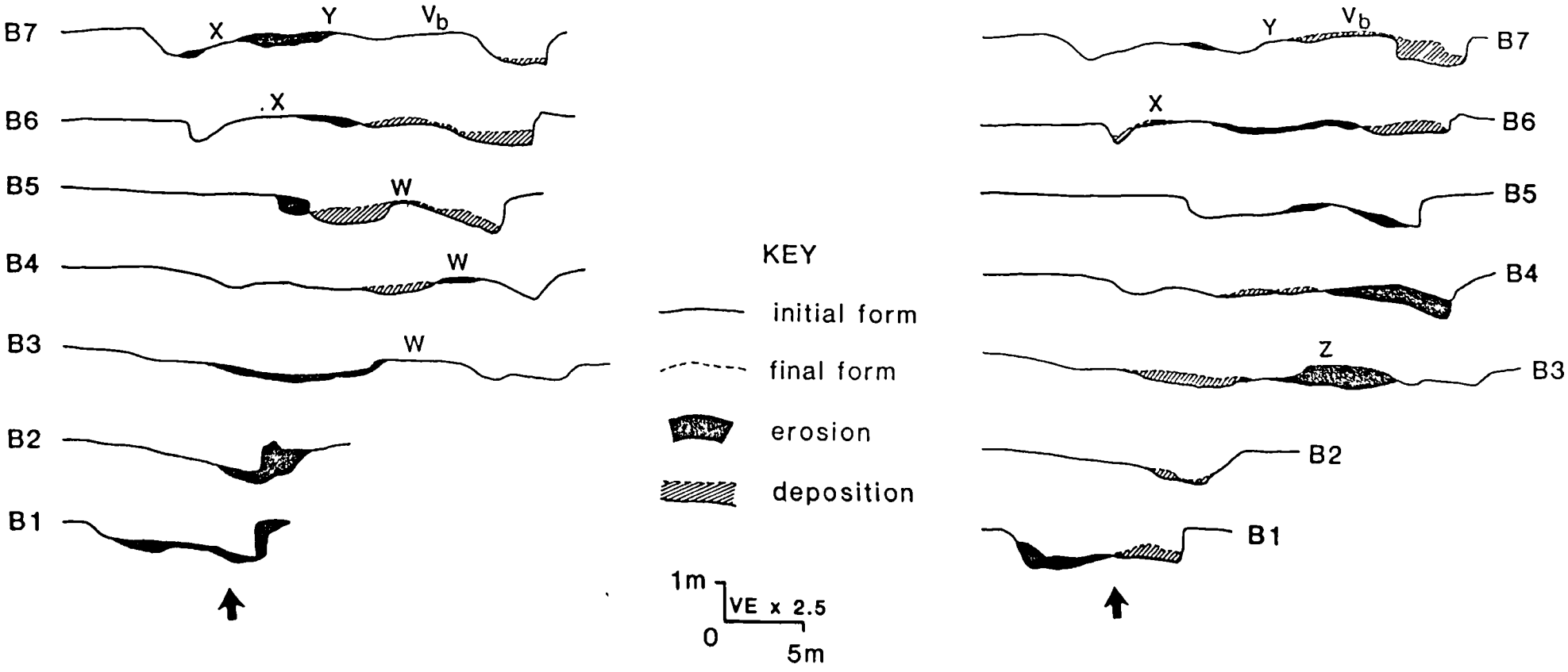

Fig. 5.5 Cross-sectional changes in the Dubhaig reach B from (a) 27.9.84 - 26.3.85, and (b) 26.9.85 - 11.12.85. Note that the cross-sections start at 10 m.

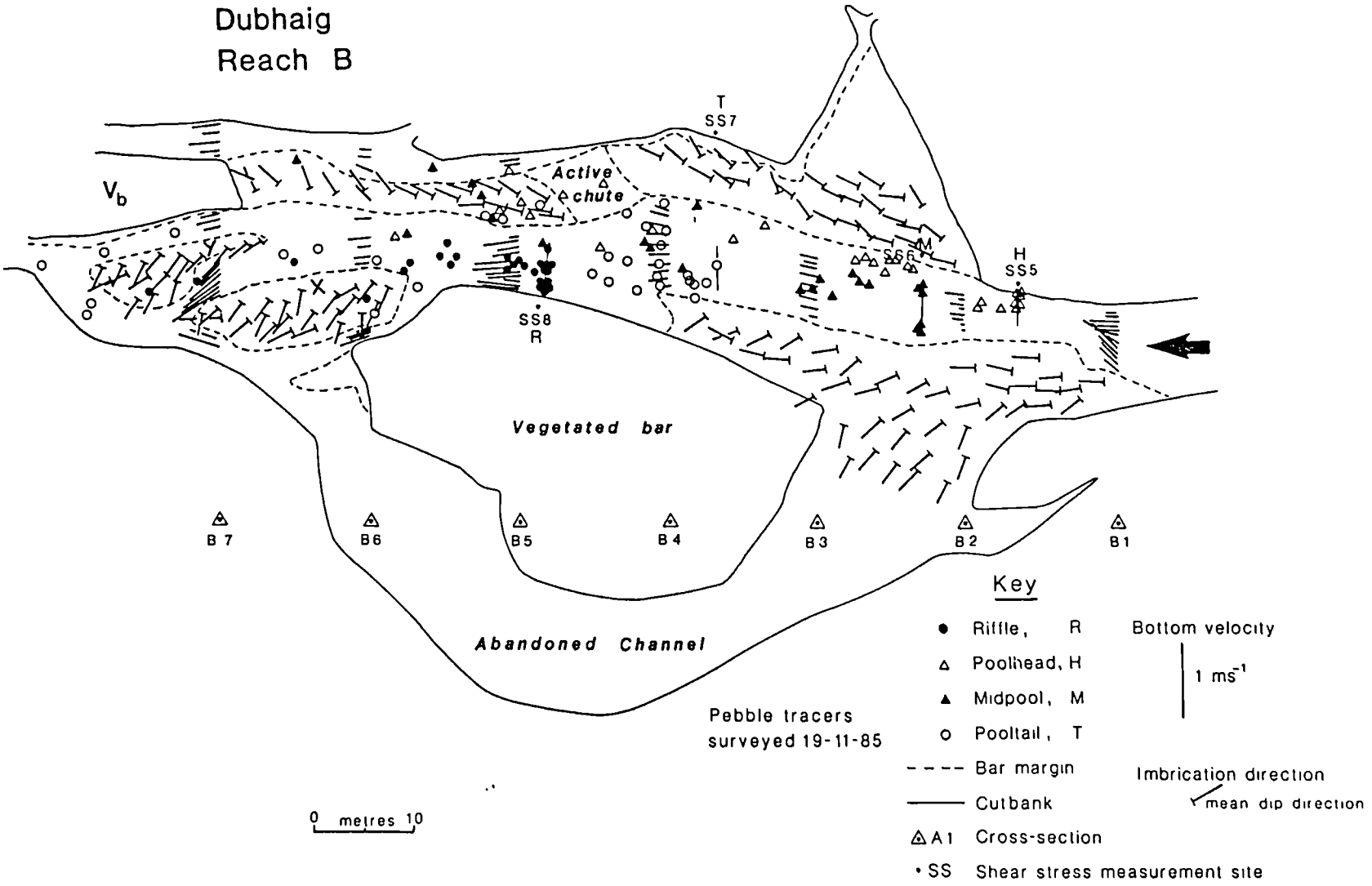

Fig. 5.6 Pebble tracer movements, bed velocities and bar imbrication directions in reach B of the Dubhaig.

directly into the bank edge at B1. The bank erosion was in the form of undercutting and large turf block collapse which paradoxically resulted in a protection of the bank from any further erosion. The channel between B1 and B3 scoured by up to 25 cm in a constant strip of erosion along the main talweg. Further bank erosion occurred at B5 where again a diagonal riffle flows directly into the bank - this time consisting of easily erodible bar remnants capped by a sparse vegetation cover. The left-hand medial bar at B6 (labelled X) was trimmed on its right margin and though there was no morphological change of the adjacent right-hand bar (labelled Y) there was bed scour along the riffle separating the bars. During the 1984/1985 winter the total reach deposition was 75 m^3 compared to 95 m^3 of erosion.

The following spring and summer months were more active than the previous year with a total of 76 m^3 of deposition but with negligible erosion. The main zone of change was at the head of the reach where 60 m^3 of material was deposited as a result of infilling of the talweg between B1 and B2. Bar X at B7 aggraded at its barhead and moved closer to the bank edge by a growth of its avalanche face.

The September-December 1985 floods caused similar amounts of channel change to the previous winter flows with a total of 81 m^3 of deposition and 89 m^3 of erosion. As Fig. 5.5b shows the talweg from B1-B4 continued to aggrade although this was partly offset by bed scour of up to 30 cm at B1 as the previously active diagonal riffle was replaced by a switching of the talweg to the left-hand side of the channel. This change in channel flow direction did not scour or widen the channel at B2 but led to 45 m^3 of erosion between sections B3 and B4 as a chute was created (labelled Z) across the bar bordering the right-hand bank edge. The change in flow pattern at the head of the reach also affected the right-hand distributary between sections B6 and B7 with some of this eroded material contributing

to the 33 m^3 of deposition that choked the channel in a band of sediment up to 50 cm thick. Bar X at B6 continued to aggrade at its barhead although the adjacent bar (Y) hardly changed its morphology.

These cross-sectional changes all tie in with the flow patterns shown by the pebble tracers, imbrication directions and to a lesser extent the bed velocities shown in Fig. 5.6. At low flow the highest measured bed velocities were again at the riffles, at B1, B5, and B7 with maximum near-bed velocities of 0.9, 1.0, and 1.2 m s^{-1}. Some indication of the flow direction and strength can be seen in Fig. 5.7 at the downstream end of reach B. The right-hand channel is confined by the vegetated bank on its right (labelled V_b) whilst the flow between the two bars (X and Y) plunges steeply down a riffle before meeting flow from upstream at the bartail which causes it to lose some of its momentum. Fig. 5.7 shows the typical flow pattern at low stage with the only possible scour zones confined to local areas of steep, fast, riffles.

At higher discharges the flow pattern changes with the bars being overtopped with diverging flow. The pebble tracers surveyed on 19/11/85 and imbrication directions clearly show this with a divergence of flow out of the main talweg between B3 and B6 leading to a lateral growth of the long bar (W) towards the right-hand bank edge and a divergence of flow at the two barheads (X and Y) between B6 and B7. The imbrication directions on bars X and Y also show the effect that the steep vegetated bank edge (V_b) visible in Fig. 5.7 has on the development of the channel at high flows. The flow direction turns almost 90° towards the right-hand distributary as the flow approaches and directly collides with the vegetated bank. It also restricts the extent of divergence of flow to the right so that the divergence is accentuated over bars X and Y. A comparison of these high flow patterns with lower stages is illustrated in Fig. 5.8. Thus at high discharges bars can not only aggrade by a

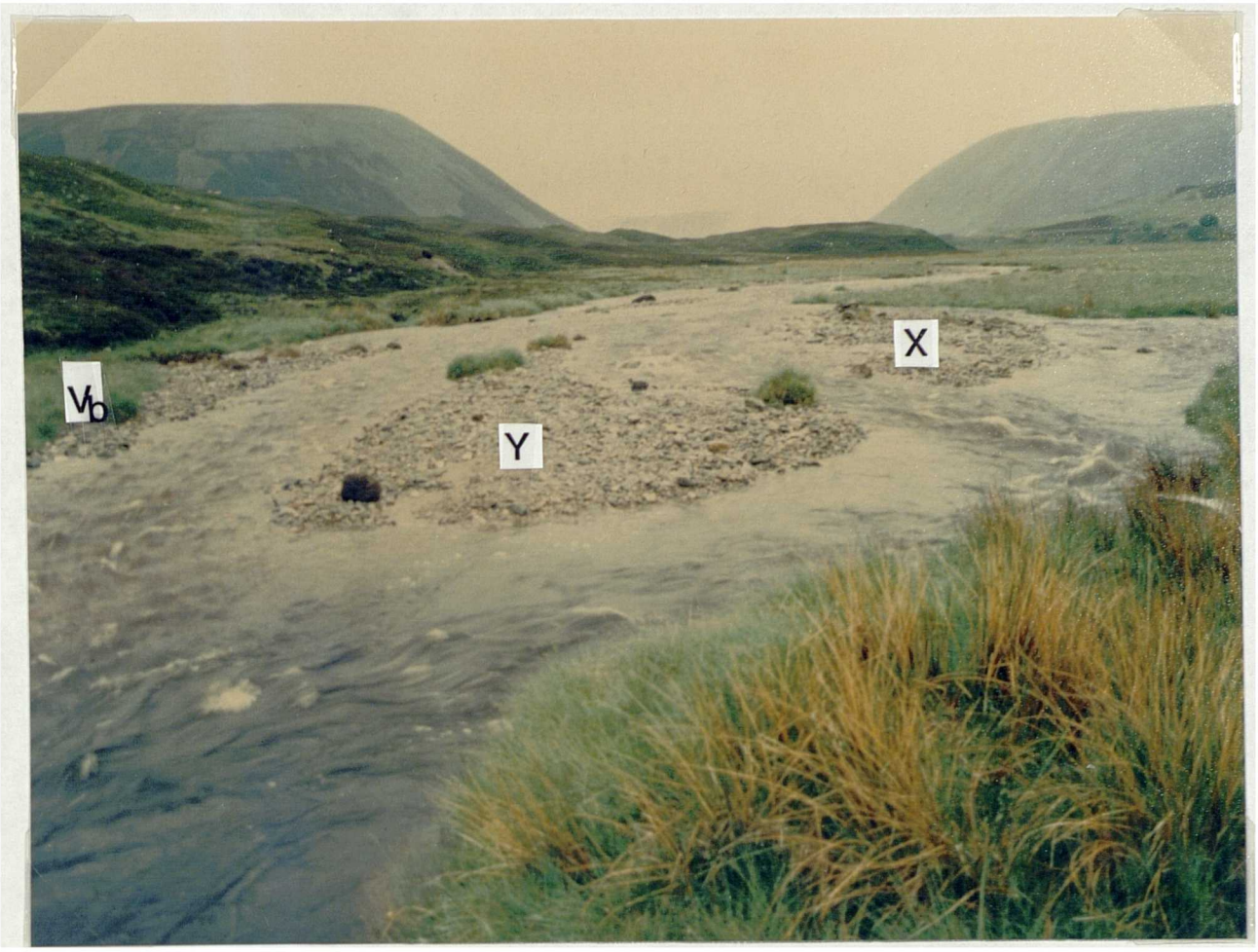

Fig. 5.7 View from B7+15 m looking upstream at the low flow pattern (discharge about 0.40 $m^3 s^{-1}$) at bars X and Y and the vegetated bank V_b of reach B of the Dubhaig. Note the confined fast flow through the steep riffles.

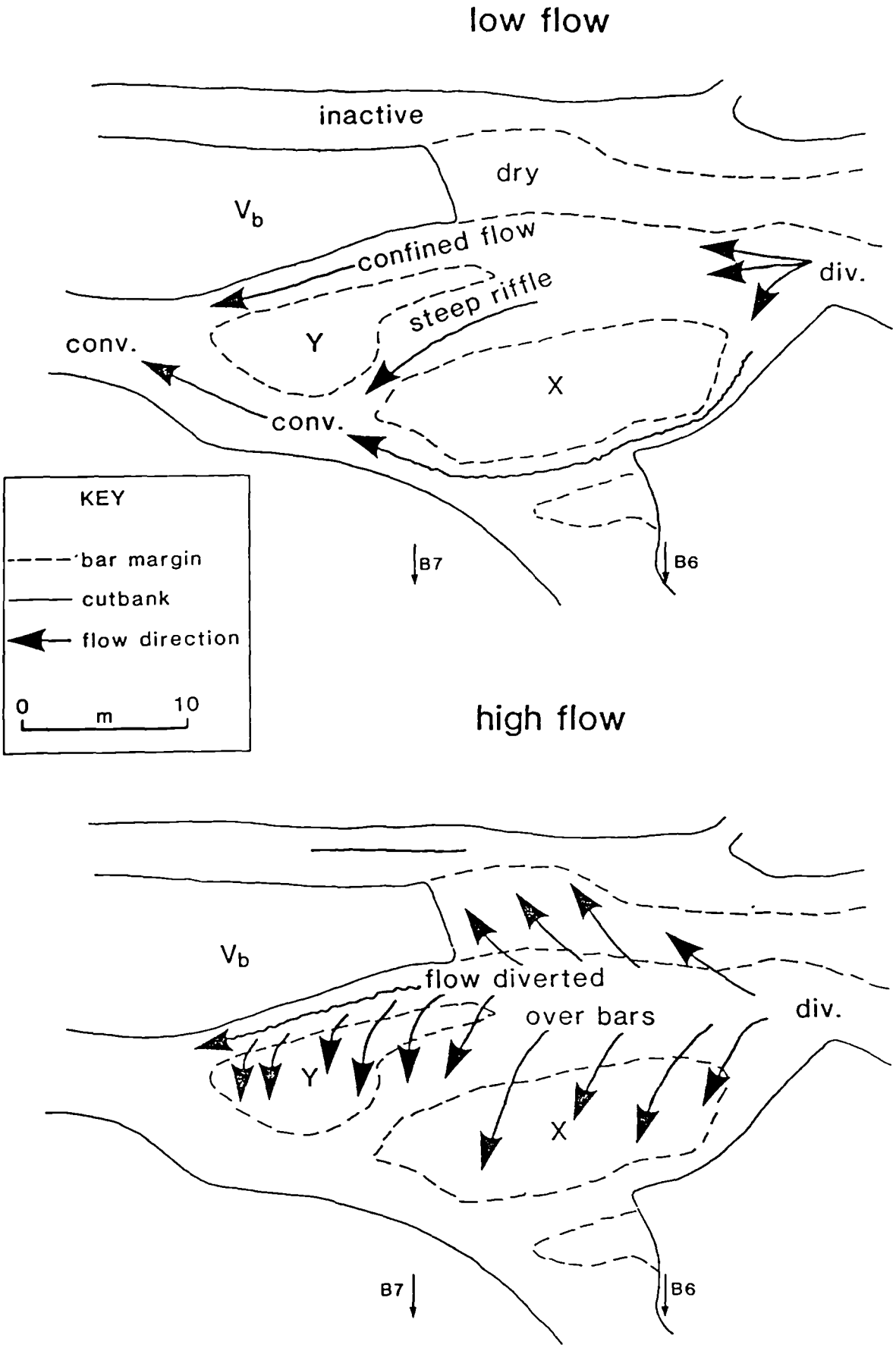

Fig. 5.8 Sketch showing the difference in flow pattern from low to high stage over and around bars X and Y of reach B of the Dubhaig (as inferred from field observations, bed velocities, pebble tracers, and imbrication directions).

near-symmetrical divergence at the barhead but also by a divergence laterally across the long axis of the bar.

The overall channel change in reach B over 21 months showed a net deposition of 17 m^3 with many parts of the channel reversing the mode of change in the subsequent floods. This was particularly true of sections B1-B3 which at first eroded and then filled, and the long right-hand bar (W) between B4 and B5 which was trimmed and then built up again. A planimetric map of the exposed bars at the end of the study period showed little change in the extent and position of the bars. Although bars X and Y between B6 and B7 and parts of the long right-hand bar (W) aggraded this was not accompanied by significant lateral growth.

5.2.4 Reach C

As mentioned in 2.1.2 the channel pattern in reach C is a transitional form between a divided and single channel. Fig. 5.9 shows the planimetric map surveyed on 29/5/84 but with the approximate bar positions at low flow superimposed from a later survey on 1/8/85. The inner chute referred to in the discussion below (labelled C_t) was also taken as the riffle site for the pebble tracing experiments described in 3.2.3. The bed velocities and pebble tracer locations from 14/12/85 are shown in Fig. 5.9 together with the imbrication directions of the semi-vegetated and stable inner relict point bar (labelled V_b). The measurement of imbrication directions was impracticable for the two segments of the mid-channel bar (labelled X_1 and X_2) which were of such low relief that they were frequently submerged in moderate discharges. The magnitude of channel change in reach C was not as great as in the previously discussed reaches A and B (and later reach D) partly due to the shortness of the study reach but also because of the lower stream power (see 5.5.1), the indefinite channel pattern, and the presence of large turf blocks which protect the foot of the outer

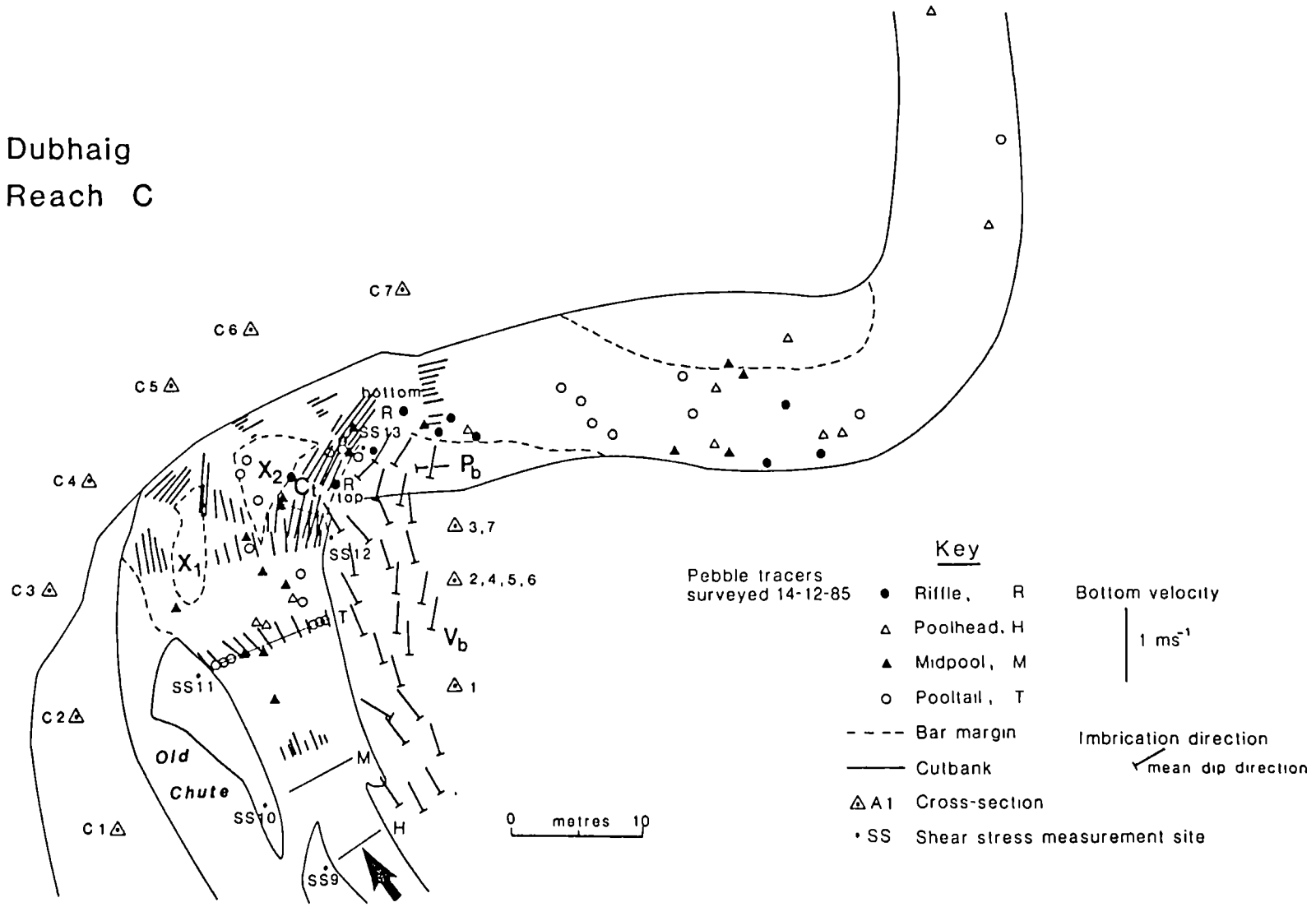

Fig. 5.9 Pebble tracer movements, bed velocities, and bar imbrication directions in reach C of the Dubhaig.

arcuate bank. However for comparison with other reaches the cross-sectional changes in the two autumn/winter periods are plotted in Figs. 5.10a-b.

During the May-October 1984 months no detectable channel change took place at all. This was followed by 16 m^3 of erosion and 2 m^3 of deposition in the winter of 1984/1985 as shown in Fig. 5.10a. A consistent scour of the talweg between C1 and C2 and the creation of a chute to divide the mid-channel bar (and create bars X_1 and X_2) accounted for most of this erosion. Sections C3 and C4 show the 7 m^3 of scour that created the chute and Figs. 5.11a-b can be compared to illustrate the altered bar morphology and the subsequent diversion of some of the flow from the main channel. The inner chute containing the main flow (C_t) eroded part of the steep avalanche face of the right-hand segment of the divided bar (X_2) as shown by C6 in Fig. 5.10a but just upstream at C5 the bar advanced towards the bank edge. A divergence of flow over the small inner exposed point bar (labelled P_b) resulted in fresh deposition of about 1 m^3 between sections C6 and C7.

The March-September 1985 period again saw little change with no new erosion and only 4 m^3 of deposition across the bed of the main chute and a thin layer on the exposed inner point bar, P_b. The following autumn/winter floods led to 1 m^3 of deposition and 11 m^3 of erosion as shown in Fig. 5.10b. The deposition occurred on the margins of the relict point bar (V_b) between C1 and C2 while the erosion was largely accounted for by a further scour of the chute between bars X_1 and X_2 and up to 40 cm of scour at the junction of the bottom of the inner chute, C_t, and the apex of the bend at C6.

In the total study period there was surprisingly little measurable deposition on the mid-channel bars X_1 and X_2. As Fig. 5.9 shows many

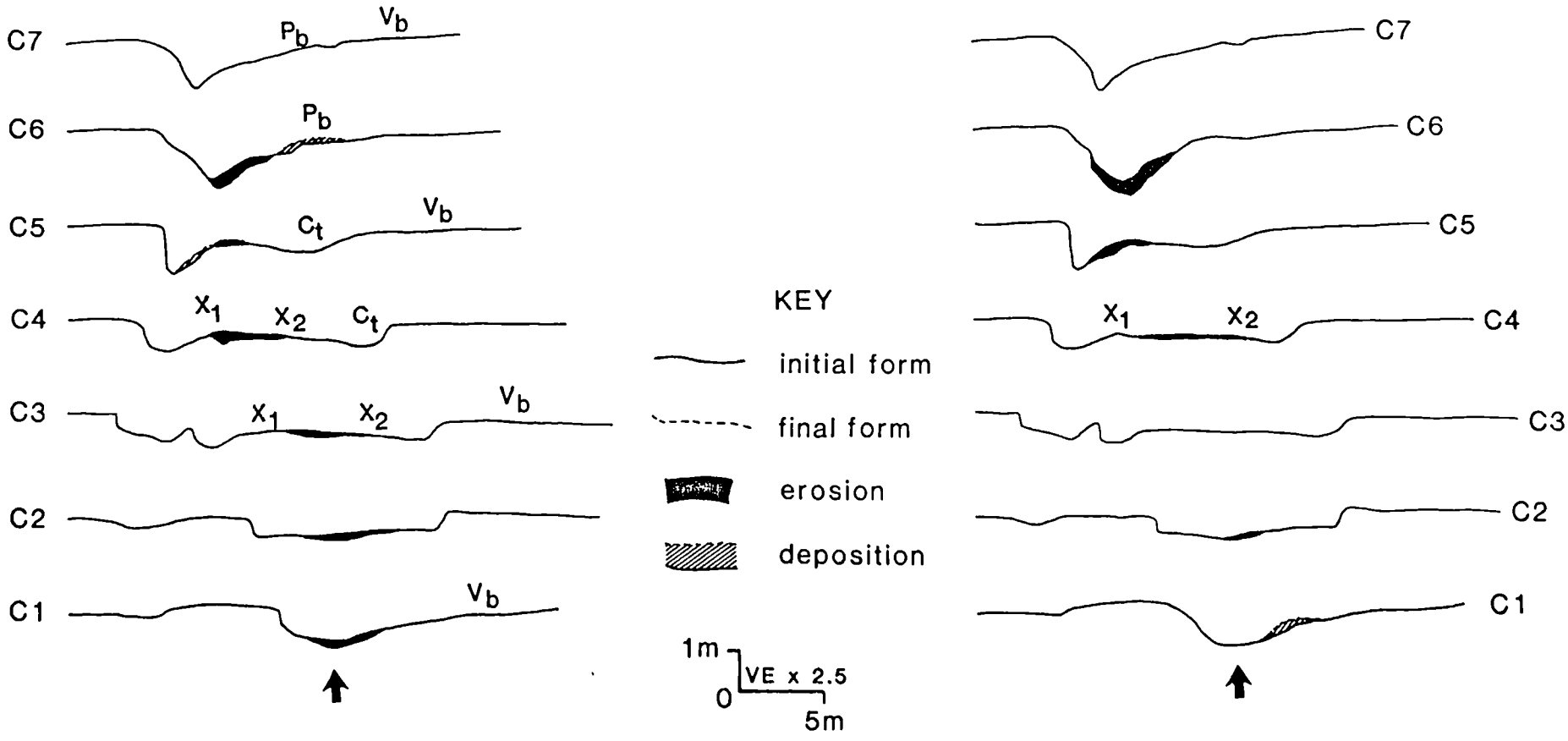

Fig. 5.10 Cross-sectional changes in the Dubhaig reach C from (a) 4.10.84 - 26.3.85, and (b) 13.9.85 - 13.11.85.

Fig. 5.11 View of reach C of the Dubhaig looking across/downstream (a) at low flow (photo taken on 4.10.84) with the mid-channel bar intact (b) the situation at low flow (discharge about 0.34 $m^3 s^{-1}$) on 17.10.84 after the bar had been dissected, and (c) during a discharge of 3.2 $m^3 s^{-1}$ showing the weak divergence of flow over the bars X_1 and X_2 and the overall dominance of the chute, C_t.


C

pebble tracers preferred to move down the fast chute C_t and through the bend (48%) although some tracers did deposit on bar X_2. This depositional pattern was identical for the other three tracer experiments showing that the chute was the fundamental control on channel development (both at low and high flow). Fig. 5.11c shows the flow pattern at a discharge of 3.2 $m^3 s^{-1}$ (which can be compared to a similar view in Fig. 5.11b at a discharge of 0.34 $m^3 s^{-1}$). Fig. 5.11c shows that at the higher discharge the fast turbulent flow through the chute is only countered by a weak and ill-defined divergence of flow over the submerged bars and a gentle flow around the outer bank edge.

The prominence of the chute C_t at low flow is also shown by the bed velocities in Fig. 5.9 with the bottom of the chute approaching velocities up to 1.0 m s^{-1} compared to a maximum of 0.9 m s^{-1} at the top. The pool stretching from upstream of C1 to C2 has very low bed velocities but as the discussion in 3.2.1 showed these pool/riffle hydraulic properties reverse at higher discharges.

The imbrication directions confirm the cross-sectional changes described above with the sediment on the exposed point bar (P_b) aligning itself to represent a divergence of flow out of the main chute at high discharges but the inner vegetated point bar (V_b) lacking any visible signs of recent flow divergence. The height of this point bar and the distance away from the present channel bend rarely allows the flow to diverge over its surface but instead it retards the flow so that the pebbles on its margin are often aligned inwards to the channel (see Fig. 5.9).

The net change for sections C1-C7 during the 21 month surveying period was an erosion of 19 m^3 of sediment which could mainly be accounted for by the erosive powers of the two chutes and upstream pool at high discharges.

5.2.5 Reach D

The meandering channel pattern of reach D is shown in Fig. 5.12 and the cross-sectional changes during the two autumn/winter periods of 1984 and 1985 in Figs. 5.13a-b. The May-October 1984 period did not alter the channel geometry significantly with only 0.5 m^3 of deposition and 3 m^3 of erosion - concentrated on the avalanche face of the point bar between D4 and D5. However as Fig. 5.13a shows both the channel and point bar's position and level changed during the following winter floods with a reach total of 43 m^3 deposition and 22 m^3 of erosion. Bank erosion at D5, D7 and a maximum of 1.1 m at D8 was accompanied by 2.1, 0.8, and 1.7 m^2 of deposition respectively on the point bar opposite. Using the prism formula between sections D7 and D8 this is equivalent to 13 m^3 of bank erosion and 9 m^3 of deposition. As Fig. 5.13a shows the deposition between D7 and D8 was essentially a result of the growth of the point bar's avalanche face, but at D5 and D6 this was also accompanied by aggradation of the point bar surface - by up to 20 cm at the apex of the bar. There was notably little other deposition on the bar surface either upstream along section D4 or downstream along D7. The source of material for this point bar aggradation was not from channel scour upstream (within the reach at least) since sections D1-D3 also showed a depositional tendency with 16 m^3 of sediment infilling the talweg and margin of the point bar. Likewise the channel banks in reach D only consist of fine floodplain material and though it may appear that the bank erosion at D5, D7, and D8 supplied the sediment to develop the point bar in its proximity, the bar growth was of much coarser material only available from the channel bed.

The March-September period led to a halt in the lateral growth of the point bar with sections D5-D8 all showing a small but measurable trimming of the avalanche face totalling 12 m^3 of erosion. At D7-D8 the

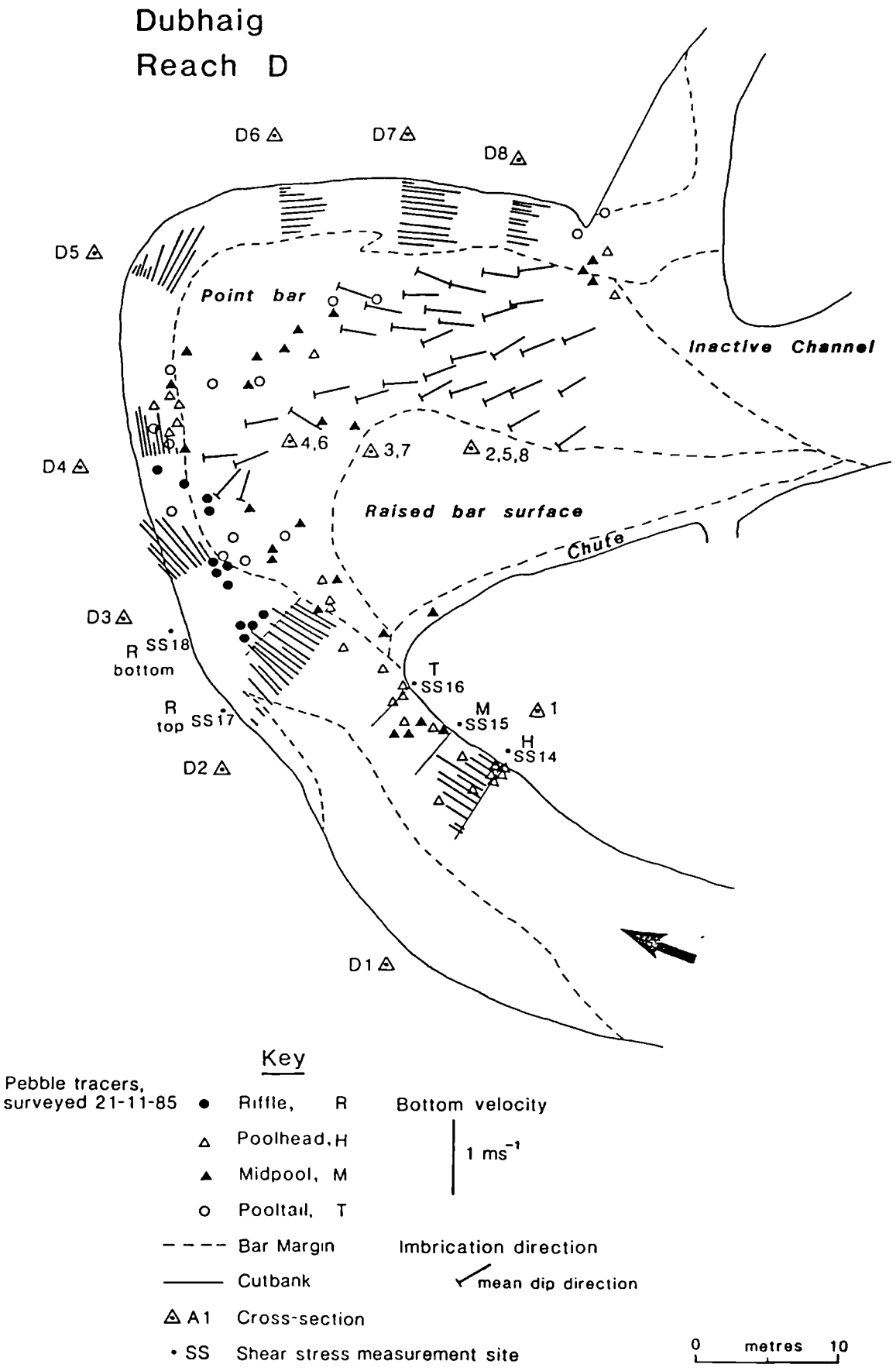

Fig. 5.12 Pebble tracer movements, bed velocities, and bar imbrication directions in reach D of the Dubhaig.

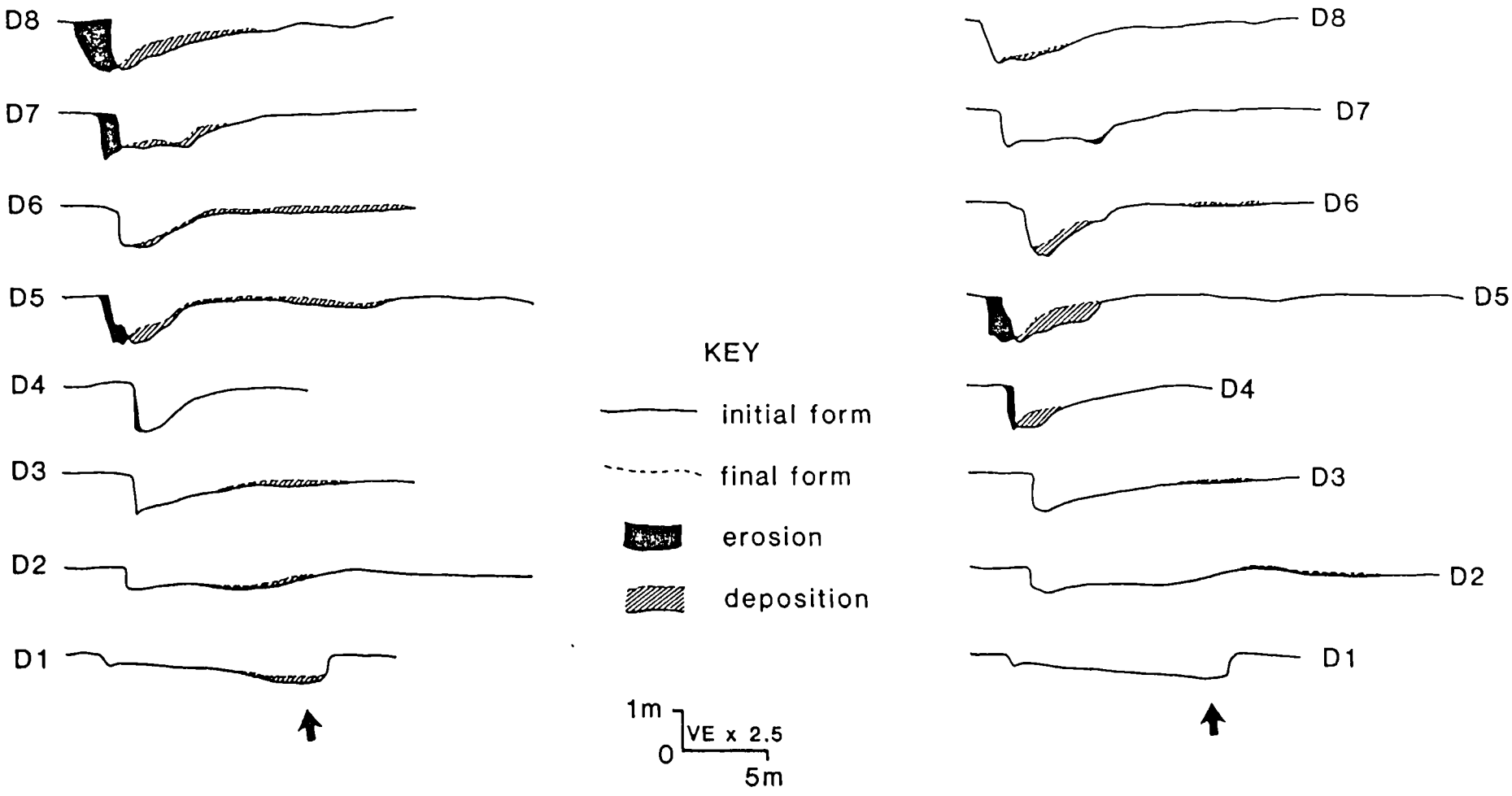

Fig. 5.13 Cross-sectional changes in the Dubhaig reach D from (a) 1.10.84 - 26.3.85, and (b) 26.9.85 - 13.12.85.

depositional and erosional trends measured in the previous winter floods were reversed with the 4 m^3 of point bar erosion accompanied by 2 m^3 of deposition in the outer (and deepest) part of the talweg. Bank erosion was again related to the greatest amount of deposition along a cross-section with this time the bank edge at D4 retreating by 0.8 m and the opposing point bar extending its position with 0.9 m^2 of deposition at the avalanche face.

The bank erosion at D4 continued during the winter floods of 1985 as shown in Fig. 5.13b. The reach total of 16 m^3 of erosion (compared to 29 m^3 of deposition) was largely a result of the bank erosion between D4 and D5, with D5 retreating by 0.4 m. Again the largest depositional areas were on the point bar opposite this erosion with 11.5 m^3 of sediment deposited at the bar's margin between D4 and D5. This growth continued around the outer limits of the point bar to D6. The bar also aggraded further upstream on the inner raised bar surface at D2 (see Fig. 5.13b) and the bar margin at D3, although these were negligible amounts.

The bed velocity map in Fig. 5.12 shows that at low flow reach D has consistently high velocities around the meander bend with a hint of flow separation at the apex at D5. The riffle between D2 and D3 has some of the highest bed velocities approaching 1.0 m s^{-1} as the bottom of the riffle nears the bank edge at D3. At higher discharges the flow overtops parts of the point bar and occupies a chute clearly identified in Fig. 5.12 by the imbrication directions. As will be shown later this flow pattern at high discharges varied in reach D according to the time period. The pebble tracer survey on 21/11/85 showed that little coarse sediment appeared to follow the main flow route around the meander bend. Instead most pebbles were deposited either as the flow diverged over the margin of the bar (between D3 and D4), or along the bed of the chute as the flow shallowed (between D3 and D6) and at its junction with the main flow (at

D8+). Recalling the cross-sectional changes for the winter 1985 period in Fig. 5.13b sections D4 and D8 showed 0.7 and 0.5 m^2 of deposition respectively (consistent with the tracer locations) but the 1.7 and 0.7 m^2 deposition at the point bar avalanche face between D5 and D6 does not correspond to any distinct tracer concentrations. The other pebble tracer experiment for this period surveyed on 13/12/85 showed an almost identical pattern. The most likely explanation for the scarcity of tracers at D5-D6 is that the pebbles were buried in the advancing avalanche face. Indeed the recovery rates were only 58 and 36% for the November and December tracer experiments respectively.

The change in the location of erosion on the outer bank and deposition on the point bar illustrated by the cross-sections in Figs. 5.13a-b is a direct result of a change in the flow pattern, which itself is dependent on the discharge. This can be illustrated using the example of the winter 1984/1985 (Fig. 5.13a) and summer 1985 channel changes. The March-September period had less frequent and lower competent discharges than in the previous winter period and this is responsible for the different spatial flow pattern and related channel changes. Figs. 5.14a-b below show the flow pattern during two high discharges on 25/10/84 (4.0 $m^3 s^{-1}$) and 27/7/85 (2.8 $m^3 s^{-1}$). The cross-sectional changes for these times are summarised in the sketches in Figs. 5.15a-b with the summer 1985 cross-sections (previously not plotted) added for comparison.

The figures show that there is a clear relationship between the flow pattern and channel changes. In the winter 1984/1985 period Fig. 5.14a shows that the flow (close to bankfull) concentrates in two areas. It divides near D3 and approximately 20% of the flow cuts across the point bar through the chute which terminates (and diverges) between D7 and D8 whilst the main flow around the bend overlaps the outer margins of the point bar between D3 and D4 on its right and follows the bank edge up to

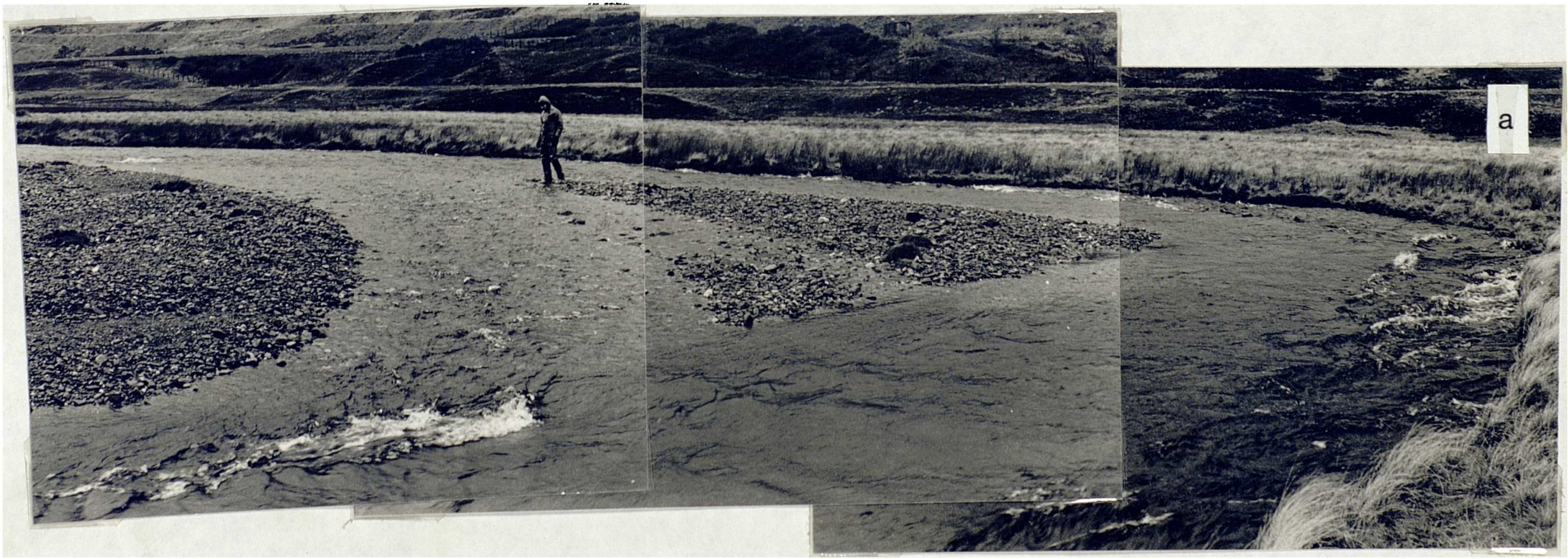

Fig. 5.14 Dubhaig reach D (a) view upstream from D8 taken on 25.10.84 during a discharge of 4.0 $m^3 s^{-1}$, and (b) view from D2 taken on 27.7.85 during a discharge of 2.8 $m^3 s^{-1}$. Note in (a) the main flow follows the bank edge from D5 onwards and in (b) the main flow direction is directly into the bank edge at D4.


b

1 Oct. 1984 - 26 March 1985

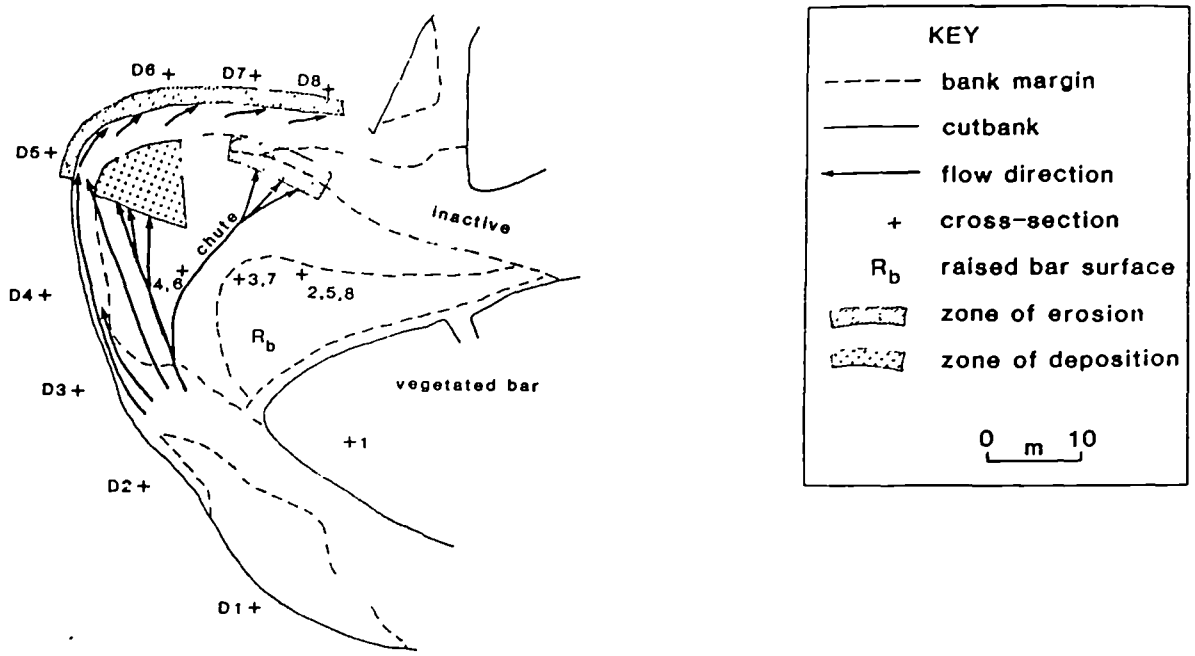

26 March 1985 - 26 Sept. 1985

cross-sectional changes

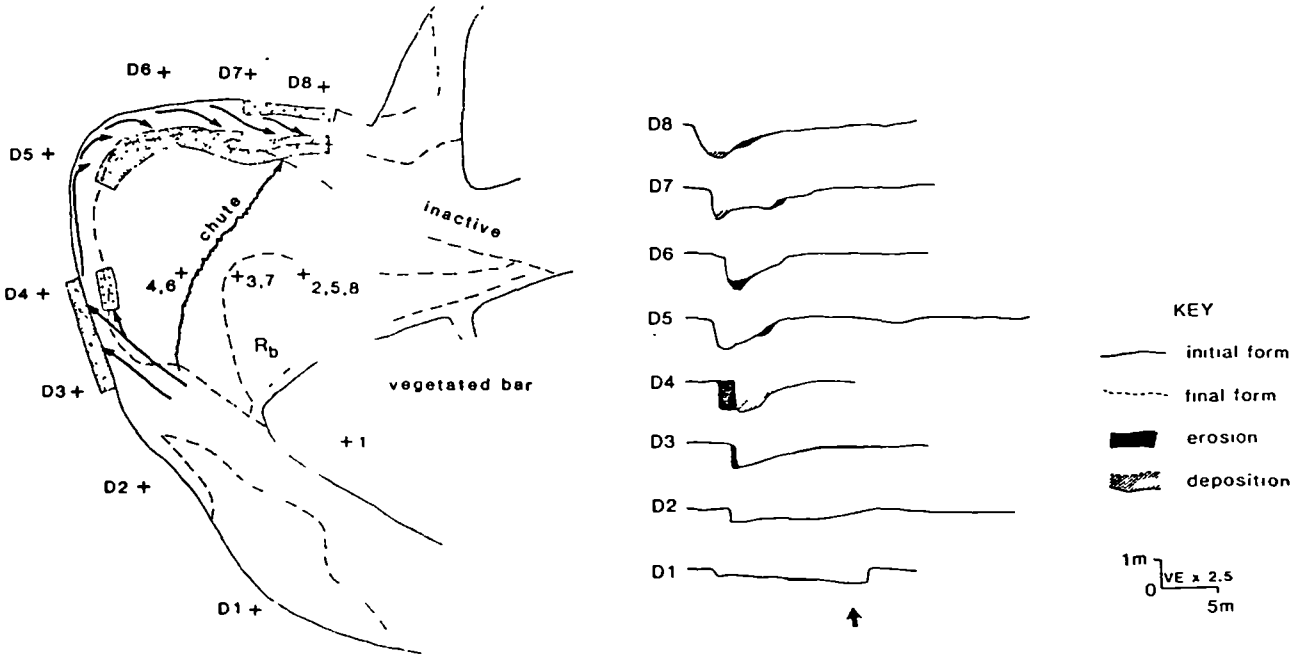

Fig. 5.15 Sketch map of the general locations of erosion and deposition in reach D of the Dubhaig (a) from 1.10.84 - 26.3.85, and (b) from 26.3.85 - 26.9.85. The cross-sectional changes for the summer 1985 period are also plotted.

the apex of the bend at D5 on its left. Here it collides directly with the bank before continuing in a rough turbulent band of flow following the bank edge up to D8 (with much gentler flow and back-eddies nearer the point bar). The resulting channel changes for the period in Fig. 5.13a and 5.15a complement this flow pattern with bank erosion at D5 and D7-D8, aggradation along the chute and outer bar margins at D3, D5, and D6, and growth of the avalanche face at the chute terminus between D6 and D8.

The range of discharge in the March-September period led to a shift in the emphasis of the main current which again was reflected in the channel changes. Fig. 5.14b shows the flow conditions at a discharge just below that required to reactivate the chute across the point bar (in Fig. 5.14b the flow is just beginning to trickle into the chute). The main flow direction does not follow the bank edge between D3 and D4 as it did in the previous winter but flows directly into the bank at D4 (compare Figs. 5.14a and b). Since the flow has lost some of its momentum at D4 it does not collide with the apex of the bend at D5 as strongly as in the previous winter and the main current at D6-D8 moves from the bank edge to leave a back-eddy separation zone below the bank edge but stronger flow towards the point bar's avalanche face. The infrequent and lower discharges during the summer period meant that the chute had less opportunity to aggrade or replace this eroded material at the point bar edge. The channel changes in Fig. 5.15b match this flow pattern with the bank at D3 and D4 eroding, the point bar at D5-D8 retreating, and the outer part of the talweg at D7-D8 infilling. This relationship between the flow pattern, channel changes, and discharge will be elaborated in 5.4.

As mentioned earlier and as shown in the above examples, in reach D there is a remarkable correlation between the locations of bank erosion and point bar deposition. In all cases where there was lateral channel movement this was compensated for by a growth of the point bar opposite

and the overall bed geometry scarcely changed. Since the banks do not contribute to the sedimentation on the point bars (it would be removed as suspended load) there is overriding evidence to suggest that the meandering channel is in a form of equilibrium so that any changes in its shape or size either by erosion or deposition is compensated for by a corresponding amount of sediment movement in or out of the bed area. Whether it is the aggradation that causes the bank erosion or vice versa cannot be determined from this study.

5.2.6 Reach E

The magnitude of channel change drops to negligible levels in the straight channel pattern of reach E despite the amount of flow passing through the reach being equivalent to that in reaches A-D. The gentler bed slope (which at times almost measures horizontal) alters the rate at which the flow passes through reach E (and therefore stream power, shear stress, and velocity) and at low flow many parts of the channel are stagnant. Fig. 5.16 shows the overall channel pattern together with the pebble tracer locations surveyed on 14/12/85 and near-bed velocities. As mentioned in 2.1.2 there is little emergent gravel (hence no imbrication directions in Fig. 5.16), possibly since the reach rarely transports large quantities of coarse sediment but also since the channel pattern (with its resistant vegetated banks) restricts the development of the divergence and convergence unit and therefore the variations between flow strength and bedload transport which scour and build the channel and bars.

The channel changes for the whole of the 21 month study period are shown in Fig. 5.17. The channel geometry shows a switching of the talweg from the poolhead on the right-hand side of E1-E2, to the left bank between E3 and E4/E5, and then back to the right from E5-E6 where it begins to diverge onto a shallow riffle. The channel changes are confined to the

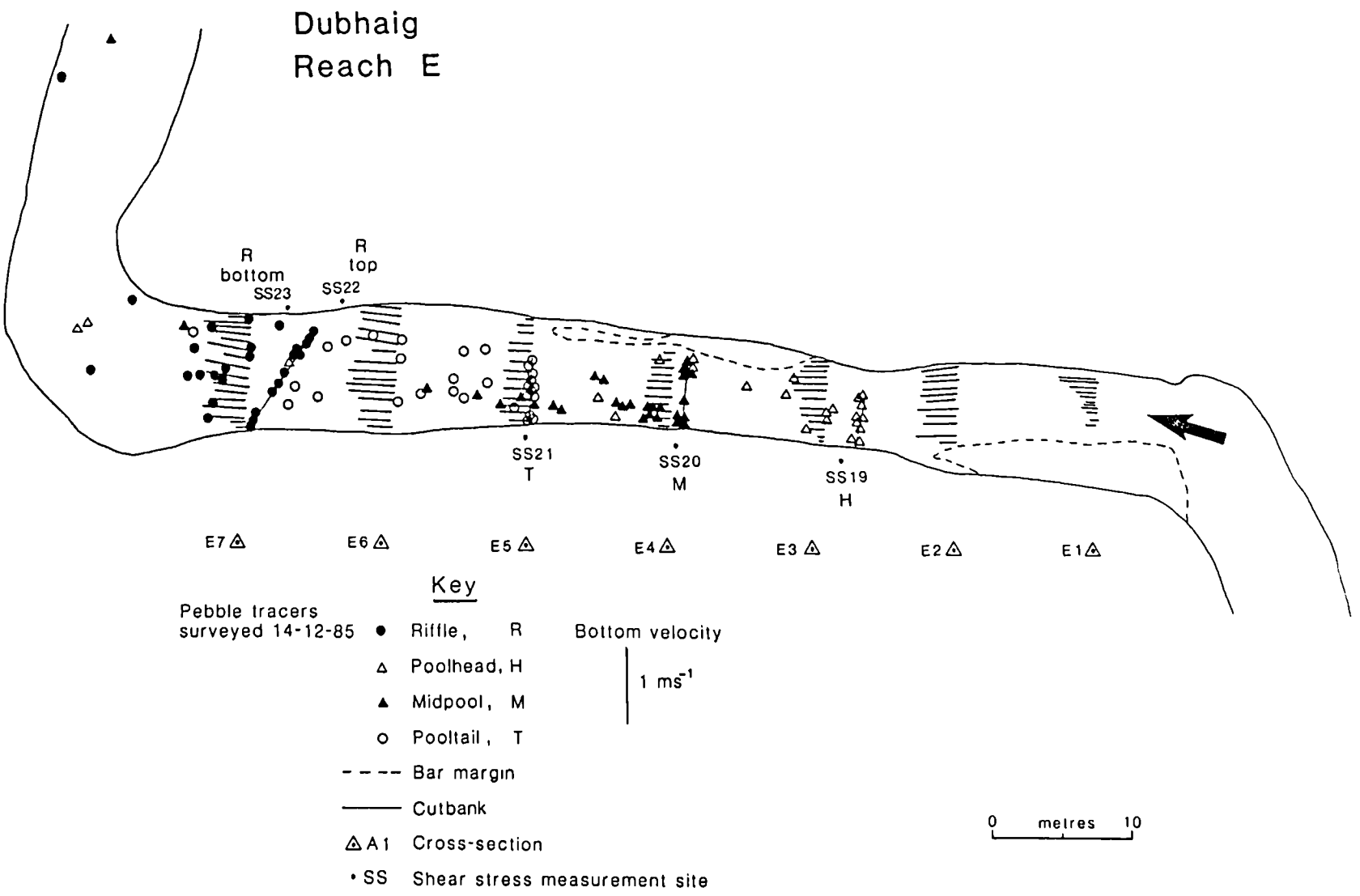

Fig. 5.16 Pebble tracer movements and bed velocities in reach E of the Dubhaig.

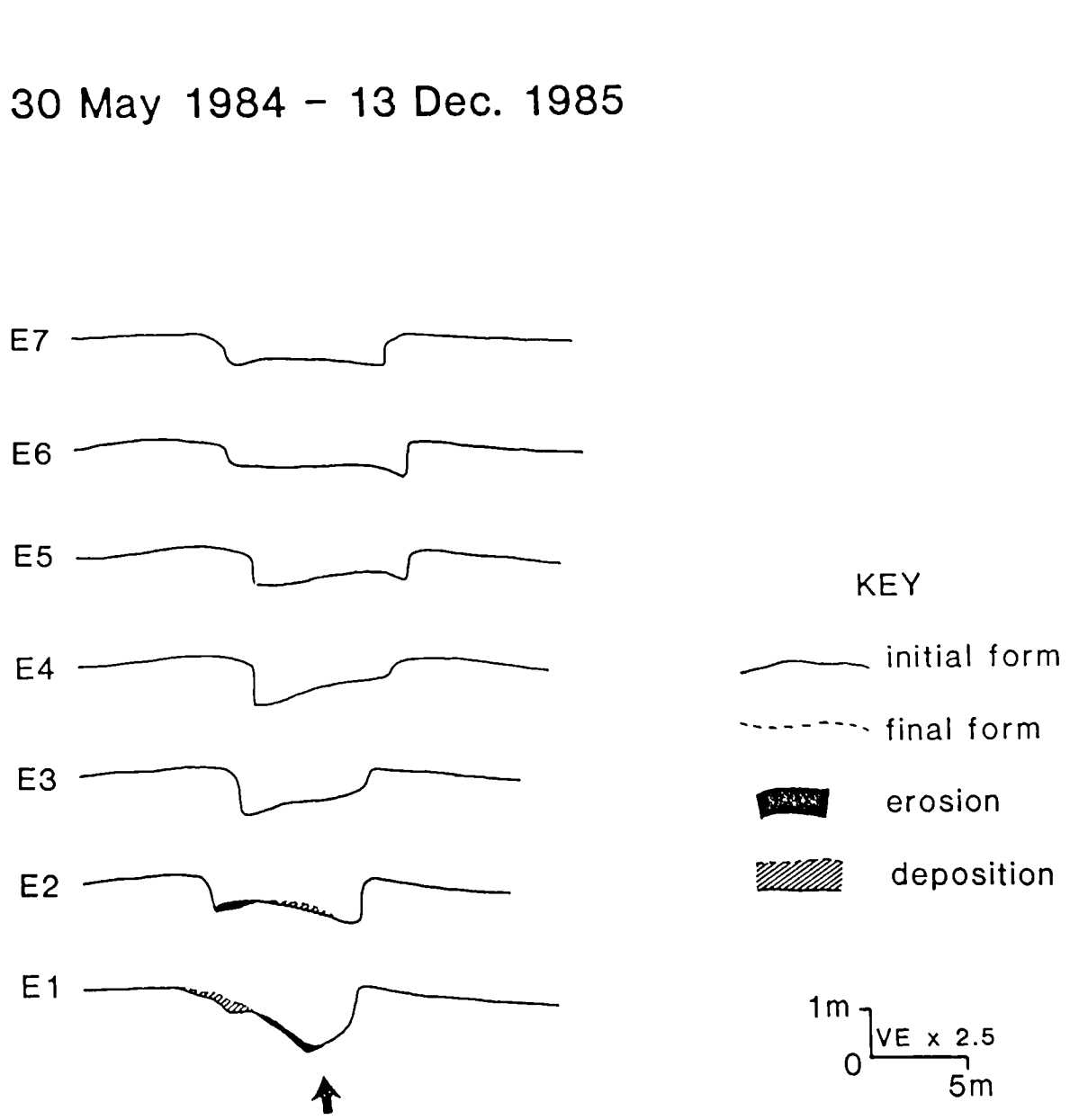

Fig. 5.17 Cross-sectional changes in the Dubhaig reach E for the whole of the study period 30.5.84 - 13.12.85.

head of the reach at E1 and E2. Here in the March-September 1985 period there was 4 m^3 of erosion concentrated at the base of the barhead and over the surface of the bartail. The same areas were built back up again on their margins in the following winter period although the total of 6 m^3 of deposition was higher up on the barhead at E1 and nearer the centre of the channel at E2. No channel change took place throughout the study period for sections E3-E7.

The bed velocity map in Fig. 5.16 can be compared with Fig. 5.18a which shows the reach at a discharge of 0.40 $m^3\ s^{-1}$. At the head of the reach the flow converges off a riffle into the right-hand bank edge (see Fig. 5.18a). This leads to a separation of flow with back-eddies on the inner left-hand part of the channel and faster flow along the smooth right-hand bank edge. This is shown both in Figs. 5.18a and at E1 in Fig. 5.16. At E2 the flow has overcome these flow irregularities from upstream and is more uniform across the section. At E3 the highest bed velocities are on the right of the channel (despite the talweg switching over to the left) but by E4-E5 the main current has crossed over and flows down the left-hand side. From E6 onwards the flow runs down a uniform riffle (just visible at the end of the reach in Fig. 5.18a) which has the highest bed velocities in the reach - up to a maximum of 0.7 m s^{-1} at the top of the riffle at E6. Fig. 5.16 also shows that all sections E1-E7 have a marked decrease in bed velocity at the channel margins. This is due to bank roughness effects from the steep, stable, well vegetated bank edges on either side of the channel.

Fig. 5.18b shows the reach at a discharge of 2.8 $m^3\ s^{-1}$. The side bar between E3 and E5 and the low lying riffle between E6 and E7 are submerged and the flow from E3 onwards now appears to concentrate along the centre of the channel (identified from the rough surface flow in Fig. 5.18b). The pebble tracers surveyed on 14/12/85 do not show any distinctive

Fig. 5.18 Views down reach E of the Dubhaig (a) from the head of the reach during a discharge of 0.40 $m^3 s^{-1}$, and (b) from E1 during a discharge of 2.8 $m^3 s^{-1}$. Note the migration of the main flow into the centre of the channel in (b).

depositional patterns since there are few exposed bars and little opportunity for divergence and convergence of flow. However the pebbles that remained at their original locations tended to be confined to the outer margins of the channel supporting the earlier suggestion that at competent discharges the current is fastest in the centre of the channel. There is therefore little evidence to show that the flow pattern changes dramatically with increasing discharge although there are still within-reach pool/riffle changes as described in 3.2.3 .

5.3 The Feshie

Channel changes were surveyed over two short periods in the latter half of 1985 for reach C and the snowmelt season of 1986 in reach B. In addition the channel processes were investigated using pebble tracers, bed velocity and shear stress measurements, and Helley-Smith bedload sampling. The Helley-Smith samples and pebble tracer experiments have already been discussed in Chapter 4 but the analysis here concentrates on a different aspect of their results. In both reaches the tracer pebbles were placed at subunits in a pool/riffle cycle (see 3.3) but in reach C an additional experiment was designed to provide information on the mobility of the barhead and tail on the active medial bar centred on sections C6-C8. This experiment is distinct from Brewster's (1986) tracer programme outlined in 3.3 but is the same pebble tracer data used in the analysis for reach C in 4.6.2.

The hydraulic measurements in reach C were confined to a single set of shear stress measurements on 4/4/85 during a moderate flood discharge of 14 $m^3 s^{-1}$ and a bed velocity map on 18/6/85 at a discharge of 3 $m^3 s^{-1}$ (approximately the mean discharge). Much more information on the channel processes was collected in reach B using a combination of velocity profiles and Helley-Smith sampling at three progressively higher

discharges during snowmelt on 2/5/86 (peaking at bankfull). Since an extensive set of process measurements was never taken in any reach of the Dubhaig, especially during active bedload transport, the Feshie reach B results are particularly important. The measurements provide information on the hydraulics at channel forming discharges and help to support the directions and rates of bedload movement that are inferred from the pebble tracers.

The discussion below will treat reaches B and C separately and begins with a brief synopsis of the channel changes, followed by a discussion of the processes that are responsible for these changes.

5.3.1 Reach B

The cross-sectional changes for the snowmelt period 18/4/86-4/6/86 are shown in Fig. 5.19 whilst the pebble tracer movements for this period and a planimetric map surveyed on 4/6/86 are shown in Fig.5.20. The reach showed a total of 112 and 102 m^3 of erosion and deposition respectively along its 100 m length. Although this indicates there was little net change in the total reach geometry Fig. 5.19 shows that most of the erosion was accounted for by bank collapse between sections B5 and B6.5. Bank retreat up to a maximum of 2.5 m at B5 led to 98 m^3 of material being removed between B5 and B6.5. Only at B7.5 did the channel scour its bed significantly with the headward erosion of the riffle/run resulting in 35 cm of scour in its talweg.

The depositional areas matched the bank erosion between B5 and B6.5 with a uniformly deposited strip along the former talweg (maximum thickness of 25 cm at B6). The riffle at B5 did not change its bed level appreciably but extended its avalanche face adjoining the poolhead by about 2 m. Further down the reach between B7 and B8 there was aggradation and growth of the

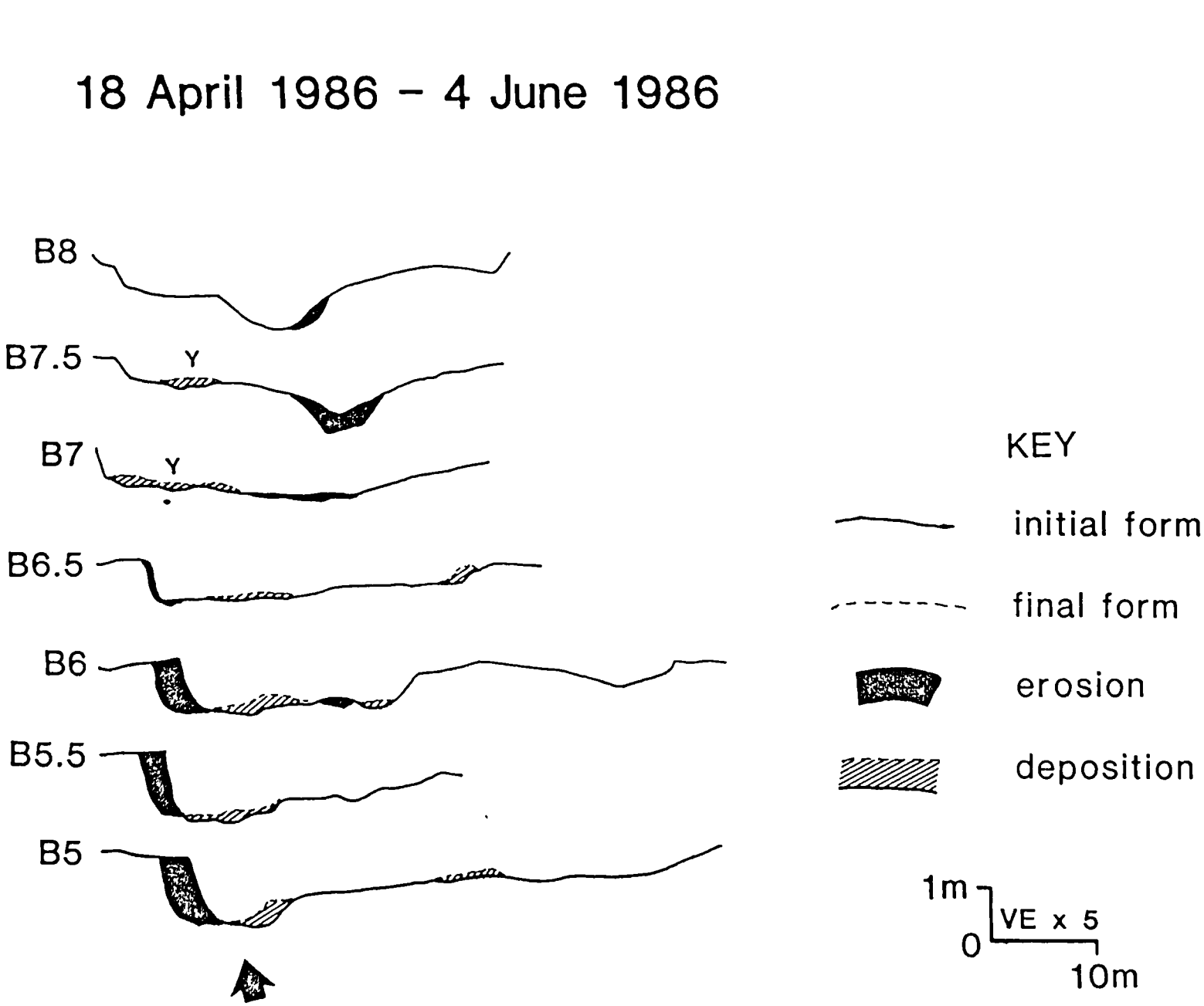

Fig. 5.19 Cross-sectional changes in the Feshie reach B during the snowmelt season 18.4.86 - 4.6.86.

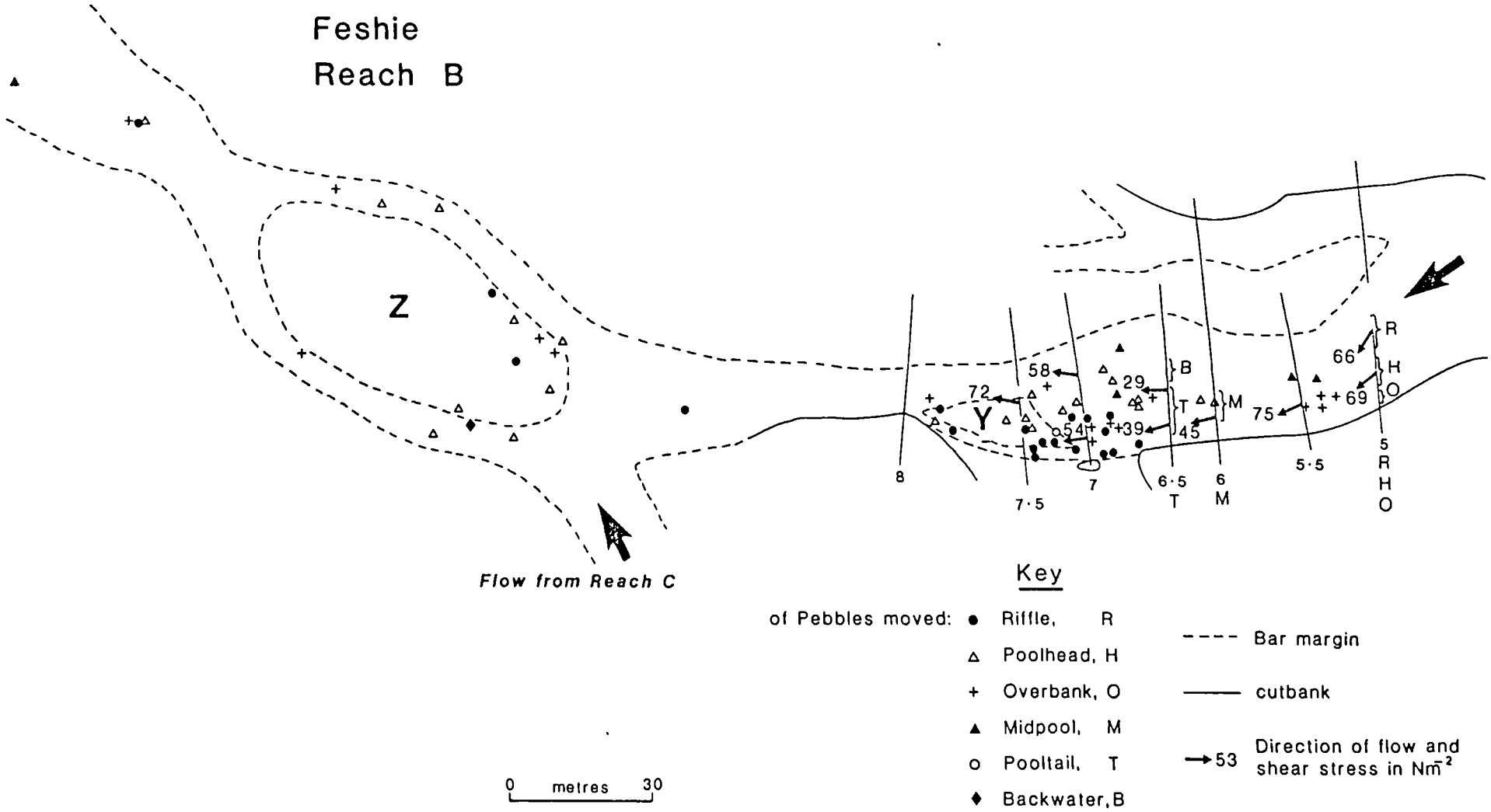

Fig. 5.20 Pebble tracer movements, shear stress measurements, and flow directions in reach B of the Feshie.

bar on the left-hand side of the channel (labelled Y). Between the barhead at B7 and the tail at B8 58 m^3 of material was deposited. The emergence of this bar (particularly on its left-hand side) and the channel changes can be seen by comparing Figs. 5.21a-b taken at the beginning and end of the study period. The change in channel curvature as a result of the bank erosion between B5 and B6.5 can clearly be seen in these figures.

Examination of the discharge record for the six week surveying (and pebble tracer) period shows that it was dominated by marked diurnal fluctuations. Six of these snowmelt floods and two other rainfloods marginally exceeded the discharge during which the process measurements were taken on 2/5/86 (see below) with a maximum discharge for the period of 33 $m^3 s^{-1}$ on 1/5/86 (snowmelt). The measurements on 2/5/86 are therefore a fairly representative guide to the magnitude and rate of channel forming processes that were operating throughout the snowmelt period.

Table 5.1 summarises the shear stress and bedload measurements taken in the three different discharges with mean values for the beginning and end of the measurement period of 14, 20, and 22 $m^3 s^{-1}$. The riffle is not included in Table 5.1 since no bedload was ever trapped (even during the peak discharge) and the hydraulics are discussed elsewhere (3.3). The sections B5.5 and B6 both constitute a midpool area although B6 was chosen as the site for pebble tracer insertion.

At the discharge of about 14 $m^3 s^{-1}$ the shear stress decreased downstream from the poolhead to the pooltail. The total transport rate generally followed this trend with a drop from 0.034 kg $m^{-1} s^{-1}$ at B5 to 0.013 kg $m^{-1} s^{-1}$ at B6.5. The amount of gravel (percentage greater than 2 mm by weight) trapped highlighted the differences in shear stress and competence at different locations with 97% of the bedload at B5 constituting gravel, falling to only 2% at B6.5.

Fig. 5.21 View taken from B8 looking upstream to B5 (a) at the beginning of the study period on 18.4.86, and (b) at the end of the snowmelt season on 4.6.86. Note the increase in channel curvature at the vegetated bar edge between B5 and B6.5.

Table 5.1 Shear stress and Helley-Smith bedload measurements during a snowmelt flood in the Feshie, 2.5.86.

Site/ unit	$\bar{Q}$ = 14 m^3s^{-1}			$\bar{Q}$ = 20 m^3s^{-1}					$\bar{Q}$ = 22 m^3s^{-1}	
	Shear stress $N\ m^{-2}$	Total trans. rate $kg\ m^{-1}s^{-1}$	% gravel by weight	Shear stress $N\ m^{-2}$	% change in shear stress	Total trans. rate $kg\ m^{-1}s^{-1}$	% change in trans. rate	% gravel by weight	Shear stress $N\ m^{-2}$	% change in shear stress from start
5 Poolhead	53 ±16	0.034	97	63 ±13	+19	0.045	+32	86	69 ±12	+30
5.5 Midpool	49 ±12	0.013	63	82 ±12	+67	0.18	+1284	84	75 ±20	+53
6 Midpool	36 ±8	0.023	8.9	45 ±8	+25	0.096	+317	69	45 ±10	+25
6.5 Pooltail	32 ±4	0.013	2.4	51 ±7	+59	0.0080	-39	3.9	39 ±7	+22

As the discharge increased to a mean of 20 $m^3 s^{-1}$ the shear stresses all increased but not at an identical rate (caution must be employed here since given the standard errors in Table 5.1 the shear stresses may actually be quite similar at B5 and B6). The most rapid rise in shear stress was at B5.5 with a 67% increase to 82 ± 12 N m^{-2}. This increase in flow strength at B5.5 was accompanied by a dramatic rise in the bedload transport rate - over a magnitude higher at 0.18 kg $m^{-1} s^{-1}$ with 84% gravel. The poolhead at B5 continued to move a high proportion of gravel (86%) and possibly as a legacy of the rise in shear stress and transport rate at B5.5, the downstream end of the midpool at B6 increased its transport rate by over 300% moving up to 69% gravel by weight. The pooltail at B6.5 seems anomalous both in the shear stress increase (which is much higher than that measured later at the peak discharge) and the drop in bedload transport rate (which could easily arise from the Helley-Smith sampler being perched on a cobble).

At the flood peak (mean discharge of 22 $m^3 s^{-1}$) the shear stress varied little from the previous measurements. No bedload was taken during this discharge (due to instrument failure) but the shear stress values in Table 5.1 and for the reach down to B7.5 in Fig.5·20 give some indication of the likely areas of bedload transport. In addition the surface flow direction was measured using a compass and a piece of string tied to the current meter (see 2.2.2) and is plotted with the shear stress values in Fig.5·20. The flow plunged down the riffle avalanche face at B5 to converge with the flow along the bank edge. The midpool at B5.5 continued to maintain the highest shear stress (75 ± 20) with the flow still converging and flowing diagonally towards the bank. From B6 onwards the flow begins to diverge with lower shear stresses at B6.5 of 39 ± 7 and 29 ± 6 across the channel and then picking up to values above 50 N m^{-2} at B7 where the flow is either diverging onto the barhead or funnelling down into the riffle/run

on the right of the channel. At B7.5 the acceleration of flow across and down the bar margins results in a shear stress of 72 ± 7 (the fourth highest recorded shear stress for the reach after the riffle at B5 and the midpool at B5.5).

Fig.5·20 also shows the direction and distance of pebble tracer movement. A large proportion of pebbles were immobile on the riffle at B5 but the rest at B5 (poolhead and overbank), B6, and B6.5 moved to cluster around two bars - the left-hand bar between B7 and B8 (bar Y) and a medial bar some 70 m downstream of B8 (labelled Z). Within the reach, the convergence of flow, bank erosion, and high bedload transport rates between B5 and B6 all combined to either move the pebble tracers downstream or bury them under other moved sediment. The low shear stresses measured at the pooltail only led to limited pebble movement - up to 30 m, depositing in a zone around the head of bar Y. The flow divergence out of the pooltail at B6.5 undoubtedly assisted the deposition of the pooltail pebbles onto this barhead but also influenced the direction of movement of incoming tracers from upstream. As Fig.5·20 shows the B5 and B6 tracers either diverged to the left and continued to build up the barhead around B7 or diverged to the right and joined the fast riffle/run which led on to the next bar system.

The overall pattern of channel processes at bankfull discharge is a good example of the convergence/divergence cycle. The flow down the riffle at B5 (with little bedload transport) converges with the flow from upstream to erode the bank between B5 and B6. This is also accompanied by some bed scour (to move the tracers) which may have been infilled on the falling limb of the flood or by collapsed bank material. The maximum flow strength, degree of convergence, and bedload transport rate is at the upstream part of the midpool (B5.5). This is probably because the flow straightens out over the riffle at B5 as the discharge approaches bankfull

and the convergent zone migrates downstream (Table 5.1 shows that the maximum shear stress and bedload transport shifts from the poolhead at B5 to the midpool at B5.5 as the discharge increases). The flow then begins to diverge as it leaves the pooltail and moves material to the left to help build a bar, or to the right to enter another convergent zone belonging to the start of the next bar system. The deposition on the right of the channel between B5 and B6 is a result not of flow divergence but of a decrease in flow strength in a backwater-type zone as the core of the convergent flow moves laterally (although this can still be termed a type of divergence).

As Fig. 5.20 shows once this sediment has moved out of the study reach little is deposited until the flow diverges again onto the next bar. The 70 m long narrow single channel linking the two depositional zones only has one pebble tracer present. The weakening of the flow strength as the flow divides around the barhead enables some pebbles to be deposited in the channel but the majority are either at the bar's head or its margins. The maximum distance moved for a tracer pebble was 308 m - managing to move through two bar systems before being deposited.

The concentration of pebble tracers in two areas of flow divergence around barheads lends further support to the observations of Mosley (1978) for the Tamaki River in New Zealand. Using limestone pebbles which were foreign to the greywacke bed material Mosley (1978) reported that there was a regular particle concentration that was related to "points of flow divergence where sediment transport capacity was below average." He also noted that "at points of convergence the particles were swept straight through" the reach. The convergent/divergent cycle therefore seems to be an important control on channel development.

In the Dubhaig the five reaches had few opportunities to establish

distinct convergent/divergent units since there was little medial deposition (excluding parts of reaches A and B). At low flow the reaches were dominated by the contrast in the nonuniformity of flow between pools and riffles. However at high discharges when more bars were brought into the active channel area the convergence into banks and divergence onto barheads became particularly important and helped to explain some of the lateral erosion and bar aggradation. The Feshie reach B results show that in a wider river, with higher discharges, and less resistant bank material this convergent/divergent cycle can develop more easily and is responsible for all the channel changes at high discharges. The hierarchy of bed and bank scour in convergent zones and aggradation in divergent zones seems to alter the channel geometry in a predictable way. This theme will be expanded on in 5.4 where the discussion of the Lyngsdalselva (with its fully braided pattern) will highlight the role and importance of the convergent/divergent unit and how it can be used to predict areas of erosion and deposition.

5.3.2 Reach C

The channel changes in reach C were surveyed on five occasions between 4/4/85 and 6/12/85. Initially only seven cross-sections were set up but after 18/6/85 an additional section C8 was surveyed to provide more information on the downstream growth of the medial bar that emerges at C6. As mentioned earlier a set of interrelated process measurements were undertaken at different times and discharges. On 18/6/85 during a discharge of 3 $m^3 s^{-1}$ a near-bed velocity map was measured for sections C1-C6 using a compass and string to determine the flow direction. This can be compared to the set of shear stress measurements taken across sections C1-C6 on 4/4/85 during a discharge of 14 $m^3 s^{-1}$. Again the flow directions were measured using a compass and string.

The September to December process measurements incorporated four sets of tracer experiments. The undergraduate study by Brewster (1986) described in 3.3 used the riffle at C1, the poolhead at C3, and the pooltail at C5 as tracer insertion sites. Movement was monitored between 24/6/85 and 9/10/85, and between 24/10/85 and 6/12/85. The maps of the tracers' depositional locations shown later are adapted from Brewster's (1986) report. The other tracer experiment which was also repeated was described in 2.2.3 and 4.6.2 and consisted of 200 pebbles seeded into the barhead (around C7) and bartail (at three locations 3.5 m upstream, along, and 1 m downstream of C8). The first experiment was undertaken between 5/9/85 and 9/10/85 and the second from 9/10/85 to 14/11/85. These experiments and Brewster's (1986) study were running concurrently for part of the time and both were supported by resurveyed cross-sectional changes (though not necessarily exactly at the start and finish of the tracer periods).

As discussed in 2.2.1 the discharge record for the Feshie was incomplete due to instrument failure. Although one of the two periods of missing data coincided with some of the tracer experiments (no flow data was available from 5/9/85 to 17/1/86) it was still possible to either reconstruct peak flows or determine what peak discharge had moved the pebbles or caused the channel changes. Fortunately the gauging station was still working during a high overbank flood on 1/9/85 which peaked at 59 $m^3 s^{-1}$ (the 3rd largest in the 31 month study period). This undoubtedly moved the pebbles in Brewster's first tracer experiment (24/6/85 to 9/10/85) and caused most of the channel changes in the 18/6/85 to 5/9/85 period. Between 5/9/85 and 6/12/85 only one more overbank flood occurred (recognised by a distinct trash line that is always left near the gauging station). Observations on 14/11/85 showed that no new trash line had been deposited, therefore no high discharge above about 20-30 $m^3 s^{-1}$ in the 5/9/85 to 14/11/85 surveying period had occurred. However on 6/12/85, after widespread channel changes including an abandonment of the

study reach, a well preserved and recent looking trash line was clearly visible at the gauging station. The height of this trash line was surveyed relative to the stageboard and the reconstructed discharge for this flood was estimated to be 89 $m^3 s^{-1}$. This represented the largest flood in the 31 month study period although higher floods have occurred in the Feshie since 1978 (Ferguson and Werritty 1983). If the discharge record for the Dubhaig discussed in 2.2.1 is recalled the highest discharge in the nine month record was 9.3 $m^3 s^{-1}$ on 3/12/85 (preceded by another high discharge on 1/12/85 peaking at 7.5 $m^3 s^{-1}$). Since the Feshie is only 30 km north-east of the Dubhaig it seems likely that the early December rainstorms at Drumochter were also experienced in the Feshie basin (and caused most of the tracer movement and channel changes measured on 6/12/85).

The main cross-sectional changes during the five month study period were due to the two high flows on 1 September and early December 1985. The initial surveying period between 4/4/85 and 18/6/85 showed no appreciable channel change - only 2 m^3 of deposition in the poolhead between C2 and C3. Likewise the 5/9/85 to 14/11/85 period showed only minor channel changes with 3 m^3 of deposition and 2 m^3 of erosion between C1 and C2 along the the riffle and its steep avalanche face. The discussion below is therefore restricted to channel changes between 18/6/85 and 5/9/85 and 14/11/85 to 6/12/85. The cross-sectional changes for these periods are shown in Figs. 5.22a-b. A planimetric map of the reach (surveyed on 24/7/85) showing the cross-section locations, approximate water edges and the pebble tracers from Brewster's (1986) first experiment is shown for reference in Fig. 5.23.

The flood on 1/9/85 led to 51 m^3 of deposition and 44 m^3 of erosion between C1 and C8. As Fig. 5.22a shows the deposition followed a long strip beginning in the talweg of the poolhead between C2 and C3 and

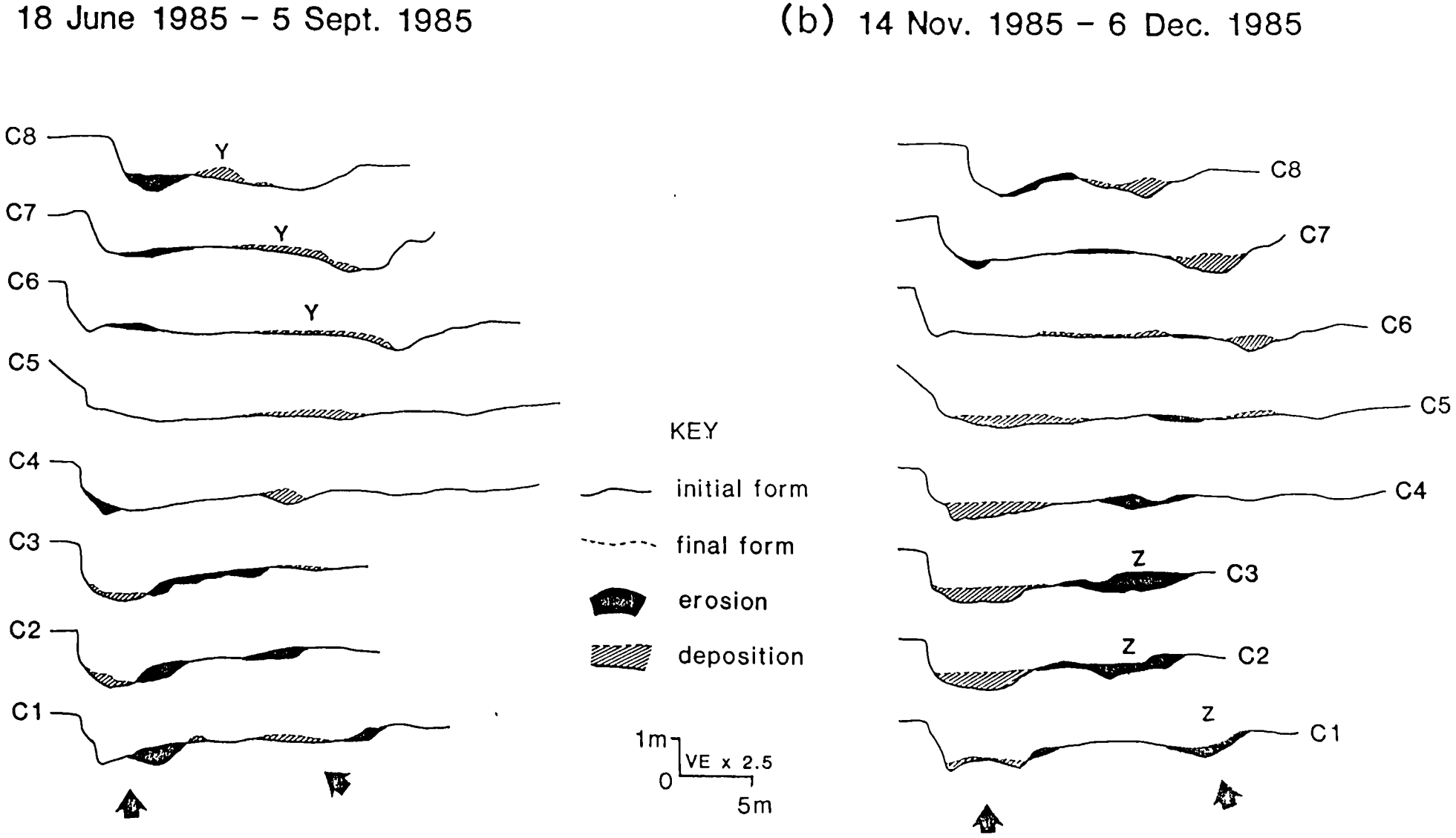

Fig. 5.22 Cross-sectional changes in the Feshie reach C from (a) 18.6.85 - 5.9.85, and (b) 14.11.85 - 6.12.85.

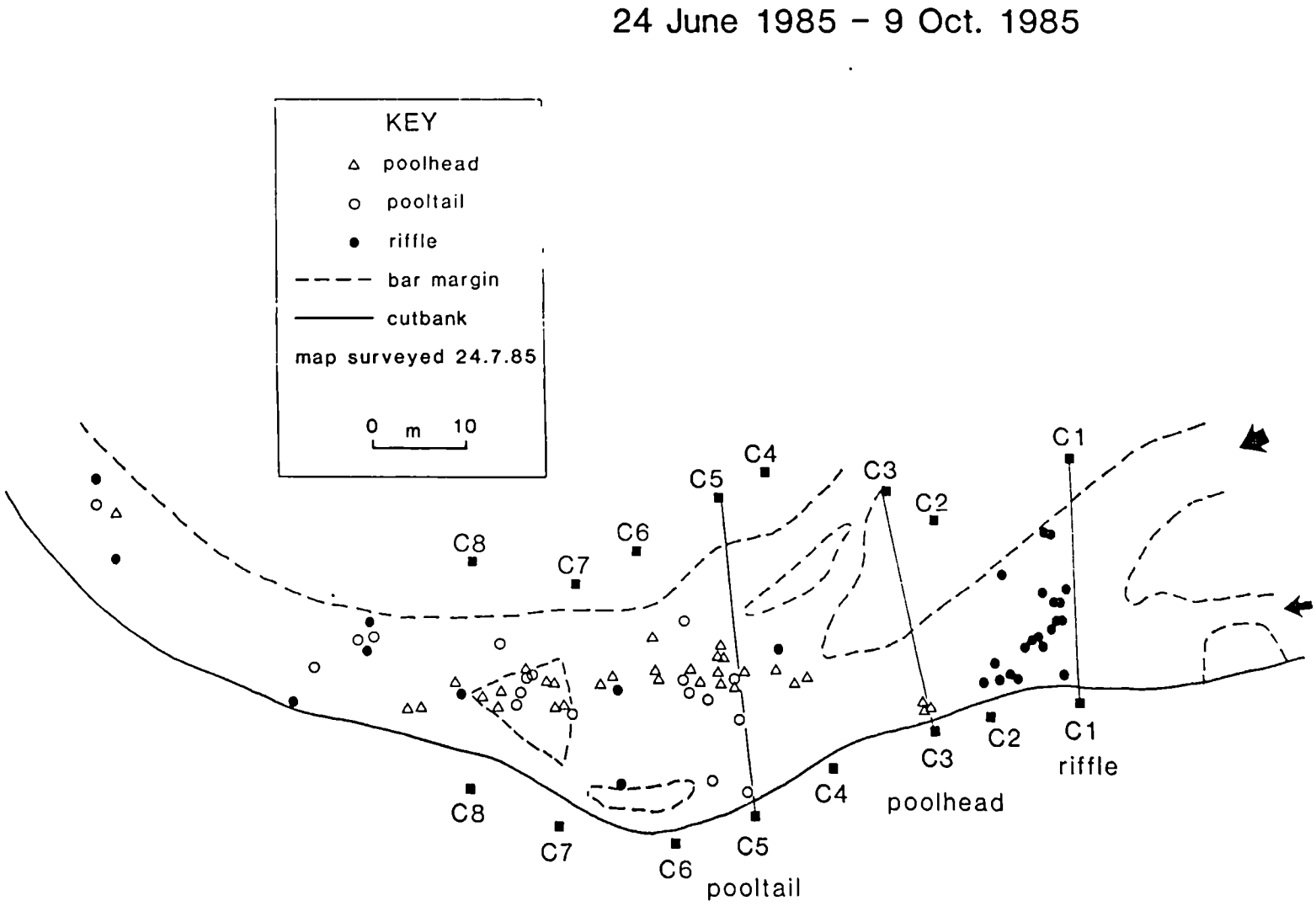

Fig. 5.23 Planimetric map of the Feshie reach C with the pebble tracer movements from the first Brewster experiment superimposed (after Brewster (1986)).

continuing over to the right of the channel between C4 and C7. There was aggradation of the medial bar (labelled Y) and lateral growth of its right margin with an increasing thickness of deposition towards the edge of the right-hand distributary. Figs. 5.24a-b show that this lateral advance of the bar's avalanche face was also accompanied by a downstream growth of the bartail with up to 35 cm of fresh material deposited along C8 (Fig. 5.22a). In addition to this widespread deposition all cross-sections except C5 also eroded some part of the channel. The bed scoured along the riffle at C1 and C3 and the avalanche face was dissected and retreated by about 3 m at C1. There was also scour of the left-hand channel around the medial bar with a deepening of 45 cm at C8. The overall pattern was of a general erosion of the riffle at the head of the reach, an infilling of the pool talweg, a broad strip of deposition building up the medial bar to its right, and an increasing dominance of the left-hand distributary around the bar.

The first of the two tracer experiments by Brewster (1986) covered the same period and highlighted the effect of the 1 September flood (Fig. 5.23). The riffle tracers (29% recovery rate) tended to move almost parallel to the C1 cross-section and deposit either a few metres downstream or in the far side of the deep pool. This is consistent with the aggradation on the top of the riffle at C1 and the deposition near the outer bank of the pool between C2 and C3 shown in Fig. 5.22a. The poolhead and pooltail tracers (recovery rates of 32 and 27% respectively) match the cross-sectional changes very closely indicating a strong divergence of flow as soon as the flow leaves the midpool at C4. The flow divergence is almost perpendicular to the long axis of the bar (and flow direction upstream) and continues down to the bartail beyond C8. It may be recalled that reach B of the Dubhaig also showed this tendency with the mid-channel bars aggrading as the flow diverged laterally across their long axes. The absence of any tracers in the left-hand channel between C7

Fig. 5.24 View from C8+ of the Feshie across the bartail of the mid-channel bar Y taken on (a) 18.6.85, and (b) 24.9.85. Note the downstream aggradation as a result of a large flood on 1.9.85.

and C8 supports the bed scour shown in Fig. 5.22a so that while the flow diverged to the right to build up the bar it must also have accelerated and concentrated its flow to the left.

Although there was no evidence of any overbank flow and little channel change from 5 September to 14 November the two pebble tracing experiments on the medial barhead and tail showed that sediment coarser than 22 mm could move by up to 73 m. The movement of different size fractions of the tracers was described in 4.6.2 (in both experiments the pebbles in the 32-45 mm class moved the furthest) but the mobility of the barhead compared to the bartail has not yet been discussed. Table 5.2 shows the percentage and mean distance of movement for the barhead and the three bartail locations. In both experiments the recovery rate was very high - 95% in the first and 70% in the second. Fig. 5.25 shows the depositional locations of pebbles after the 5 September to 9 October tracing period. The directions of movement for the barhead pebbles are added to indicate the approximate flow directions at or near the peak discharge (only eight bartail pebbles moved so their directions are not plotted).

Both Fig. 5.25 and Table 5.2 show that the barhead is much more mobile than the bartail. In the first experiment 40% of the barhead pebbles moved (but only a mean distance of 3.4 m) while in the second experiment 80% moved (a mean distance of 13 m). This greatly exceeds any of the pooltail pebble movements which in experiment two showed a clear decrease in mobility downstream for the pooltail sites (mean distances of movement of 4.1, 3.1, and 2.4 m for each successive site downstream). Field observations showed that the flow overtopped all of the bar (since many bartail tracer pebbles were covered by fresh gravel) so this difference in mobility cannot be explained by the lack of opportunity for entrainment. More likely the downstream increase in bar height (see Fig. 5.22a) leads to a decrease in the water depth and therefore flow strength (if the slope

Table 5.2 The movement of pebble tracers from the barhead and bartail of an active mid-channel bar, River Feshie.

Site	1st tracer experiment			2nd tracer experiment		
	No. pebbles	Mean distance moved m	% movement	No. pebbles	Mean distance moved m	% movement
Barhead	100	3.4	40	89	13	80
Bartail 1 *	50	0.41	6.0	50	4.1	36
Bartail 2	30	0.57	10	30	3.1	27
Bartail 3	20	0.43	10	20	2.4	17

* Bartail sites 1-3 in downstream order (see text for details).

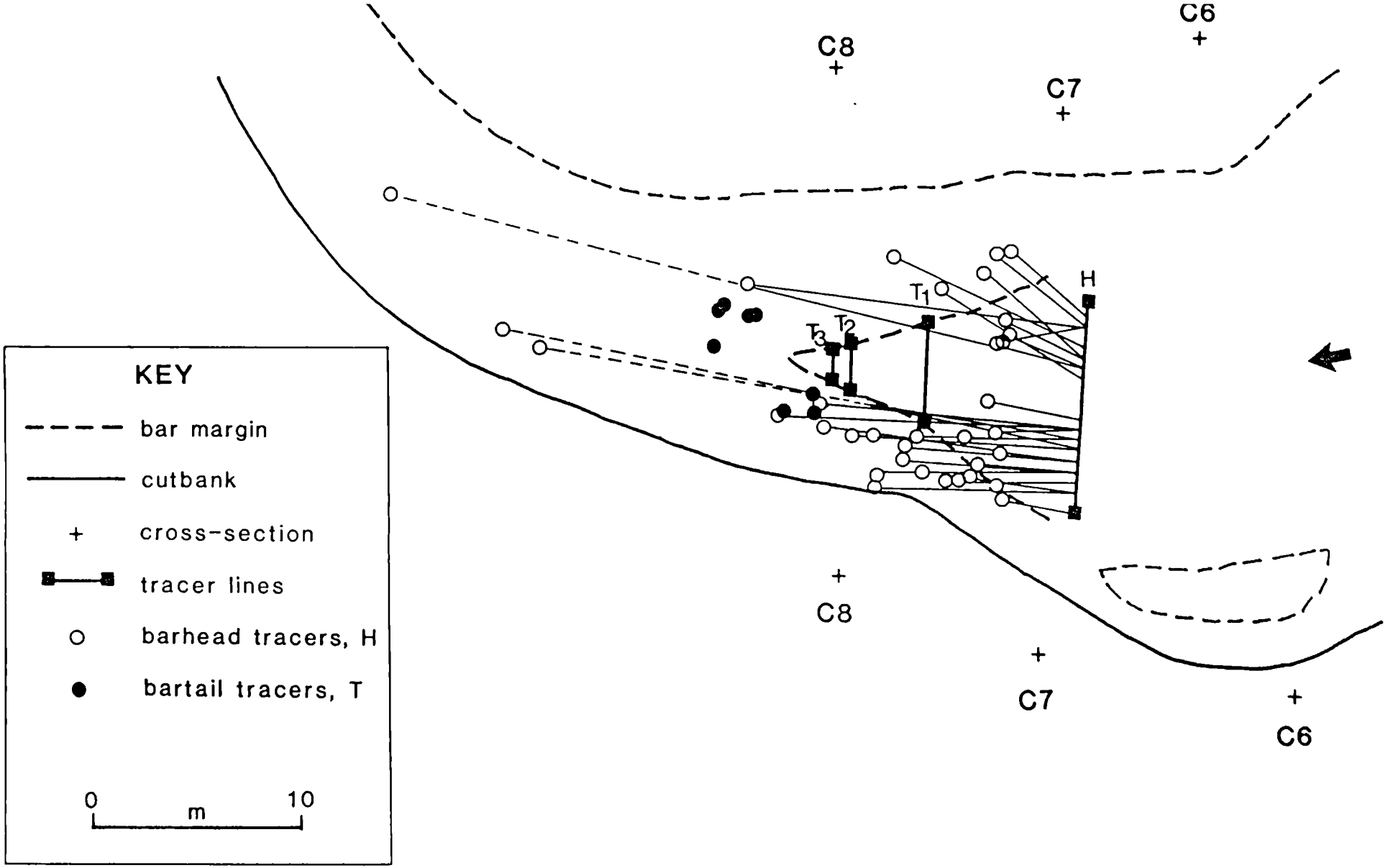

Fig. 5.25 Movements of tracer pebbles (in the first experiment) from the barhead and bartail of the mid-channel bar Y in reach C of the Feshie. Note the divergent depositional pattern of the barhead tracers and the small amount of movement from the bartail.

is assumed constant in the Du Boys equation) so that flow over the bartail is not as competent to move most sizes of material as flow over the barhead. The entrainment from the bartail is further restricted by burial under fresh sediment since the tail is a depositional zone.

The differences in mobility between the barhead and tail may seem predictable but what is interesting is that the barhead does not seem to be responsible for the growth and deposition of the bartail (using pebbles in the five most common phi classes of the bed material). Fig. 5.25 clearly shows that of all the pebbles that moved from the barhead (89% were recovered) none moved down to the bartail but instead diverged off the right and left bar edges. The second tracer experiment gave the same pattern (so is not plotted here) with only 7 (11%) of the re-located barhead tracers moving onto the bartail. Both of the experiments show that the barhead is mobile (and not a static feature as Leopold and Wolman (1957) suggest) and that at high discharges the flow diverges with an interchange of sediment at the barhead as material from upstream is deposited at the avalanche face and sediment is moved off the barhead into the adjacent channels. Fig. 5.23 showed that during a discharge of about 59 $m^3 s^{-1}$ this divergence can be very pronounced (and biased towards one side of the bar) but also that sediment from outside of the bar system can contribute to the growth of the bartail. This is important since the barhead/tail tracer experiments showed there was little scope for bartail development at discharges which just submerged the bar surface. The medial bar seems to be active at the barhead during moderate discharges but this does not lead to downstream bartail growth. Only at high (overbank) discharges does the bartail have the opportunity to advance with the majority of the sediment supplied from upstream and not as a result of the reworking of bar material. Much more work is needed to confirm these interpretations (particularly with pebble tracers at different discharges) but it does seem that the barhead and tail behave as

two separate subunits within the bar system.

The channel changes from 14/11/85 to 6/12/85 were much more dramatic as a result of the peak discharge estimated at 89 $m^3 s^{-1}$ in early December. During this flood the head of the right-hand distributary which contributes the main proportion of the flow to the study reach at C1 was blocked and infilled. This led to a switching of the flow to the east side of the floodplain (to feed reach B) and the study reach being abandoned and left dry. The cross-sectional changes shown in Fig. 5.22b show that before this there were extensive channel changes with 107 m^3 of new deposition compared to 67 m^3 of erosion. The former deep pool from C1 to C5 infilled with 58 m^3 of fresh sediment - up to 45 cm thick at C2. The barhead at C6 aggraded with a uniform layer about 10 cm thick and the right-hand channel around the medial bar repeated the depositional trend from upstream and infilled with up to 55 cm of sediment (at C7). This deposition was countered (and possibly assisted) by the formation of a new channel almost perpendicular to the riffle's former flow direction between C1 and C3. This new channel cut into the relict bar surface on the right-hand side and led to 50 cm of scour at C3 and a total of 49 m^3 of material being removed from C1-C3. Comparison of Figs. 5.26a-b taken before and after the December floods shows the formation of this new channel (labelled Z) and the widespread deposition in the former pool between C1 and C5. It is noteworthy that the former left-hand channel around the medial bar between C7 and C8 did not infill as the other main channels did but even scoured slightly at C7 and trimmed the bar at C8. The overall channel change however was a transformation to a much wider, flatter and more uniform channel geometry with the bar/pool/riffle irregularities smoothed out by selective erosion and deposition. This type of change is similar to the channel changes described for reaches A and B of the Lyngsdalselva in 5.4 which also resulted from an avulsion and an abandonment of the study reaches.

Fig. 5.26 View down reach C of the Feshie (a) on 14.7.85, and (b) on 19.3.86 after a major flood which created a new channel (Z) and eventually led to the abandonment of the study reach.

The direction of sediment movement during the early December floods is shown by the second Brewster (1986) tracer experiment plotted in Fig. 5.27. Although the pattern of tracer movement is not as clear as the earlier experiment (possibly due to the large-scale channel changes) there are still discernible trends. The riffle tracers at C1 (28% recovery) were mostly moved along the new channel cut across the former riffle's course and adjacent relict bar (Z). Only 8% of the poolhead pebbles were found (the rest presumably buried in the 40 cm of aggradation) mainly having travelled through the left-hand distributary around the medial bar which had not infilled during the flood. Of the 36% of the pooltail tracers recovered most either moved a few metres downstream in an evenly distributed zone of deposition (consistent with the bar aggradation at C6 in Fig. 5.22b) or moved out of the study reach and into the narrow single channel. This is the channel that eventually joins the downstream end of reach B as discussed in 5.3.1.

The overall flow pattern at high discharges inferred from the pebble tracer locations is not very clear. At some point during the flood the riffle at C1 must have been abandoned in favour of a more direct path down the right-hand side of the channel. The flow convergence through this new scour channel transported the riffle tracers down as far as C8 near the bartail. The pronounced divergence out of the pooltail at C5 appears to have been replaced by a weaker and more uniform divergence over the whole of the barhead. The left-hand distributary around the medial bar seems to have transported most of the pebbles that moved out of the reach whilst the right-hand distributary infilled and probably blocked any movement through its channel. The even distribution of pebble tracers (excluding the rapidly aggrading zones) is probably a reflection of the change in channel geometry to a more uniform topography.

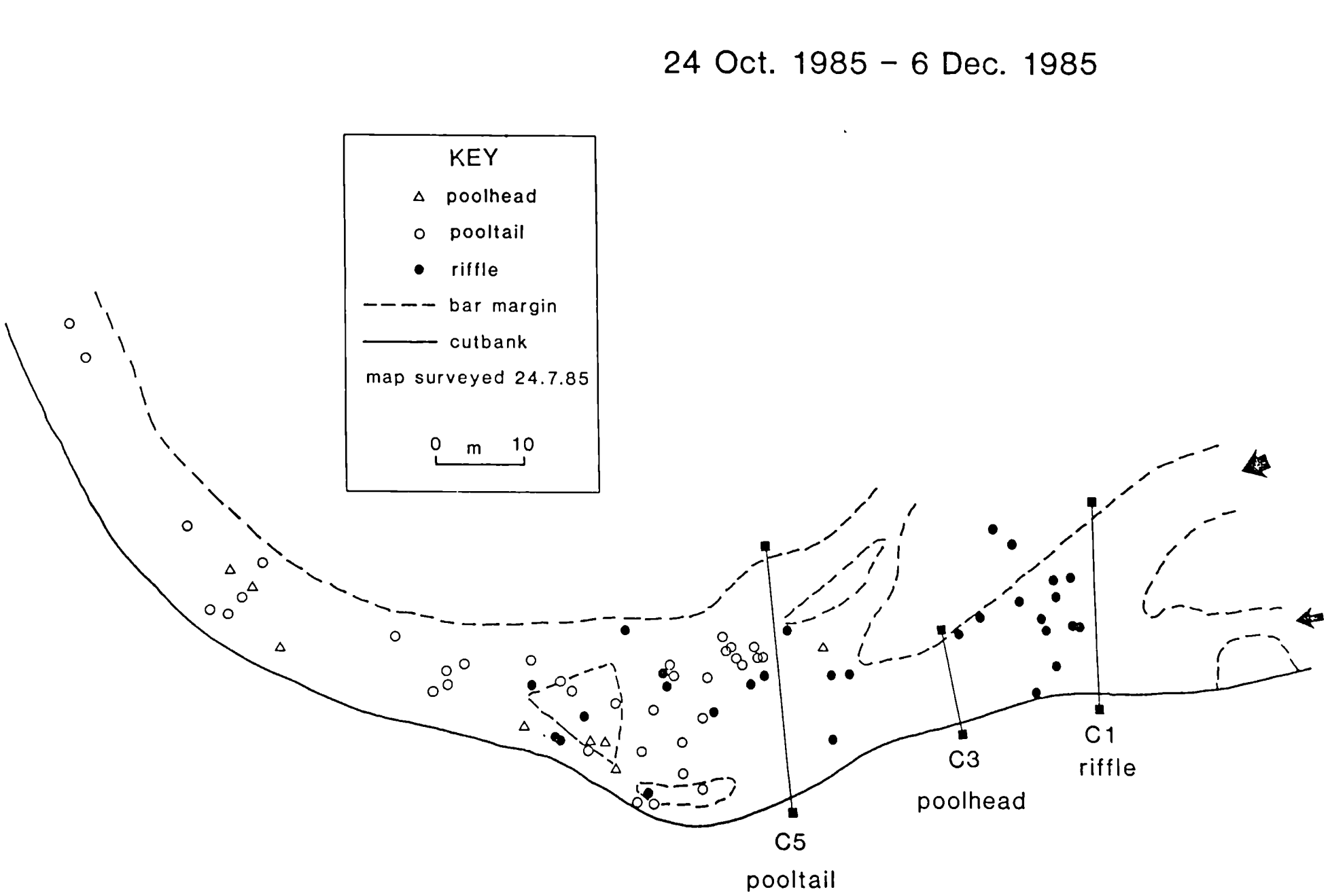

Fig. 5.27 Pebble tracer movements during the second Brewster experiment (after Brewster (1986)) in reach C of the Feshie.

Finally, although the flow patterns in reach C have been described for high flows using the positions of moved pebble tracers, the flow direction and strength was also measured at low and moderate discharges (previous to the 1 September flood). Fig. 5.28 shows the magnitude and direction of the near-bed velocities and shear stresses for discharges of 3 and 14 $m^3 s^{-1}$ respectively. At low flow the riffle (at C1) again has the strongest flow with a distinctive divergent pattern off its avalanche face into the pool. The gentle flow through the pool begins to diverge at the midpool at C4 and by C6 is flowing perpendicular to the channel and bank edges. This is an exaggerated form of the divergent pattern described earlier for the 1 September flood. At moderate discharges the flow direction remains roughly the same but as discussed in 3.3 the pool has a rapid rise in shear stress and exceeds the riffle stresses. The poolhead flows parallel to the steep left-hand bank edge with a decrease in shear stress towards the shallow right channel margin. At C4 the flow begins to diverge again with the strongest flow shifting to the right-hand side of the channel with shear stresses up to 60 $N m^{-2}$. This is in contrast to the weaker divergence to the left-hand side which reaches shear stresses of around 12 $N m^{-2}$. If the cross-sectional changes in Fig. 5.22a are recalled it was noted that whilst the bar aggraded along the entire length of its right-hand margin the left-hand channel trimmed the bar face and scoured its bed. Thus it seems that the strong flow off the right bar margin at low flow may be replaced by a much weaker divergence at high flow (which is possibly assisted by the clogging of the right-hand distributary). Similarly the gentle low flow channel to the left appears to become a much stronger convergent zone at high discharges. Such a reversal in convergent and divergent zones has already been mentioned in 5.2 and will be discussed at length in 5.4.

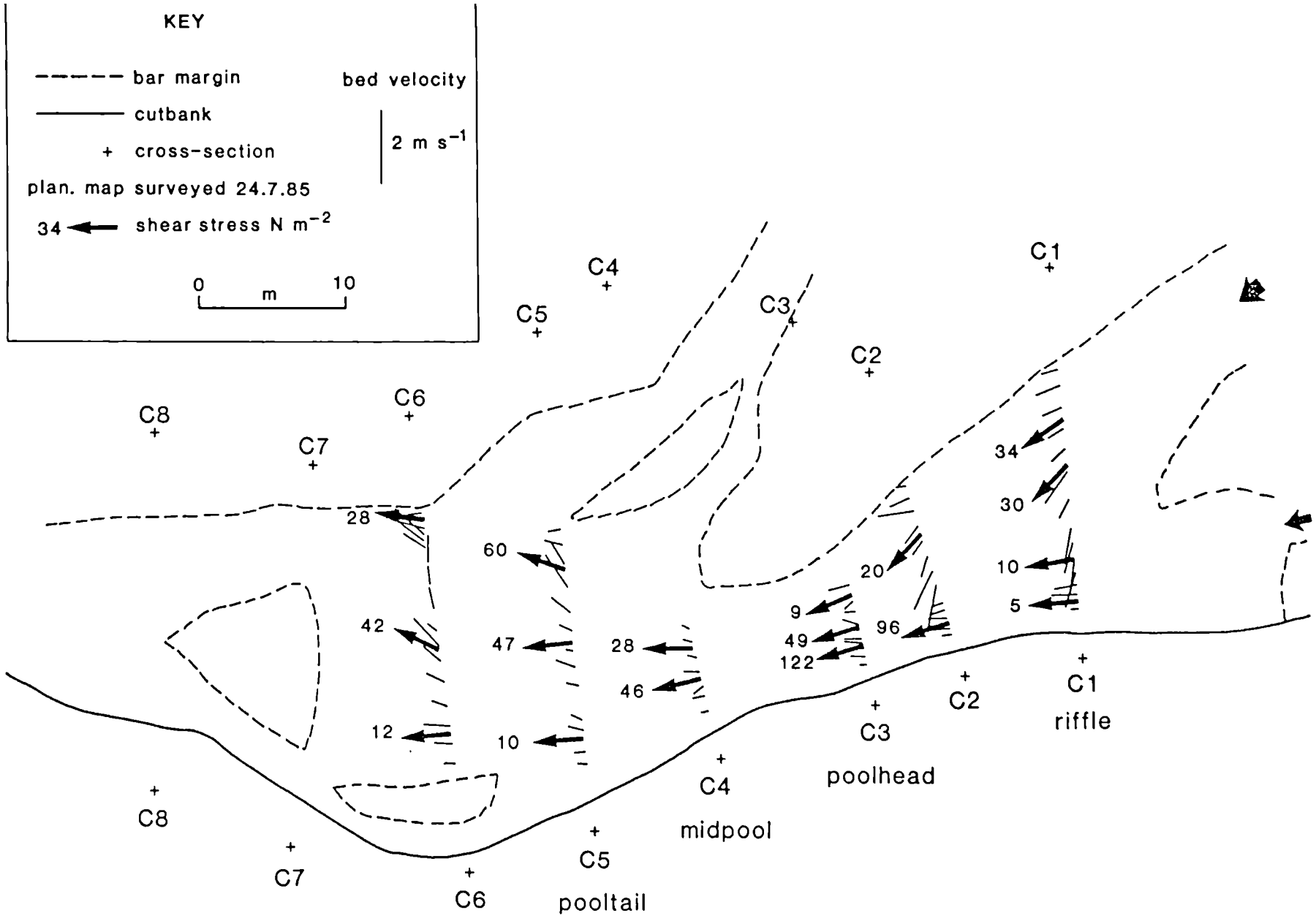

Fig. 5.28 Magnitude and direction of bed velocity at low flow (discharge about 3 $m^3 s^{-1}$) and shear stress during a moderate snowmelt discharge (about 14 $m^3 s^{-1}$) in reach C of the Feshie.

5.4.1 Measurement procedure

Reaches A-C of the Lyngsdalselva were briefly described in 2.1.4 and details of the Helley-Smith bedload catches and pebble tracing given in Chapter 4. In order to understand the channel changes during the five week study period the discharge variations described in 2.2.1 must be briefly recalled. The discharge varied from 1.3 $m^3 s^{-1}$ on 29 August to the only bankfull conditions following a rain storm on 7 August of 8.1 $m^3 s^{-1}$. The discharge varied little in late July (around 4.0 $m^3 s^{-1}$), was higher with more pronounced diurnal peaks (from about 5.0 to 7.0 $m^3 s^{-1}$) in early August, and after the peak flow on the night of 7/8 August progressively dropped to its minimum on 29 August at the end of the study period. As will be shown later the flood on 7/8 August led to an avulsion and abandonment of reaches A and B so that the discussion of their channel changes is restricted to the period of high meltwater flows and the even higher rainflood. Channel changes were surveyed more frequently in reach A (four times in the 12 day observation period) and since measurements of near-bed velocity, shear stress and bedload were also concentrated here the discussion of channel changes below relates mainly to reach A. Reach B showed changes which were similar in overall tendency to reach A but they were different in detail and magnitude. The new reach C set up after the avulsion was surveyed on 24 August but changed little in the low flows recorded for the end of the study period and is therefore not discussed.

Unlike the Dubhaig and Feshie channel changes described in 5.2 and 5.3 which were surveyed over long time periods, the Lyngsdalselva changes can be linked to each day's flow strength and pattern together with the variations in the transport rate of bedload through the reach. Although it was not feasible to obtain a complete set of interrelated hydraulic measurements for each day with high channel forming discharges, a comprehensive series of measurements were obtained in a wide range of flow

conditions. This enabled the reconstruction of the temporal and spatial differences in the flow strength and direction, and the size distribution and magnitude of bedload transport rates. Thus the Lyngsdalselva provides the opportunity to quantify both the processes (cause) and the changes (effect) resulting from each brief period of varying discharge.

The discussion below for reach A (where the detailed process measurements were taken) will begin with a description of the hydraulics and bedload, then outline the channel changes, and finally bring them together in a discussion of the cause-effect interrelationships operating in gravel-bed rivers. The analysis for reach B is confined to a description of the channel changes only.

5.4.2 Reach A

As mentioned above reaches A and B had three distinct periods with different flow conditions; the early moderate flows, the high meltwater discharges, and the rainflood. The moderate flows between 28 July and 3 August only led to slight channel change since the discharges were only high enough in the last two days for appreciable bedload transport to occur. The discussion below will therefore concentrate on the contrast between the high meltwater discharges and the rainflood on 7 August.

5.4.2.1 Hydraulics during high meltwater discharges

With an alternation along reach A between diverging, decelerating flow and converging, accelerating flow, the velocities and shear stresses estimated from velocity profiles varied in space as well as over time. Fig. 5.29 illustrates the pattern of near-bed velocities in reach A during a high meltwater discharge of 6 $m^3 s^{-1}$. The general appearance of the reach in these conditions is illustrated in Fig. 5.30a.

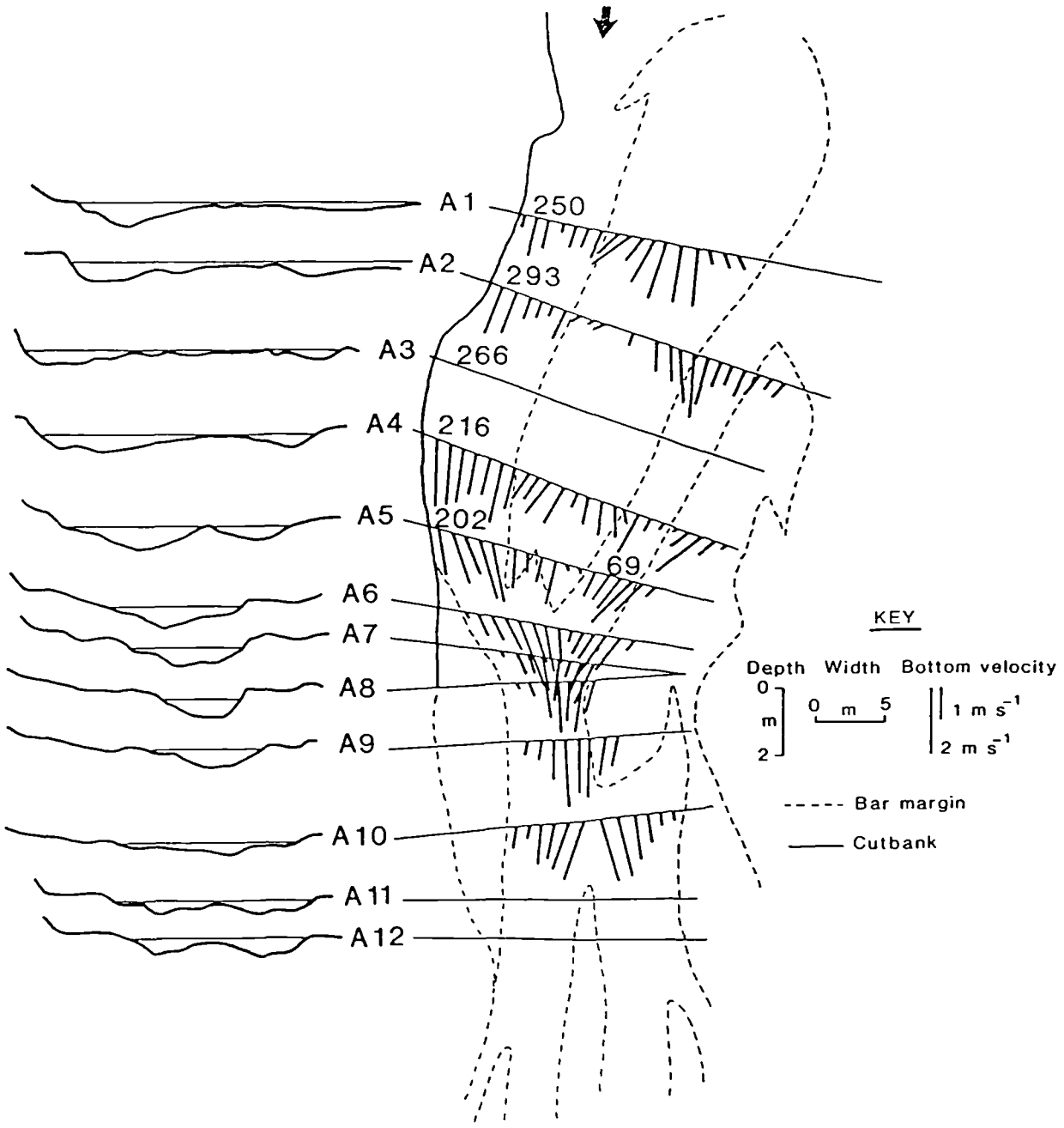

Fig. 5.29 Bed velocity map in reach A of the Lyngsdalselva during a high meltwater discharge on 6 August. Cross-sections are as surveyed the following day. Numbers by sections A1 and A5 indicate the shear stress (N m^{-2}) measured at the same discharge on a different day.

Fig. 5.30 Views of reach A of the Lyngsdalselva from true right end of A12 (a) during high meltwater flow on 6 August, river discharge about 6 m^3 s^{-1}, and (b) at peak of rainflood on night of 7/8 August, river discharge about 8 m^3 s^{-1}.

Two main zones of flow convergence are apparent. At the head of the reach the combination of divergence off the medial bar, and curvature of the main (true right) channel, gave a skewing and acceleration of flow from section A1 to A4 where both velocity and depth reached maxima (2.0 m s^{-1} and 50 cm) near the outer bank, before decreasing slightly through the more riffle-like sections at A5 and A6. The confluence of the smaller true left channel at A7-A9 caused a second convergence of flow with velocity and depth increasing to 2.0 m s^{-1} and 70 cm, before decreasing again beyond A10 as the channel divided around the next medial bar, a situation much like A1 again.

As mentioned in 2.2.2 the velocity map of Fig. 5.29 is also a guide to the spatial distribution of shear stress if the vertical velocity profiles are logarithmic and roughness height is constant. Velocity profiles along the talweg at A1-A5 showed consistently high shear stresses (greater than 200 N m^{-2} at each section, with standard errors from 35 to 110 N m^{-2}) with a slight downstream increase as far as A3 then a decrease past A4 to A5 (Fig. 5.29). The smaller and slower left-hand distributary had a much lower shear stress (69 $\pm$ 6 N m^{-2}) as expected. The shear stress at the A8-A9 confluence was probably higher still but wading was impossible.

5.4.2.2 Hydraulics during a rainflood

The river rose to the highest level of the summer on the night of 7 August following intense rain at the end of a day of high meltwater flow. As the stage rose in reach A (Fig. 5.30b) the flow became less confined within the non-uniform channel and began to overtop first the bar alongside the confluence (A8-A9 in Fig. 5.29, near right in Fig. 5.30b), then the medial bar in the upper part of the reach (A1-A5 in Fig. 5.29, mid/right background in Fig. 5.30b), and finally the lowest points of the true right

floodplain (A7-A9, left foreground in Fig. 5.30b). Velocity mapping was not feasible, but the drowning out of the A8-A9 confluence must have reduced the degree of convergence here and once the A1-A5 medial bar was overtopped the pattern of surface currents suggested that convergence in the head of the main channel had been replaced by a less pronounced divergence over the bar. This is supported by velocity profiles measured in the right bank talweg which gave shear stress estimates of 364 ± 59 N m^{-2} at A1, dropping to only 198 ± 7 N m^{-2} at A3 where depth and velocity were also lower.

Flow deceleration in this area was compounded by the rapid channel changes taking place during the flood (see later). Erosion of the right bank widened the channel to a progressively greater extent downstream from A1, causing surface divergence that was reinforced by medial bar deposition centred on A7. At the peak of the flood the main current at A5 was switching from side to side of this new bar. Velocity profiles in the right-hand channel at different times gave shear stresses of 319 N m^{-2} and 81 ± 21 N m^{-2}, the latter at a time when the main current was on the other side of the bar with a shear stress estimated at 406 ± 59 N m^{-2}.

Further down the reach no velocity profiles were measured but some evidence on flow patterns was gained from the positions in which painted pebbles were found after being thrown in at section A1 at the peak of the flood (see map in 4.6.4). Those that travelled out of the reach all appeared to have moved through the left-hand distributary at A11-A12, before being deposited to form a new bar further left.

5.4.2.3 Bedload transport

The spatial and temporal variations in bedload transport rate in reach A are also important for understanding the channel changes discussed later.

Observed spatial differences in transport rates can mostly be explained by differences in flow strength, though not just in a simple proportional way.

Bedload sampling at the same times and places in reach A as the shear stress measurements mapped in Fig. 5.29 revealed a rise in the transport rate of sand plus gravel from about 0.16 kg m^{-1} s^{-1} at A1 to 0.24 at A2 and 0.31 at A3, then a fall to 0.20 at A4 and 0.08 kg m^{-1} s^{-1} at A5. Unreplicated samples such as these are not very reliable but the rising and falling trend is the same as that of shear stress, only more pronounced. This is consistent with a cumulative addition of sediment entrained from the bed between A1 and A3 to the load entering the reach at A1, then deposition as shear stress falls from A3 to A4 to A5. The lower shear stress in the smaller left-hand distributary at A5 was accompanied as expected by a very low transport rate, 0.01 kg m^{-1} s^{-1}, and the bedload here was mainly sand whereas that at A1-A3 was predominantly, and at A4 and A5 mainly, gravel.

During the August 7-8 rainflood, when as already noted the downstream trend of shear stress was radically different with a big fall from A1 to A3 and fluctuating conditions at A5, transport rates again correlated reasonably closely with flow strength. Replicate samples at A1 indicated 2.3 and 3.5 kg m^{-1} s^{-1} of mainly cobble-sized bedload, whereas those at A3 were lower at 0.8 and 0.5 kg m^{-1} s^{-1}, again predominantly cobbles. Three samples at A5 gave a transport rate of about 0.8 kg m^{-1} s^{-1} at the highest shear stress and 0.3 kg m^{-1} s^{-1} at two other times, with a higher proportion of sand (40-60 %) than at A1 and A3.

5.4.2.4 Channel changes during high meltwater discharges

Over the four days of high meltwater discharge between 4 and 7 August

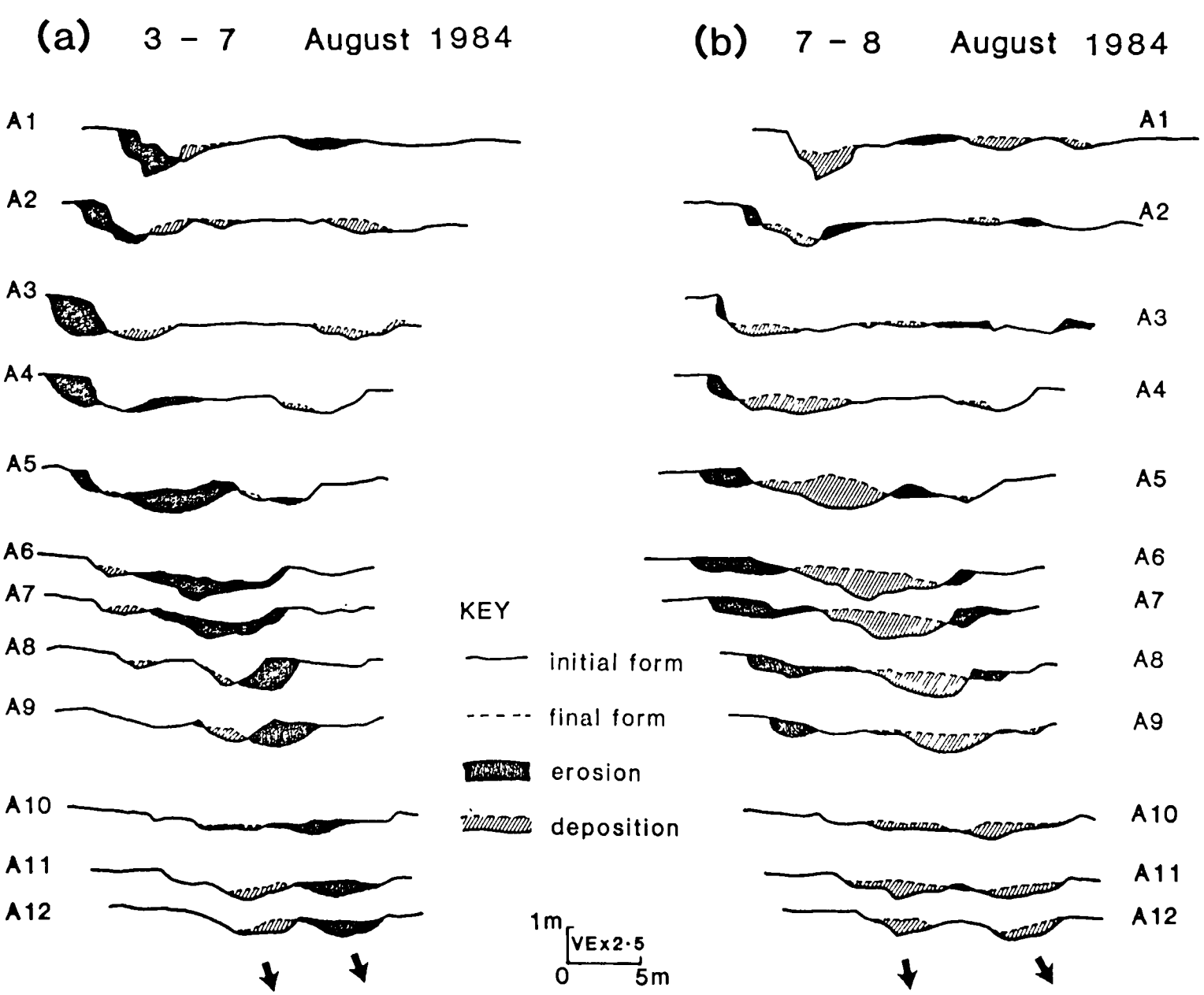

Fig. 5.31 Cross-sectional changes in reach A of the Lyngsdalselva during (a) a period of high meltwater flows (3-7 August), and (b) a high rainflood (7-8 August).

there was considerable erosion and deposition as shown in Fig. 5.31a. The general pattern was one of lateral erosion and scour in the two zones of flow convergence demonstrated by velocity mapping (Fig. 5.29), one along the right bank of sections A1-A4 and the other diagonally from A5 through the A8/A9 confluence and beyond. Lateral erosion of up to 3 m in both zones, but in the opposite directions, caused an increase in talweg sinuosity. The channel deepened in both zones, but this lateral and vertical erosion was partly offset by deposition in areas of lower velocity and shear stress: on the inside of the migrating upper main channel, downstream of its eroding bank, and in the lower-discharge distributaries at both ends of the reach. Application of the prism formula between successive cross-sections indicated a total of 139 m^3 of erosion from the 55 m long reach with only 40 m^3 of deposition.

5.4.2.5 Channel changes during the rainflood and discussion

Changes during the overnight flood on August 7-8 were even more dramatic (Figs. 5.31b and 5.32a-b). Even before the peak of the flood the steep outer banks at A1-A6 were visibly eroding by frequent small-scale collapse and the rumble of bedload was clearly audible. Measurements during the flood and a re-survey the following day showed bank retreat of up to 6 m (Fig. 5.31b), nearly all of it in a four hour period. The sediment thus mobilised together with the considerable input from upstream of A1 began to form a new medial bar which was first visible at A7 (Fig. 5.32a), though the maximum depth of aggradation (1.0 m) was at A5. Subsequent bulk sampling revealed particularly coarse sediments, with a surface median diameter of 83 mm. Deflection of flow around both sides of this growing bar undoubtedly explains why erosion of both the right and left banks was greatest at A5-A8, and the medial deposition itself is consistent with the previously discussed fall in shear stress and bedload transport rate from A1 to A3. The whole process is reminiscent of the

Fig. 5.32 Effects of the 7-8 August flood in reach A of the Lyngsdalselva (a) view downstream from A1 at flood peak showing new medial bar emerging at A7, and (b) view upstream from A12 the following morning showing abandonment of reach after avulsion and bank retreat compared to Figs. 5.30a and b.

initial stages of Leopold and Wolman's (1957) laboratory example of braid development.

Meanwhile, channel changes further upstream were leading to a progressive avulsion of the main flow away from reach A, which 12 hours later was almost dry (Fig. 5.32b) so that the subsequent re-survey of cross sections gave an unambiguous measure of the effects of the flood. It indicated 56 m^3 of lateral erosion, but this was far exceeded by 144 m^3 of deposition along the central strip.

This is quantitatively almost the opposite of what had happened during the preceding four days of high meltwater flows, and the spatial pattern of erosion and deposition was likewise reversed (Fig. 5.33). During high meltwater flows the river was only locally competent to move coarse bed material, in discrete zones of locally high shear stress, so that selective scour (and associated deposition elsewhere) maintained a non-uniform channel geometry characterised by narrow chutes. During the rainflood, in contrast, the river was competent everywhere but the abundant supply of coarse sediment from upstream and from rapid bank erosion within the reach evidently led to overloading, triggered by what was now a downstream decrease in shear stress given the different pattern of flow convergence and divergence at the higher discharge. This overloading led to the deposition of a coarse medial bar which grew by headwards accretion and in turn deflected the main current to cause even more bank erosion than was already under way as a direct result of the increase in discharge. The outcome of these changes was a transformation to a wider, shallower, and more uniform channel containing a new, low relief medial bar.

Whether this reversal of response is site-specific or more widely applicable is unclear. Certainly some of the observations in the Dubhaig

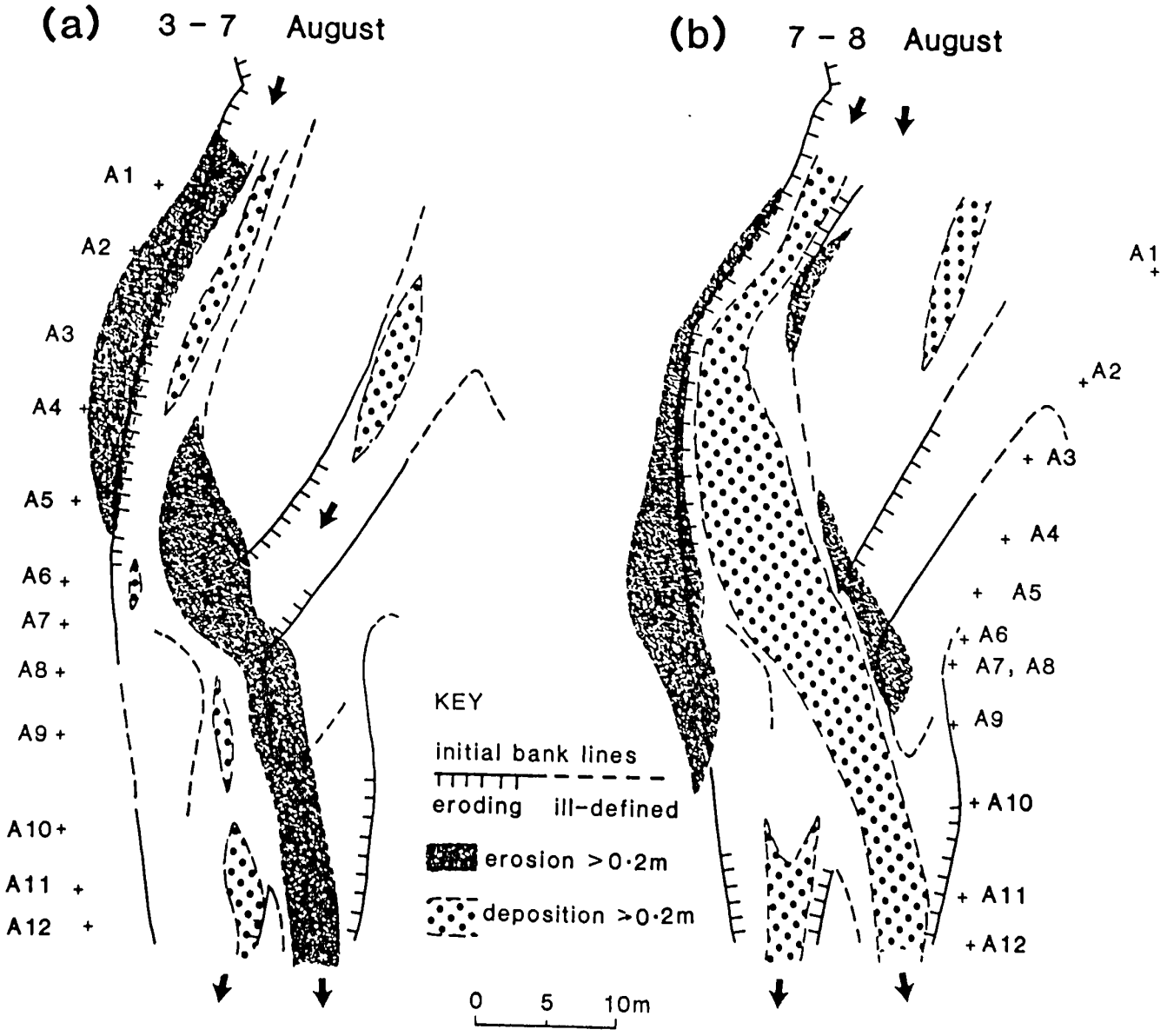

Fig. 5.33 Spatial pattern of erosion and deposition in reach A of the Lyngsdalselva during (a) high meltwater flows (3-7 August), and b) higher rainflood 7-8 August.

and Feshie described in 5.2 and 5.3 (but in most cases using pebble tracers and imbrication directions after the event) point towards a change in flow pattern from low to high stage. It is reminiscent of the tendency noted by Andrews (1982) for sustained overbank snowmelt flows in the meandering East Fork river to even out spatial variations in channel width, but the two rivers differ greatly in character and in the present case the aggrading tendency was probably assisted by the gradual avulsion away from reach A, and indeed the overall downstream decrease in slope and increase in total channel width at the head of the braidplain. Furthermore the Lyngsdalselva results do not fully bear out Cheetham's (1979) suggestion that distributaries become bedload bottlenecks in high flows, for in reach A there was aggradation in the undivided A7-A9 confluence as well as the A1-A6 distributary (similar to the Feshie reach C avulsion in December 1985 during which one distributary scoured even though the other filled).

5.4.3 Reach B

The 12 cross-sections in reach B were surveyed on three occasions and their changes are shown in Figs. 5.34a-b. The surveying data from 9 August for sections B1-B3 is unavailable and so comparisons can only be made for sections B4-B12 (although B1-B3 are plotted in Fig. 5.34a). Unfortunately the times of surveying did not coincide exactly with the changes in river discharge (as in reach A) and Figs. 5.34a-b represent a slight overlap in discharge conditions.

The moderate and high meltwater discharges up to the 5 August led to almost equal amounts of deposition and erosion between sections B4 and B12 (28 and 31 m^3 of change respectively). As in reach A the erosion led to an increase in talweg sinuosity with the bank edge from B3-B4 and B9-B11, and the bar avalanche face on the opposite side of the channel between B6

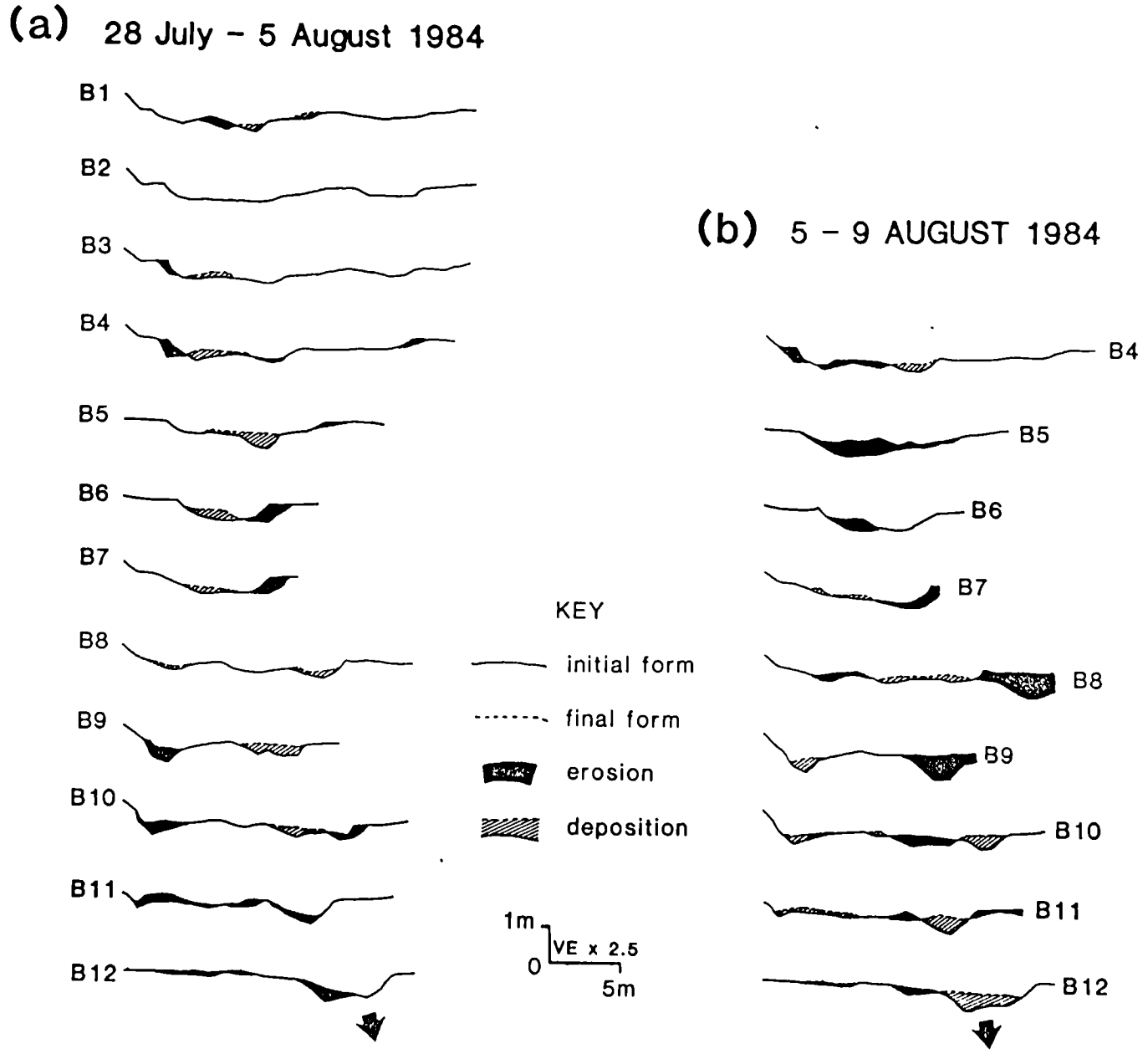

Fig. 5.34 Cross-sectional changes in the Lyngsdalselva reach B during (a) high meltwater discharges (28 July - 5 August), and (b) the rainflood (5-9 August).

and B7 all retreating (by up to 2.0 m at B6). Despite this lateral erosion there was little channel scour and only sections B9-B12 eroded their channel bed. The depositional locations matched the lateral erosion and served to accentuate the increase in talweg sinuosity. Between B3 and B10 the parts of the channel opposite the erosion aggraded by up to 45 cm (at B5). The only exception to this trend was at B11 and B12 where the cross-sections scoured along most of their lengths.

The further two days of high meltwater discharges and the rainflood in the evening of 7 August led to an almost complete opposite pattern of deposition and erosion. Although the net reach total of channel change showed over twice as much erosion as deposition (71 m^3 compared to 31 m^3) there was a good correlation between the locations of change in the rainflood and the opposite mode of change shown by the previous survey (compare Figs. 5.34a and b). Previous areas of deposition were replaced by extensive channel scour (B5-B10) with 2.5 m^2 of material removed from the bar at the left end of B8 and a maximum of 65 cm of scour (and 2.4 m^2 of erosion) at B9. Although the bank continued to erode at B4 (by 1.2 m) the bank erosion at B9-B11 ceased and was replaced by an infilling of the channel and a building of a side bar skirting the channel margin. Sections B10-B12 also infilled with up to 50 cm of aggradation in the centre of the channel at B12. The combination of all this erosion and deposition led to reach B assuming a much wider, flatter, and more uniform channel geometry.

The overall pattern of channel change between 28 July and 8 August (the reach was abandoned after this) bears a striking resemblance to the changes observed in reach A. The initial increase in talweg sinuosity during the meltwater discharges, the reversal in the mode of channel change during the rainflood, and the resulting uniform channel geometry all support the measurements and observations discussed for reach A in

5.4.2. It seems likely therefore that as in reach A the channel changes in reach B can be explained by a cross-over in the flow pattern with an interchange of the convergent and divergent flow zones with increasing discharge.

5.4.4 Planimetric changes

Channel pattern changes in the wider study area are illustrated in Fig. 5.35. Comparison of the maps shows that the flood of August 7-8 left intact many of the larger bar fragments in the central and downstream part of the area, though not without erosional trimming and dissection by chutes. But in the entrance to the braidplain, on its southern margin (including reaches A and B) where the main flow was concentrated before the flood, and on the northern margin (including reach C) which took over as the main channel system after the flood, very few bars are recognisable in both maps. Changes of the magnitude described for reaches A and B appear to have been widespread with the creation of new bars, choking of existing channels, and rapid retreat of eroding banks - by up to 24 m on parts of the northern margin. Almost all these changes took place during the flood with no detectable scour or fill in reaches A, B, and C over the following two weeks, although some local reorganisation took place along the new northern channels in the first few days after the flood.

5.5 Comparison between rivers and reaches

As stated in 1.3 one of the principal objectives of this study was to compare the channel processes and changes in several different channel patterns. The five reaches in the Dubhaig, two in the Feshie, and three in the Lyngsdalselva were chosen to represent a continuum from straight to braided river types. These rivers have contrasting discharge regimes and provide a broad range of channel forms and sizes with different rates and

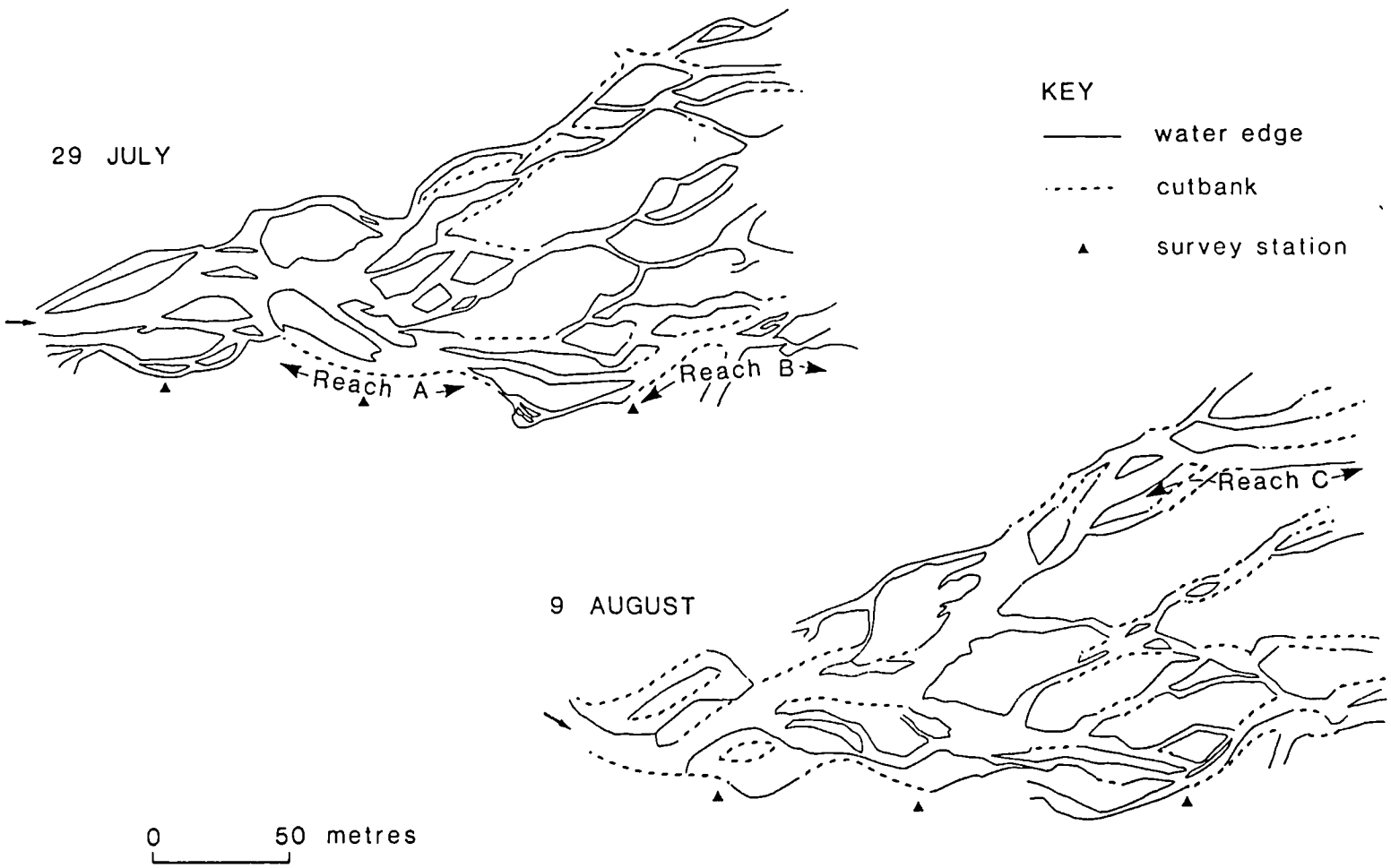

Fig. 5.35 Planimetric map of study area before and after the August 7-8 flood and avulsion. Bulk of river discharge was through reaches A and B initially, but reach C after the avulsion.

magnitudes of activity. So far Chapters 3-5 have only compared and discussed the differences between river and reaches in specific topic areas (for example 3.4, 4.5, and 5.4.2.5) and an overall comparison is still required. The discussion below looks at two subject areas that were quantified in most of the reaches (allowing comparisons) but which also have implications for channel change. These are (1) the rate of channel change and bank retreat (measured from cross-sections), and (2) the rate and distance of bedload movement (measured from Helley-Smith sampling and pebble tracing).

5.5.1 Rates of channel change

Sections 5.2-5.4 described the mode of channel change in the Dubhaig, Feshie, and Lyngsdalselva and briefly discussed the magnitude of sediment movement through each reach (measured using the digitised areas of change and the prism formula). Table 5.3 summarises the volumetric calculations of channel change averaged over the measurement period (expressed as the amount of change in the reach, per metre stream length, per year, to enable comparisons to be made between different reaches and surveying time periods). Unfortunately the results in Table 5.3 are not always averaged over a long time span partly because some reaches were abandoned (for example reaches A and B of the Lyngsdalselva and C of the Feshie), or because measurements were only taken over a specific period (for example reach B of the Feshie in the snowmelt season). In the cases of the reaches that were abandoned the rates of channel change shown in Table 5.3 are undoubtedly exaggerated when they are expressed as an annual rate of change. Indeed it is not unreasonable to argue that the modification of the channel geometry prior to abandonment may be the only channel change that the reach experiences in a year. Table 5.3 therefore shows both the minimum and maximum (in brackets) rates of channel change, though the former is preferred and will be used in the comparisons and discussion

Table 5.3 Digitised volumetric rates of channel change for the nine reaches of the Dubhaig, Feshie, and Lyngsdalselva.

River/ reach	Reach length m	Surveying period days	Total reach volumetric erosion m^3	Total reach volumetric deposition m^3	Annual** rate of erosion/ stream length $m^3 m^{-1} yr^{-1}$	Annual** rate of deposition/ stream length $m\ m^{-1} yr^{-1}$	Peak shear stress at bankfull $N\ m^{-2}$
Dubhaig							
A	70	636	127	61	1.0	0.50	217
B	90	610	206	232	1.4	1.5	131
C	34	565	27	7.3	0.51	0.14	111
D	72	536	63	77	0.60	0.73	61
E	60	535	4.4	6.0	0.050	0.068	58
Feshie							
B	100	77	112	102	(5.3) 1.1	(4.8) 1.0	82
C	64	246	113	162	(2.6) 1.7	(3.8) 2.5	NA
Lyngsdal'							
A	55	10	202	187	(134) 3.7	(124) 3.4	407
B*	55	11	101	59	(61) 1.8	(36) 1.1	NA

* Sections B4-B12 only

** The figure in brackets assumes that the rate of change continues throughout the year (the minimum rate of change assuming no other change for the rest of the year is given below this figure).

NA = No shear stress data available

below.

The annual rate of erosion or deposition per metre stream length ($m^3\ m^{-1}\ y^{-1}$) in Table 5.3 gives a good indication of the differences in rates of channel change between reaches and rivers. As expected the divided channel patterns of the Lyngsdalselva and Feshie have the highest rates of channel change. This can be explained by the high stream powers associated with these patterns (Ferguson 1981) and the widespread availability of sediment from the uncohesive banks (which usually consist of relict bars incorporated into the floodplain) and numerous bars. Table 5.3 also shows the peak shear stress measurements taken in the three rivers (and five reaches for the Dubhaig) at bankfull discharge. The highest shear stress value of the nine reaches was measured in reach A of the Lyngsdalselva during the bankfull rainflood on 7/8 August. The peak shear stress was 406 $N\ m^{-2}$, but shear stresses of 319 and 364 $N\ m^{-2}$ were also measured at different times during the flood. This compares with the Feshie reach B maximum shear stress at bankfull of 82 $N\ m^{-2}$ and the Dubhaig reaches A-E (extrapolated using the mean reach values from ratings of shear stress and discharge shown in 3.2) of 217, 131, 111, 61, and 58 $N\ m^{-2}$ respectively. The Feshie reach B peak shear stress is surprisingly low (it was replicated three times) but is consistent with the low transport rates measured immediately after the velocity profiles (see Table 5.1 and the discussion in 5.5.2). Given the within-reach spatial variations in shear stress and the differences in channel geometry and bed grain size the shear stresses at bankfull discharge in Table 5.3 are only general guidelines to the variations in hydraulics between reaches. Despite this the Lyngsdalselva shear stresses indicate that it is probably the most competent of the three rivers at bankfull discharge. This will be elaborated in 5.5.2.

The downstream decrease in peak bankfull shear stress shown in Table 5.3

for reaches A-E of the Dubhaig helps to explain the differences in channel pattern described in 5.2. As Fig. 2.3 showed there is a rapid decrease in channel gradient from 0.021 at reach A to 0.004 at reach E which accounts for the change from braided to straight channel pattern over the 2 km. The magnitude of shear stress is related to this slope change which in turn affects the rate of channel change and indirectly the channel pattern. Table 5.3 shows that the hierarchy in shear stress at bankfull discharge is generally matched by the rate of channel change. The moderately braided reaches A and B have the highest rates of channel change (taken as the sum of the erosion and deposition rates) with reach B moving sediment at rates similar to the Feshie reach B (it is more braided than reach A as shown by comparing Figs. 5.2 and 5.6). As noted in 5.2.4 the transitional channel pattern of reach C does not change its channel geometry significantly (due to the lack of bank erosion and aggradation of the mid-channel bars) and therefore measures a lower rate of change compared to the fully meandering form of reach D. Reach E is comparatively inactive with rates of change about a magnitude less than reaches A-D.

As well as expressing the rate of channel change in terms of volumetric erosion or deposition per reach, the rate of bank erosion (either from digitised volumes or lateral measurements) can be used to distinguish between different rates of activity of channel patterns. Table 5.4 shows the annual rates of bank erosion for the nine reaches expressed in three ways: volume removed per stream length, mean bank retreat per section, and maximum for the reach (measured from cross-section surveys). Bank erosion was defined as being the retreat of the floodplain (not erosion of the avalanche faces of channel bars), so that in the cases of reaches A and B of the Lyngsdalselva and B of the Feshie, the bank erosion was only calculated for one of the channel banks (usually steep, well defined, and partly vegetated). Again the extrapolation of rates of change from one or

Table 5.4 Volumetric and lateral rates of bank erosion for the nine reaches of the Dubhaig, Feshie, and Lyngsdalselva.

River/ reach	Drainage area km^2	Total Reach volumetric bank erosion m^3	** Annual volumetric bank erosion/ stream length $m^3 m^{-1} yr^{-1}$	*** Total reach bank erosion m	** Mean Annual bank erosion/ section $m\ yr^{-1}$	** Maximum annual bank erosion $m\ yr^{-1}$
Dubhaig						
A	14	0	0	0	0	0
B	15	30	0.20	3.7	0.32	1.8
C	15	0	0	0	0	0
D	16	53	0.50	3.8	0.32	0.75
E	17	0	0	0	0	0
Feshie						
B	107	100	(4.7) 1.0	7.5	(5.1) 1.1	(11) 2.3
C	107	0	0	0	0	0
Lyngsdal'						
A	23	96	(64) 1.7	29	(88) 2.4	(237) 6.5
B*	23	3.5	(2.1) 0.064	2.5	(9.2) 0.28	(58) 1.8

* Sections B4-B12 only

** The figure in brackets assumes that the rate of change continues throughout the year (the minimum rate of change assuming no other change for the rest of the year is given below this figure).

*** Total bank erosion from all sections in the study period

two floods to an annual rate can give unrealistic results (for example see Lyngsdalselva reach A in Table 5.4), so the minimum rate of bank erosion is used for comparisons between reaches.

Table 5.4 shows that the channels in reaches A, C, and E of the Dubhaig and C of the Feshie did not move laterally. This can be explained by the nature of the bank material and the flow pattern. In the cases of reaches A and C there is negligible bank erosion because the main current does not flow directly into the banks. This is particularly true for reach C where the outer bank is protected by two mid-channel bars and the main flow moves down a chute on the inner part of the channel (see 5.2.4). In addition all reaches of the Dubhaig have well vegetated stable banks which if attacked by the flow often collapse as large turf blocks. In reach A the turf blocks tend to drape over the bank edge whilst in reach C they fall into the deep pool and lie as immobile obstructions protecting the foot of the bank from any further erosion. During the study period the position and morphology of these turf blocks was scarcely modified. In reach E there is no distinct convergence/divergence cycle (see 5.2.6) and this together with the low stream gradient (and therefore power, velocity, and shear stress) means that the banks are rarely attacked.

The stability of the left-hand bank of the Feshie reach C is more surprising since it had retreated at a rate of 7 m yr^{-1} in the past (Ferguson and Werritty 1983) and consists of uncohesive gravels capped by vegetation that readily collapse even when stood on. Despite the high rate of channel change shown in Table 5.3 the flow pattern at high discharges must have concentrated on reworking the bed material via the convergent/divergent cycle discussed in 5.3.2 rather than widening the channel.

For the reaches that did have some bank erosion Table 5.4 shows the

differences in rates of retreat between channel patterns. In the Dubhaig the moderately braided reach B had an equivalent rate of bank erosion to the meandering reach D showing that single channels can be just as efficient at shifting their channel positions as divided channels. Surprisingly both reaches B and D had rates of bank retreat marginally greater than reach B of the Lyngsdalselva but the high rates of erosion and deposition in Table 5.3 and the discussion of channel changes in 5.4.3 show that the flow in reach B of the Lyngsdalselva must have concentrated on the reworking of the within-channel bars rather than eroding the outer bank. There is a progressive increase in the rate of bank erosion from the more active reach B of the Feshie to the Lyngsdalselva - which had a maximum bank retreat of 6.5 m during a flood (see 5.4.2.5).

The annual bank erosion per section and maximum bank erosion in each reach can be compared to the compilation of erosion rates from 42 rivers by Hooke (1980). As Hooke (1980) notes her plot of rate of erosion (m yr^{-1}) against drainage area is complicated by the different methods of calculation and terms representing bank erosion reported in published works. Her plot therefore incorporates a mixture of mean and maximum erosion rates (taken from a variety of sources including aerial photographs, maps, erosion pins, and ground surveys). Fig. 5.36 shows Hooke's (1980) plot with the maximum and mean section bank erosion rates from Table 5.4 superimposed. Hooke claims that her plot only includes published rates of bank erosion for meandering streams but as Fig. 5.36 shows the rates for the four divided channels reported here do not plot in substantially different positions from other studies (though at the upper end of the range). This suggests that the scatter in Hooke's plot maybe partly related to deviations in the channel pattern. In particular some of the meander bends of referenced works may just be parts of a larger stream network (for example Rundle (1985) notes there is a universal tendency for "braided streams to meander").

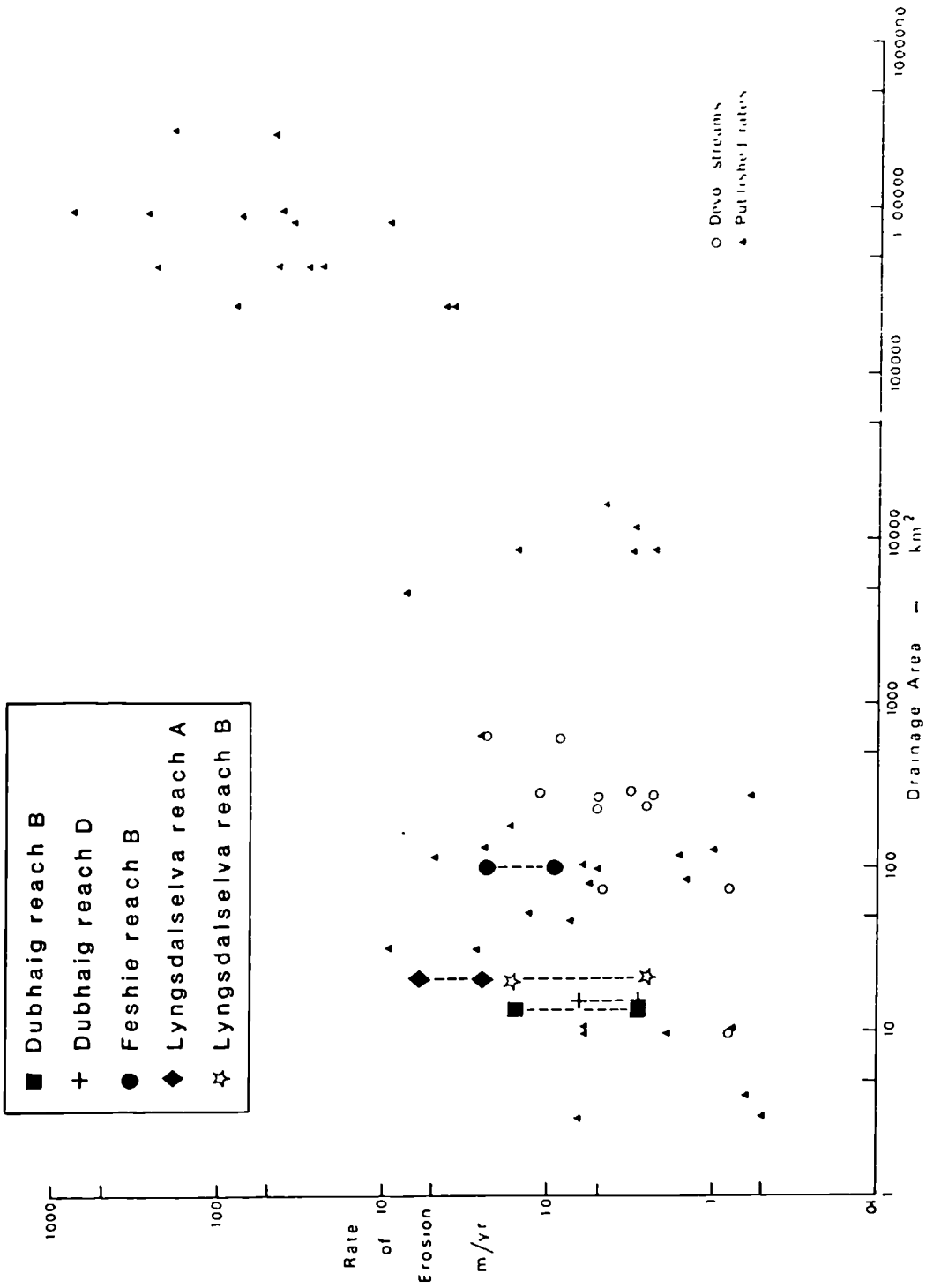

Fig. 5.36 Relationship between bank erosion rates and catchment area from Hooke (1980) with the maximum and mean erosion rates from five of the study reaches superimposed for comparison.

The only meandering channel pattern, reach D of the Dubhaig, plots along the trend of other rivers supporting Hooke's (1980) conclusion that there is a relationship between the rate of bank erosion and drainage area and indicating that the Dubhaig rate of erosion is not abnormally high compared to other rivers of a similar drainage area.

5.5.2 Rates and distances of bedload transport

Bedload transport was investigated in most of the study reaches directly by Helley-Smith sampling (with the exception of reach C of the Feshie) and indirectly using pebble tracers (reach B of the Lyngsdalselva excluded). Although Chapters 3 and 4 have documented and discussed the within-reach variations in bedload transport the data have not yet been compiled into a form that allows between-reach comparisons. The average distances of movement from over 3700 pebble tracers and the transport rates from 72 Helley-Smith bedload catches are used to provide information on the variations in transport efficiency in different channel types.

Table 5.5 shows the size range of tracers and the average distances of pebble tracer movement for each reach. The minimum and maximum b-axes of the tracers are shown together with the mean b-axis for all tracers used in the reach - expressed as a percentile of the bed surface grain size. It must be noted that the bed surface grain size distributions used for each reach in Table 5.5 are derived from an amalgamation of several bulk samples <u>not</u> Wolman counts, hence the pebble tracers appear to be relatively coarse compared to the sampled bed surface.

Table 5.5 shows that reaches B-D of the Dubhaig had pebbles inserted of approximately the same size range compared to the bed surface and despite having different channel patterns, moved them a similar mean distance.

Table 5.5 Summary of pebble tracer results for each of the nine study reaches in the Dubhaig, Feshie, and Lyngsdalselva.

River/ reach	No. pebbles inserted	% recovery	% moved of those found	Mean dist. moved of all found m	Mean dist. moved of those moved m	Pebble tracer b-axis mm		Mean b-axis as percentile of surface grain size D_x
						Min.	Max.	
Dubhaig								
A	745	66	63	7.7	12	24	147	D_{36}
B	488	68	78	14	18	26	238	D_{83}
C	522	76	72	13	19	24	153	D_{79}
D	453	61	82	13	17	24	170	D_{73}
E	366	89	54	5.1	10	24	135	D_{96}
Feshie								
B	379	40	74	35	47	25	171	D_{84}
C	389	84	36	4.4	12	24	136	D_{79}
Lyngsdal'								
A	188	26	100	21	21	90	170	D_{78}
C	255	89	74	5.0	6.7	35	200	D_{46}

The tracers in reaches A and E however did not move as far. In the case of reach E the tracers were undoubtedly too large (and heavy) to be moved or transported a long distance (the mean b-axis was the D_{96} of the surface) and consequently had a low percentage and mean distance of movement and a high percentage of recovery. On the other hand reach A had tracers inserted that were small relative to the bed surface but paradoxically these moved a shorter distance than those in reaches B-D. This situation can possibly be explained by the coarse grain size and physical structure of the bed surface. Reach A is much coarser than reaches B-E (D_{50} from bulk samples of 98 mm, compared to a range of 46-23 mm for B-E), with many boulders which protrude and form a rough bed surface topography. Pebble clusters are common in reach A (for example see Fig. 5.3) where the large cobbles collide and then stack up against each other (c.f. Brayshaw et al. 1983). The presence of these bedforms and coarse cobbles reduces the amount and distance of pebble movement by hiding pebbles within their structures or forming obstructions that pebbles have to climb over. The finer fractions are particularly prone to these effects and since smaller (relative to the surface D_{50}) tracers were used in the reach A experiments the mean distance of movement in Table 5.5 is lower than in other reaches. This explanation is supported by the Helley-Smith bedload catches (see later), field observations (where many tracers were found in pebble clusters or in deep sheltered voids between large boulders), and the analysis of tracer movement for different size fractions in 4.6.2 (which showed that in reach A the 90-128 mm size class had the furthest mean distance of movement). The results from reach A are in agreement with the arguments put forward in Chapter 4 that in coarse heterogeneous bed material the movement of the finer fractions is restricted. In the case of reach A the bed is so coarse that the 'finer fractions' can include pebbles with b-axes up to 77 mm (D_{36} of the bed surface).

Recalling the results in 4.6.2 the sizes of tracers that were most commonly moved (and over the greatest mean distance) were those close to or just coarser than the D_{50} of the bed surface. Therefore if a coarser tracer size range had been inserted in reach A there would probably have been a greater overall mobility of the tracers. Likewise if smaller tracer pebbles had been used in reach E the mean distance of movement would probably have increased. Table 5.5 shows that reaches B-D had very similar mean distances of tracer movement. If the differences in tracer sizes for reaches A and E are taken into account then all five reaches transported their bed material approximately the same distances. At first sight this may seem as though the pebbles move from riffle to riffle but the distance of movement is only an average and the riffle spacing in reaches A-E is at least double this distance. The discussion of rates of channel change in the Dubhaig in 5.5.1 showed that there was a difference in the rate of change (i.e. the amount of material removed over time) between reaches with the divided channel patterns of A, and particularly B, being the most active. The tracer results in Table 5.5 however show that the difference in the sediment transport between channel patterns is not matched by a corresponding variation in the distance this sediment is moved.

Table 5.5 shows that the Feshie and Lyngsdalselva tracers were transported much further distances than the Dubhaig tracers. The Feshie reach B tracers moved a mean distance (of all those found) of 35 m whilst the Lyngsdalselva reach A pebbles moved a mean distance of 21 m. The low recovery rate in the Lyngsdalselva (26%) is a result of the poor visibility in the turbid water and the burial of the tracers after the widespread channel changes during the 7/8 August rainflood (see 5.4.2.5). The map of the locations of the tracers after the flood (Fig. 4.19) shows that whilst most were found within the 55 m long study reach only one out of 50 that were thrown in at the flood peak was recovered. This suggests

that the pebbles may have been moved well out of the reach before the channel changes. Hence the mean distance of tracer movement in Table 5.5 may be an underestimate of the true mean length of travel. The Feshie reach B and Lyngsdalselva reach A tracer results support the discussion in 5.5.1 that these river types are both in high energy environments with high stream powers. This leads to rapid channel changes and the movement of sediment over long distances.

The different tracer experiments in reaches within these channel patterns can show a vast difference in the mobility of sediment. Table 5.5 shows that the mean distance of tracer movement (of those found) in reach C of the Feshie and C of the Lyngsdalselva is 87% and 76% less than the corresponding reaches B and A respectively. The reasons for this are connected to the individual tracer experiments. The tracers in reach C of the Feshie were seeded into a medial bar and consequently higher discharges were needed before the bars could be overtopped and the tracers entrained. Furthermore the discharge never exceeded bankfull during the two tracer experiments in reach C and therefore did not give the tracers the same opportunity to move as in the reach B snowmelt tracer experiment. The difference between the tracer movements in the two reaches (despite the size range of tracers relative to the bed surface being very similar) can also be explained by the use of the overbank pebbles in the reach B experiment. As discussed in 3.3 because of the special circumstances involved with the mobility of these pebbles they moved the greatest distance out of all the other tracer insertions in the experiment. Consequently the mean distance of movement for the whole of reach B is inflated and cannot be directly compared with the mobility of the reach C tracers.

The contrast between the tracer results of reaches A and C in the Lyngsdalselva is a function of the magnitude of discharge during the two

tracing periods. As discussed in 4.6.4 the reach A tracers were all inserted during the highest discharge of the five week study period. The reach C tracers however were only inserted near the end of the study period (22 August) when the discharge was progressively falling as the temperatures dropped and the snowmelt ceased. The river was still competent to move some of the pebbles and gravel in strong convergent zones but this sediment was soon deposited in the slower adjoining divergent areas downstream (the maximum pebble tracer movement was 49 m).

The differences in the rates of sediment transport between different channel patterns can be investigated using the 72 Helley-Smith bedload catches. Table 5.6 shows the maximum total transport rates and the corresponding discharge at the time of sampling for each reach. Comparisons between different reaches can only be made in general terms since the bedload samples were taken in a wide range of flows. Nevertheless the transport rates in Table 5.6 correspond fairly well with the rates of channel changes shown in Table 5.3.

The Dubhaig reach A has a lower transport than reach B (despite the shear stress being much higher in A at bankfull and the sample being taken at 153% of the bankfull discharge). As discussed previously this is due to the restriction on sediment movement by bedforms and the coarse nature of the bed surface (the maximum size that can be trapped in the Helley-Smith is only the D_{34} of the bed surface). The maximum reach B transport rate is close to the Lyngsdalselva transport rates showing that the formation and destruction of bars characteristic of divided channels can lead to a high supply of sediment passing through the system. Reaches C-E of the Dubhaig have progressively lower transport rates (but were also taken at lower discharges) with the maximum transport rate in reach E over two magnitudes less than reach B.

Table 5.6 Maximum transport rates and discharges for Helley-Smith bedload samples from the Dubhaig, Feshie, and Lyngsdalselva.

River/ reach	No. bedload samples	Maximum transport rate $kg\ m^{-1}s^{-1}$	Discharge bedload taken at $m^3 s^{-1}$	Discharge as % of bankfull %
Dubhaig				
A	6	0.21	9.2	153
B	10	1.6	4.9	82
C	8	0.10	4.0	66
D	4	0.015	3.3	55
E	3	0.0044	2.9	48
Feshie				
B	8	0.18	20	100
Lyngsdal'				
A	16	3.5	8.1	100
B	9	0.47	6.4	79
C	8	0.11	6.1	75

The maximum transport rate in the Feshie reach B (taken at bankfull) is surprisingly low but is supported by the shear stress measurements reported in Table 5.3. This suggests that discharges above bankfull are needed before the sediment transport rate increases substantially. In comparison the bankfull conditions during the Lyngsdalselva rainflood led to some of the highest bedload transport rates ever recorded (see 4.7.2). As the analysis in 4.3 and the discussion in 4.5 showed the bed armour during the flood was totally destroyed and all sizes of sediment were almost equally mobile. Although the Helley-Smith samples could only trap sediment finer than 76 mm in diameter the high transport rate still reflects this rapid increase in sediment availability (see 4.2). Reaches B and C of the Lyngsdalselva were not sampled during the rainflood but within channel meltwater peaks still transported sediment at rates greater than 0.1 kg m^{-1} s^{-1} at sites of flow convergence.

The overall picture of channel change and sediment transport in the 10 study reaches seems to follow a predictable pattern. Channels that are steep and have high shear stress tend to be divided channel forms. As such they have a regular source of sediment via the uncohesive banks and rapidly changing bars. Consequently these channel patterns have some of the highest transport rates and mean distances of sediment movement. Furthermore with a broad floodplain of uncohesive gravels the channels can freely migrate and change the channel geometry and so have high rates of channel change.

At lower flow strengths and gradients the river is less able to switch its position and the pattern takes the form of a single channel. Reach C of the Dubhaig shows that if the channel pattern is midway between a divided and single channel type the rate of erosion and deposition decreases. Once the pattern truly meanders (as in reach D of the Dubhaig with the classic bank erosion on its outer banks and point bar growth) the flow is

competent to change the channel geometry. However if the gradient (and therefore stream power) is so low that the channel is straight there is minimal channel change, bank erosion, and bedload transport.

These observations are consistent with many other studies concerned with the threshold for different channel pattern development (for example Lane (1957), Leopold and Wolman (1957), Ackers and Charlton (1971), Schumm and Khan (1972)) which show that there is a pattern sequence from straight to meandering to braided with increasing bed slope (and discharge). The flume study of Schumm and Khan (1972) is particularly relevant since they also looked at the effect of sediment load on the development of channel patterns. Their conclusions that "as slope and sediment loads increased, threshold values of these variables were encountered, at which channel patterns altered significantly" bears out the results from the study reported here.

6 CONCLUSIONS

6.1 Interrelationships of channel processes and changes in gravel-bed rivers

Throughout the analyses and discussions in Chapters 3-5 the underlying theme to emerge has been that though different rivers, reaches, and channel types have their own pattern, rate, and magnitude of channel processes and changes, there is a common set of interrelationships which can explain the way each channel functions and develops. In 1.3 a general model was put forward showing the cause-effect relationships operating in gravel-bed rivers (Fig. 1.1). The results reported here from 10 study reaches, representing seven different channel patterns, support this model and highlight the complexities of the linkages in the system which can have substantial feedback, both positive and negative.

The unsteady discharge through a system of highly nonuniform channels with rough beds produces a complicated spatial and temporal pattern of water velocity (or shear stress). As the discussion in 3.1 showed many field workers now recognise that the pool/riffle unit is one of the fundamental controls on flow strength, sediment transport, and channel development in gravel-bed rivers. The results from the tracer experiments and shear stress measurements at varying discharges in the Dubhaig and Feshie (see 3.2 and 3.3) showed that there is a common response of this pool/riffle unit to a changing discharge. The Keller (1971) velocity-reversal hypothesis holds true in most channel patterns and explains why riffles tend to be coarser than pools and aggrade at high flows. The results in 3.2 and 3.3 point to variations in Keller's model but show that the

velocity reversal still holds true for subunits of the pool/riffle cycle.

On a broader scale the discharge of a river affects the flow pattern which tends to be dominated by a series of convergent/divergent cycles. The measurements of flow strength and direction and the locations of channel change for all three rivers presented in Chapter 5 show that the convergent flow zones are responsible for bank erosion and channel scour whilst the divergent flow areas lead to bar growth and channel aggradation. Using pebble tracers the divergent zones can easily be recognised by distinct tracer concentrations. Measurements during a major flood (in the Lyngsdalselva reach A) showed that these convergent/divergent zones can shift (and even reverse) their positions with increasing discharge so that channel changes at moderate competent discharges may be the opposite (in magnitude and location) of those in high flows (overbank).

The vertical velocity gradient at any point determines the shear stress or fluid force acting parallel to the bed surface. The shear stress interacts with the character of the bed material to determine the sizes and amounts of sediment transported. The results in Chapter 4 showed that there is not a simple proportional relationship between the flow strength and the size of material entrained (as traditionally assumed). A complex combination of hiding, protrusion and pivoting of different size fractions leads to most sizes of sediment having an almost equal opportunity of entrainment. If the bed armour is broken then there is no restriction on sediment movement of different sizes but if the armour is still intact there are varying degrees of selective transport with sizes near to or just coarser than the surface D_{50} being the most mobile.

The detailed discussion throughout Chapter 4 highlighted the complexity of the interrelationships between the shear stress, bed material, and subsequently the bedload transport. However there are still discernible links which can best be illustrated using an example from one of the rivers.

The Lyngsdalselva had 33 Helley-Smith bedload samples taken in shear stresses ranging from 6 to 406 N m^{-2}. The grain size distributions of these bedload samples are plotted in Fig. 6.1. The bedload curves fall into four distinct envelopes which turn out to correspond to progressively higher, though overlapping, ranges of shear stress. The fine-grained bedload of envelope A (n=4) corresponds to low discharges with a mean shear stress of 11 N m^{-2}. Envelope B (n=11, mean shear stress = 104 N m^{-2}) has no sediment coarser than 32 mm and is a medium shear stress/flow set. Envelope C (n=8, mean shear stress = 148 N m^{-2}) differs from envelope B due to the lack of sediment in the 1 to 8 mm size range, giving a bimodal size distribution. Such a 'grain size gap' has been reported by many other workers. Envelope D (n=10, mean shear stress = 276 N m^{-2}) represents the higher shear stresses and has a correspondingly coarse distribution, with all sizes within the sampler's capacity of 76 mm being trapped.

Fig. 6.1 also shows grain size curves for bulk samples of up to 45 kg from three distinctive and common channel deposits: a fine backwater fill, the topset unit from the cross-bedded sand at a bartail, and the eroding bank of the main channel just upstream of reach A. This 'floodplain' sample represents the surface and subsurface layers of an older medial bar, whereas the backwater and topset samples represent falling-stage deposits. These different deposits are seen to correspond in size to bedload

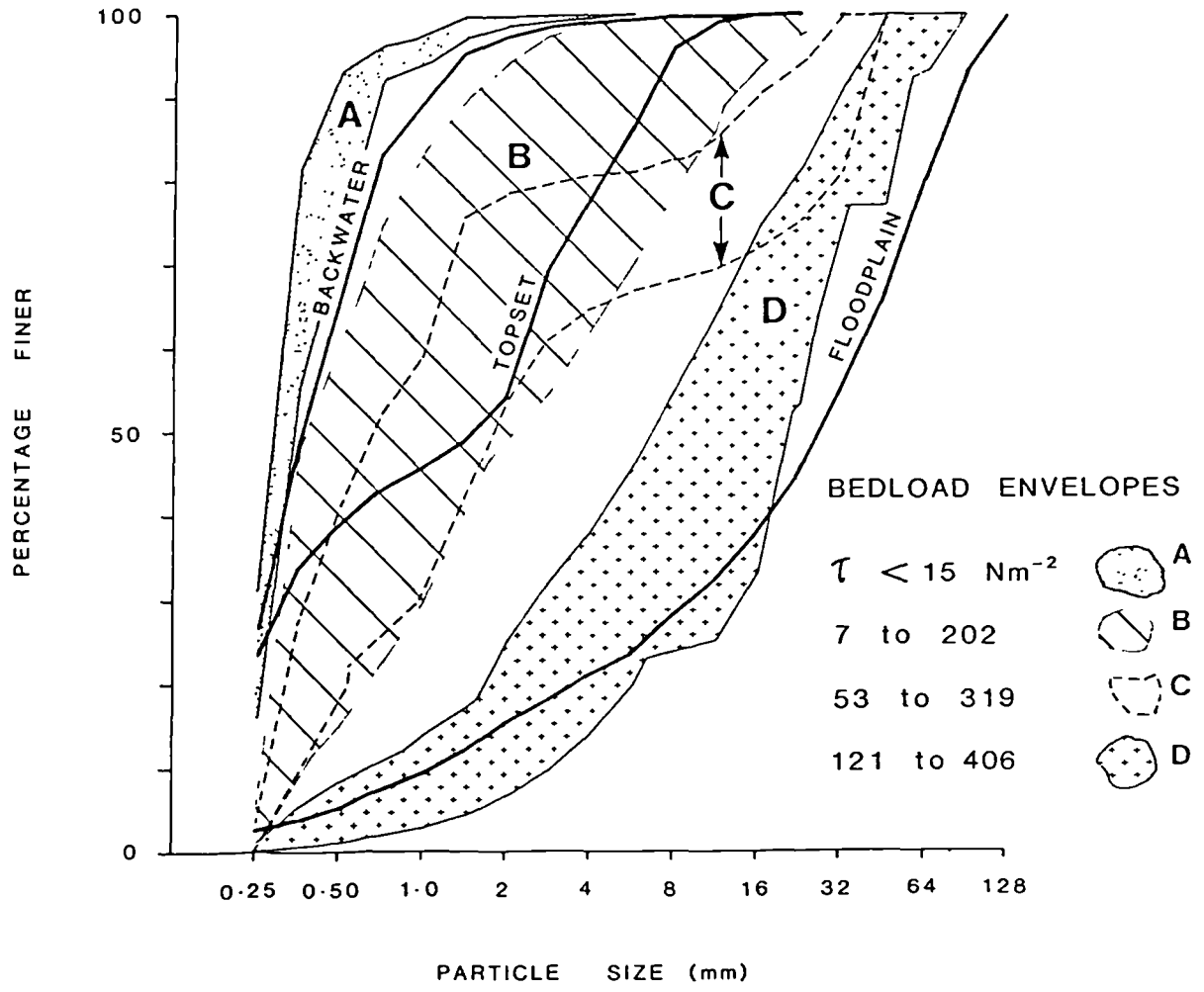

Fig. 6.1 Grain size curves (by weight) of floodplain sedimentary units compared with those of bedload sampled in different ranges of shear stress. Bedload distributions are truncated at 0.25 and 76 mm.

transported under different flow conditions. The backwater sample matches grain size envelope A for bedload at the lowest shear stresses. The topset plots in the medium-flow envelope B, though its curve is complicated by a grain size gap between 0.35 mm and 2 mm, and the floodplain (cutbank) curve resembles the bedload envelope for the highest shear stresses, especially when it is remembered that the coarse tail of the bedload envelope is truncated by the limited size of the sampler. Allowing for this the Lyngsdalselva example shows that there seems to be a close relationship between the bedload movement at different discharges and shear stresses and the deposit found in the floodplain.

The amount of bedload transport determines whether a channel maintains its existing geometry (and maybe position) or alters it by scour, fill, or lateral migration. The results in 5.5 showed that the maximum rates of bedload transport for each study reach correspond fairly well with the volumetric rates of channel change. This channel change also correlates with the channel pattern with progressively more erosion or deposition as the river changes from a straight to multi-braided system. Furthermore the results in Chapter 5 show that if a reach was abandoned (during a flood) the erosion and deposition would alter the channel form to create a wider, shallower, and more uniform channel geometry.

The resulting channel form determines the hydraulic geometry (i.e. velocity distribution, slope and so on) which brings the gravel-bed system (Fig. 1.1) back to the start again with the velocity distribution in nonuniform channels. As stated in 1.3 the cause-effect relationships in the system have numerous feedbacks and in conditions of fluctuating discharge the system is dynamic not static. However the findings of this study (see below) show that there are certainly discernible links between

the spatial and temporal patterns of velocity and shear stress, of bedload transport rate, and of consequent erosion or deposition, but more research is needed before general patterns of response can be expected to emerge.

6.2 Summary of findings

The results from the study of bedload transport and channel changes in seven different channel patterns of the rivers Dubhaig, Feshie, and Lyngsdalselva lead to six general conclusions.

(1) The velocity-reversal hypothesis put forward by Keller (1971) holds true in gravel-bed rivers of different channel patterns. The flow strength increases at different rates through various subunits of the pool/riffle cycle as the discharge rises. At discharges at or just below bankfull the poolhead is the first to exceed the riffle shear stress followed by the midpool and then pooltail. The distances of pebble tracer movement for these subunits matches this hierarchy of shear stress at high discharges. The grain size distribution of the bed surface differentiates between the coarser riffle and finer pool but does not show a clear pattern of within-pool sediment sorting. Exceptions to Keller's hypothesis can be found where the channel is free to migrate over low-lying bars. In such circumstances a rise in the discharge can be accommodated by an increase in the channel width so that the shear stress does not change substantially.

(2) Bedload transport rates increase with flow strength but depend on the availability and mobility of appropriate-sized sediment at the surface. The traditional and often relied-upon bedload predictive formulae of Shields (1936), Meyer-Peter and Müller (1948), Brown (1950), Einstein

(1950), and more recently Parker (1978) all fail to take into account the differences in the probability of entrainment of different fractions from coarse heterogeneous bed material. Using analyses similar to Parker et al. (1982b) and Andrews (1983) on 72 Helley-Smith bedload catches shows that the hiding of finer particles (relative to the bed surface) and protrusion and pivoting of the coarser pebbles almost cancels out the variations in mobility of all size fractions caused by weight differences. The bed surface is therefore almost equally mobile.

(3) The interrelationships between the discharge, shear stress, and grain size and physical structure of the bed material determines the proportions and sizes of sediment that are either equally mobile or selectively entrained. Helley-Smith samples and shear stress measurements taken during a major flood showed that when the bed armour is destroyed all sizes of the surface and subsurface become equally mobile. However for the majority of flow conditions when the bed behaves jointly as a mobile and static armour there is considerable scope for selective entrainment. This is supported by the distances and percentages of movement of different sized pebble tracers. The tracer results showed that there is a weak inverse relationship between the distance moved and particle weight and that sizes near to or just coarser than the D_{50} of the bed surface were the most mobile (the movement of the finer and coarser fractions was restricted presumably by hiding and weight effects respectively). The pebble tracers also showed that there was some selective transport according to a particle's shape with the spherical and triaxial ellipsoids moving the furthest distance.

(4) The work and reasoning of Parker and Andrews, although the closest to arriving at a predictive bedload transport equation for use in gravel-bed

rivers, needs to be refined. In particular the results from this study show that any explanation of down-bar of downstream fining must incorporate some selective entrainment and cannot, as Parker and Andrews argue, depend solely on selective deposition.

(5) The pattern of converging accelerating flow and diverging decelerating flow helps explain channel changes and bar formation. The locations of the convergent/divergent cells may alter radically as the discharge increases and can lead to a reversal of channel response as the river becomes generally, rather than locally, competent to transport coarse bed material.

(6) The annual rates of erosion and deposition for different channel patterns can be explained by each channel's shear stress, sediment availability, and bank stability. There is a general order of increasing rate of channel change from the remarkably stable straight channel, through the meandering and then moderately divided patterns, to the active multi-braided system.

Finally, the cause-effect relationships operating in gravel-bed rivers depicted in the flow diagram in Fig. 1.1 seem to be consistent for all channel types. If the recent upsurge in gravel-bed research continues to provide more sets of integrated and intensive field measurements it may soon be possible to model these relationships for different channel patterns given detailed information on the flow strength, bedload transport, and sedimentology.

BIBLIOGRAPHY

Ackers, P. and Charlton, F.G. (1971): The slope and resistance of small meandering channels. *Proceedings of Institute of Civil Engineers Supplement* XV, Paper 7362S, 349-370.

Ackers, P. and White, W.R. (1973): Sediment transport: new approach and analysis. *Journal of Hydraulics Division, American Society of Civil Engineers*, 99, 2041-2060.

Andrews, E.D. (1979): Scour and fill in a stream channel, East Fork River, Western Wyoming. *United States Geological Survey Professional Paper*, 1117, 49p.

Andrews, E.D. (1982): Bank stability and channel width adjustment, East Fork River, Wyoming. *Water Resources Research*, 18, 1184-1192.

Andrews, E.D. (1983): Entrainment of gravel from naturally sorted riverbed material. *Geological Society of America Bulletin*, 94, 1225-1231.

Andrews, E.D. (1984): Bed-material entrainment and hydraulic geometry of gravel-bed rivers in Colorado. *Geological Society of America Bulletin*, 95, 371-378.

Andrews, E.D. and Erman, D.C. (1986): Persistence in the size distribution of surficial bed material during an extreme snowmelt flood.

Water Resources Research, 22, 191-197.

Andrews, E.D. and Parker, G. (in press): The coarse surface layer as a response to gravel mobility. *In* Thorne, C.R., Bathurst, J.C., and Hey, R.D. (eds.): *Sediment Transport in Gravel-Bed Rivers*, Wiley, Chichester, 880p.

Arkell, B., Leeks, G., Newson, M., and Oldfield, F. (1983): Trapping and tracing: some recent observations of supply and transport of coarse sediment from upland Wales. *In:* Collinson, J.D. and Lewin, J. (eds.): *Modern and Ancient Fluvial Systems*, Special Publication of International Association of Sedimentologists, 6, 107-109.

Ashmore, P.E. (1982): Laboratory modelling of gravel braided stream morphology. *Earth Surface Processes and Landforms*, 7, 201-225.

Ashworth, P.J. and Ferguson, R.I. (1986): Interrelationships of channel processes, changes and sediments in a proglacial river. *Geografiska Annaler*, 68, 361-371.

Bagnold, R.A. (1956): The flow of cohesionless grains in fluids. *Philosophical Transactions Royal Society (London)* 249, 235-297.

Bagnold, R.A. (1966): An approach to the sediment transport problem from general physics. *United States Geological Survey Professional Paper*, 422-I, 37p.

Bagnold, R.A. (1973): The nature of saltation and of bedload transport in water. *Proceedings of Royal Society (London)*, A, 332, 473-504.

Bagnold, R.A. (1977): Bedload transport by natural rivers. *Water Resources Research*, 13, 303-312.

Bagnold, R.A. (1980): An empirical correlation of bedload transport rates in flumes and natural rivers. *Proceedings Royal Society (London)*, A, 372, 453-473.

Baker, V.R. (1974): Paleohydraulic interpretation of Quaternary alluvium near Golden, Colorado. *Quaternary Research*, 4, 94-112.

Baker, V.R. and Ritter, D.F. (1975): Competence of rivers to transport coarse bedload materials. *Geological Society of America Bulletin*, 86, 975-978.

Bathurst, J.C, Thorne, C.R. and Hey, R.D. (1979): Secondary flow and shear stress at river bends. *Journal of Hydraulics Division, American Society of Civil Engineers*, 105, 1277-1295.

Bathurst, J.C. (1982): Theorectical aspects of flow resistance. *In:* Hey, R.D., Bathurst, J.C., and Thorne, C.R. (eds.): *Gravel-Bed Rivers*, 83-109.

Baumgart-Kotarba, M. (in press): Formation of coarse gravel bars and alluvial channels, braided Bialka River, Carpathians, Poland. *In:*

Gardiner, V. (ed.): *Proceedings of First International Geomorphology Conference, Manchester*, Wiley, Chichester.

Bhowmik, N.G. and Demissie, M. (1982): Bed material sorting in pools and riffles. *Journal of Hydraulics Division, American Society of Civil Engineers*, 108, 1227-1231.

Billi, P. and Tacconi, P. (in press): Bedload transport processes from Virginio Creek measuring station, Italy. *In:* Gardiner, V. (ed.): *Proceedings of First International Geomorphology Conference, Manchester*, Wiley, Chichester.

Bluck, B.J. (1971): Sedimentation in the meandering River Endrick. *Scottish Journal of Geology*, 7, 93-138.

Boothroyd, J.C. and Ashley, G.M. (1973): Processes, bar morphology, and sedimentary structures on braided outwash fans, Northeastern Gulf of Alaska. *In:* Jopling, A.V., and McDonald, B.C. (eds.): *Glaciofluvial and Glaciolacustrine Sedimentation*, Special Publication of Society of Economic Paleonotologists, and Mineralogists, 23, 193-222.

Bradley, W.C. and Mears, A.I. (1980): Calculations of flows needed to transport coarse fractions of Boulder Creek alluvium at Boulder, Colorado. *Geological Society of America Bulletin*, 91, 1057-1090.

Bray, D.I. (1972): Generalized regime-type analysis of Alberta rivers. *Unpublished Ph. D Thesis*, University of Alberta, 241p.

Bray, D.I. and Church, M. (1980): Armoured versus paved gravel-beds. *Journal of Hydraulics Division, American Society of Civil Engineers*, 106, 1937-1940.

Brayshaw, A.C., Frostick, L.E., and Reid, I. (1983): The hydrodynamics of particle clusters and sediment entrainment in coarse alluvial channels. *Sedimentology*, 30, 137-143.

Brewster, C. (1986): Bedload transport experiments in the River Feshie, Scottish Cairngorm Mountains, U.K. *Unpublished B. Sc dissertation*, University of Stirling, 94p.

Brice, J.C. (1974): Evolution of meander loops. *Geological Society of America Bulletin*, 85, 581-586.

Bridge, J.S. (1985): Paleochannel patterns inferred from alluvial deposits: a critical evaluation. *Journal of Sedimentary Petrology*, 55, 579-589.

Brown, C.B. (1950): Sediment Transportation. *In:* Rouse, H. (ed.): *Engineering Hydraulics*, 769-857.

Cailleux, A. (1947): L'indice d'emousse: Definition et premiere application. *Comptes Rendues de la Societe Geologique Francaise*, 10 October, 250-252.

Campbell, A.J. and Sidle, R.C. (1985): Bedload transport in a pool-riffle sequence of a coastal Alaska stream. *Water Resources*

Bulletin, 21, 579-590.

Cant, D.J. and Walker, R.G. (1978): Fluvial processes and facies sequences in the sandy braided South Saskatchewan River, Canada. *Sedimentology*, 25, 625-648.

Carling, P.A. (1981): Discussion of Bray, D.I. and Church, M. 'Armoured versus paved gravel beds', Journal of Hydraulics Division, American Society of Civil Engineers, 106, 1937-1940. *In: Journal of Hydraulics Division, American Society of Civil Engineers*, 107, 1117-1118.

Carling, P.A. (1983): Threshold of coarse sediment transport in broad and narrow natural streams. *Earth Surface Processes and Landforms*, 8, 1-18.

Carling, P.A. (1984): Deposition of fine and coarse sand in an open-work gravel bed. *Canadian Journal of Fisheries and Aquatic Sciences*, 41, 263-270.

Carson, M.A. (1984): The meandering-braided river threshold: a reappraisal. *Journal of Hydrology*, 73, 315-334.

Carson, M.A. (1986): *Transport of Gravel in Alluvial Channels*, North Canterbury Catchment Board and Regional Water Board, Christchurch, New Zealand, 299p.

Carson, M.A., and Griffiths, G.A. (1985): Tractive stress and the onset of bed particle movement in gravel stream channels. *Journal of*

Hydrology, 79, 375-388.

Charlton, F.G., Brown, P.M., and Benson, R.W. (1978): The hydraulic geometry of some gravel rivers in Britain. *Report IT-180*, Hydraulics Research Station, Wallingford, 48p.

Cheetham, G.H. (1979): Flow competence in relation to stream channel form and braiding. *Geological Society of America Bulletin*, 90, 877-886.

Chien, N. (1956): The present status of research on sediment transport. *Transactions of American Society of Civil Engineers*, 121, 833-868.

Church, M. (1972): Baffin Island sandurs: a study of arctic fluvial processes. *Geological Survey of Canada Bulletin*, 216, 280p.

Church, M. (1978): Paleohydrological reconstructions from a Holocene valley. *In.* Miall, A.D. (ed.): *Fluvial Sedimentology*, Canadian Society of Petroleum Geologists Memoir 5, 743-772.

Church, M. and Gilbert, R. (1975): Proglacial fluvial and lacustrine environments. *In:* Jopling, A.V. and McDonald, B.C. (eds.): *Glaciofluvial and Glaciolacustrine Sedimentation*, Special Publication of Society of Economic Paleontologists and Mineralogists, 23, 22-100.

Church, M. and Jones, D. (1982): Channel bars in gravel-bed rivers. *In:* Hey, R.D., Bathurst, J.C., and Thorne, C.R. (eds.): *Gravel-Bed Rivers*, 291-339.

Church, M., Moore, D., and Rood, K. (1981): *Catalogue of Alluvial River Channel Regime Data.* Department of Geography, University of British Columbia, 300p.

Church, M., McLean, D.G., and Wolcott, J.F. (in press): River bed gravels: sampling and analysis. *In:* Thorne, C.R., Bathurst, J.C., and Hey, R.D. (eds.): *Sediment Transport in Gravel-Bed Rivers*, Wiley, Chichester, 880p.

Collinson, J.D. and Lewin, J. (1983): *Modern and Ancient Fluvial Systems*, Special Publication of International Association of Sedimentologists, 6, Blackwell Scientific Publications, 575p.

Cowan, I.R. (1968): Mass, heat and momentum exchange between stands of plants and their atmospheric environment. *Quarterly Journal Royal Meteorology Society*, 94, 524-544.

Davoren, A. and Mosley, M.P. (1986): Observations of bedload movement, bar development and sediment supply in the braided Ohau River. *Earth Surface Processes and Landforms*, 11, 643-652.

Dietrich, W.E. and Smith, J.D. (1984): Processes controlling the equalibrium bed morphology in river meanders. *In:* Elliott, C.M. (ed.): *River Meandering*, Proceedings of the Conference Rivers '83, 759-769.

Du Buat, P. (1786): *Principles d'hydraulique*, 2nd ed. De l'Imprimerie de Monsieur, Paris, 220p.

Einstein, H.A. (1942): Formulas for the transportation of bed load. *Transactions of American Society Civil Engineers*, 107, 561-577.

Einstein, H.A. (1950): The bed-load function for sediment transportation in open channel flows. *United States Department of Agriculture Technical Bulletin*, 1026, 71p.

Elliott, C.M. (1984): *River Meandering*, Proceedings of the Conference Rivers '83, American Society of Engineers, New York, 1036p.

Emmett, W.W. (1975): The channels and waters of the upper Salmon River area, Idaho. *United States Geological Survey Professional Paper*, 870-A, 116p.

Emmett, W.W. (1976): Bedload Transport in two large gravel-bed rivers, Idaho and Washington. *Proceedings of Third Federal Inter-Agency Sedimentation Conference*, Denver, Colorado, 15p.

Emmett, W.W. (1980): A field calibration of the sediment-trapping efficiency characteristics of the Helley-Smith bedload sampler. *United States Geological Survey Professional Paper*, 1139, 44p.

Emmett, W.W. (1982): Variability of bedload and some hydraulic characteristics along a reach of East Fork River. *In:* Leopold, L.B. (ed.): *American Fieldtrip Guidebook 1982 Conference*, Pinedale, Wyoming, 49-56.

Engel, P. and Lau, L. (1980): Calibration of bedload samplers. *Journal of Hydraulic Division, American Society of Civil Engineers*, 106, 1677-1685.

Ergenzinger, P.J. and Custer, S.G. (1983): Determination of bedload transport using natural magnetic tracers: first experiences at Squaw Creek, Gallatin County, Montana. *Water Resources Research*, 19, 187-193.

Fahnestock, R.K. (1963): Morphology and hydrology of a glacial stream, White River, Mount Rainier, Washington. *United States Geological Survey Professional Paper*, 422-A, 70p.

Fenton, J.D. and Abbott, J.E. (1977): Initial movement of grains on a stream bed: the effects of relative protrusion. *Proceedings of Royal Society (London)*, A, 352, 523-537.

Ferguson, R. I. (1981): Channel form and channel changes. *In:* Lewin, J. (ed.): *British Rivers*, 90-125.

Ferguson, R. I. (1984): Kinematic model of meander migration. *In:* Elliott, C.M. (ed.): *River Meandering*, Proceedings of the Conference Rivers '83, 942-951.

Ferguson, R. I. (1986): River loads underestimated by rating curves. *Water Resources Research*, 22, 74-76.

Ferguson, R. I. (in press): Discussion of Andrews, E.D. and Parker, G., 'The coarse surface layer as a response to gravel mobility'. *In:* Thorne, C.R., Bathurst, J.C., and Hey, R.D. (eds.): *Sediment Transport in Gravel-Bed Rivers*, Wiley, Chichester, 880p.

Ferguson, R.I. and Werritty, A. (1983): Bar development and channel

changes in the gravelly River Feshie, Scotland. *In:* Collinson, C.D. and Lewin, J. (eds.): *Modern and Ancient Fluvial Systems*, Special Publication of Association of Sedimentologists, 6, 181-193.

Garde, R.J. and Ranga Raju, K.G. (1977): *Mechanics of Sediment Transportation and Alluvial Stream Problems*, Wiley, New Delhi, 483p.

Gessler, J. (1965): The beginning of bed load movement of mixtures investigated as natural armoring in channels. *Laboratory of Hydraulics Research and Soil Mechanics Report*, Swiss Federal Institute of Technology, Zurich, 69, 89p.

Gilbert, G. K. (1914): The transportation of debris by running water. *United States Geological Survey Professional Paper*, 86, 363p.

Gomez, B. (1983): Temporal variations in bedload transport rates: the effect of progressive bed armouring. *Earth Surface Processes and Landforms*, 8, 41-54.

Gomez, B. (1984): Typology of segregated (armoured/paved) surfaces: some comments. *Earth Surface Processes and Landforms*, 9, 19-24.

Gomez, B. (1987): Bedload. *In:* Gurnell, A.M. and Clark, M.J. (eds.): *Glacio-Fluvial Sediment Transfer*, 355-376.

Hack, J.T. (1957): Studies of longitudinal stream profiles in Virginia and Maryland. *United States Geological Survey Professional Paper*, 294-B, 10p.

Hall, J.D. and Lantz, R.L. (1969): Effects of logging on the habitat of coho salmon and cutthroat trout in coastal streams. *In:* Northcote, T.G. (ed.): *Symposium on Salmon and Trout in Streams*, 335-376.

Hammond, F.D.C., Heathershaw, A.D. and Langhorne, D.N. (1984): A comparison between Shields' threshold criterion and the movement of loosly packed gravel in a tidal channel. *Sedimentology*, 31, 51-62.

Harris, G.S. (1970): Some aspects of the biology of Welsh sea trout (*S. trutta trutta* L.). *Unpublished Ph.d thesis*, University of Liverpool, 320p.

Harvey, A.M. (1975): Some aspects of the relations between channel characteristics and riffle spacing in meandering streams. *American Journal Science*, 275, 470-478.

Hayward, J.A. (1979): Mountain stream sediments. *In:* Murray, D.L. and Ackroyd, P. (eds.): *Physical Hydrology*, 193-212.

Hayward, J.A. and Sutherland, A.J. (1974): The Torlesse Stream vortex-tube sediment trap. *Journal of Hydrology, (NZ)*, 13, 41-53.

Hein, F.J. (1974): Gravel transport and Stratification origins. *Unpublished M. Sc thesis*, McMaster University, Hamiliton, 135p.

Hein, F.J. and Walker, R.G. (1977): Bar evolution and development of stratification in the gravelly, braided, Kicking Horse River, British Columbia. *Canadian Journal of Earth Sciences*, 14,

562-570.

Helley, E.J. and Smith, W. (1971): Development and calibration of a pressure-difference bedload sampler. *United States Geological Survey Open-File Report*, 18p.

Hey, R.D. (1982): Gravel-bed rivers: form and processes. *In:* Hey, R.D., Bathurst, J.C. and Thorne, C.R. (eds.): *Gravel-Bed Rivers*, 5-15.

Hey, R.D. and Thorne, C.R. (1983): Accuracy of surface samples from gravel bed material. *Journal of Hydraulic Engineering, American Society of Civil Engineers*, 109, 842-851.

Hey, R.D., Bathurst, J.C. and Thorne, C.R. (1982): *Gravel-Bed Rivers*, Wiley, Chichester, 875p.

Hirsch, P.J. and Abrahams, A.D. (1981): The properties of bed sediments in pools and riffles. *Journal of Sedimentary Petrology*, 51, 757-760.

Hjulström, F. (1935): Studies of the morphological activity of rivers as illustrated by the River Fyris. *Bulletin of Geological Institute, University of Uppsala*, 25, 221-527.

Hooke, R.B. (1975): Distribution of sediment transport and shear stress in a meander bend. *Journal of Geology*, 83, 543-565.

Hooke, J.M. (1977): The distribution and nature of changes in river bends. *In:* Gregory, K.J. (ed.): *River Channel Changes*, 265-280.

Hooke, J.M. (1980): Magnitude and distribution of rates of river bank erosion. *Earth Surface Processes and Landforms*, 5, 143-157.

Ikeda, S., Parker, G. and Sawai, K. (1981): Bend theory of river meanders, Part 1, linear development. *Journal of Fluid Mechanics*, 112, 363-377.

Jackson, P.S. (1981): On the displacement height in the logarithmic velocity profile. *Journal of Fluid Mechanics*, 111, 15-22.

Keller, E.A. (1970): Bed Load movement experiments, Dry Creek, California. *Journal of Sedimentary Petrology*, 40, 1339-1344.

Keller, E.A. (1971): Areal sorting of bed-load material: the hypothesis of velocity reversal. *Geological Society of America Bulletin*, 82, 753-756.

Keller, E.A. (1972a): Development of alluvial stream channels: a five-stage model. *Geological Society of America Bulletin*, 83, 1531-1536.

Keller, E.A. (1972b): Areal sorting of bed material: the hypothesis of velocity reversal: reply. *Geological Society of America Bulletin*, 83, 915-918.

Keller, E.A. and Melhorn, W.N. (1978): Rhythmic spacing and origin of pools and riffles. *Geological Society of America Bulletin*, 89, 723-730.

Kellerhals, R. and Bray, D.I. (1971): Sampling procedures for coarse

fluvial sediments. *Journal of Hydraulics Division, American Society of Civil Engineers*, 97, 1165-1180.

Klingeman, P.C. and Emmett, W.W. (1980): Field progress in describing sediment transport. *Paper Presented to the International Workshop on Engineering Problems in the Management of Gravel-Bed Rivers*, Newton, U.K.

Klingeman, P.C. and Emmett, W.W. (1982): Gravel bedoad transport processes. *In:* Hey, R.D., Bathurst, J.C. and Thorne, C.R. (eds.): *Gravel-Bed Rivers*, 141-179.

Klingeman, P.C. and Milhous, R.T. (1970): Oak Creek vortex bedload sampler. *Paper Presented to 17th Annual Pacific Northwest Regional Meeting*, American Geophysical Union, Tacoma, Washington.

Klingeman, P.C., Milhous, R.T. and Heinecke, T.L. (1979): Oak Creek vortex bedload sampler. *Oak Creek Sediment Transport Report F2*, Water Resources Research Institute, Oregon State University, Corvallis.

Knighton, A.D. (1974): Variation in width-discharge relation and some implications for hydraulic geometry. *Geological Society of America Bulletin*, 85, 1059-1076.

Knighton, A.D. (1977): Short-term changes in hydraulic geometry. *In:* Gregory, K.J. (ed.): *River Channel Changes*, 101-119.

Komar, P.D. and Zhenlin, L. (1986): Pivoting analysis of the selective

entrainment of sediments by shape and size with application to gravel threshold. *Sedimentology*, 33, 425-436.

Kondolf, G.M. and Williams, W.V.G (1986): Transport of tracer gravels on a coastal California River. *Journal of Hydrology*, 85, 265-280.

Krigström, A. (1962): Geomorphological studies of sandur plains and their braided rivers in Iceland. *Geografiska Annaler*, 44, 328-346.

Krumbein, W.C. (1941): Measurement and geological significance of shape and roundness of sedimentary particles. *Journal of Sedimentary Petrology*, 11, 64-72.

Lane, E.W. (1957): A study of the shape of channels formed by natural streams flowing in erodible material. *United States Army Corps of Engineers Division*, Missouri River, M. R. D. Sedimentological Series, 9, 106p.

Langbein, W.B. and Leopold, L.B. (1966): River meanders: theory of minimum variance. *United States Geological Survey Professional Paper*, 422-H, 15p.

Laronne, J.B. and Carson, M.A. (1976): Interrelationships between bed morphology and bed material transport for a small gravel-bed channel. *Sedimentology*, 23, 67-85.

Leopold, L. B. (1982): Water surface topography in river channels and implications for meander development. *In:*. Hey, R.D., and Bathurst, J.C. and Thorne, C.R. (eds.): *Gravel-Bed Rivers*, 359-389.

Leopold, L.B. and Emmett, W.W. (1976): Bedload measurements, East Fork River, Wyoming. *Proceedings of National Academy of Science, USA*, 73, 1000-1004.

Leopold, L.B. and Emmett, W.W. (1977): 1976 bedload measurements, East Fork River, Wyoming. *Proceedings of National Academy of Science, USA*, 74, 2644-2648.

Leopold, L.B. and Emmett, W.W. (1981): Some observations on the movements of cobbles on a streambed. *In: Sediment Transport Measurement (Proceedings of the Florence Symposium, 22-26 June 1981)*, Publication of International Association of Hydrological Sciences, 133, 49-59.

Leopold, L.B. and Emmett, W.W. (1984): Bedload movement and its relation to scour. *In:* Elliott, C.M. (ed.): *River Meandering*, Proceedings of the Conference Rivers '83, 640-649.

Leopold, L.B. and Langbein, W.B. (1966): River Meanders. *Scientific American*, 214, 60-70.

Leopold, L.B. and Wolman, M.G. (1957): River channel patterns: braided, meandering, and straight. *United States Geological Survey Professional Paper*, 282-B, 85p.

Leopold, L.B. and Wolman, M.G. (1960): River meanders. *Geological Society of America Bulletin*, 71, 769-794.

Leopold, L.B., Bagnold, R.A., Wolman, M.G. and Brush, L.M. (1960): Flow resistance in sinuous or irregular channels. *United States Geological Survey Professional Paper*, 282-D, 111-134.

Leopold, L.B., Wolman, M.G. and Miller, J.P. (1964): *Fluvial Processes in Geomorphology*, Freeman, San Francisco, 522p.

Leopold, L.B., Emmett, W.W. and Myrick, R.M. (1966): Channels and hillslope processes in a semi-arid area, New Mexico. *United States Geological Survey Professional Paper*, 352-G, 61p.

Lewin, J. (1972): Late-stage meander growth. *Nature Physical Science*, 240, 116.

Lewin, J. (1983): Changes of channel patterns and floodplains. *In:* Gregory, K.J. (ed.): *Background to Palaeohydrology*, 303-319.

Lewin, J. and Weir, M.J.C. (1977): Morphology and recent history of the lower Spey. *Scottish Geographical Magazine*, 93, 45-51.

Lisle, T.E. (1979): A sorting mechanism for a riffle-pool sequence. *Geological Society of America Bulletin*, 90, 1142-1157.

Lisle, T.E. (1982): Effects of aggradation and degradation on riffle-pool morphology in natural gravel channels, Northwestern California. *Water Resources Research*, 18, 1643-1651.

Maizels, J.K. (1983): Proglacial channel systems: change and thresholds for change over long, intermediate and short time-scales. *In:* Collinson, J.D.and Lewin, J. (eds.): *Modern and Ancient Fluvial Systems*, Special Publication of International Association of Sedimentologists, 6, 251-267.

Mark, D.M. and Church, M. (1977): On the misuse of regression in Earth

Science. *Mathematical Geology*, 9, 63-75.

Mavis, F.T., Ho, C. and Tu, Y.C. (1935): The transportation of detritus by flowing water - I. *Studies in Engineering*, University of Iowa, 5, 68p.

Mavis, F.T., Liu, T.Y. and Soucek, E. (1937): The transportation of detritus by flowing water - II. *Studies in Engineering*, University of Iowa, 11, 112p.

McNeil, W.J. (1966): Effect of the spawning bed environment on reproduction of pink and chum salmon. *United States Fish Wildlife Service Bulletin*, 65, 495-523.

McNeil, W.J. and Ahnell, W.H. (1964): Success of pink salmon spawning relative to size of spawning bed materials. *Special Scientific Report to United States Fish and Wildlife Service*, 469p.

Meland, N. and Normann, J.O. (1969): Transport velocities of individual size fractions in heterogeneous bedload. *Geografiska Annaler*, 51, 127-144.

Meyer-Peter, E., Favre, H., and Einstein, H.A. (1934): Neueve Versuchsresultate uben den geschiebetrieb. *Schweizerische Bauzeitung*, 103.

Meyer-Peter, E. and Müller, R. (1948): Formulas for bedload transport. *Proceedings of 2nd Congress, International Association of Hydraulic Research*, Stockholm, Sweden, 39-64.

Miall, A.D. (1978): Fluvial sedimentology: an historical review. *In:* Miall, A.D. (ed.): *Fluvial Sedimentology*, Canadian Society of Petroleum Geologists Memoir, 5, 1-47.

Milhous, R.T. (1973): Sediment transport in a gravel-bottomed stream. *Unpublished Ph. D Thesis*, Oregon State University, Corvallis, 232p.

Milne, J.A. (1980): Hydraulic regularity and environment distortion in some stream channels of upland Britain. *Unpublished Ph. D Thesis*, University of Hull, 301p.

Milne, J.A. (1982): Bed-material size and the riffle-pool sequence. *Sedimentology*, 29, 267-278.

Milner, N.J., Scullion, J., Carling, P.A. and Crisp, D.T. (1981): The effects of discharge on sediment dynamics and consequent effects on invertebrates and salmonids in upland rivers. *Advances in Applied Biology*, 6, 153-220.

Misri, R.L., Garde, R.J. and Ranga Raju, K.G. (1984): Bed load transport of coarse nonuniform sediments. *Journal of Hydraulic Engineering, American Society of Civil Engineers*, 110, 312-328.

Mosley, M.P. (1978): Bed material transport in the Tamaki River, near Dannevirke, North Island, New Zealand. *New Zealand Journal of Science*, 21, 619-626.

Mosley, M.P. (1983): Response of braided rivers to changing discharge. *Journal of Hydrology (NZ)*, 22, 18-64.

Mosley, M.P. and Tindale, D.S. (1985): Sediment variability and bed material sampling in gravel-bed rivers. *Earth Surface Processes and Landforms*, 10, 465-482.

Neill, C.R. (1968): A re-examination of the beginning of movement for coarse granular bed materials. *Report IT-68*, Hydraulics Research Station, Wallingford, 37p.

Neill, C.R. and Hey, R.D. (1982): Gravel-bed rivers: engineering problems. *In:* Hey, R.D., Bathurst, J.C. and Thorne, C.R. (eds.): *Gravel-Bed Rivers*, 15-27.

Nixon, M. (1959): A study of bankfull discharges of the rivers of England and Wales. *Proceedings of the Institution of Civil Engineers*, 12, 157-174.

O'Neill, M.P. and Abrahams, A.D. (1984): Objective identification of pools and riffles. *Water Resources Research*, 20, 921-926.

Paintal, A.S. (1971): Concept of critical shear stress in loose boundary open-channels. *Journal of Hydraulics Research*, 9, 91-113.

Parker, G. (1978): Self-formed straight rivers with equalibrium banks and mobile bed. Part 2. The gravel river. *Journal of Fluid Mechanics*, 89, 127-146.

Parker, G. (1980): Experiments on the formation of mobile pavements and static armour. *Department of Civil Engineering Technical Report*, University of Alberta, Edmonton, 57p.

Parker, G. and Peterson, A.W. (1980): Bar resistance of gravel-bed

streams. *Journal of Hydraulics Division, American Society of Civil Engineers*, 106, 1559-1575.

Parker, G., Sawai, K. and Ikeda, S. (1982a): Bend theory of river meanders, Part 2, nonlinear deformation of finite-amplitude bends. *Journal of Fluid Mechanics*, 115, 1303-1314.

Parker, G., Klingeman, P.C. and McLean, D.C. (1982b): Bedload and size distribution in paved gravel-bed streams. *Journal of Hydraulics Division, American Society of Civil Engineers*, 108, 544-571.

Peterson, A.W. and Howells, R.F. (1973): A compendium of solids transport data for mobile boundary channels. *Department of Civil Engineering, Report HY-ST3*, University of Alberta, 122p.

Proffitt, G.T. (1980): Selective transport and armouring of non-uniform alluvial sediments. *Department of Civil Engineering, Research Report 80-22*, Univeristy of Canterbury, 203p.

Proffitt, G.T. and Sutherland, A.J. (1983): Transport of non-uniform sediments. *Journal of Hydraulic Research*, 21, 33-43.

Reid, I. and Frostick, L.E. (1984): Particle interaction and its effect on the threshold of initial and final bedload motion in coarse alluvial channels. *In:* Koster, E.H. and Steel, R.J. (eds.): *Sedimentology of Gravels and Conglomerates*, Canadian Society of Petroleum Geologists Memoir, 10, 61-68.

Reid, I. and Frostick, L.E. (1986): Dynamics of bedload transport in Turkey Brook, a coarse-grained alluvial channel. *Earth*

Surface Processes and Landforms, 11, 143-147.

Reid, I., Brayshaw, A.C. and Frostick, L.E. (1984): An electomagnetic device for automatic detection of bedload motion and its field applications. *Sedimentology*, 31, 269-276.

Reid, I., Frostick, L.E. and Layman, J.T. (1985): The incidence and nature of bedload transport during flood flows in coarse-grained alluvial channels. *Earth Surface Processes and Landforms*, 10, 33-44.

Richards, K.S. (1976a): The morphology of riffle-pool sequences. *Earth Surface Processes and Landforms*, 1, 71-88.

Richards, K.S. (1976b): Channel width and the riffle-pool sequence. *Geological Society of America Bulletin*, 87, 883-890.

Richards, K.S. (1978): Simulation of flow geometry in a riffle-pool stream. *Earth Surface Processes and Landforms*, 3, 345-354.

Riou, C. (1984): Simplified calculation of the zero-plane displacement from wind-speed profiles. *Journal of Hydrology*, 69, 351-357.

Rottner, J. (1959): A formula for bedload transportation. *La Houille Blanche*, 4, 301-307.

Rundle, A. (1985): Braid morphology and the formation of multiple channels The Rakaia, New Zealand. *Zeitschrift fur Geomorphologie*, Suppl.-Bd. 55, 15-37.

Rust, B.R. (1972): Structure and process in a braided river. *Sedimentology*, 18, 221-245.

Rust, B.R. (1975): Fabric and structure in glaciofluvial gravels. *In:* Jopling, A.V. and McDonald, B.C. (eds.): *Glaciofluvial and Glaciolacustrine Sedimentation*, Special Publication of Society of Economic Paleontologists and Mineralogists, 23, 238-248.

Rust, B.R. (1978): The interpretation of ancient alluvial successions in the light of modern investigations. *In:* Davidson-Arnott, D. and Nickling, W. (eds.): *Research in Fluvial Geomorphology*, 67-105.

Schubauer, G.B. and Tchen, C.M. (1961): *Turbulent Flow*, Princeton University Press, 280p.

Schumm, S.A. and Khan, H.R. (1972): Experimental study of channel patterns. *Geological Society of America Bulletin*, 83, 1755-1770.

Shields, A. (1936): Application of similarity principles and turbulence research to bedload movement. *Mitt. Preuss. Vershsanst., Berlin, Wasserbau Schiffbau, In:* Ott, W.P. and Uchelen, J.C. (translators): *California Institute of Technology*, Pasadena, California, 167, 43p.

Simons, D.B. and Richardson E.V. (1966): Resistance to flow in alluvial channels. *United States Geological Survey Professional Paper*, 422-J, 61p.

Sissons, J.B. (1974): A Late-glacial ice cap in the central Grampians, Scotland. *Transactions of Institute of British Geographers*, 62, 95-113.

Smith, N.D. (1974): Sedimentology and bar formation in the upper Kicking Horse River, a braided meltwater stream. *Journal of Geology*, 82, 205-223.

Smith, N.D. (1978): Some comments on terminology for bars in shallow rivers. *In:* Miall, A.D. (ed.): *Fluvial Sedimentology*, Canadian Society of Petroleum Geologists Memoir, 5, 85-88.

Smith, D.G. (1983): Anastomosed fluvial deposits: modern examples from western Canada. *In:* Collinson, J.D. and Lewin, J. (eds.): *Modern and Ancient Fluvial Systems*, Special Publication of International Association of Sedimentologists, 6, 155-169.

Smith, D.G. and Putnam, P.E. (1980): Anastomosed river deposits: modern and ancient examples in Alberta, Canada. *Canadian Journal of Earth Science*, 17, 1396-1406.

Southard, J.B. and Middleton, G.V. (1985): Turbulent Flow. *In: Society of Economic Paleontologists and Mineralologists Short Course, 3*, (2nd edition).

Southard, J.B., Smith, N.D., Drake, T.G. and Kuhnle, A. (1981): Field and laboratory studies of braiding in shallow gravel-bed streams. *In:* Abstracts: *Modern and Ancient Fluvial Systems: sedimentology and processes*, University of Keele, 115.

Southard, J.B., Smith, N.D. and Kuhnle, R.A. (1984): Chutes and lobes: newly identified elements of braiding in shallow gravelly streams. *In:* Koster, E.H. and Steel, R.J. (eds.): *Sedimentology*

of Gravels and Conglomerates, Canadian Society of Petroleum Geologists Memoir, 10, 51-59.

Stanhill, G. (1969): A simple instrument for the field measurement of turbulent diffusion flux. *Journal of Applied Meteorology*, 8, 509-513.

Sutherland, A.J. (in press): Static armour layers by selective erosion. *In:* Thorne, C.R., Bathurst, J.C. and Hey, R.D. (eds.): *Sediment Transport in Gravel-Bed Rivers*, Wiley, Chichester, 880p.

Task Force on Friction Factors in Open Channels, Committee on Hydrodynamics, Hydraulics Division (1963): Friction factors in open channels. *Journal of Hydraulics Division, American Society of Civil Engineers*, 89, 97-143.

Teleki, P.G. (1972): Areal sorting of bedload: the hypothesis of velocity reversal: Discussion. *Geological Society of America Bulletin*, 83, 911-914.

Thompson, A. (1986): Secondary flows and the pool-riffle unit: a case study of the processes of meander development. *Earth Surface Processes and Landforms*, 11, 631-641.

Thompson, A. (in press): Channel response to flood events in a divided upland stream. *In:* Gardiner, V. (ed.): *Proceedings of First International Geomorphology Conference, Manchester*, Wiley, Chichester.

Thorne, C.R. and Lewin, J. (1979): Bank processes, bed material movement

and planform developments in a meandering river. *In:* Rhodes, D.D. and Williams, G.P. (eds.): *Adjustments of the Fluvial System*, 117-137.

Thorne, C.R., Bathurst, J.C. and Hey, R.D. (in press): *Sediment Transport in Gravel-Bed Rivers*, Proceedings of the Pingree Park Workshop. August 12-17, 1985, Wiley, Chichester, 880p.

Turpenny, A.W.H. and Williams, R. (1980): Effects of sedimentation on the gravels of an industrial river system. *Journal of Fish Biology*, 17, 681-693.

Van Rijn, L.C. (1984): Sediment pick-up functions. *Journal of Hydraulic Engineering, American Society of Civil Engineers*, 110, 1494-1502.

Vanoni, V.A. (1975): *Sedimentation Engineering*, American Society of Civil Engineers - Manuals and Reports on Engineering Practice, 54, 745p.

Werritty, A. and Ferguson, R.I. (1980): Pattern changes in a Scottish braided river over 1, 30, and 200 years. *In:* Cullingford, R., Davidson, D.A. and Lewin, J. (eds.): *Timescales in Geomorphology*, 53-68.

Wiberg, P.L. and Smith, J.D. (in press): Calculations of the critical shear stress for motion of uniform and heterogeneous sediments. *Water Resources Research*.

Williams, G.P. (1970): Flume width and water depth effects in sediment transport experiments. *United States Geological Survey*

Professional Paper, 562-H, 37p.

Wilkinson, R.H. (1984): A method for evaluating statistical errors associated with logarithmic velocity profiles. *Geo-Marine Letters*, 3, 49-52.

Wolman, M.G. (1954): A method for sampling coarse river-bed material. *Transactions of American Geophysical Union*, 35, 951-956.

Yalin, M.S. (1972): *Mechanics of Sediment Transport*, Pergamon Press, New York, 290p.

Yang, C.T. (1971): Formation of riffles and pools. *Water Resources Research*, 7, 1567-1574.

Zhenlin, L. and Komar, P.D. (1986): Laboratory measurements of pivoting angles for applications to selective entrainment of gravel in a current. *Sedimentology*, 33, 413-423.

Appendix A: Hydraulic measurements, transport rates, and sizes of the Helley-Smith bedload samples.

River	Sample location	Date of sampling	Shear stress	Stream power	Mean velocity	Depth
			$N\ m^{-2}$	$W\ m^{-2}$	$m\ s^{-1}$	m
Lyngsdal'	A1	1.8.84	250	502	2.01	0.65
Lyngsdal'	A2	1.8.84	293	469	1.90	0.45
Lyngsdal'	A3	1.8.84	266	513	1.93	0.47
Lyngsdal'	A4	1.8.84	216	486	2.25	0.54
Lyngsdal'	A5R	1.8.84	202	343	1.70	0.53
Lyngsdal'	A5L	1.8.84	69	88	1.28	0.30
Lyngsdal'	B1	3.8.84	169	341	2.02	0.36
Lyngsdal'	B2	3.8.84	138	246	1.78	0.60
Lyngsdal'	B3	3.8.84	121	262	2.17	0.50
Lyngsdal'	B6	3.8.84	193	323	1.67	0.55
Lyngsdal'	B1	4.8.84	271	945	3.49	0.38
Lyngsdal'	A1.1	7.8.84	364	1110	3.05	0.50
Lyngsdal'	A1.2	7.8.84	364	1110	3.05	0.50
Lyngsdal'	A3.1	7.8.84	198	469	2.37	0.36
Lyngsdal'	A3.2	7.8.84	198	469	2.37	0.36
Lyngsdal'	A5.1	7.8.84	319	504	1.58	0.32
Lyngsdal'	A5.2	7.8.84	406	938	2.31	0.40
Lyngsdal'	A5.3	7.8.84	80	160	2.00	0.40
Lyngsdal'	A6	8.8.84	6	5	0.83	0.28
Lyngsdal'	A8	8.8.84	12	9	0.75	0.15
Lyngsdal'	A9	8.8.84	12	7	0.58	0.15
Lyngsdal'	B9	12.8.84	7	10	1.43	0.47
Lyngsdal'	B9.5	12.8.84	48	77	1.60	0.40
Lyngsdal'	B10	12.8.84	37	64	1.73	0.40
Lyngsdal'	B10.5	12.8.84	15	26	1.73	0.40
Lyngsdal'	C1L	21.8.84	186	271	1.46	0.47
Lyngsdal'	C1R	21.8.84	132	180	1.36	0.29
Lyngsdal'	C2	21.8.84	279	493	1.77	0.64
Lyngsdal'	C3	21.8.84	53	82	1.55	0.52
Lyngsdal'	C4	21.8.84	71	123	1.73	0.45
Lyngsdal'	C5	21.8.84	56	117	2.09	0.42
Lyngsdal'	C6	21.8.84	60	121	2.07	0.45
Lyngsdal'	C7	21.8.84	45	61	1.36	0.30
Dubhaig	SS13	27.7.85	36	53	1.42	0.40
Dubhaig	SS20	27.7.85	10	12	1.19	0.77
Dubhaig	SS21	27.7.85	12	14	1.23	0.59
Dubhaig	SS22	27.7.85	24	24	0.99	0.49

Dubhaig	SS6	2.10.85	59	123	2.08	0.54
Dubhaig	SS7	2.10.85	36	42	1.17	0.40
Dubhaig	SS8	2.10.85	72	95	1.33	0.42
Dubhaig	SS1	3.12.85	123	337	2.75	0.95
Dubhaig	SS2	3.12.85	232	684	2.95	0.69
Dubhaig	SS3	3.12.85	149	338	2.28	0.82
Dubhaig	SS4	3.12.85	123	312	2.53	0.63
Dubhaig	SS4	3.12.85	123	312	2.53	0.63
Dubhaig	*	3.12.85	172	360	2.09	0.66
Dubhaig	SS5	3.12.85	58	89	1.45	0.67
Dubhaig	SS6	3.12.85	70	116	1.68	0.52
Dubhaig	SS6	3.12.85	96	205	2.15	0.60
Dubhaig	SS8	3.12.85	98	179	1.83	0.43
Dubhaig	SS9	3.12.85	63	103	1.64	0.79
Dubhaig	SS10	3.12.85	60	125	2.08	1.07
Dubhaig	SS11	3.12.85	48	87	1.79	0.63
Dubhaig	*	3.12.85	32	52	1.63	0.47
Dubhaig	SS12	3.12.85	24	35	1.43	0.35
Dubhaig	SS13	3.12.85	57	68	1.19	0.44
Dubhaig	SS5	5.12.85	55	73	1.33	0.62
Dubhaig	SS6	5.12.85	28	48	1.72	0.58
Dubhaig	SS7	5.12.85	53	74	1.40	0.69
Dubhaig	SS13	5.12.85	57	76	1.34	0.34
Dubhaig	SS15	5.12.85	16	21	1.34	0.44
Dubhaig	SS16	5.12.85	12	14	1.13	0.55
Dubhaig	SS17	5.12.85	26	28	1.07	0.36
Dubhaig	SS18	5.12.85	21	20	0.99	0.51
Feshie	B5	2.5.86	53	91	1.73	0.72
Feshie	B5	2.5.86	63	149	2.38	0.82
Feshie	B5.5	2.5.86	49	77	1.58	0.69
Feshie	B5.5	2.5.86	82	60	1.94	0.86
Feshie	B6	2.5.86	36	53	1.49	0.73
Feshie	B6	2.5.86	45	83	1.87	0.79
Feshie	B6.5	2.5.86	32	46	1.45	0.68
Feshie	B6.5	2.5.86	51	96	1.89	0.75

Sample location	Date of sampling	Total transport rate $kg\ m^{-1}\ s^{-1}$	Transport rate > 2 mm $kg\ m^{-1}\ s^{-1}$	Bedload D_{50} mm	Bedload max. mm	Bed Surface D_{50} mm
A1	1.8.84	0.16	0.093	6.5	54	69
A2	1.8.84	0.24	0.19	6.7	38	69
A3	1.8.84	0.31	0.29	12	38	69
A4	1.8.84	0.20	0.075	1.2	54	69
A5R	1.8.84	0.080	0.040	2.1	27	69
A5L	1.8.84	0.010	0.0012	0.50	9.5	69
B1	3.8.84	0.016	0.0039	0.80	14	69
B2	3.8.84	0.015	0.0034	0.80	27	69
B3	3.8.84	0.056	0.045	20	38	69
B6	3.8.84	0.0054	0.0023	1.3	14	69
B1	4.8.84	0.47	0.41	18	54	69
A1.1	7.8.84	2.3	1.7	7.7	70	69
A1.2	7.8.84	3.5	2.2	3.6	54	69
A3.1	7.8.84	0.79	0.65	14	54	69
A3.2	7.8.84	0.48	0.46	17	38	69
A5.1	7.8.84	0.29	0.10	0.70	70	69
A5.2	7.8.84	0.78	0.48	4.0	38	69
A5.3	7.8.84	0.28	0.15	4.0	38	69
A6	8.8.84	0.016	0.000010	0.30	1.7	69
A8	8.8.84	0.024	0.000011	0.30	2.4	69
A9	8.8.84	0.0048	0.000049	0.70	3.3	69
B9	12.8.84	0.0002	0.000028	0.80	4.8	69
B9.5	12.8.84	0.0017	0.00017	0.90	4.8	69
B10	12.8.84	0.0002	0.000039	0.90	4.8	69
B10.5	12.8.84	0.0002	0.0000012	0.30	2.4	69
C1L	21.8.84	0.0082	0.00050	0.40	6.7	69
C1R	21.8.84	0.0020	0.00015	0.30	9.5	69
C2	21.8.84	0.11	0.089	18	54	69
C3	21.8.84	0.0099	0.0029	0.60	27	69
C4	21.8.84	0.020	0.0075	1.0	27	69
C5	21.8.84	0.014	0.0056	0.50	14	69
C6	21.8.84	0.020	0.0089	1.9	38	69
C7	21.8.84	0.064	0.032	1.7	27	69
SS13	27.7.85	0.0067	0.0039	5.5	27	41
SS20	27.7.85	0.0044	0.00013	0.40	6.7	23
SS21	27.7.85	0.0044	0.0015	1.1	9.5	23
SS22	27.7.85	0.0037	0.0021	3.3	14	23
SS6	2.10.85	0.016	0.011	23	27	46
SS7	2.10.85	0.0015	0.00095	3.2	9.5	46
SS8	2.10.85	0.0046	0.0041	5.9	14	46

SS1	3.12.85	0.011	0.0066	4.3	14	98
SS2	3.12.85	0.14	0.11	46	54	98
SS3	3.12.85	0.21	0.20	28	54	98
SS4	3.12.85	0.027	0.020	18	27	98
SS4	3.12.85	0.034	0.025	7.2	27	98
*	3.12.85	0.19	0.18	34	54	98
SS5	3.12.85	1.2	0.90	6.3	38	46
SS6	3.12.85	0.023	0.015	3.6	19	46
SS6	3.12.85	1.6	1.6	16	38	46
SS8	3.12.85	1.5	1.3	17	38	46
SS9	3.12.85	0.046	0.034	16	38	41
SS10	3.12.85	0.059	0.039	3.3	19	41
SS11	3.12.85	0.0091	0.0063	5.0	27	41
*	3.12.85	0.0020	0.00075	0.70	14	41
SS12	3.12.85	0.044	0.024	2.6	19	41
SS13	3.12.85	0.099	0.081	17	54	41
SS5	5.12.85	0.023	0.015	4.5	19	46
SS6	5.12.85	0.019	0.014	14	27	46
SS7	5.12.85	0.022	0.011	2.1	27	46
SS13	5.12.85	0.031	0.026	13	38	41
SS15	5.12.85	0.0081	0.0016	0.90	6.7	42
SS16	5.12.85	0.0021	**	0.50	2.4	42
SS17	5.12.85	0.015	0.012	10	38	42
SS18	5.12.85	0.0027	0.00082	0.60	14	42
B5	2.5.86	0.034	0.033	20	38	88
B5	2.5.86	0.045	0.039	34	54	88
B5.5	2.5.86	0.013	0.0083	14	27	50
B5.5	2.5.86	0.17	0.15	17	54	50
B6	2.5.86	0.023	0.0021	0.80	14	38
B6	2.5.86	0.096	0.066	8.3	54	38
B6.5	2.5.86	0.013	0.00032	0.60	6.7	33
B6.5	2.5.86	0.0080	0.00031	0.70	4.8	33

* No specific site used in the text.

** No sediment coarser than 2 mm in the sample.

Appendix B: Mathematical procedure for the bisection of a forwards and inverse multiple regression as used to calculate bedload hiding functions (R. I. Ferguson, personal communication, 1986).

Let $y = \log W_i^*$, $x = \log \tau_i^*$, $z = \log D_i/D_{50}$

Forwards regression: $y = a_1 + b_1x + c_1z$

which corresponds to: $y - \overline{y} = b_1(x - \overline{x}) + c_1(z - \overline{z})$

Inverse regression: $x = a_2 + b_2y + c_2z$

which corresponds to: $y - \overline{y} = 1/b_2.(x - \overline{x}) - c_2/b_2.(z - \overline{z})$

Bisector in yx plane through $\overline{x}$, $\overline{y}$, $\overline{z}$:

$$y - \overline{y} = (b_1/b_2)^{0.5}.(x - \overline{x}) + k.(z - \overline{z})$$

where k is determined by:

Bisector also in yz plane through $\overline{x}$, $\overline{y}$, $\overline{z}$:

$$y - \overline{y} = (b_1/b_2)^{0.5}.(x - \overline{x}) + (-c_1.c_2/b_2)^{0.5}.(z - \overline{z})$$

If simplified: $y = A + Bx\ Cz$

where $B = (b_1/b_2)^{0.5}$

$C = (-c_1.c_2/b_2)^{0.5}$

$A = \overline{y} - B\overline{x} - C\overline{z}$

Expressed in terms of a hiding function:

$$\tau^*_{ir} = 10^{-A/B} .W^*_{ir}{}^{1/B} .(D_i/D_{50})^{-C/B}$$

Appendix C: Some example velocity profiles

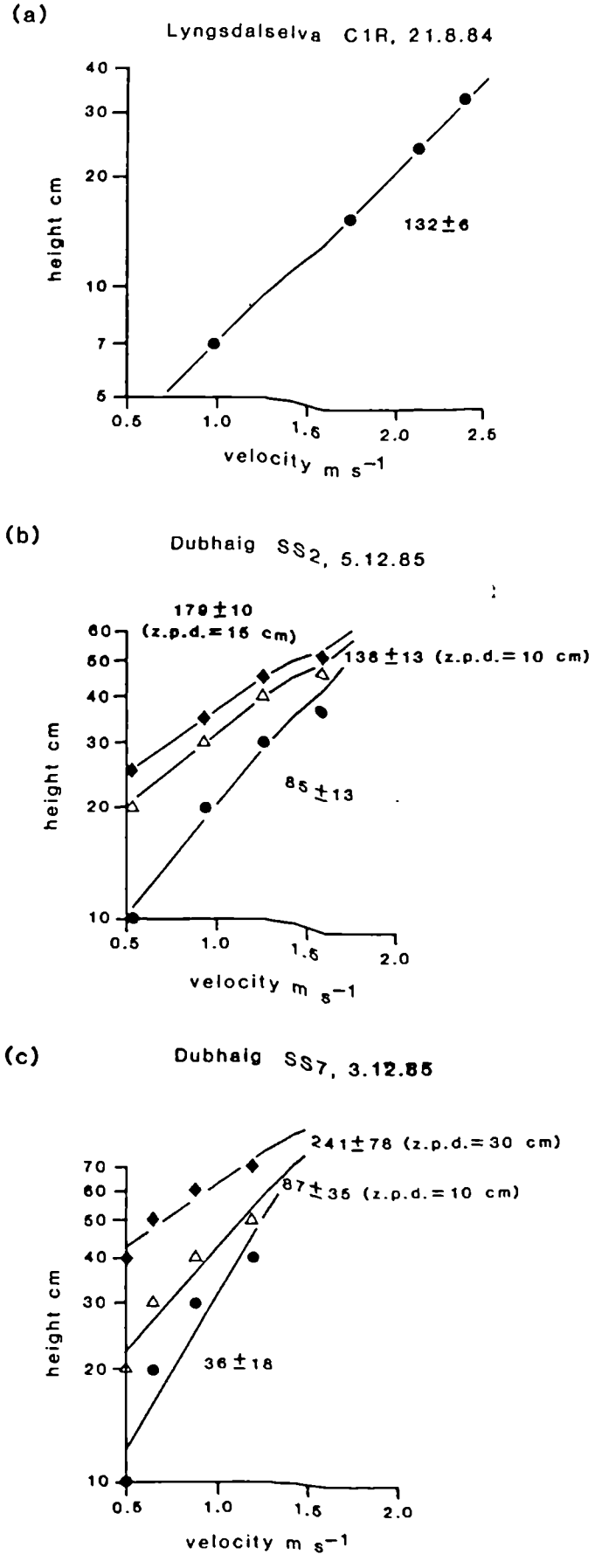

Example (a) is where the profile was almost linear (for over 90% of the profiles measured), (b) in a few cases a zero-plane displacement was added to linearise the profile, and (c) very occasionally a profile was rejected since the addition of a realistic z.p.d. still failed to overcome the curvilinearity in the profile.